DEVELOPMENT AND CHARACTERISATION OF NOVEL FLUORAPATITE CONTAINING DENTAL COMPOSITE MATERIALS

Asmaa Mohammed Basil Jasim Al-Taie

Submitted in accordance with the requirements for the degree of
Doctor of Philosophy

The University of Leeds
School of Dentistry

May 2017

The candidate confirms that the work submitted is her own and that appropriate credit has been given where reference has been made to the work of others.

Acknowledgements

I would like to thank my mentor and supervisor David Wood who has been with me in every step since we first met. Your support, advice and help have been tremendous and I am very blessed to have you as my mentor and call you a friend. You stood by me at the hardest of times which I am forever grateful for. I am also very happy that you can now tick off another box from your “blue sky research ideas” list!

Paul Franklin, I thank you for your kindness, support and for your understanding throughout this journey and for protecting my research time allowing me to complete this piece of work which I dedicate to you. And thank you for all the coffee and cake breaks when I was so busy writing.

Nigel Bubb, thank you for your help throughout this journey, and thank you for teaching me “the hard space”!

Matt German, thank you for your support and for always welcoming me in Newcastle.

Adam, Ola and Zara, I am so blessed to have such supportive siblings like you.

My little nephews Joseph and Ali, you bring so much joy and happiness to my life. Now I am finished with my PhD you can have as many sleepovers as you want.

My parents, I am truly blessed to have you and I am so grateful to all your support throughout my life and I really thank you for everything you have done for me.

My best friend Layth, although you chose to stay at the Ozzy lands, I never felt that you are away; I thank you for being there at all times.

And finally to the true happiness in my life Robin, thank you for holding my hand at each step I take, you bring so much love and happiness to my life which I am forever grateful for. Your support and encouragement has been so great and I dedicate this thesis to you…

Abstract

Objectives: The objectives of this study were to develop model dental composites incorporating fluorapatite (FA) as secondary filler and to characterise their physical and mechanical properties and fluoride ion release.

Methods: Experimental composites were formulated containing BisGMA/TEGDMA/BisEMA and barium aluminium silicate glass as the primary filler. FA rod-like crystals and bundles were synthesised using a hydrothermal method and incorporated at 0 (0FA), 10 (10FA), 20 (20FA), 30 (30FA) and 40% (40FA) by mass into the previously identified optimum experimental composite, maintaining an overall filler content of 80%wt. 0FA and TetricEvoCeram (TC) were used for comparison as the experimental and the commercial controls, respectively. Two-body wear, Vickers Hardness (HV), Degree of Conversion (DC), Flexural strength (FS), Flexural modulus (FM), Fracture Toughness (K_{1C}) and fluoride ion release were measured for each composition. Quantitative analysis of wear volume was carried out using a noncontact profilometer. Qualitative imaging of wear and fracture surfaces was undertaken using Scanning Electron Microscopy (SEM) and Energy Dispersive X-ray Spectroscopy (EDX). Statistical analysis was conducted using SPSS version 21.

Results: All experimental composites showed similar wear resistance ($p > 0.05$) and enhanced microhardness compared to TC ($p < 0.05$). DC for all composites ranged between 56-60% at 20s polymerisation ($p > 0.05$). FA composites showed higher FM ($p < 0.05$) and similar FS ($p > 0.05$) to TC but lower FM and FS when compared to 0FA. 30FA and 40FA showed similar K_{1C} to TC and 0FA ($p > 0.05$), whereas 10FA and 20FA showed lower K_{1C} when compared to the other groups ($p < 0.05$). Under neutral pH, no fluoride release was detected from FA containing composites. However, under acidic conditions (pH 4), FA containing composites released fluoride when compared to the controls ($p < 0.05$), the amount of which was proportional to the amount of FA incorporated within the samples, i.e. 40FA> 30FA > 20FA > 10FA ($p < 0.05$).

Conclusions: Experimental dental composites were successfully produced incorporating FA as secondary filler. The addition of FA did not affect the key physical and mechanical properties when compared to the commercial control. FA composites showed short and long term fluoride release under acidic conditions showing a promising step towards a potential “smart” fluoride releasing dental composite.

Table of Content

List of main abbreviations

ANOVA: Analysis of variance

BisGMA: bisphenol A glycidyl dimethacrylate

BisEMA: Bisphenol A polyethylene glycol diether dimethacrylate

CQ: Camphoroquinone

DC: Degree of conversion

DMAEMA: Di-methyl-aminoethyl methacrylate

EDX: Energy dispersive X-ray spectroscopy

FS: Flexural Strength

FM: Flexural Modulus

FA: Fluorapatite

FTIR: Fourier transform infrared spectroscopy

HV: Vickers Hardness

K_{1C}: Fracture toughness

PPF: pre-polymerised filler

RI: Refractive Index

TC: Tertic Evo Ceram

TEGDMA: Triethylene glycol dimethacrylate

SEM: Scanning electron Microscopy

UDMA: Urethane dimethacrylate

List of Figures

List of Tables

Chapter 1: Introduction

1.1 General introduction

Resin composites have acquired a prominent place amongst direct restorative materials as a posterior restorative exceeding amalgam use in several countries (Burke, 2004, Mitchell et al., 2007, Vidnes-Kopperud et al., 2009, Burke et al., 2017). Around 800 million composite resin restorations were placed worldwide in 2015; ~80% were placed in the posterior region and 20% in the anterior region (Jäggi F, 2015). In the UK, resin composite is used in ~48% of cases when restoring Class II cavities in permanent molars and ~66% in premolars. The popularity of resin composites is driven by their superior aesthetic properties and conservative nature, in addition to their reasonable clinical performance (Beazoglou et al., 2007, Lynch et al., 2007, Lynch et al., 2011). More recently the introduction of the Minimata convention and the calls for a phase down in the use of mercury containing products has placed composite as the most suitable alternative to amalgam as a direct restorative material (Lynch and Wilson, 2013a). Current composite formulations exhibit enhanced mechanical and physical properties allowing them to be used as a posterior restorative (Manhart et al., 2009, Da Rosa Rodolpho et al., 2011, Demarco et al., 2012a, Opdam et al., 2014, da Veiga et al., 2016). However, the average life span of composite restorations remains just under 10 years after which clinical intervention may be required (Ástvaldsdóttir et al., 2015). Recurrent caries and restoration fracture remain as the primary reasons of clinical failures of composite restorations (Bernardo et al., 2007, Soncini et al., 2007, Sunnegardh-Gronberg et al., 2009, Demarco et al., 2012a, Beck et al., 2015a). Recent systematic reviews reported that restoration fracture is the most common reason of failure when composite resin is used as a posterior restorative (Opdam et al., 2014, Ástvaldsdóttir et al., 2015, Heintze et al., 2015). Therefore, concerns still exist when composite is used in high load bearing areas, especially in patients with parafunctional habits (van de Sande et al., 2013). Recurrent caries remains as a primary issue leading to restoration failure due to the lack of effective antimicrobial

properties in current composite formulations (Wiegand et al., 2007, Cury et al., 2016). Therefore, it is essential to develop new innovative composite formulations with novel chemistries to further enhance their physical and mechanical properties and more importantly exhibit effective bioactive properties against recurrent caries. The idea of a “smart” resin composite that reacts with its surrounding environment remains the focus of many researchers in the field of resin composites.

1.2 Composition of resin based composites

Fundamentally, dental composite consists of an inorganic filler, organic matrix and coupling agent. The incorporation of fillers is the main strategy used to enhance the poor mechanical and physical properties of the unfilled resin. Therefore the ratio of resin/filler content directly affects the material’s properties. Increasing the filler content results in enhanced wear resistance, strength and reduced shrinkage properties (Kim et al., 2002, Turssi et al., 2005, Randolph et al., 2016). A surface coupling agent is required to enhance the bond between the filler and the resin matrix and an initiator is also required to initiate the polymerisation process when an external energy source is applied. To prolong the monomer shelf life and improve its ambient light stability, an inhibitor may also be added. Furthermore, pigments may also be incorporated to improve the optical properties and shade match of resin composites.

1.2.1 Resin matrix

Resin composites are typically prepared from a compound of bisphenol A and two molecules of glycidyl methacrylate called 2,2-bis[4(2-hydroxy-3 methacryloyloxy-propyloxy)-phenyl] propane (BisGMA), (Bowen RL, 1962), Figure 1. BisGMA is the first resin that was successfully incorporated into resin based composites and remains the primary resin used in contemporary dental composites to date. It is a relatively large methacrylate molecule which has two aromatic rings and hydroxyl groups that contribute to its weight and stiffness. Consequently, it is a very viscous material which has low reactivity and degree of conversion (Pfeifer et al., 2009b).

Furthermore, the viscosity of the material compromises the composite handling properties and makes more difficult the incorporation of enough reinforcing filler for sufficient physical and mechanical properties to be achieved. Therefore, di-functional monomers with low molecular weight and reduced viscosity are usually added and act as diluents for the resin matrix (Silikas and Watts, 1999).

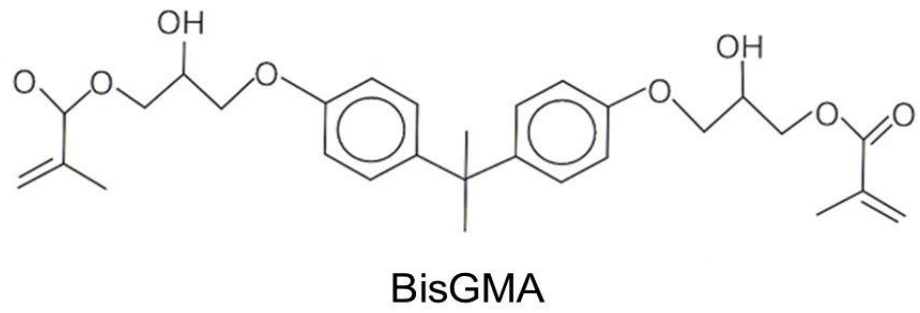

Figure 1: The chemical structure of the base monomer Bisphenol A glycidyl methacrylate (BisGMA)

The use of diluting monomers facilitates the incorporation of large amounts of filler particles to improve the mechanical properties of the material. In addition, these monomers contain reactive (C=C) bonds at each end which can undergo addition polymerisation and therefore increased reactivity and degree of conversion. Various diluting monomers are available such as TEGDMA, UDMA and BisEMA. The commonly used diluent triethyleneglycol dimethacrylate (TEGDMA) has a reduced viscosity due to its low molecular weight, Figure 2, which also aids in increased reactivity and degree of conversion. However the presence of ether groups (C-O-C) and the lack of aromatic rings along its structure reduce its mechanical properties in comparison to BisGMA. Furthermore, the increased reactivity and conversion results in increased polymerization shrinkage which is a highly undesirable property (Asmussen, 1982, Braga et al., 2005). Another disadvantage is the reduced hydrophobicity of TEGDMA which results in increased susceptibility to staining and leaching of the monomer in the oral environment (Sideridou and Achilias, 2005).

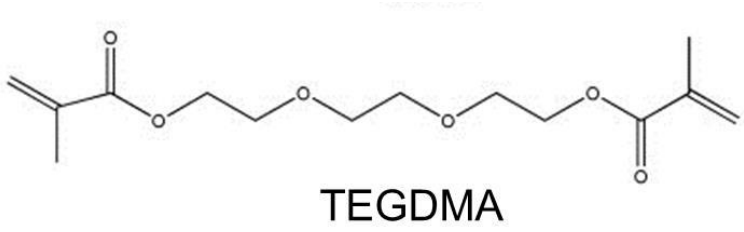

Figure 2: The chemical structure of Triethyleneglycol dimethacrylate (TEGDMA)

Other methacrylate-based monomers such as urethane dimethacrylate (UDMA) may also be used to either completely substitute for BisGMA or be used in combination with BisGMA. UDMA contains a urethane group which provide greater functionality to the monomer, Figure 3. This functionality adds toughness and flexibility to the monomer back bone. Although the molecular weight of UDMA is similar to BisGMA, the lack of aromatic rings results in reduced viscosity and consequently enhanced conversion and handling properties.

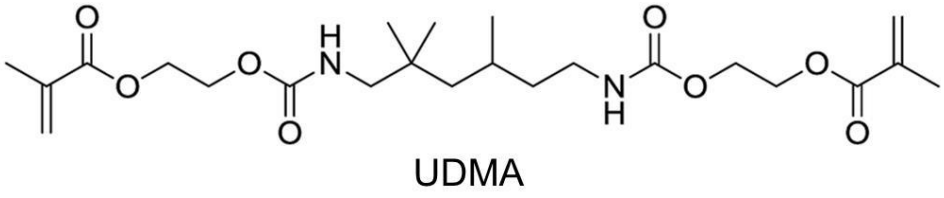

Figure 3: The chemical structure of urethane dimethacrylate (UDMA)

Another monomer system which can be used as either a base monomer or a diluting monomer is ethoxylated bisphenol A dimethacrylate (BisEMA). BisEMA structure is similar to BisGMA as it has a stiff central phenyl ring core but differs from BisGMA due to the absence of the pendant hydroxyl groups which are mainly responsible of the increased viscosity of BisGMA, Figure 4. Therefore, BisEMA maintain a high molecular weight (496 g/mol) comparable to BisGMA but it has a significantly lower viscosity (Cook, 1992, Sankarapandian et al., 1997) which significantly improves the handling properties.

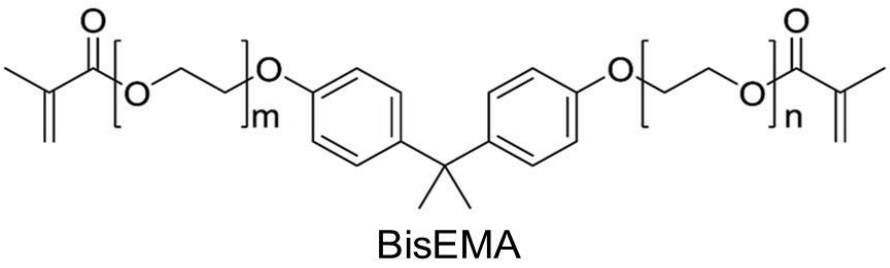

BisEMA

Figure 4: The chemical structure of ethoxylated bisphenol A dimethacrylate (BisEMA)

1.2.2 The filler content

The fillers are the inorganic component of resin composites which are incorporated to enhance the mechanical properties and reduce polymerisation shrinkage of resin composites. It was recognised that the size and the amount of filler content are critical in determining the materials' mechanical and physical properties. Generally increasing the filler content results in increased wear resistance, surface microhardness and strength and reduced polymerisation shrinkage of resin based composites (Jun et al., 2013a, Shah and Stansbury, 2014, Randolph et al., 2016). It was identified that a filler content of 60%vol is necessary to achieve the aforementioned properties (Lohbauer et al., 2006, Randolph et al., 2016). Therefore researchers continued to focus on refining the filler particles to produce materials with enhanced mechanical and physical properties. However, the relatively small filler particle size limits the amount of filler volume fraction that can be incorporated. Therefore pre-polymerised fillers (PPF) were introduced which are larger in size to improve the filler volume fraction. PPFs are processed using ground cured composite containing a variety of submicron particles. The addition of PPFs also aids in reducing the polymerisation shrinkage and provides improved polishability when compared to conventionally filled resin composites (Senawongse and Pongprueksa, 2007, Ferracane et al., 2014). However, PPF lack the active binding sites for surface coupling which results in reduced bonding to the resin matrix and consequently compromised mechanical properties (Kim et al., 2002, Ilie et al., 2013b, Randolph et al., 2016). The type of filler particle is also crucial in determining the materials' optical and physical properties.

Initially quartz filler particles were used as they provide excellent optical match to the resin matrix. However, it has several drawbacks such as abrasiveness to the opposing enamel, reduced polishability and radiopacity which limits its aesthetic properties. Therefore amorphous silica (i.e. glass) particles were developed to address these issues and most modern composites currently contain radiopaque silicate particles based on barium, strontium, zinc, aluminium, or zirconium. The filler morphology also affects the filler loading rate which consequently affects the materials' physical and mechanical properties (Kim et al., 2002, Leprince et al., 2010, Ilie et al., 2013b, Jun et al., 2013a, Randolph et al., 2016). Most modern materials contain fillers with various morphologies including spherical and irregularly shaped particles and pre-polymerised fillers (Randolph et al., 2016). It was shown that composites containing pre-polymerised fillers had the lowest filler content whereas composites incorporated with round filler particles had the highest filler content (Kim et al., 2002).

1.2.3 Photoinitators

The photo-polymerisation process involves the use of an external light source to produce free radicals to start the polymerisation process; this allows command set of the material once the light is applied. Therefore, the use of photo-polymerisation rather than chemical curing allows greater flexibility in controlling the clinical working time. The most common photoinitiator system used in dentistry consists of two components; photoinitiator and co-initiator. Camphorquinone (CQ) is the most widely used photoinitiator in resin composites. It absorbs visible blue light in the wavelength range of 400-500nm (λmax = 470 nm). The co-initiator is conventionally a tertiary aliphatic amine reducing agent, which reacts with CQ in its excited state to generate free radicals. Dimethylaminoethyl dimethacrylate (DMAEMA) is the most commonly used reducing agent in resin composites. Appropriate photoinitiator chemistry is essential for optimum polymerisation and hence satisfactory physical and mechanical properties (Ogunyinka et al., 2007). Optimising the correlation between the photoinitiator and co-initiator type and concentration allows maximum photon absorbance and consequently increased depth of cure (Chen et al.,

2007, Dos Santos et al., 2008). However, the concentration of the photoinitiator system should be limited to achieve optimum polymerisation and monomer conversion while limiting the amounts of unreacted photoinitiator and monomers that may cause cytotoxicity (Pagoria et al., 2005). Furthermore, increasing the concentration of CQ beyond a certain level affects the aesthetics properties of resin composites due to the yellow nature of CQ, in which any unreacted molecules would turn back to their original state causing polymer discolouration (Ogunyinka et al., 2007). More recently, alternative photoinitiators were introduced such as phenyl proanedione (PPD), Benzil (BZ) and Norrish Type I photoinitiator systems such as mono- (Lucirin TPO) and bi-(Irgacure 819) acylphosphine oxides (Neumann et al., 2005, Neumann et al., 2006, Ogunyinka et al., 2007). Most of these materials are not pigmented and therefore are used in bleached shades of resin composites, Figure 5. They can be used as a standalone photoinitiator or in combination with CQ which may provide improved polymerisation kinetics, mechanical properties and aesthetics (Weinmann et al., 2005, Neumann et al., 2006). However, a crucial difference to CQ is the different absorbance characteristics of these photoinitiators which are mostly in the range of 370-393 λmax (nm), Table 1. Therefore most of the new photoinitiators require light curing units that could emit light at wide range of spectral emission; halogen lights (380-550 nm) would be a suitable option in this case however their use in dentistry is almost obsolete. Alternative polywave lights have recently been introduced emitting light at two intensity maxima, one in the visible region and one covering the shorter wavelength region. However, polywave lights exhibit local differences in irradiance distribution and spectral inhomogeneity (Shortall et al., 2015), which in turn affect the extent and quality of curing of resin composites (Arikawa et al., 2008, Palin et al., 2008, Vandewalle et al., 2008, Alshaafi et al., 2016). Therefore the clinical acceptance of these photoinitators is still questionable.

Figure 5: The colour differences between the photoinitiators used in resin based composites showing CQ (left), PPD (middle) and TPO (right), *(Bluephase LED user guide, Ivoclar Vivadent)*

Table 1: The absorption characteristics of photoinitiators used in resin based composites

Photoinitiator	Absorption Range (nm)	λmax (nm)	Molar extinction coefficient at λmax ($L.mol^{-1}.cm^{-1}$)
Camphorquinone	400-550	470	~35
Lucirin TPO	300-430	381	~550
Irgacure	300-440	370	~300
PPD	300-480	393	~150
Benzil	300-460	385	~50

1.2.4 Inhibitors

Inhibitors are commonly used to prevent spontaneous polymerisation and to increase the shelf life of resin composites. The most commonly used photo-inhibitor is hydroquinone or butyl hydroxytoluene (BHT). Inhibitors react with the free radicals and therefore reduce the rate of initiation and increase the rate of termination (Moad and Solomon, 1995). Consequently the rate of polymerisation is reduced. The conversion of monomer to polymer proceeds at a reduced rate until the inhibitor is fully consumed. Therefore, the inhibitor may also increase the “pre-gel” phase allowing shrinkage forces to be dissipated (Braga and Ferracane, 2002). Inhibition of the polymerisation process may also occur when large amount of oxygen

is present which may prevent optimal restoration curing and therefore compromised properties (Gauthier et al., 2005).

1.3 Development and classification of resin composites

The composition of dental composites has significantly evolved since they were first introduced more than 50 years ago. The development of resin composite materials remains heavily researched in academia and industry aiming to enhance their clinical longevity by addressing their perceived shortcomings such as mechanical strength (Ilie and Hickel, 2009a, Ilie and Hickel, 2009b, Jun et al., 2013a), polymerisation stress (Eick et al., 2007, Gonçalves et al., 2010), inadequate depth of cure (Leprince et al., 2012), handling (Lee et al., 2006) and aesthetic properties (Mikhail et al., 2013). Until recently the most important changes have been related to the filler type, morphology and size (Ferracane, 2011, Randolph et al., 2016). Researchers continued to focus on refining the filler particles. With the advancement of processing techniques such as jet-milling, the size of filler particles have decreased from tens of microns to a sub-micron level, with a consequent enhancement in wear resistance and polishing properties. Nano-fillers were also introduced to enhance the aesthetic properties of resin composites and have been used both as agglomerated nano-clusters and as discrete particles to enhance the mechanical performance (Curtis et al., 2009). The use of discrete nano-particles could also offer a significantly increased depth of cure due to their reduced refraction and scattering when exposed to visible blue light (Fujita et al., 2011). More recently, “Bulk-fill” dental composites have been introduced and they are claimed to enable restoration build-up in thick increments of up to 4-6 mm. This new class includes flowable and higher viscosity sculptable materials. The use of bulk-fill composites has become a popular trend amongst dentists due to their ease of use and reduced clinical time. The main advancement of bulk-fill materials in the increased depth of cure which is mostly attributed to their increased translucency (El-Safty et al., 2012), in addition to that, their reduced shrinkage stress is related to modifications in the filler content and/or the organic matrix. However these perceived improvements are not indicative of the mechanical performance of these materials. Some

concerns were raised regarding the low surface hardness, flexural strength and flexural modulus properties of bulk-fill materials when compared to conventional resin composites (Garoushi et al., 2013, Ilie et al., 2013a, Leprince et al., 2014). The classification of dental composites continued to evolve following the evolution of the material composition. Generally the classification is focused on the filler size distribution and filler content. “Micro-filled” and “nano-filled” composites contain only micro and nanofillers respectively. However most modern dental composites fall under the category of “hybrid” materials, and are typically marketed as “nano-hybrids”. This terminology refers to composites containing a portion of nanoparticles (<100 nm) and of sub-micron particles (≤1 µm, mostly averaging 0.5–1.0 µm). Nano-hybrids usually contain a larger fraction of nanoparticles when compared to micro-hybrids (Ferracane, 2011), Figure 6.

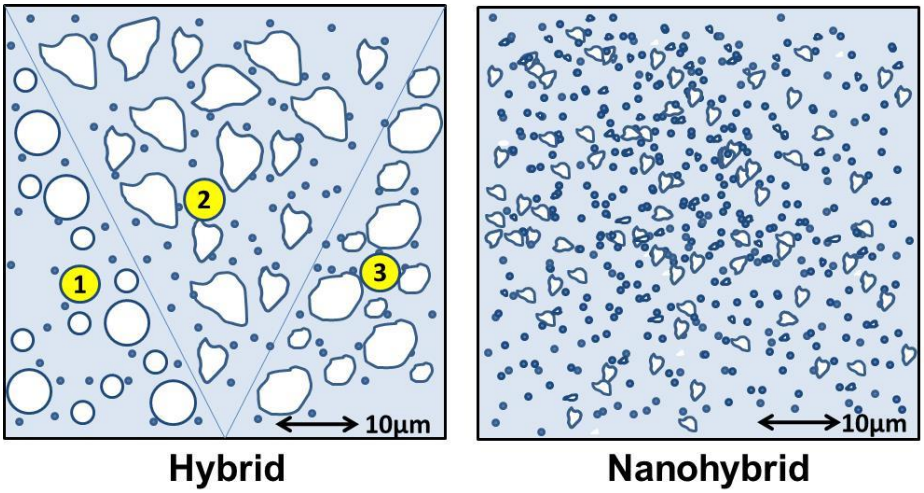

Figure 6: Schematic description of filler distribution of resin composites. Hybrid resin composites include a combination of micro and nanoparticles (left figure). Continuous distribution is shown (1 and 2) with spherical (1) or irregular particles (2) and a bimodal distribution (3) of micro particles, (Randolph et al., 2016)

However, this classification has been recently criticised as it does not completely reflect the filler composition, morphology or filler specifications (Randolph et al., 2016). Many commercial dental composites which are claimed to be “nano-hybrid” in fact have a significant proportion of large

filler particles (>1 µm), (Kim et al., 2002, Scougall-Vilchis et al., 2009), therefore it is questionable whether all nano-hybrids composites would have the same properties. Comparisons of the mechanical and physical properties of dental composites are well documented in the literature; these properties vary between different materials or testing centres. Resin composite properties are interrelated and predominantly dependent on filler characteristics (geometry, composition, size distribution) and filler content (filler mass and volume content) (Kim et al., 2002, Leprince et al., 2010, Ilie et al., 2013b, Jun et al., 2013a, Randolph et al., 2016). Therefore the current classification which is solely based on filler particle size may not be appropriate for accurate representation of the material's performance. A recent study evaluating the mechanical properties and filler characteristics of a wide range of contemporary dental composites showed significant variations amongst modern materials (Randolph et al., 2016). However, it was not possible to accurately illustrate these variations using the current classification. Since direct correlations were found between the filler content and the materials' mechanical and physical properties, a simpler classification based on the materials' filler volume content was suggested instead. This classification is based on the filler content at two levels: 50% and 74%vol, the terms "Ultra low-fill", "Low-fill" and "Compact" would apply to materials with filler contents lower or higher than 50% or higher than 74vol%, respectively, schematic diagram is shown in Figure 7.

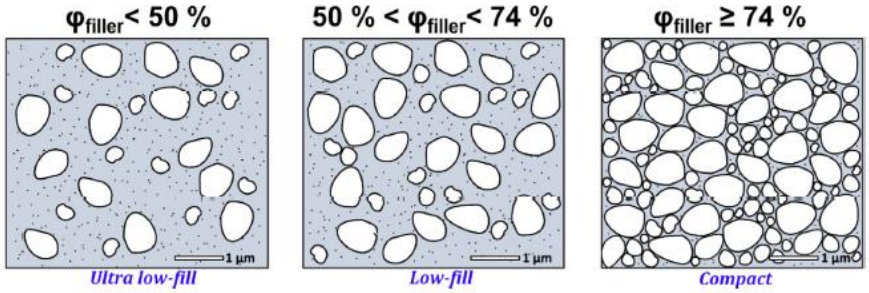

Figure 7: New classification based on the inorganic filler volume content of composite containing nano and micron-sized particles. The filler content also reflecting the elastic modulus. (*Randolph et al., 2016*)

1.4 Longevity and shortcomings of resin composites

Based on meta-analyses on posterior resin restorations it has been shown that at least ~5% of such restorations will fail due to fracture of the material and ~12% will show noticeable wear within an observation period of 10 years (Heintze and Rousson, 2012, Beck et al., 2015a). In other words, based on the data presented in Section 1.1, at least ~32 million posterior resin restorations placed in 2015 will be replaced or will need repair work due to fracture by 2025. Therefore there is an increasing demand to continue enhancing resin composite properties in terms of strength, fracture resistance and reducing the polymerization shrinkage of the material (Ferracane, 2011, Randolph et al., 2016). The lack of effective antimicrobial properties in the current composite materials places them in a compromised position in tackling the recurrent caries issue (Wiegand et al., 2007, Cury et al., 2016). Based on the recent observations, ~4.5% of posterior composites would fail due to recurrent caries over 10 years' time; therefore around 28.8 million of the posterior restorations placed in 2015 would also require clinical intervention by 2025 (Beck et al., 2015b). Therefore, research is also focused on developing new materials that can resist/prevent recurrent caries development by including antibacterial components capable of enhancing the material's remineralising potential and responsiveness to the changing oral environment (Beyth et al., 2014). The idea of "smart" restorative that react to the surrounding environment remains very attractive amongst researchers (McCabe et al., 2011, Davis et al., 2014, Hyun et al., 2015). Therefore, due to the continuous material development among researchers and manufactures, it is essential that new materials are subjected to various testing modalities to characterise their properties and compare them to already existent successful formulations (Ferracane, 2013a). Ideally clinical trials should be conducted to evaluate the performance of new dental composites, however due to their expensive and time consuming nature, well designed laboratory studies remain necessary in trying to predict the performance of new materials. Furthermore, it is also essential to correlate the laboratory tests to the clinical performance of resin composites to ensure accurate predictions of

clinical behaviour. Based on the main reasons of failure of resin composites; strong/moderate correlations were found between the material's fracture toughness and clinical fractures and the flexural strength properties and the clinical wear (Ferracane, 2013a, Heintze et al., 2017). Therefore assessment of new materials should include clinically relevant tests to provide a better insight into the materials performance.

1.5 Wear resistance of dental composites

Wear of resin composites remains an important limiting property of large posterior composite restorations especially when used in patients with heavy occlusal loads and parafunctional habits (van Dijken, 2000, Soderholm et al., 2001). Earlier studies suggested that excessive wear of posterior composite restorations is caused by several factors related to filler composition, filler size and filler-resin matrix bonding. The new formulations of dental composites are composed of smaller filler particles which allow higher filler loading with improved mechanical properties which ultimately increase the survival rates. The general consensus is that the wear resistance of resin composite is dominated by the filler constituent which can be tailored by adjusting the filler volume fraction, diameter or density (Lim et al., 2002, Hu et al., 2003, Pick et al., 2011, Hahnel et al., 2012, Finlay et al., 2013). Hanel *et al* conducted a two-body wear test on fourteen dental restorative materials with variable filler size; they concluded that microfilled composites had lower wear compared to hybrid and macrofilled composites and that the highest wear was in composites containing larger filler particles (>1 μm)(Hahnel et al., 2011). Palaniappan *et al* compared the clinical wear performance of nanohybrid, microfilled and conventional hybrid composite in a 5 year clinical trial; they reported that nanohybrid composite showed significant lower material volume loss compared to the other two, which showed comparable volume loss (Palaniappan et al., 2012). The filler-matrix bonding could also play a major role in the wear resistance of dental composites. The silane coupling agent forms a bond between the inorganic and the organic components of dental composite. It also protects the filler surface from fracture and hydrolytic degradation (Mohsen and Craig, 1995). In general the efficiency of silane coupling agent

is determined by the degrees of reaction of the silane with the glass fillers and with the polymer matrix. The oxygen bond (silicon-oxygen-silicon) that forms between the silane agent and the mineral filler is vulnerable to hydrolysis because of its significant ionic character. By contrast, the carbon-carbon bond that forms between silane and the polymer matrix is more stable to hydrolytic attack (Antonucci et al., 2005). In an attempt to improve the quality and the durability of the filler-matrix interface, the use of more hydrophobic silane coupling agents was suggested. Nihei *et al* (2008) evaluated the wear resistance of resin composite materials containing fillers with novel hydrophobic silane coupling agent containing hydrophobic phenyl group (3-methoxy-4-methacryloyloxy-phenyl) and they concluded that composites containing the hydrophobic coupling agent showed higher wear resistance compared to composite materials without hydrophobic group in the coupling agent (3-methacryloyloxypropyl-trimethoxysilane) (Nihei et al., 2008). Although the wear resistance of resin composite is mainly dominated by the filler constituent, wear is described as a "complex process" and not all resin formulations behave similarly (Finlay et al., 2013, Altaie et al., 2017). The complexity of the wear process is attributed to the four fundamental wear mechanisms (abrasion, adhesion, fatigue or corrosion) involved in the wear process (Mair et al., 1996). A combination of wear mechanisms is mostly involved during the wear process of resin composites. However, a predominant wear process is usually present which is determined by the resin composite chemical composition (Altaie, 2012). Recent findings showed that certain commercial composite formulations presented exacerbated wear due to the presence of secondary adhesive wear mechanisms resulting from material transfer from the composite to the opposing antagonist (Altaie et al., 2017). Therefore due to the increase of use of resin composites as a posterior restorative and the different wear behaviour of recent composite formulations it was concluded that '*wear should continue to be a screening tool for new composites prescribed for posterior teeth*' (Ferracane, 2013a).

1.5.1 *In-vitro* wear testing of dental composites

The wear performance of resin composites has been heavily researched in the literature. A variety of *in-vitro* wear testing devices have been used to replicate the *in-vivo* wear process (Lambrechts et al., 2006). However, to date there has been no single *in-vitro* wear simulator that can mimic the complex masticatory process in the oral environment. Most devices provide the relative ranking of new composite formulations and compare to already successful formulations (Finlay et al., 2013, Benetti et al., 2016). However, the most robust laboratory studies are conducted on a wide range of commercial materials in the form of round-robin tests (Heintze et al., 2005a, Heintze et al., 2011, Heintze et al., 2012). Determining the wear parameter and the accurate measurement of wear is also essential in accurate prediction of wear *in-vivo*. Too frequently in dentistry, the wear depth or wear area are reported, however the wear in the mouth is dependent upon occlusal factors which constantly change with time and wear progression. Therefore, the parameter of choice for reporting wear should be the volume loss rather than wear depth (DeLong, 2006, Fleming et al., 2016). Furthermore, interruption of wear should consider the complex wear process and the tribology of wear to provide a greater insight into the material's behaviour. Therefore a combination of analytical techniques should be employed when wear is evaluated including surface analysis or the wear facets on the material and the opposing antagonist. However regardless of the technique employed, the accuracy and precision of these measurement techniques should also be reported (DeLong, 2006). Three dimensional (3D) scanning is the preferred method for measuring wear which is accurate and able to provide a quantitative 3D database which can be stored and compared to other data. Contact and non-contact scanners are available which are able to measure the material loss (depth/volume), surface topography and roughness. 3D profilometric scanners are widely used in measuring the wear of resin composites (Palaniappan et al., 2010, Theocharopoulos et al., 2010, Benetti et al., 2016, Altaie et al., 2017). Contact profilometers consist of a diamond stylus of varying radius (5-20 µm). The stylus moves along the surface of the specimen in vertical and

lateral directions for a specified distance at a predetermined reference point. It moves under a constant force and speed recording the vertical surface variations as a function of position ranging from 10 nm to 1 mm. The vertical position of the stylus generates an analogue signal which is converted into a digital signal for analysis. The advantages of the contact scanners are the low costs and their effectiveness regardless of the materials' colour or transparency (DeLong, 2006). However, the accuracy of the measured volume loss using a stylus scanner is limited when spherical abraders were scanned, in addition to discrepancies in the readings due to wear of the tip of the stylus (Wassell, McCabe and Walls 1994b). The non-contact or laser profilometer overcame the issues of contact scanners. Non-contact scanners project a light beam from a semi-conductor laser source focused on the specimen as a focal spot. It is controlled by a moveable lens in the sensor to ensure that the focal spot is always in a constant contact with the object surface. The sensor records any displacement on the specimen surface in the direction of the light beam which provides the desired surface displacement measurement, surface contour and roughness parameters. However, regardless of the techniques used, the key factor is employing accurate and precise measurement techniques that are relevant to clinical wear (DeLong, 2006). In addition of qualitative analysis, evaluating the pattern of wear facets on the material and the opposing antagonist provide a better understanding of the materials behaviour. Scanning Electron Microscopy (SEM) has been widely used to determine wear patterns of dental composites and to evaluate the different wear mechanisms involved (Hu et al., 2002, Yap et al., 2002b). More recently elemental mapping of the wear facets on the opposing antagonists using energy dispersive X-ray spectroscopy (EDX) showed characteristics of predominatly adhesive wear mechanisms in certain composite formulations (Altaie et al., 2017). Therefore it is suggested that employing a variety of analytical techniques when evaluating the wear performance of resin composites provide a better insight into the materials behaviour rather than relying on simple ranking.

A wide range of wear testing machines had been developed and are available today with varying complexity and sophistication trying to simulate the oral cavity during mastication. One of the earliest chewing machines was described in the nineteen fifties by Cornell *et al*. In this machine the upper teeth were mounted on a movable arm while the lower teeth were mounted on a rigid arm (Cornell et al., 1957). Harrison and Lewis (1975) developed a wear testing machine using the same pin and plate principle but they simulated the masticatory cycle by using a pin which moved in the vertical and the horizontal axes allowing impact and slide motion. The machine was later modified allowing the use of various antagonist materials such as steatite balls to be placed on the vertical pins which is opposed by samples placed in a custom plate with individual compartments (Mian, 2011). The wear machine was then revalidated by conducting several preliminary investigations on composite controls to calibrate and estimate the test parameters. In the study the number of cycles required to create a wear track of at least 10 µm depth were determined against steatite antagonist balls of 8 mm in diameter. During the pilot study measurements were made at 2000, 3000, 4000 and 5000 cycles. The study showed that a linear wear rate was evident following 2000 cycles (r^2=0.99), data also showed that after 5000 cycles the mean depth of the wear track was approximately 50 µm (Mian, 2011). Several different devices are also available using different principles but those with the highest citation in the literature are detailed in Table 2, (Heintze, 2006).

Table 2: Available wear testing devices used to evaluate composite resin wear.

Wear machine	Principle used
The Alabama wear simulator	Impact and sliding
The Academisch Centrum Tandheelkunde Amsterdam (ACTA) wear machine	Two metal rotating wheels
The Oregon Health sciences University Oral wear simulator (OHSU)	Vertical contact with 30º rotation
Zurich Computer-controlled masticator	Palatal cusps mounted on rubber cup impacting at 45º
Minnesota: MTS wear simulator	Impact and sliding

As all simulators and wear methods follow different approaches, the results cannot be compared. However regardless of the simulator used; the key factors are the use of the right mix of controllable variables and precise analytical techniques for a wear study to be predictive of the materials of clinical performance (DeLong, 2006, Heintze, 2006, Fleming et al., 2016). It is suggested that a device that is used to test dental materials for wear should ideally have the following features, (Ilie et al., 2017):

- Force and force impulses should be reproducible.
- A lateral stylus movement should be integrated in the system.
- Constant water exchange should be integrated between the stylus and the specimen.
- Movements should be adjustable.

1.6 Fracture toughness

Fracture toughness is described as the intrinsic property of a material to resist fracture or the amount of stress required to propagate a pre-existing flaw (Beer F, 2008). Fracture toughness has been identified as one the most important factors to determine the clinical performance of composite resin. Since all restorations are likely to contain internal flaws, fracture toughness may be the most critical factor in determining the fracture resistance *in-vivo* which could be presented as chipping or bulk fracture of the restoration (Ferracane, 2013a, Heintze et al., 2017). During mastication, the ability of a composite restoration to withstand fracture is critically dependant on the nucleation and growth of micro and macro voids, mechanisms of dislocation, propagation of micro cracks, and the geometry of the material. According to the Griffith energy-balance approach, while a crack is growing through a material, strain energy is released through the surroundings and absorbed by the growth of the crack (Beer F, 2008, Wachtman JB, 2009). Therefore a restorative material can withstand a crack stress up to a critical value. Failure of the material starts when the strain energy release rate attains a peak value at a critical crack length, beyond which the crack becomes self-propagating. Several studies were conducted to investigate impeding crack propagation by increasing the filler content in dental composites (Stgermain et al., 1985, Rodrigues Junior et al., 2008b). The presence of filler particles distributes the propagating force into many components causing the crack front to dissipate between particles and eventually it becomes energetically unfavourable for a crack to grow. Theoretically increasing the filler content and decreasing the filler particle size and inter-particle spacing would increase the fatigue limit. This is due to the increase of obstacles for crack growth and limiting of stresses at the crack tip around a plastic zone to finite values below the maximum stresses allowed. Therefore with new composite filler advancements going from a macro to a micro and to a nano- scale, restoration defects become progressively smaller and are eliminated, which leads to increased material strength (Beer F, 2008, Rodrigues Junior et al., 2008b, Wachtman JB, 2009). However studies on dental composites showed that the critical strain

energy release rate can be increased by incorporation of a specific filler volume fraction, beyond which it decreases. Thus, there may be a more favourable filler volume fraction and particle size that could produce an optimal critical stress-intensity factor (Kim et al., 2002, Masouras et al., 2008b). This was supported by Lien *et al* (2010), who reported no significant difference in the fracture toughness between moderately filled composite, nanocomposites and highly filled composite (in contrast to compomers with the lowest percentage of filler by volume fraction) (Lien and Vandewalle, 2010).

1.6.1 Fracture toughness testing

Fracture toughness of dental composite has been presented in the literature with a wide dispersion of values. This variation is attributed to the different composite formulations and testing methods employed. The single edge notched beam method following the ASTM (E399-12-e2) is the most widely used methodology in determining the fracture toughness of resin composites (Heintze et al., 2017). Fracture toughness measurements using this method are usually conducted by means of three or four point bending apparatus. The sharp crack requirement is replaced by a narrow notch which could be transformed into a very sharp notch by various methods. However the results of this test are very sensitive to the notch depth and width (Schneider, 1991). The narrow notch can be introduced by various techniques, most commonly using a razor blade built-in in a custom made mold where the notch can be introduced during composite preparation and curing (Fujishima and Ferracane, 1996, Toparli and Aksoy, 1998, Kim et al., 2002, Thomaidis et al., 2013). Other techniques include using diamond saw, diamond disc and razor blade which can be introduced into the composite sample following polymerisation (Balkenhol et al., 2009, Ilie et al., 2012). Some researchers also used knife edge spilt molds to prepare the samples for fracture testing (Lien and Vandewalle, 2010, Zakir et al., 2013). Other fracture toughness evaluation techniques include compact tension specimen where fracture resistance is evaluated by the fracture resistance crack approach (*R*-curve) (Fujishima and Ferracane, 1996, Shah et al., 2009a). The *R*-curves describe the fracture resistance of the

material toughened by extrinsic mechanisms such as crack bridging. Therefore further crack extension requires higher driving forces until a plateau is reached. A short rod fracture toughness test was also used in testing dental composites; in this test, stable crack growth occurs initially, and assessment of the crack growth is based on the load to cause crack growth instability (Pilliar et al., 1986). Other tests including the double torsion (Fujishima and Ferracane, 1996) and the Chevron notched Brazilian disk test were also used (Scherrer et al., 2000, Watanabe et al., 2008). Nevertheless fracture toughness is an intrinsic property of the material therefore different testing methods should provide the same values without significant differences. However, fracture toughness has been shown to be dependent on many variables including the sample geometry and the crack tip sharpness (Fujishima and Ferracane, 1996). Nevertheless, the single edge notched beam test remains to be the most popular method reported in the literature in determining the fracture toughness of resin composites (Soderholm, 2010, Heintze et al., 2017).

1.7 Flexural strength and Flexural modulus

Strength assessments seem to be an important property to evaluate since all composite restorations are likely to have internal flaws. Therefore, based on the main reasons of failure of dental composites, flexural strength (FS) and flexural modulus (FM) have been identified as important mechanical properties in predicting the clinical performance of dental composites (Ferracane, 2013a, Heintze et al., 2017). Flexural testing is the standard means for strength testing of dental composites as per (ISO 4049). Significant correlations were found between FS and the wear resistance of dental composites (Peutzfeldt and Asmussen, 1992, Ferracane et al., 1997a, Heintze et al., 2017). Therefore it remains one of the key mechanical parameters necessary to assess in new composite formulations. The ISO4049 classifies two types of light cured direct resin composites according to their flexural strength; Type 1: indicated for occlusal restorations (flexural strength values ≥ 80 MPa) and Type 2: classified as filling for other indications (flexural strength ≥ 50 MPa). Therefore these values could be used as a baseline when evaluating new composite

formulations. Dental composite flexural strength has been previously related to the filler volume, a general trend for enhanced mechanical properties was observed when a filler volume of 60% was reached (Ilie and Hickel, 2009a). However it was shown that increasing the filler content beyond 80% by weight results in a significantly lower tensile strength (Htang et al., 1995). Consequently increasing the filler content does not necessarily increase the flexural strength of dental composites. Kim *et al* (2002) investigated the effect of filler loading and morphology on the flexural properties of resin composites; it was concluded that round fillers enabled higher filler loading which resulted in high flexural strength, whereas irregular and per-polymerised filler allowed intermediate filler loading which reflected on the flexural properties of the materials (Kim et al., 2002). More recently, Randolph *et al* (2016) evaluated the FS of various commercial dental composites; however no general trend was found between the filler size or content and the materials' flexural strength (Randolph et al., 2016). The lack of general trend was attributed to the differences in filler content at similar size distribution, the different matrix compositions and strength measurement sensitivity in relation to sample surface preparations (Randolph et al., 2016).

1.8 Degree of conversion

The degree of polymerisation is one of the key factors that affect the mechanical and clinical performance of resin composites (Ferracane and Greener, 1986b). Conversion occurs as carbon double bonds of monomers are converted to extended networks of carbon single bonds. It has been shown that the degree of conversion (DC) directly affects the strength, modulus and the hardness (Ferracane, 1985), wear resistance (Ferracane et al., 1997c), volumetric shrinkage (Dewaele et al., 2006) and monomer elution (Ferracane, 1994, Hofmann et al., 2002). The materials' DC is dependent on several intrinsic factors such as the chemical structure of the dimethacrylate monomer and the photo-initiator and extrinsic factors such as the polymerisation conditions (Leprince et al., 2013). Many studies also evaluated the effect of filler loading, size and geometry on the DC of resin composites (Turssi et al., 2005, Baroudi et al., 2007, Amirouche-Korichi et

al., 2009). It was shown that the DC decreases by increasing the opaque filler content and by decreasing the filler particle size. The use of particle size that approaches the output wavelength of the curing unit (470 nm) results in a significant decrease in the DC; this could be explained by the scattering effect of the small fillers on the penetrating light during photoactivation. However the filler geometry was not shown to affect the DC of experimental composites. Resin matrix polymerisation results in a change in the materials optical properties and an increase in the refractive index due to the increasing viscosity and the density of the cross-linked polymer. As the refractive index of the resin approaches to that of the filler, the scattering at the interfacial/resin reduces which results in higher light transmission. Polymerisation rate increases with time, however a time delay in reaching maximum light transmission could result in lower maximum rates of polymerisation despite a possibly higher ultimate DC (Lovell et al., 1999, Shortall et al., 2008).

The most common method used to determine the degree of conversion is by spectroscopic methods which infer the quantity of remaining double bonds, the techniques used are either mid-infrared Fourier transform (FT) (Ferracane and Greener, 1984) or Raman spectroscopy (Pianelli et al., 1999). FT mid-IR is based on the reflection of the infrared radiation and has been widely used for many years to measure the DC by comparing the peak height of 1640cm^{-1} which corresponds to –CH=CH2 stretching vibration before and after polymerisation (Ferracane and Greener, 1984). Another peak corresponding to the aromatic ring at 1608cm^{-1} is used as a reference as its intensity does not change with curing. The Raman spectroscopy measurements is based on the dispersion of the light by the polymer using similar measurement peaks as mid-IR spectroscopy (Pianelli et al., 1999). FT mid-IR techniques uses microscopic attachments and Raman spectroscopy uses a focused beam to enable the measurements of the DC at specific time points by mapping the sample surface under high magnification, this is evidently useful when considering polymerisation in depth. However, the disadvantage of the mid-IR remains to be the high absorption in this wavelength range, therefore this might lead to a decrease

in the signal/noise ratio and consequently an increase the variability of the results. More recently near-infrared FT spectroscopy (FT-NIR) was introduced (Stansbury and Dickens, 2001), it is based on transmission which was shown to be more efficient and more reliable in measuring the DC in real time. Accurate measurements are based on transmission and monitoring the decrease of the vinyl peak at 6164cm^{-1}. It also allows detecting small differences in the DC and analysis of thick samples. Nevertheless it was shown that FT-NIR spectroscopy provides equivalent methacrylate conversion values to those obtained by traditional FT mid-IR techniques (Stansbury and Dickens, 2001).

The DC of Bis-GMA based resin composites has been widely evaluated using the infrared techniques, DC reported values ranges between 52-75% with most materials in the range of 55-60% (Ruyter and Svendsen, 1978, Asmussen, 1982). However the DC required for adequate clinical performance has not been established yet. Nevertheless a negative correlation has been established between the *in-vivo* abrasive wear and the DC, accordingly the DC values below 55% is not recommended for occlusal restorative materials (Ferracane et al., 1997c, Silikas et al., 2000).

The depth of cure of resin composite is also an important property especially when used as a posterior restorative in deep cavities. Insufficient curing of resin composites at depth results in reduced mechanical properties and biocompatibility. The depth of cure is usually referring to the thickness of resin composite that is “adequately” cured. It is limited by light absorption and scatter within the material, which are influenced by several factors, including the amount, size and type of fillers (Shortall et al., 2008), composite shade (Moore et al., 2008), photoiniator system used (Leprince et al., 2011), refractive index mismatch (Shortall et al., 2008) and the light curing source (Lindberg et al., 2005). The limited depth of cure of resin composites requires clinicians to place composite restorations in thin layers (~2mm) to ensure adequate curing. However, incremental techniques are associated with various disadvantages such voids incorporation composite layers, failures in bonding between layers, placement difficulty due to limited access and extended procedure time (Abbas et al., 2003).

Therefore, different approaches have been employed to increase the depth of cure of resin composites including increasing light transmission through filler particle modifications (Shortall et al., 2008) increasing light intensity (Lindberg et al., 2005). In addition to that, higher depth of cure was suggested through using alternative photoinitatior systems such as Lucirin-TPO at low concentration in conjunction with CQ which also requires higher intensity light source emitting specifically around 400 nm (Leprince et al., 2011). More recently, dental manufacturers introduced “Bulk-fill” dental composites which are claimed to enable restoration build-up in thick increments of up to 4-6 mm. The increased depth of cure of bulk-fill composites is mostly attributed to their increased translucency and reduced filler content (El-Safty et al., 2012). However these perceived improvements are not indicative of the mechanical performance of these materials. Some concerns were raised regarding the low surface hardness, flexural strength and flexural modulus properties of bulk-fill materials when compared conventional resin composites (Garoushi et al., 2013, Ilie et al., 2013a, Leprince et al., 2014).

1.9 Other Physical Properties

There are several other physical properties that could potentially influence the longevity of dental composite restorations. The most important physical property to evaluate dental composite is polymerization shrinkage, shrinkage stress and the adhesion of the restoration to the tooth surface. Shrinkage of resin composite causes internal stresses which may potentially distribute to the adhesive material. This may damage the bonded interface, the tooth or the restoration. Clinically this may manifest as tooth cusp deflection, enamel microcracks, microleakage, marginal discoloration and recurrent caries (Hilton, 2002, Alvarez-Gayosso et al., 2004, Baroudi et al., 2007). It is therefore useful to assess the internal stresses generated during curing to evaluate the material's clinical performance. Different approaches have been proposed to reduce polymerisation shrinkage and to reduce the stresses of resin based restorative materials. This included incremental placement techniques (Lutz et al., 1986), the development of soft start polymerization (Kanca and Suh, 1999), the development of alternative chemical formulations of dimethacrylate based resins (Condon and Ferracane, 2002) and more recently the introduction of the silorane based composite which showed reduced volumetric shrinkage and reduced cuspal deflection compared to conventional dimethacrylate based composites (Weinmann et al., 2005, Bouillaguet et al., 2006, Ilie et al., 2007, Gregor et al., 2013). Other properties such as the depth of cure, solubility and sorption properties are also important. Biocompatibility concerns arise over leaching of residual monomer and the long term stability of the composite due to degradation from the uptake of the solvent and the wash-out of poorly cured material. In general the solubility of the composite material is strongly influenced by the degree of conversion of the monomers (Tanoue et al., 2003, Kopperud et al., 2013). The mechanical properties of dental composite are also affected by the extent of cure. Improvement of the mechanical properties of dental composite has been correlated with the increase of the degree of conversion (Ferracane et al., 1997b, Rencz et al., 2012).

1.10 Antimicrobial properties

Resin based composites have been continuously developed and improved to enhance the longevity and increase their clinical service (Ferracane, 2011). However numerous studies indicate that secondary caries remains one of the main reasons of failure of composite restorations (Burke et al., 1999, Mjor et al., 2000, Bernardo et al., 2007, Demarco et al., 2012c, Opdam et al., 2014). Evidence suggests that composite restorations accumulate more dental biofilm when compared to enamel and other restorations on the long run (Beyth et al., 2010b). The presence of the biofilm and the lack of inhibitory effect against cariogenic bacteria lead to chemical and mechanical degradation of dental composites (Skjorland, 1973, Beyth et al., 2010b). The adhered bacteria also affect the neighbouring enamel and dentine which consequently may result in recurrent caries. Therefore several strategies have been adopted by researchers to introduce antimicrobial dental composites by modifications to the resin matrix, the filler components and the use of novel antibacterial polymers (Beyth et al., 2014). Antimicrobial components used have included fluoride (Wiegand et al., 2007, Xu et al., 2010a, Xu et al., 2010b), chlorhexidine (Leung et al., 2005), zinc oxide (Aydin Sevinc and Hanley, 2010), silver ions (Tanagawa et al., 1999, Yoshida et al., 1999) and quaternary ammonium compounds (Beyth et al., 2010a).

1.10.1 Filler particles modifications

Modifications to the filler components were made by incorporating soluble and non-soluble antimicrobial agents. Soluble agents are able to diffuse into an aqueous environment. Fluoride is a widely documented anticariogenic agent which is effective through various mechanisms such as reduction of the demineralization process, enhancement of the remineralization, interference with pellicle and biofilm formation, and the inhibition of microbial growth and metabolism (Fejerskov O, 1996, Rølla G, 1996, ten Cate JM, 1996) . Thus, it has been reported that fluoride releasing filler systems, such as strontium fluoride (SrF_2), ytterbium trifluoride (YbF_3) or leachable glass fillers have an antibacterial effect (Yap et al., 1999,

Kawashita et al., 2000, Xu and Burgess, 2003b). Fillers release fluoride by an exchange reaction due to water diffusion into the resin composite which is followed by a diffusion gradient driven movement into the environmental solution (water and saliva). However, one of the major disadvantages is the formation of voids within the resin matrix as fluoride leaches out from the material. In addition to that, most of the fluoride is released during the setting reaction followed by smaller amount in the long term. Other factors that also affect the amount of fluoride release is the fluoridated filler type and particle size, type of resin used, silane treatment and material porosity (Dijkman et al., 1993, Arends et al., 1995, Xu and Burgess, 2003a). It was also reported that the use of hydrophilic and acidic polymers increase the fluoride release from resin composites (Arends et al., 1995). Other antibacterial components added to the filler include silver and zinc oxide agents. It was reported that pure silver ions added into SiO_2 filler particles exhibit antimicrobial effect against oral streptococci (Yamamoto et al., 1996). Other studies also reported that composite resin loaded with high concentrations of silver containing fillers showed antibacterial activity due to the anti-adherence activity of the silver supported substratum (Yoshida et al., 1999). More recently bioactive glasses (BAG) have been used in experimental resin composites (Hyun et al., 2015, Alania et al., 2016). BAG has been suggested as a promising bioactive material that can interact with the surrounding environment (Hench, 2006). BAGs are represented by amorphous calcium, sodium phosphosilicate materials which are able to precipitate biologically active hydroxycarbonate layer on their surfaces when they are exposed to bodily fluids. Fluorapatite (FA) has also been suggested as a potential suitable filler for experimental bioactive dental restoratives (Chen et al., 2006b). FA is the fluorine substituted form of HA, in which the (OH^-) in HA is substituted with (F^-). Various clinical applications of apatites have been suggested; including coating of dental implants to improve the bioactivity and osteointegration (Carradò et al., 2017), direct application to exposed dentine to manage dentine hypersensitivity (EARL, 2007), dental prophylactic agents (Kensche et al., 2017) and the development of experimental bioactive dental restoratives (Arcís et al., 2002, Taheri et al., 2015). Fluorapatite is hexagonally shaped with a highly

symmetrical crystallographic structure. It is chemically stable but known to release fluoride in an acidic environment. The unique morphology of FA crystals may also aid in maintaining good mechanical properties in addition to fluoride ion release.

1.10.2 Resin matrix modifications

Released and non-released antibacterial agents have been used to incorporate antibacterial properties within the resin matrix. Non-released agents are more readily available within the resin matrix when compared to the filler modifications. Soluble fluoride has been used to obtain antibacterial properties, e.g. organic fluoride components such as acrylic-amine- HF salts, methacryloyl acid fluoride and acrylic-amine-BF_3. However lower concentrations of fluoride leached from these materials when compared to glass ionomer materials (Hicks et al., 2003). Chlorohexidine was also used which was shown to inhibit bacterial growth by 50% within 14 days (Leung et al., 2005). Quaternary ammonium compound benzalkonium chloride was also used and was shown to enhance the antimicrobial properties without significantly changing the material's physical properties (Sehgal et al., 2007). Non-released insoluble agents can inhibit bacterial growth by inactivating target microorganisms. This mechanism has the advantage of being non-volatile and chemically stable, e.g. Triclosan, which has been shown to inhibit bacterial growth by acting on the bacterial cell wall (Wicht et al., 2005).

1.10.3 Antibacterial polymers

Cationic or positively charged polymers can act as a disinfectant when in contact with the negatively charged cell wall. Cationic polymers bearing quaternary ammonium groups were found to be particularly potent. Therefore a number of polymers have been developed including soluble and insoluble pyridinium-type polymers which exhibit antibacterial properties (Tiller et al., 2002). Several reports have described incorporation of a methacryloyloxydodecyl pyridinium bromide (MDPB) monomer in composite resins that showed no release of the incorporated monomer but

still exhibited antibacterial properties (Imazato et al., 1995). Insoluble crosslinked quaternary ammonium polyethylenimine (PEI) nanoparticles were also incorporated in composite resin materials which showed strong antibacterial activity up to 1 month without leach-out of the nanoparticles and without compromising its mechanical properties (Beyth et al., 2006).

1.11 Fluoride effect

Fluoride interferes with the caries process by reducing demineralisation and enhancing remineralisation of enamel and dentin (Cury and Tenuta, 2009). As the pH falls below a critical level, the tooth tissues start to dissolve and lose calcium and phosphate ions. However, in the presence of fluoride the amount of dissolving minerals decreases and returns back to the tooth as fluorapatite. When the pH rises again, fluoride enhances the natural phenomenon of tooth remineralisation. Consequently the progression of caries lesions is slowed down (Fejerskov O et al., 2015). Fluoride is widely used in dentistry in various forms including toothpastes, vanishes and mouthwashes. Tooth brushing using a fluoridated tooth paste is by far the most effective caries prevention tool (Marinho et al., 2004). Therefore, fluoride releasing restoratives are very attractive to maintain constant fluoride in the mouth. A fluoride releasing restorative would provide fluoride at the right place (biofilm/tooth tissue), amount and time to interfere with the caries process. In addition to that, having a fluoride releasing restorative would overcome patients' compliance and interrupted uses of fluoridated dentifrices. Although fluoride is by far the most widely incorporated antimicrobial agent, the effectiveness of fluoride releasing restorative materials has been critically reviewed (Wiegand et al., 2007, Cury et al., 2016). To date, there has been no consensus on the amount of fluoride required for a restorative material to be effective against recurrent caries; however it is generally suggested that the effect of fluoride releasing restoratives is mostly attributed to the localised fluoridation adjacent to the demineralisation zones rather than elevating of fluoride levels in saliva. It has been reported that localised small amounts of fluoride are sufficient to shift the equilibrium from demineralisation to re-mineralisation (Rawls, 1995, Wiegand et al., 2007).

1.12 Fluoride releasing restorative materials

Fluoride-releasing dental materials present the necessary properties to be effective against caries progression, however their effectiveness have been critically reviewed (Wiegand et al., 2007, Cury et al., 2016). Various fluoride releasing restoratives are currently available such as glass ionomer cements (GIC), resin modified glass ionomers (RMGIC), compomers and fluoride containing composites. The amount of daily and accumulative fluoride release from these restoratives varies in the literature and is dependent on the type of storage medium (Wiegand et al., 2007). Generally, the highest amount of fluoride release is shown to be in acidic environments and lowest in artificial saliva (Karantakis et al., 2000, Imazato et al., 2001, Moszner and Salz, 2001). However, the kinetics and pattern of fluoride release is similar amongst all restoratives. Most materials initially release high amounts of fluoride (within 24-48 hours), however this initial burst rapidly diminishes with time and long term release continues at much lower rates (Karantakis et al., 2000, Yap et al., 2002a, Attar and Turgut, 2003). Composites have been shown to release the lowest amounts of fluoride in the long term when compared to GIC, RMGIC and compomers (Karantakis et al., 2000, Vermeersch et al., 2001, Wiegand et al., 2007). Studies on different composite brands reported initial fluoride release with range of 0.04-2.7 ppm into deionized water within the first 24 hours, but the amount released soon decreases to 0.02-2 ppm within 30-60 days (Attar and Onen, 2002, Attar and Turgut, 2003). Other studies reported a decrease of fluoride release from 3-4 ppm to 1-2 ppm within few weeks (Cooley et al., 1988). Cumulative fluoride release studies reported values less than 0.5 $\mu g/mm^2$ during a period of 90-120 days (Karantakis et al., 2000, Vermeersch et al., 2001). Studies show that commercial and experimental fluoride releasing dental composites continue to release fluoride for up to five years (Tantbirojn et al., 1992, Dijkman et al., 1993, Furtos et al., 2005). Experimental composites containing BAG fillers were shown to have cumulative fluoride release ranging between 1.40–1.47 ppm (22 hours) and around 3.5-4 ppm by day 18 in deionised water (Davis et al., 2014). Highly fluoridated experimental composite (Ariston pHc) was

shown to release much higher amounts of fluoride (140 µg/cm^2 cumulative release over one year) when compared to conventional fluoridated composites (Dijkman et al., 1993, Attar and Turgut, 2003). Unlike other available composites the fluoride release from this material was linear in proportion to time. The high fluoride release was due to the high fluoride content (F-Al-silicate and YbF_3) in combination of the high water solubility of the filler and the high water uptake and diffusion of the polymer matrix. However evident clinical failures were soon identified due to the latter two reasons (Braun et al., 2001). Regardless of the antibacterial agent used, it was concluded that agents have various releasing rates with mostly short term effectiveness. The release into the surrounding environment could also affect the mechanical properties of the carrier over an extended period of time. However it is suggested that polymeric antibacterial agents with low molecular weight have an improved integration within the composite resin due to their chemical stability and non-volatile nature (Beyth et al., 2006).

1.13 Fluoride release testing

The fluoride release of restorative materials has been thoroughly investigated in the literature. However, no standard protocol is currently followed for fluoride release measurement. Researchers have used different sample size and geometry under different storage media including distilled water, deionised water, lactic acid and acidic buffer solutions (Williams et al., 1999, Karantakis et al., 2000, Dhondt et al., 2001). It was found that the storage media affected the amount of fluoride release; saliva for example reduces the fluoride release in comparison to distilled water (Bell et al., 1999). This can be explained by the reduced diffusion gradient between the restorative material and ion-enriched saliva. In addition to that, saliva compounds may form a pellicle on the specimen surface which interferes with the ion release (Williams et al., 2001). Increasing amount of fluoride release was reported in acidic media which is explained by the dissolution of the material under acidic conditions (Karantakis et al., 2000, Imazato et al., 2001, Nicholson and Czarnecka, 2004). Furthermore, increasing the temperature from 4°C to 37°C was also shown to increase the amount of fluoride released (Yan et al., 2007, Madhyastha et al., 2013).

Different methods have been used to measure the amount of fluoride release by materials, including ion selective electrode (ISE) and ion chromatography (IC).The ion selective electrode method (ISE) has been widely used by researchers to measure the total fluoride ions (free and complex fluoride ions) released from dental restoratives. Following this methodology acetic buffer solution (TISAB) is usually added to release free fluoride ions from the complex fluoride species (Itota et al., 2004a, Itota et al., 2004b, Durner et al., 2012). The popularity of this method is related to its high reliability, great selectivity and specificity for fluoride ions and generally being easy to use.

1.14 Summary

The literature shows that dental composites have evolved from their beginning in the early 1950s to the present generation of nano-featured hybrid composites. Nowadays, they have acquired a prominent place amongst modern filling materials as a so-called ‘universal restorative’. The increase of popularity of composite resin among patients is most likely because it is tooth coloured with excellent aesthetic properties, also it is preferred by practitioners as a more conservative restorative option, in addition to the governmental legislation on the use of mercury. Following the recently agreed Miniamata Convention leading to a worldwide reduction and cessation in the use of mercury containing products including amalgam, this will therefore lead to a phase down in the use of dental amalgam. In this case the most suitable alternative to directly restore posterior teeth would be dental composites. This will have a great impact on dental training as well as increasing the demand for a better performance of these restorations (Lynch and Wilson, 2013a, Lynch and Wilson, 2013b). Therefore research should focus on enhancing the performance of posterior composites in clinical service. The basis of failures of the current dental composites should be used as a baseline to improve the properties of these materials for enhanced and prolonged clinical service. Recurrent caries and restoration fracture remain the primary reasons of failure of resin composites. Therefore the idea of “smart” restorative materials capable of responding to their environment by

releasing antimicrobial agents and/or having a remineralising effect remains an attractive focal point in dental materials research. In addition, research focusing on developing new filler/resin formulations to further enhance the mechanical properties for use in high load bearing areas should be encouraged.

Several studies evaluated the clinical performance of dental composites. However it is still not possible to identify the precise level of the required properties to ensure clinical success of the new formulations. Therefore it is crucial to analyse the primary reasons for clinical failure or success of dental composite followed by different testing methods to evaluate the material's performance. Based on the main reasons of clinical failure of dental composites; assessment of the strength parameters of dental composite should involve clinically relevant tests including fracture toughness, flexural strength and wear (Ferracane, 2013a, Heintze et al., 2017, Ilie et al., 2017).

Chapter 2: Aims, Objectives and program of work

2.1 Aims

1- To develop highly filled model resin composites incorporating fluorapatite (FA) as secondary filler.
2- To measure the degree of conversion of the experimental FA containing resin composites.
3- To characterise the mechanical properties including wear resistance, vickers microhardness, flexural strength, flexural modulus and fracture toughness.
4- To measure fluoride ion release under acidic (pH 4) and neutral (fresh distilled water) conditions.

2.2 Objectives

1- To prepare model resin composites suitable for FA incorporation as secondary filler.
2- To synthesise fluorapatite crystals and incorporate them as a secondary filler in resin composites.
3- To establish the effect of FA incorporation on the degree of conversion of the experimental materials.
4- To establish the effect of FA incorporation on the mechanical properties of resin composites including wear resistance, vickers microhardness, flexural strength, flexural modulus and fracture toughness.
5- To establish the relationship between the FA concentration and the amount of fluoride ion release under neutral and acidic conditions.

2.3 Program of work

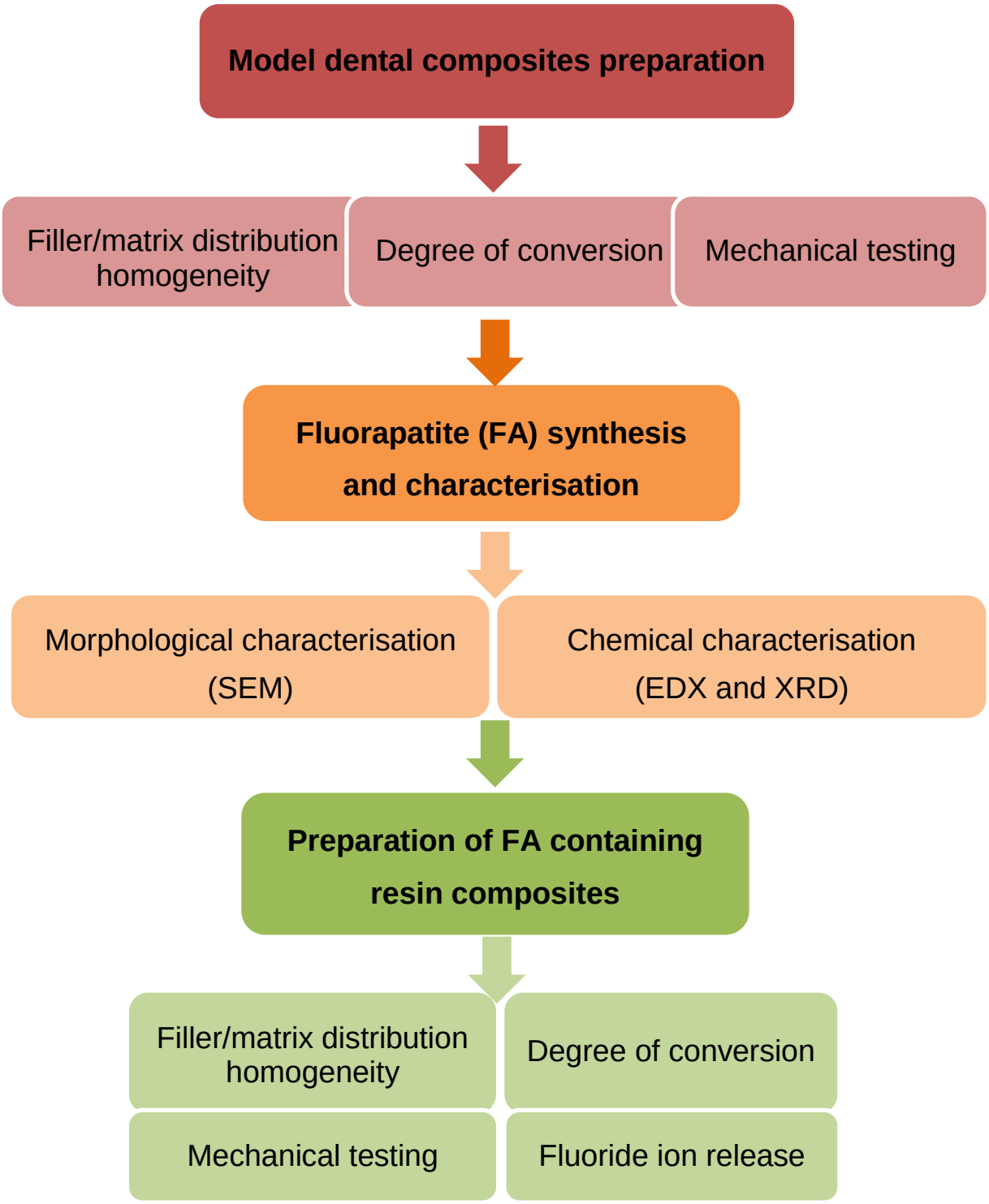

Chapter 3: Preparation and characterisation of model experimental dental composites

3.1 Introduction

The main aim of this project is to develop and characterise experimental dental composites with fluorapatite (FA) crystals incorporated as secondary filler. Selecting an appropriate model dental composite to act as a vehicle for the secondary FA filler is essential. Therefore the purpose of this part of the study was to prepare model highly filled dental composites and to characterise their physical and mechanical properties. Having an insight into the performance of different composite formulations is highly valuable to enable the selection of an appropriate model dental composite formulation suitable for the next part of this project. The selected model composite formulation would also act as a control (0FA) once FA containing composites had been prepared. Having a contemporary commercial control is also essential to evaluate the experimental materials properties in relation to the available commercial composites. Tetric Evo Ceram (TC) (Ivoclar-Vivadent, Liechtenstein) was selected as representative commercial control since it is highly filled (83%wt, 63%vol) with barium glass as a primary filler and BisGMA as a base monomer. The composition of the experimental composites was based on careful evaluation of the literature and the range of commercially available dental composites. The filler content has been widely reported to influence the mechanical and the physical properties of dental composites. Generally it was concluded that the surface hardness, modulus and wear resistance increase and the volumetric shrinkage decreases by increasing the filler content (Jun et al., 2013a, Shah and Stansbury, 2014). A threshold of 60% filler volume fraction has been identified as the necessary level required for an acceptable performance (Lohbauer et al., 2006, Randolph et al., 2016). The degree of conversion (DC) is a key factor influencing the materials mechanical, physical and optical properties in addition to their solubility (Ferracane, 1985, Ferracane and Greener, 1986a, Hofmann et al., 2002, Durner et al., 2012). Therefore

it was essential to evaluate the DC of the prepared experimental materials and compare it to the commercial control. Fourier transform infrared spectroscopy (FTIR) was used in this study which has been widely reported by several researchers measuring the DC of dental composites (Imazato et al., 2001, Ilie and Hickel, 2007, Durner et al., 2012, Walters et al., 2016). In addition to that, two-body wear and surface microhardness tests were also conducted to further evaluate the mechanical performance of the different composite formulations. This chapter will describe the preparation of the model experimental composites and the characterisation of their physical and mechanical properties.

3.2 Aims

1- To develop model experimental dental composites with different resin formulations and to characterise their mechanical and physical properties.
2- To select a suitable monomer mixture for incorporation of fluorapatite as secondary filler.

3.3 Hypotheses

The null hypotheses are below:

1- There are no significant differences in the degree of conversion, wear resistance and microhardness between the different experimental dental composite formulations and the commercial control (TC).
2- There are no significant differences in the degree of conversion, wear resistance and microhardness between the different experimental composite formulations regardless of the resin mixture used.

3.4 Materials and methods

3.4.1 Model dental composite preparation

Different composite formulations were prepared with monomer: filler ratio of 20:80% by weight (%wt). Four monomer groups were prepared by mixing different ratios of BisGMA/TEGDMA/UDMA/BisEMA (ESSTECH Inc, Essington, PA, US) and using CQ (camphorquinone, Sigma-Aldrich) as an initiator and DMAEMA (dimethylamino ethyl methacrylate, Sigma-Aldrich) as an activator. Silanised barium aluminium silicate glass with D_{50}=0.7 µm (First Scientific Dental GmbH, Elmshorn, Germany) was then added to each monomer mix to maintain a glass filler content of 80%wt. Details of the materials used and the monomer ratios are detailed in Table 3 and Table 4. The commercial control composite composition is also shown in Table 4.

Table 3: List of materials and their manufacturers used for preparations of experimental materials

Materials	Description	Manufacturer
BisGMA	Bisphenol A diglycidal ether dimethacrylate	ESSTECH inc., USA
TEGDMA	Tri ethylene glycol dimethacrylate	ESSTECH inc., USA
BisEMA	Bisphenol A polyethylene glycol diether dimethacrylate	ESSTECH inc., USA
UDMA	Urethane dimethacrylate	ESSTECH inc., USA
CQ	97% Camphorquinone	Sigma-Aldrich Company Ltd., UK
DMAEMA	98% 2- (Dimethylamino)ethyl methacrylate	Sigma-Aldrich Company Ltd., UK
Glass	6% Silanised barium aluminium silicate glass with D_{50}=0.7 µm	First Scientific Dental GmbH, Germany

Table 4: Compositions of the experimental dental composites by weight (wt%).

Group	BisGMA (%wt)	TEGDMA (%wt)	UDMA (%wt)	BisEMA (%wt)
A	70	30	-	-
B	70	20	-	10
C	70	10	-	20
D	70	-	-	30
E	70	-	30	-
F	70	20	10	-
G	70	10	10	10

Table 5: Composition of Tetric Evo Ceram composite

Tetric Evo Ceram (Ivoclar Vivadent)	
Resin matrix	Dimethacrylates (17–18%wt); (Bis-GMA) 5–10%; Urethane dimethacrylate (UDMA) 5–10%wt.
Filler content	Barium glass, ytterbium trifluoride, mixed oxide, prepolymer, 82–83%wt inorganic fillers, particle size of inorganic fillers 40–3000 nm, with mean 550 nm.

3.4.1.1 Monomer preparation

BisGMA was placed in a glass container and pre-heated to 50º C for 60 minutes to enable easier handling of the material. The different monomers were then added depending on the ratio required, see Table 4, and placed in amber glass bottles (500 ml, Sigma-Aldrich) to prevent accidental activation of the photoinitiator. 0.5%wt CQ and 0.5%wt DMAEMA were then added to the monomer mix and mixed for 60 minutes using a magnetic stirrer (VELP, Scientifica, Italy). Each prepared mixed monomer ‘master batch’ was then stored in amber bottles and wrapped in the aluminium foil

until use. All components were weighted using a digital scale (0.01 g readability) (PERCISION Advanced, OHAUS, USA).

3.4.1.2 Mixing glass filler with the monomer

Different composite formulations were prepared in batches of 20 grams for each group with a content of 80%wt filler and 20%wt monomer mix. The selected monomer mix was pre-weighed (4 grams) and placed in a plastic mixing container and added to an overall glass filler weight of 16 grams, the glass filler was divided into four equal increments (wt) which were then sequentially added to the monomer. The container was then placed in a centrifugal mixer (SpeedMixerTM DAC 150.1 FVZ, Hauschild Engineering and Co. KG, Hamm, Germany) ready for mixing. All formulations were mixed four times following a specific protocol to achieve a homogenous mix. The below protocol was followed:

1- First mix: Add the overall monomer weight + first glass increment then mix for 30000 cycles x 3 minutes.

2- Second mix: First mix+ second glass increment then mix for 30000 cycles x 3 minutes.

3- Third mix: Second mix+ third glass increment then mix for 30000 cycles x 3 minutes.

4- Fourth mix: Third mix+ fourth glass increment then mix for 15000 cycles x 3 minutes.

The above protocol was established after several attempts to prepare a homogenous mix, similar techniques were previously used by researchers to prepare experimental dental composites (Schneider et al., 2009b, Palin et al., 2014, Ismail, 2016). Once mixing was complete, the containers were sealed with Parafilm (Parafilm®M, Bemis company, Inc., UK) and wrapped in aluminium foil to prevent accidental light exposure and then stored at 4°C until use.

3.4.2 Model experimental materials characterisation

3.4.2.1 Scanning Electron Microscope (SEM)

To evaluate the homogeneity of the mixed composite formulations qualitative analysis was conducted using the SEM (Hitachi-S-3400N, variable pressure SEM, Japan). Experimental composite specimens were compared to a contemporary commercial dental composite, Tetric Evo Ceram (TC) (Ivoclar Vivadent, Schaan, Liechtenstein) (for composition see box overleaf) which was used as a control. Disc shaped composite specimens were prepared for each group with dimensions of 6 × 2 mm using a custom made steel mould (n=3). Specimens were prepared following the ISO 4049 standard. Composite was packed incrementally and covered by a cellulose acetate separating strip and a glass microscope slide onto which was placed a 1 kg mass for 20 s in order to compress and level the material. The microscope slide was then removed and each specimen was photo-polymerised for 40 s using a light emitting diode (LED) light curing unit with 8 mm diameter tip (Demi Plus, Kerr, Orange Co., CA, USA), irradiance of 1200mW/cm^2, at 23 ± 1ºC. The irradiance was checked prior to use by employing a checkMARK (Bluelight Analytics Inc., Halifax, Canada). Composites were polished using 400 grit silicon carbide (SiC) abrasive papers (Struers, Copenhagen, Denmark). Prepared specimens were then mounted on aluminium stubs and sputter coated with approximately 5 nm of gold using an argon sputter coating unit (Agar Scientific, Stanstead, UK) for SEM imaging. Samples were mounted at a 5 mm distance and scanned under low vacuum with an accelerating voltage of 20Kv.

3.4.2.2 Degree of Conversion

The degree of conversion (DC) of experimental and commercial composites was measured using FTIR-ATR (Spectrum 100, PerkinElmer, Bucks, UK). Five specimens were prepared for each group by placing the material into stainless steel washers (4 mm internal diameter and 0.8 mm thick), (A2 stainless steel plain washer metric BS4320). Materials were light cured using a light emitting diode (LED) light curing unit (LCU) (Demi Plus, Kerr, Orange Co., CA, USA) at ambient room temperature (23 ± 1ºC) with a spectral range of 450 - 470 nm and an irradiance of 1200 mW/cm^2. The irradiance was checked prior to use by employing a checkMARK (Bluelight Analytics Inc., Halifax, Canada). The FTIR spectra were recorded for samples irradiated for 5, 10, 20, 30, 40 and 60s. For each material five spectra were measured in the unpolymerised state, materials were placed in the washers directly on the ATR sensor. The upper surface of the specimen was covered with a Mylar strip and a glass slide of 1 mm thickness and slightly pressed against the ATR to ensure good contact of the specimen and to prevent formation of the oxygen inhibited layer. The diameter of the measured surface of each specimen was 800µm, the wave number range of the spectrum was 4000–650 cm $^{-1}$ and the FTIR spectra were recorded with 32 co-additions at a resolution of 4 cm $^{-1}$ using dedicated software (Spectrum, PerkinElmer). To calculate the DC the standard baseline method to assess the peak heights were followed (Rueggeberg et al., 1990a). The percentage of uncured double carbon bond (C=C) at any time was determined from the ratio of absorbance intensities of the aliphatic peak at 1640cm^{-1} and the aromatic peak at 1607cm^{-1} (as the internal standard) (Atai and Watts, 2006, Rodrigues Junior et al., 2008a, Amirouche-Korichi et al., 2009, Kopperud et al., 2013). The following equations were used:

Equation 1

$$(\%C = C) = \frac{[Abs\,(1640\ cm^{-1})/(Abs(1607\ cm^{-1})]polymer}{[Abs\,(1640\ cm^{-1})/(Abs(1607\ cm^{-1})]monomer} \times 1$$

Equation 2

$$DC\% = 100 - \%C = C$$

3.4.3 *In-vitro* wear testing

3.4.3.1 Two-body wear simulator

Wear testing was conducted using a newly modified pin-on-plate wear testing apparatus originally developed by Harrison and colleagues (Harrison and Lewis, 1975, Harrison and Draughn, 1976). The original device allowed five pairs of pin and plate to be tested simultaneously against each other; the sample material was placed on the end of the pin and in contact with the antagonist which was attached to the plate. Weights were used to maintain an independent contact force between each pair of pin and plate and the contact time could also be regulated independently for each pair. Modifications were made by introducing custom made antagonist holders which could be attached to the vertical rods holding the abrader using a locking screw. This modification allowed the choice of variable antagonists to be selected. Figure 8 shows a schematic diagram illustrating a cross section cut through one of the ten stations, the antagonists were fixed in a holder in the lower end of the vertical pins and the specimens where imbedded in the previously described custom made tray in line with the antagonists. Differences between the original and the modified pin-on-plate wear testing apparatus are detailed in Table 6.

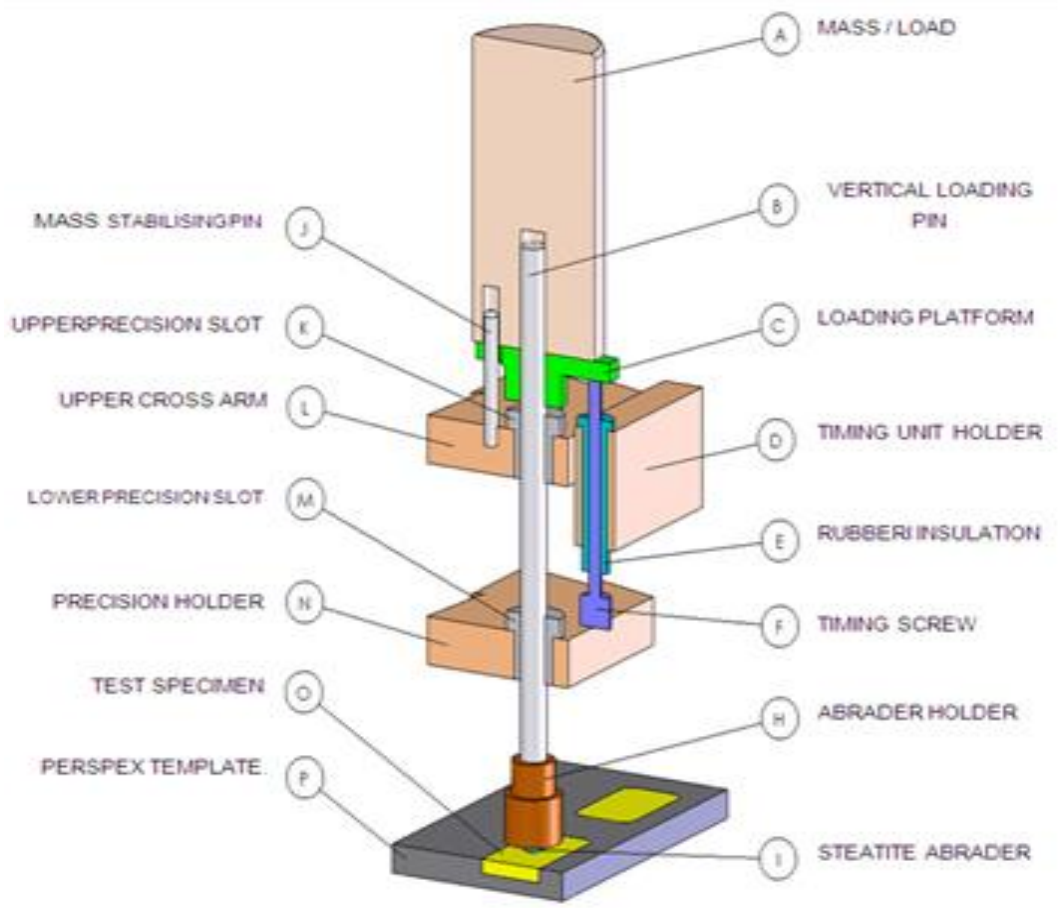

Figure 8: Schematic diagram showing the wear machine components, (*Altaie et al, 2017*)

Table 6: Comparisons between the old and the new versions of the wear testing apparatus

Variable	Old version	New version
Abrader	Individual silicon carbide paper held on the table	Steatite balls 8 mm in diameter, can be modified to fit any diameter
Sample	4.5 mm diameter cylinders cemented into the pin ends	20×10×3 mm rectangular slabs placed in Perspex templates, held in the table using locking screws
Number of test samples	10	10
Pin/Plate contact frequency	70 per minutes	100 per minutes
Pin/Plate contact time	0.2 seconds, can be adjusted for each sample	0.2 seconds, can be adjusted for each sample
Pin/Plate vertical lift	4 mm	4 mm
Pin/Plate contact distance	1 mm	1 mm
Stroke frequency	2.10Hz	2.14 Hz
Environment	Liquid or slurry solution	Liquid or slurry
Measurement of wear	Vertical height loss of specimen using a specially designed bench micrometer	Maximum depth in µm and volume loss in mm^3 , using noncontact profilometer
Load used	50-1000 grams	50-1000 grams

The “wear cycle” is defined as the *“synchronised horizontal and vertical movement of the lower and upper cross arms respectively maintaining conformal contact between the abrader and specimen, during which the lower cross arm travels 32 mm to and from the start position and the abrader strikes 100 contacts along this course at frequency of 2.1 Hz to create a wear track of 16 mm length”* (Altaie, 2012), Figure 9.

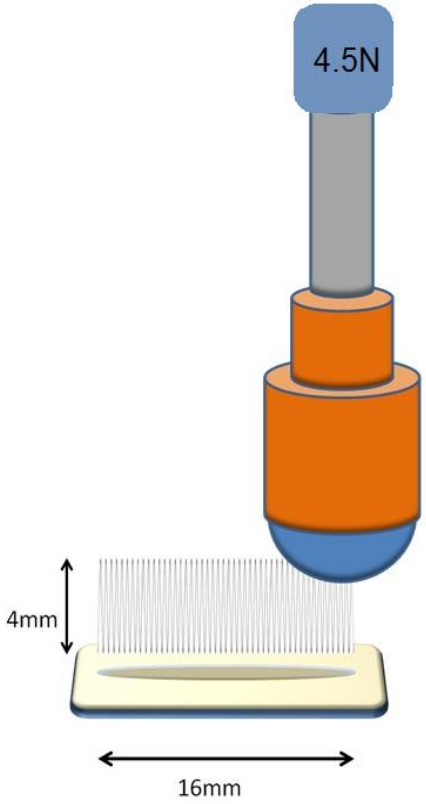

Figure 9: Schematic diagram showing a 16 mm wear track created during the testing cycle.

The wear machine used in this study was previously re-validated following the modifications conducted by Mian 2011. Based on the findings of the study, a linear wear rate was evident following 2000 cycles (r^2=0.99), data also showed that after 5000 cycles the mean depth of the wear track was approximately 50 µm. The initial run of 2000 cycles was not taken into consideration to allow the wear process to stabilise and attain an equilibrium state. This was also observed as high wear rates were reported in the initial phase below 2000 cycles and it was considered as a ‘running-in phase’ of the specimen and the abrader. Therefore for this study, it was

decided that all composite samples should be abraded for 4000 cycles before measurements, this is equivalent to three months simulation wear in the oral cavity (Altaie et al., 2017).

3.4.3.2 Specimen preparation

Rectangular bar-shaped composite specimens (20 x 10 x 3 mm) were prepared using a custom made Perspex template (n=10), Figure 10. Composite was incrementally placed into the mould and covered with a cellulose acetate strip and a glass microscope slide and a weight of 1 kg was applied for 20 s to ensure consistent and reproducible packing of the specimens. The weight and microscope slide were removed and the specimen was light irradiated using a light emitting diode (LED) light curing unit (LCU) (Demi Plus, Kerr, Orange Co., CA, USA) at ambient room temperature (23 ± 1ºC) with a spectral range of 450 - 470 nm and an irradiance of 1200 mW/cm^2. The irradiance was checked prior to use by employing a checkMARK (Bluelight Analytics Inc., Halifax, Canada). The entire length of each specimen was light irradiated using the ISO 4049 specimen manufacture protocol by placing the tip of the light guide in direct contact with the cellulose acetate strip in the centre of the specimen (ISO4049, 2009). Both the top and the lower surface of the specimens were light irradiated by moving the tip of the light guide to the section next to the centre, overlapping the previous section by half the diameter of the tip (4 mm), and irradiating for the appropriate time; the section on the other side of the centre was then irradiated in the same way, Figure 11. This process continued until the entire length of the specimen had been irradiated. Following light irradiation, the cellulose acetate strip was discarded and specimen checked for surface imperfections. The specimens were wet ground by hand lapping using P400, P600, P800, P1000 and P1200 grit silicon carbide (SiC) abrasive papers (Struers, Copenhagen, Denmark) under copious water irrigation to remove the oxygen inhibited, resin rich layer and produce a planar surface with a consistent surface topography. The specimens were stored in a light-proof container and placed in distilled water-bath maintained at 37 ± 1ºC for seven days prior to

testing and analysis. Most studies evaluating the mechanical properties of resin composite use a certain storage time for the specimens before testing.

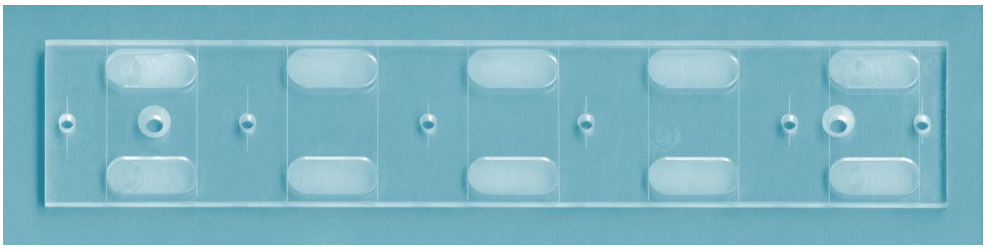

Figure 10: Custom made Perspex template

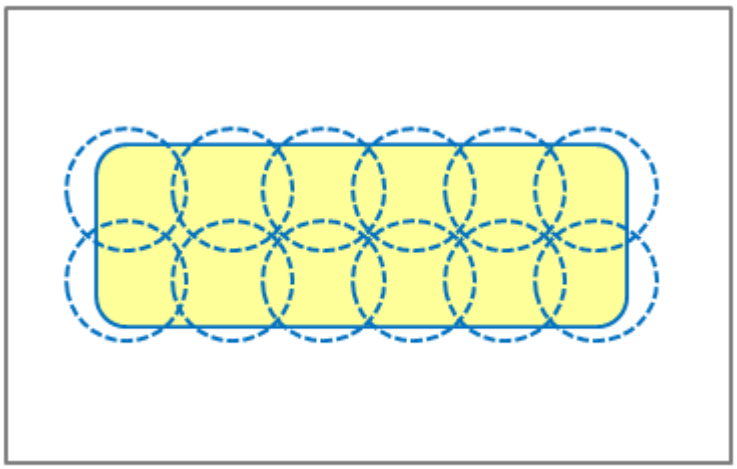

Figure 11: Specimen light curing process using overlaying curing cycles

Composite specimens were confined within their Perspex template and attached to a horizontal plate moving at a frequency of 2.14 Hz. Steatite antagonist spheres (8 mm diameter) were fixed to the vertically moving pins at a loading force of 4.5 N. The choice of steatite was based on the numerous studies which confirmed the suitability of steatite as an antagonist material for *in-vitro* wear testing (Wassell et al., 1994b, Wassell et al., 1994a, Shortall et al., 2002, Ghazal et al., 2008). A spherically shaped antagonist was selected to simulate a human molar cusp which has a greater contact area with the material than a sharp pointed antagonist thus producing less fatigue stress on the material (Lutz et al., 1992). The loading force used was also based on previous studies which reported that the human masticatory force in tooth to tooth contact ranges from 3 – 36 N

(Harrison and Lewis, 1975). During the test, specimens were maintained in a neutral buffer solution (pH 7) to simulate the *in-vivo* oral environment (human saliva pH~6.7) (Yap et al., 2002b, Correr et al., 2006, Antunes and Ramalho, 2009).

Fresh buffer solution was made for each test run. Solutions were made using pH 7 buffer tablets (VDR, Belgium) which were dissolved in distilled water following manufacturer's instructions. The pH values were confirmed using a pH meter (ORION-920A model Orion Research, Sussex, UK) which was calibrated before each test.

3.4.3.3 Profilometry

Wear tracks were scanned using a non-contacting laser profilometer (Proscan 2000, Scantron, Taunton, Somerset, UK) with a scan speed of 2 mm/s. Longitudinal traces were taken at 40 µm intervals with step size of 0.01 µm (x-direction) across the wear facet with a measurement recorded at every 60 µm interval with 0.02 µm step size (y-direction). S5/03 sensor was used to scan all the samples with resolution of 0.01 µm and a spot size of 4 µm. The stylus probe used was sensitive to record a minimum of 0.01 µm and a maximum of 150 µm. Three-dimensional profiles (3D) were then generated using Proscan analysis software (Proform 2000 by Scantron version, 2011), Figure 12 . The unworn areas around the wear track were used as the baseline from which it was possible to calculate both the mean maximum wear depth (µm) and the mean volume loss (mm^3) for each material tested (Finlay et al., Benetti et al., 2016, Fleming et al., 2016).

The volume loss (mm^3) was calculated across three selected areas in the scanned wear track using the Proscan software. The mean of the three readings was then recorded for each sample, Figure 13.

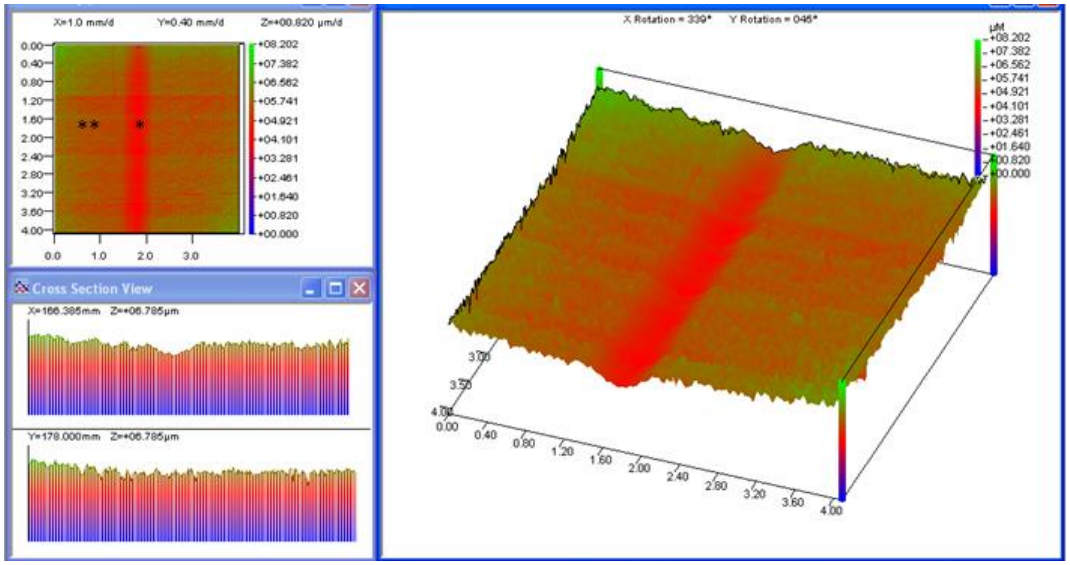

Figure 12: Profilometric scan of Tetric Evo Ceram composite sample showing cross-sectional and 3D views of the land area (**) and the wear track (*).

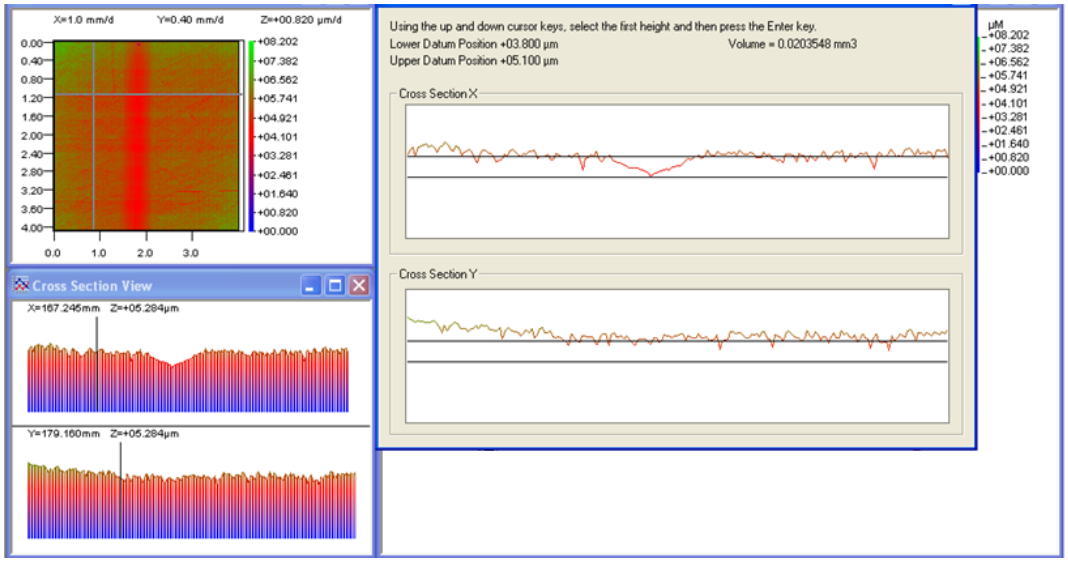

Figure 13: An example of mean volume loss estimation at a selected point of Tetric Evo Ceram composite sample.

3.4.3.4 Scanning Electron Microscopy (SEM)

Qualitative analysis of the wear tracks was conducted using SEM (Hitachi-S-3400N, variable pressure SEM, Japan) to determine the different wear mechanisms and the wear patterns involved. The wear-tested composite specimens and their corresponding steatite antagonists were mounted on aluminium stubs and sputter coated with approximately 5 nm of gold using an argon sputter coating unit (Agar Scientific, Stanstead, UK). Samples were mounted at a 5 mm distance and scanned under low vacuum.

3.4.3.5 Energy dispersive X-ray spectroscopy (EDX)

EDX was additionally used to analyse the wear facets on the steatite antagonist by generating elemental spectral maps for each specimen using a BRUKER–X-Flash detector-5010-129 (Bruker, Inc, Berlin, Germany) attached to the SEM.

3.4.4 Vickers Microhandess (HV)

3.4.4.1 Specimen preparation

Disc shaped composite specimens were prepared for each group with dimensions of 6 × 2 mm using a custom made steel mould (n=5). Specimens were prepared following the ISO 4049 standard using the same technique reported in section (3.4.3.2). Composites were then photo-polymerised in one cycle for 40 s. Composites were polished using 400 grit silicon carbide (SiC) abrasive papers (Struers, Copenhagen, Denmark). The specimens were then stored in distilled water in an incubator maintained at 37 ± 1ºC for seven days before testing.

3.4.4.2 Vickers microhardness (HV) testing

HV measurements were carried out using a Duramin 5 microhardness tester (Struers, Copenhagen, Denmark) equipped with a diamond pyramidal micro-indentor to apply a load of 100 g for 15 s. A series of five measurements were recorded for each specimen and mean value was then recorded.

3.5 Results

Composite mixtures containing UDMA monomer (Group E-G) showed visible air blows within the mix regardless of the mixing protocol used. Therefore, it was decided to exclude the monomer mixtures containing UDMA to avoid preparation of composite samples with voids inclusion.

3.5.1 Scanning Electron Microscope (SEM)

Analysed SEM images showed even distribution of the glass filler within the resin matrix of experimental dental composites. This was comparable to the glass distribution within the commercial control (TC). Therefore the homogeneity of the mixed composites was confirmed. Figure 14 shows representative examples of the experimental and commercial composites.

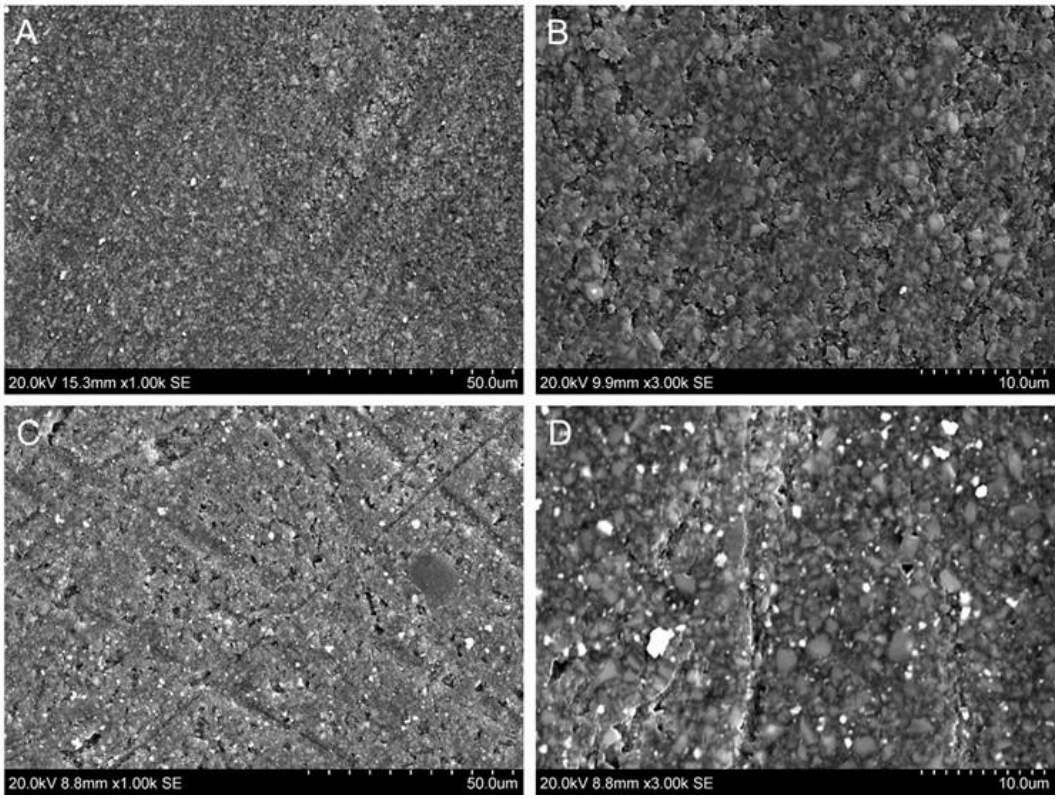

Figure 14: SEM images showing the glass filler distribution within the matrix in experimental composites; [70 BisGMA: 30 TEGDMA] with 80%wt filler (A,B) and Tetric Evo Ceram samples (C,D).

3.5.2 *In-vitro* wear resistance

3.5.2.1 Data distribution

Statistical analysis was conducted using SPSS version 21. The Shapiro-Wilk test was conducted to evaluate the data distribution. Data is considered to follow a normal distribution when $p \geq 0.05$. The results showed that all groups were normally distributed in (Table 7), therefore parametric multi comparison tests One-way ANOVA and the Post Hoc Tukey were carried out.

Table 7: Normality test for experimental and commercial dental composites wear data.

Tests of Normality		
Group	**Shapiro-Wilk**	
	Statistic	Sig.
TC	0.903	0.429
A (30%TEG)	0.883	0.325
B (20%TEG)	0.786	0.062
C (10%TEG)	0.891	0.363
D (0%TEG)	0.881	0.314

3.5.2.2 Descriptive and statistical analysis

The mean volume loss was variable between the groups as shown in Table 7 and Figure 15. The One-way ANOVA test showed that the differences were statistically significant with $p < 0.05$, Appendix A. The Post Hoc Tukey test showed that Group A had a significantly higher wear loss compared to all the tested groups ($p < 0.05$). Group D also showed significantly higher wear loss when compared to group C and B ($p < 0.05$), while group B,C and D showed no statistically significant difference to TC ($p > 0.05$), Appendix B.

Table 8: Group comparisons of the measured volume wear loss (mm^3), groups presented according to the content of TEGDMA (%TEG).

Group	Mean	Median	Std. Deviation
TC	0.023	0.021	0.004
A (30%TEG)	0.060	0.060	0.007
B (20%TEG)	0.019	0.020	0.004
C (10%TEG)	0.021	0.020	0.004
D (0%TEG)	0.031	0.030	0.003

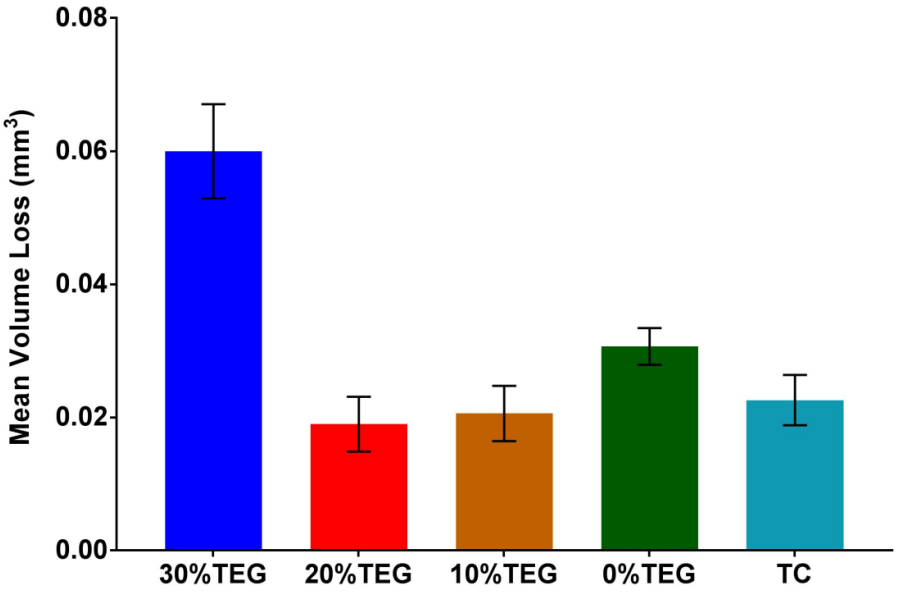

Figure 15: Composite groups mean volume loss (mm^3) with their standard deviation, groups presented according to the content of TEGDMA (%TEG).

3.5.2.3 Profilometric analysis

Figure 16 shows the generated 3D profiles for all tested groups, tested specimens showed characteristic shallow wear tracks with exception of Group A which showed a deeper track in comparison to the other groups. The unworn areas around the wear track were used as a datum to calculate the mean volume loss (mm^3).

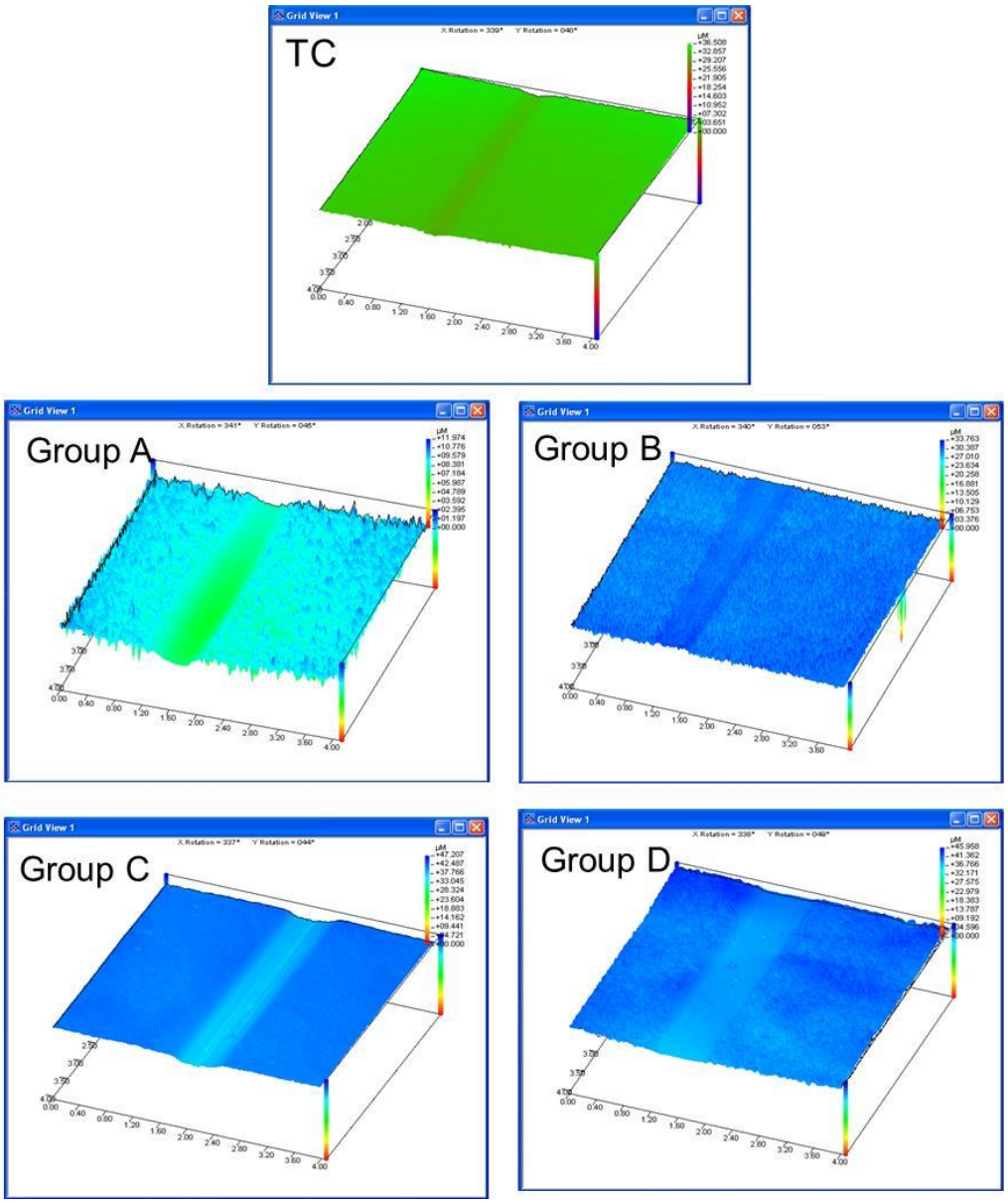

Figure 16: Profilometric scans showing representative wear tracks from the tested composite groups.

3.5.2.4 SEM analysis

Analysis of the wear tracks showed shallow wear tracks with predominant micro grooves running in the direction of the wear, and occasionally pull out of the large filler particles. Figure 17 shows the wear track (TC) and the wear facet in the abrading antagonist and Figure 18 show representative examples of the wear tracks of the experimental composite groups. The abrading steatite antagonist surfaces showed distinct wear facets corresponding to the opposing wear tracks (Figure 19).

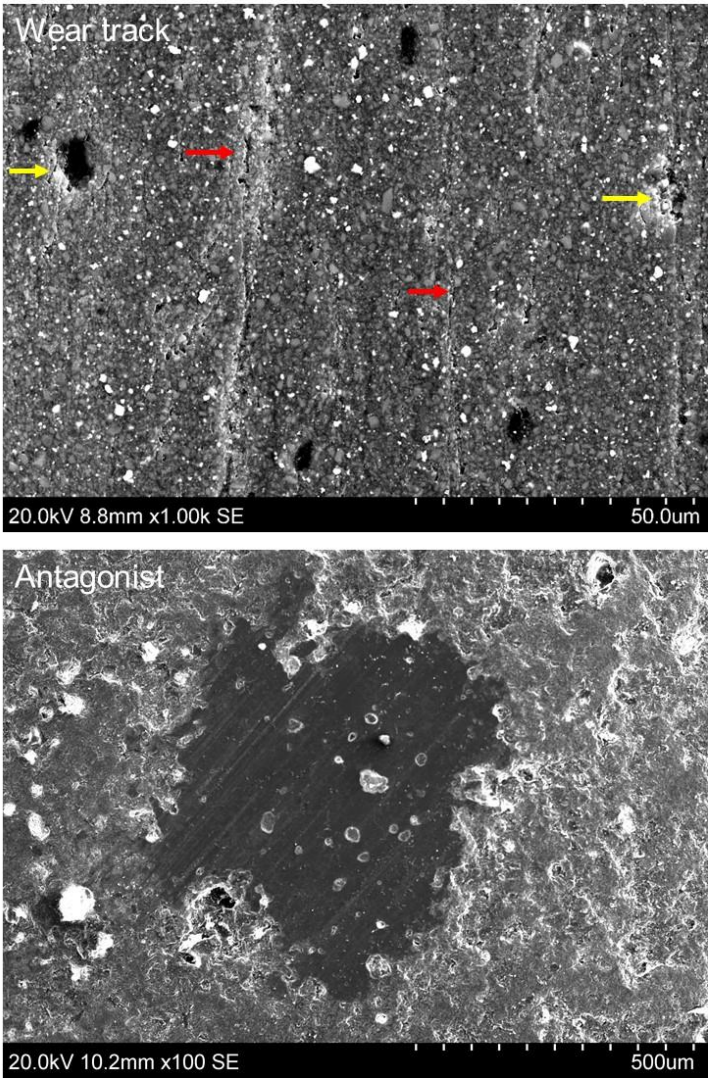

Figure 17: SEM images showing the wear track and the corresponding steatite antagonist of a TC sample. Evident micro-grooves running in the direction of the wear track (red arrows) and voids corresponding to pulled-out filler particles (yellow arrow). Distinctive round wear facet is shown on the abrading antagonist.

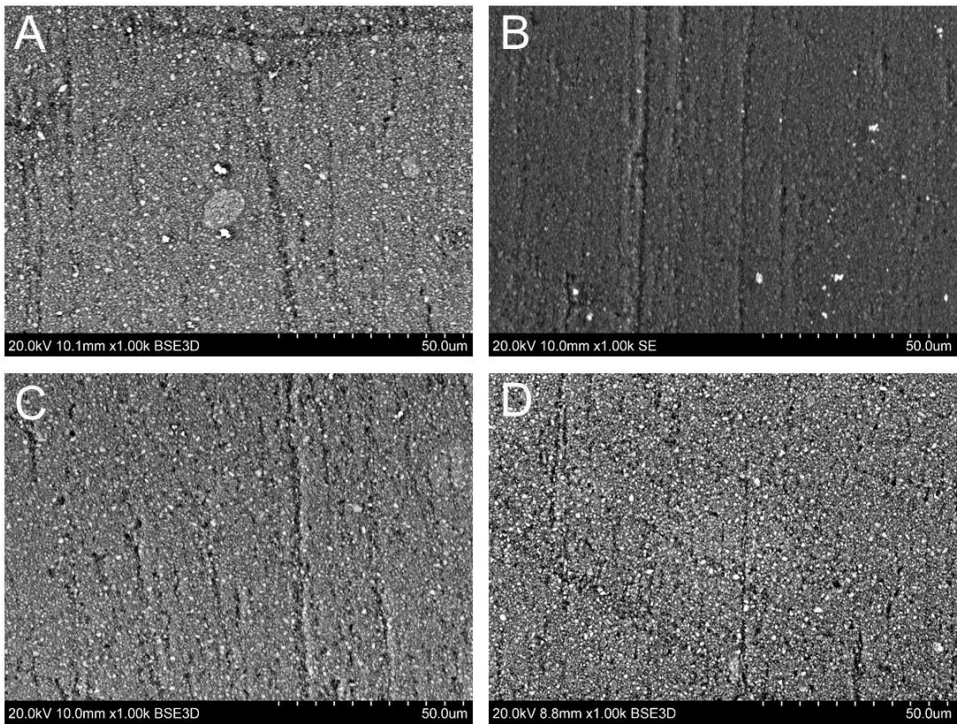

Figure 18: SEM images of experimental dental composites (A-D) showing micro grooves within the wear tracks.

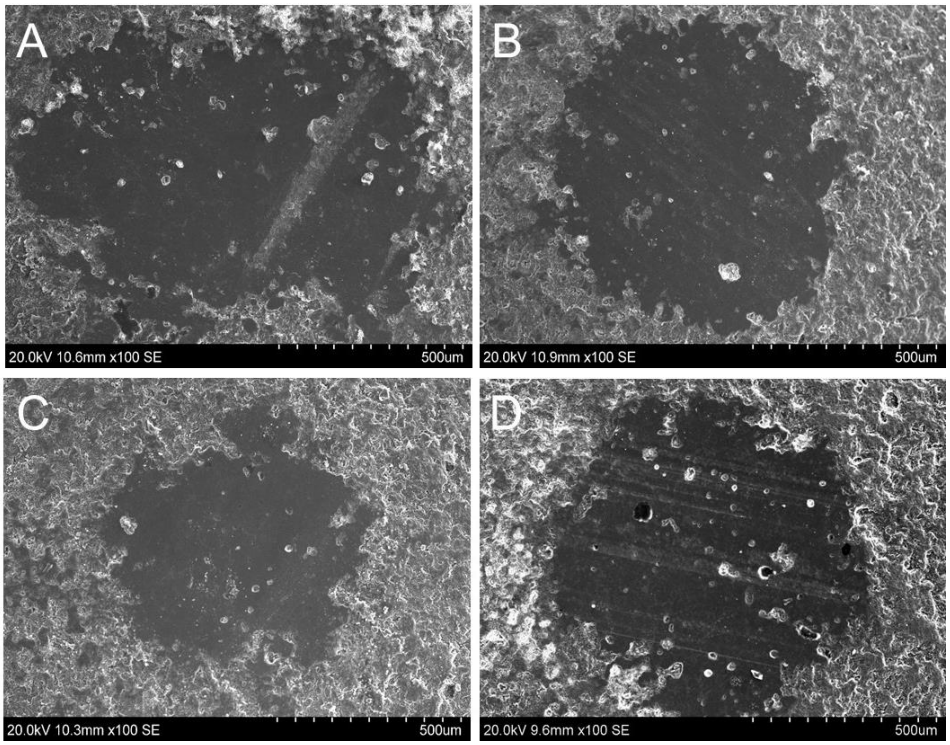

Figure 19: SEM images of the steatite antagonists showing the wear facets which correspond to the wear tracks of (A-D) composites.

3.5.3 Vickers Microhardness

3.5.3.1 Data distribution

The Shapiro-Wilk test was conducted to evaluate the data distribution. The results showed that all groups were normally distributed, Table 9. Therefore parametric multi comparison tests One-way ANOVA and the Post Hoc Tukey were carried out.

Table 9: Normality test for experimental and commercial dental composites microhardness values.

Tests of Normality		
Group	**Shapiro-Wilk**	
	Statistic	**Sig.**
TC	0.904	0.430
A (30%TEG)	0.962	0.819
B (20%TEG)	0.867	0.254
C (10%TEG)	0.867	0.254
D (0%TEG)	0.908	0.457

3.5.3.2 Descriptive and statistical analysis

The mean microhardness values were variable between the groups as shown in Table 9 and Figure 20. The One-way ANOVA test showed that the differences were statistically significant with $p < 0.05$, Appendix C. The Post Hoc Tukey test showed that TC has a significantly lower HV compared to all the experimental composite groups ($p < 0.05$). Group D also showed a significantly lower HV value when compared to group B and C ($p < 0.05$), Appendix D.

Table 10: Group comparison of HV values between experimental composites and TC.

Group	Mean	Median	Std. Deviation
TC	53.4	54.3	3.5
30%TEG	89.7	88.6	4.0
20%TEG	93.2	91.9	2.8
10%TEG	94.8	95.0	2.0
0%TEG	89.0	89.4	3.3

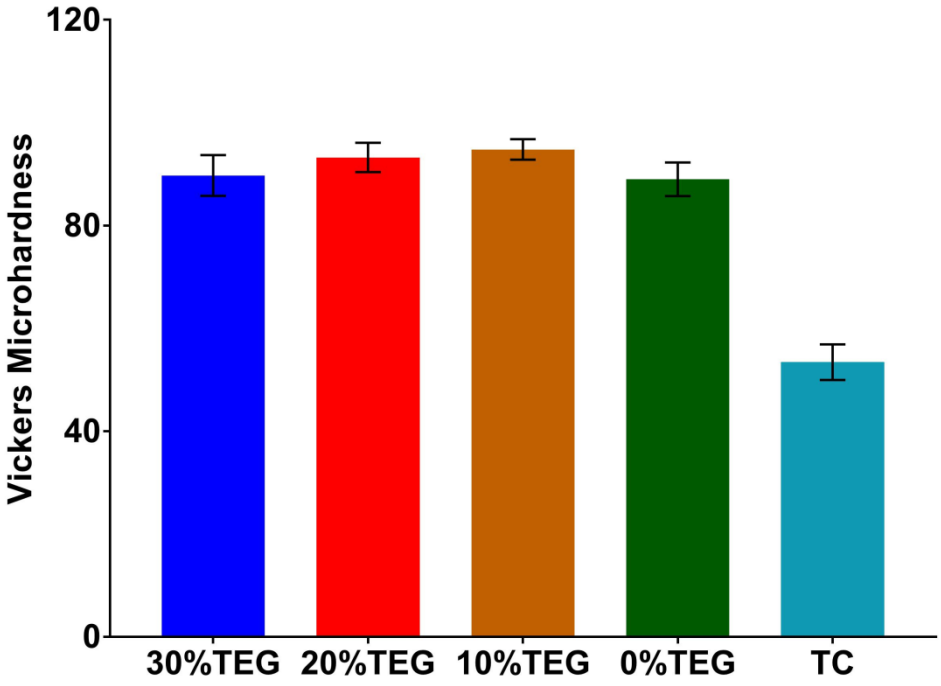

Figure 20: Group comparisons of HV values with their standard deviation (error bars) between experimental composites and TC. Experimental groups presented according to the content of TEGDMA (%TEG).

3.5.4 Degree of Conversion

Figure 21 and Figure 22 show representative FTIR spectra of experimental and commercial composite groups focusing on two key peaks at each time point. The absorption aliphatic (C=C) peak at 1640 cm $^{-1}$ changes with polymerisation, while the absorption aromatic peak (C=C) at 1604 cm $^{-1}$ does not change at polymerisation and therefore was chosen as the internal standard. The graph shows that the aliphatic (C=C) peak decreased with the light exposure whereas the aromatic (C=C) peak remains relatively stable during polymerisation.

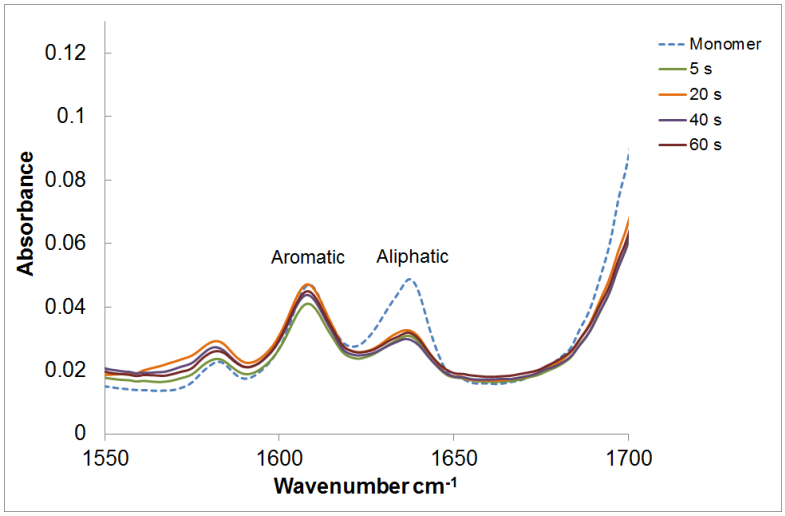

Figure 21: A representative FTIR spectra in region of 1550-1700 cm $^{-1}$ from experimental composite specimen group B (20%TEG).

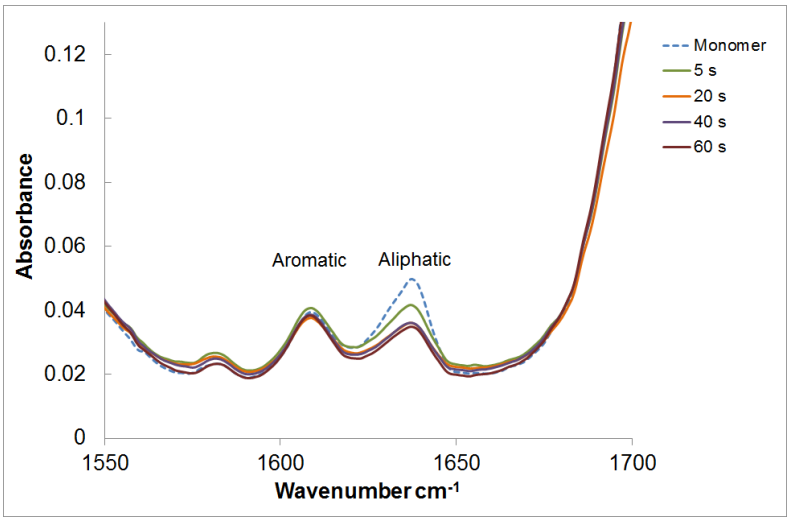

Figure 22: A representative FTIR spectra in region of 1550-1700 cm $^{-1}$ from commercial composite specimen (TC).

3.5.4.1 Data distribution

The Shapiro-Wilk test was conducted to evaluate the data distribution. The results showed that all groups were normally distributed as shown in Appendix E, therefore a parametric multi comparison tests One-way ANOVA and the Post Hoc Tukey were carried out.

3.5.4.2 Descriptive and statistical analysis

The mean percentages of the degree of conversion (DC) are shown in Table 10 and Figure 23. Experimental dental composites showed mean DC of 52-62%. Statistical analysis carried out using the one-way ANOVA and the post hoc Tukey tests (Appendix F and Appendix G) showed that all experimental composite groups had significantly higher DC compared to TC at all curing times ($p < 0.05$). However there were no significant differences between the different experimental composite groups at all curing times ($p > 0.05$). The results showed that the DC for all composite groups started to plateau at 20 s and with no significant increase in relation to extending the curing times up to 60 s ($p > 0.05$), Figure 24.

Table 11: Group comparisons showing the mean Degree of Conversion with their standard deviation (SD) for experimental and commercial composites

Time	TC		30%TEG		20%TEG		10%TEG		0%TEG	
	Mean	SD	Mean	SD	Mean	SD	Mean	SD	Mean	SD
5 s	41.3	7.5	52.2	1.1	57.7	1.2	53.9	1.8	53.0	3.3
10 s	41.4	1.3	54.0	1.4	58.4	2.6	58.0	4.2	54.4	2.9
20 s	47.3	0.8	55.5	2.4	59.0	2.9	56.5	4.1	58.0	1.3
30 s	49.2	1.1	60.5	0.6	60.9	4.7	58.1	3.9	60.1	2.3
40 s	51.8	0.5	59.9	2.4	59.8	3.5	61.0	4.6	61.9	1.9
50 s	53.0	4.1	60.4	2.6	58.6	3.3	62.1	5.1	61.7	1.9
60 s	55.0	3.9	62.7	1.5	62.0	0.9	62.9	3.6	61.8	2.0

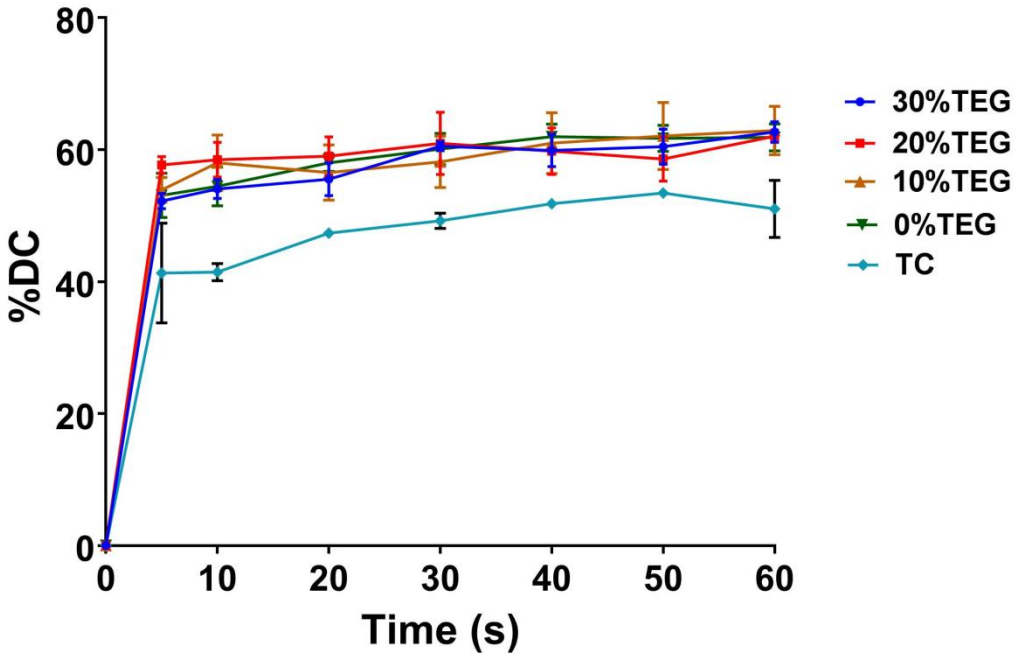

Figure 23: The mean DC with the standard deviation (error bars) for the experimental and the commercial composite groups at different curing times (5-60 s).

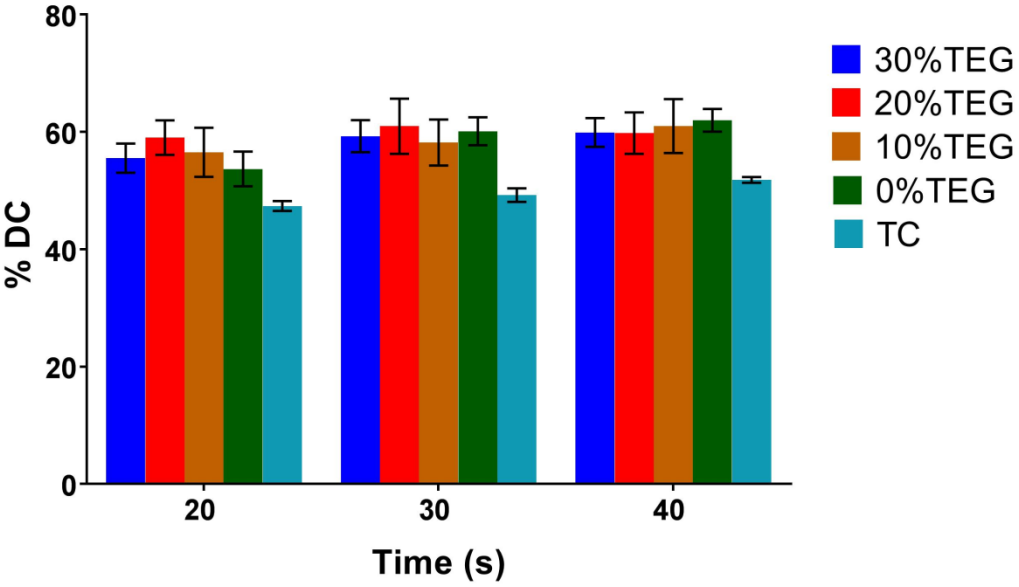

Figure 24: The mean DC with the standard deviation (error bars) for the experimental and the commercial composite groups between 20-40 s curing times.

3.6 Discussion

3.6.1 Selection and preparation of the materials

Conventional monomer systems were selected in this study to prepare model dental composites and to select a suitable monomer mixture for FA incorporation. BisGMA was selected as the main base monomer which was diluted with co-monomers at various ratios. BisGMA is the most commonly used base monomer in experimental and commercial dental composite. It has a large molecule with two aromatic rings and hydroxyl ring which increase its molecular weight (512.5 g/mol) and stiffness. This allows good handling properties and lower shrinkage due to its high viscosity. Adversely the reactivity and the degree of conversion remain low for this material (Pfeifer et al., 2009b). Furthermore, the high viscosity of the material limits the amount of reinforcing filler that can be incorporated to achieve sufficient mechanical and physical properties. Therefore, TEGDMA and BisEMA were selected as the co-monomers to dilute the main BisGMA monomer. UDMA was also initially included as a diluting monomer, however it was found that composite mixtures containing UDMA monomer showed visible air blows within the mix regardless of the mixing protocol used. Therefore it was decided to exclude the monomer mixtures containing UDMA to avoid preparation of composite samples with voids inclusion. TEGDMA is a low molecular weight monomer (286.2 g/mol) with low viscosity; it allows easier handling and incorporation of a larger amount of inorganic fillers to enhance the material's mechanical properties. It also contains reactive double carbon double bonds at each end which allows additional polymerisation and therefore increased reactivity and degree of conversion. However due to the presence of the ether groups (C-O-C) and the lack of aromatic rings in its structure, its mechanical properties are inferior to BisGMA. Furthermore, the lower molecular weight and the high concentration of C=C bonds results in higher conversion rates and polymerisation shrinkage (Asmussen, 1984, Braga et al., 2005). BisEMA structure is similar to BisGMA which has a stiff central phenyl ring core with the absence of the pendant hydroxyl groups which are mainly responsible of the high viscosity

of BisGMA. Therefore, BisEMA maintains a high molecular weight (496 g/mol) comparable to BisGMA but it has a significantly lower viscosity (Cook, 1992, Sankarapandian et al., 1997). In this study monomer mixtures were prepared with 70/30 molar ratio (base monomer/co-monomers), mimicking most of the conventional commercial and experimental composites resin mixtures (Manojlovic et al., 2016, Fonseca et al., 2017, Manojlovic et al., 2017). Camphorquinone (CQ) photoinitiator mixed DMAEMA co-initiator was used which is considered the mostly widely used photoinitiator system in commercial dental composites. Silanated barium aluminium silicate glass filler (D_{50} 0.7 µm) was used as the primary filler in this study and it was incorporated at 80 wt% (67 vol%). It has been widely reported that the mechanical and the physical properties of dental composites are directly dependant on the filler content and its various characteristics (geometry, composition, surface, size distribution). Generally it was concluded that the surface hardness, modulus and wear resistance increase and the volumetric shrinkage decreases by increasing the filler content (Jun et al., 2013a, Shah and Stansbury, 2014). A filler content of 60 vol% is necessary to achieve the aforementioned properties (Lohbauer et al., 2006, Randolph et al., 2016). To produce a homogenous composite mix, experimental materials were prepared using a centrifuge mixture (Speedmixer, DAC 150, Hauschild and Co. KG,Hamm, Germany). This technique has been widely used by many researchers preparing experimental dental composites (Schneider et al., 2009a, Palin et al., 2014, Alania et al., 2016). The aim was to produce highly filled dental composites; the use of the Speedmixer aided in producing homogeneously mixed composites. Composite specimens were analysed using the SEM to evaluate the mixture and compare it to the commercial control. SEM images showed even distribution of the glass filler within the resin matrix of experimental dental composites. This was comparable to the glass distribution within the commercial control (TC), representative examples are shown in Figure 14. Therefore the homogeneity of the mixed experimental composites was confirmed and efficiency of the mixing protocol was confirmed.

3.6.2 Degree of conversion

One of the aims of this study was to characterise the physical properties of the experimental materials by measuring their degree of conversion.

The degree of conversion is a crucial determining factor of the material's mechanical, physical and optical properties in addition to their solubility (Ferracane, 1985, Ferracane and Greener, 1986a, Hofmann et al., 2002, Durner et al., 2012). Generally the degree of conversion of dental composites vary widely ranging between 35-77% (Schmalz, 2009). Although the DC required for adequate clinical performance has not yet been established, a negative correlation has been established between the *in-vivo* abrasive wear and the DC. Therefore, it was suggested that materials with DC values below 55% are not recommended for occlusal restorations (Ferracane et al., 1997c, Silikas et al., 2000).

The results showed that experimental composites with different monomer mixtures showed mean DC ranging between 52-62%, (Table 4). There were no significant differences between the experimental groups at all curing times regardless of the monomer mixture used ($p > 0.05$).Group A and D contained only one of the diluting monomers at 30%wt (TEGDMA and BisEMA respectively), whereas group B and C contained both diluting monomers at different ratios (Detailed description is shown in Table 4). TC composite which was the commercial control showed a lower degree of conversion when compared to all experimental groups at all tested time intervals ($p < 0.05$). The maximum DC measured for TC was 55.0% at 60 seconds curing. It was also noted that the DC of all tested composite groups started to plateau at 20 s without a significant increase in the DC when the curing times were extended. Therefore the null hypothesis was rejected when comparing the experimental composites to the commercial control. Durner *et al* (2012) reported that TC degree of conversion increased from 38±2.0% after 5 s polymerisation to 47±2.1% after 40 s polymerisation time. It was also found that there was a significant inverse correlation between the DC and the amount of eluted monomers from TC. TC specimens cured for 5-10 s showed higher amount of elutable BisGMA when compared specimens polymerised at extended curing times (20-40 s), (Durner et al.,

2012). TC also contains pre-polymerised filler particles used as a secondary filler, therefore any remaining unreacted or pendant double carbon bonds (C=C) could also increase the final amount of leachable monomers. Furthermore, the absence of TEGDMA may also lead to insufficient polymerisation resulting in increased amounts of leachable monomer (Sideridou et al., 2002).

Fourier transform infrared spectroscopy (FTIR) was used in this study which is a well-established methodology for measuring the degree of conversion of the experimental composite materials (Imazato et al., 2001, Ilie and Hickel, 2007, Durner et al., 2012, Walters et al., 2016). Most dental composites are methacrylate based materials containing monomers such as BisGMA, TEGDMA, BisEMA with at least two C=C bond that are able to form a three-dimensional network. The degree of conversion was calculated by comparing the aliphatic and the aromatic bands around 1607cm^{-1} which was taken as the internal standard (Rueggeberg et al., 1990b). Spectra were taken with 32 co-addition scans to increase the signal to noise ratio (SNR). It was previously suggested that SNR ratio is 10 times better in 100 co-additions when compared to a single scan. Specimens were prepolymerised at different time intervals (5, 10, 20, 30, 40, 50 and 60 s), the short curing time of 5 second was included to identify potential differences between the materials, however there was a potential delay between the light exposure and the analysis which could have led to post-curing effect (Burtscher, 1993, Par et al., 2014). Therefore extended curing times were included to avoid the post curing potential.

The nature and the amount of monomer used in dental composites primarily influence their degree of conversion (Amirouche-Korichi et al., 2009). BisGMA is predominantly used as the base monomer in most dental composites; it is a highly viscous monomer due to its large molecular size and rigid structure which provide lower polymerisation shrinkage. However, its lower mobility does not allow high degree of conversion. Therefore, BisGMA is traditionally mixed with diluting low viscosity monomers such as TEGDMA, UDMA and BisEMA in order to achieve higher degree of polymerisation (Lemon et al., 2007, Stansbury, 2012, Ferracane et al.,

2014). UDMA and BisEMA can also be used as base monomers (Floyd and Dickens, 2006, Moraes et al., 2010). The use of BisEMA as a base monomer mixed with the co-monomer TEGDMA was shown to have higher degree of conversion when compared to BisGMA based co-monomer mixture (Fonseca et al., 2017). The amount of filler incorporated also affected the degree of conversion, higher filler content lead to increased materials viscosity and increased light scattering during polymerisation which consequently results in lower degree of conversion (Ferracane et al., 1998, Hadis et al., 2011).

The type and the concentration of the photo-initiator system used is a key factor affecting the polymerisation efficiency. It was reported that increasing the concentration of the photo-initiator increases the DC and the surface hardness of dental composites due to the increase in the maximum rate of polymerisation (Musanje et al., 2009, Pfeifer et al., 2009a). However, increasing the photo-initiator concentration above a certain optimal co-initiator level does not translate into an increased polymerisation efficiency (Pfeifer et al., 2009a). In addition to that, an increase in the shrinkage stress might also occur when the concentration is increased (Furuse et al., 2011). To date, CQ-tertiary amine is considered the most widely used photo-initiator system, however the optimal ratio of photoinitator to co-initiator is still not specified due to the large existent differences within the various resin-based composite components (Leprince et al., 2013). CQ with DMAEMA co-initiator system was used in this study with ratios comparable to most commercial and experimental dental composites (Aljabo et al., 2015, Alania et al., 2016).

Polymerising the resin matrix changes the materials optical properties and increases the refractive index due to the fast increase in the crosslinking and the viscosity. Light transmission increases as the refractive index of the resin approaches that of the filler particles which results in a decrease in the interfacial resin/filler scattering effect (Shortall et al., 2008). Therefore it is recommended to optimise the filler/resin refractive index mismatch to provide increased curing depth and assist in shade matching. The refractive indices of the materials used in this study are as follows: barium glass

(1.53), BisGMA (1.55), TEGDMA (1.46), BisEMA (1.51) and the reported BisGMA: TEGDMA (70:30%) is around 1.52 (Shortall et al., 2008). The filler and monomer mixtures used in this study had closely matched refractive indices containing BisGMA as the base monomer, therefore this may also explain the lack of significant differences in the DC between the different composite mixtures. Based on the results of this part of the study, it was concluded that using BisGMA as a base monomer with TEGDMA and BisEMA as co-monomers at different ratios did not affect the DC of the experimental composite materials, the DC was within the recommended required values for adequate mechanical properties and reduced shrinkage necessary for occlusal restorations (Ferracane et al., 1997c, Silikas et al., 2000).

3.6.3 *In-vitro* wear resistance

The wear resistance of dental composites has been identified as one of the key mechanical properties to predict the materials clinical performance (Ferracane, 2013b). The wear behaviour remains as an important property for dental composites specially when used in large restorations with heavy occlusal contacts and for patients with parafunctional habits (eg. bruxism). Therefore it is recommended that wear should continue as a screen tool for new dental composites designed for posterior use (Ferracane, 2013b). The current knowledge suggests that the mechanical properties including the wear resistance of resin based composites are mainly dependent of the filler content rather than the resin matrix (Musanje et al., 2001, Ilie and Hickel, 2009a, Hahnel et al., 2012). Over the past decade, significant improvements have been made due to the reduction in the filler size and the increase in the amount of reinforcing filler incorporated, consequently dental composites are currently showing superior mechanical properties and reduction in wear (Ferracane, 2011). Increasing the filler volume loading enhances the mechanical properties (Braem et al., 1989, Condon and Ferracane, 1997, Ilie and Hickel, 2009a), however reducing the filler particle size limits the allowable amount of filler volume fraction but increases the wear resistance (Suzuki et al., 1995, Venhoven et al., 1996, Turssi et al., 2005).

The wear data showed that there was generally very minimal wear across the experimental groups and the commercial control; the mean volume loss ranged between (0.02-0.06 mm^3), (SD=0.003-0.007). However Group A showed a significantly lower wear resistance when compared to all tested groups including the commercial control, ($p < 0.05$). Group D also showed lower wear resistance when compared to B and C, ($p < 0.05$), whereas there were no statistical differences between group B, C and TC ($p > 0.05$). Generally the *in-vitro* wear is dominated by the filler content, therefore since all experimental materials contained the same amount and type of filler particles (80 wt%, 67 vol%), high wear resistance was expected. TC also showed minimal wear which again mostly related to its high filler content (83 wt%, 63 vol%). Ilie *et al* (2009) identified that a filler volume fraction of 60% is necessary for adequate mechanical performance of resin composites (Ilie and Hickel, 2009a). Although composite wear behaviour is mainly affected by the filler content, the wear remains as a complex process and not all monomer mixtures would be expected to behave in a similar manner. Data showed that group A (70 BisGMA: 30 TEGMA) had the lowest wear resistance and followed by group D (70 BisGMA: 30 BisEMA). Although short term wear was shown not to be able to differentiate between the different composite formulations when compared to long term testing, it provided researchers with significant insights into the materials *in-vitro* wear performance (Finlay et al., 2013, Altaie et al., 2017). Therefore, extended wear testing is proposed to gain further insight into the wear behaviour of different composite formulations. Group A and D showed slightly deeper wear tracks when compared to the other groups which was consistent with the mean volume loss measurements. The pattern of wear was similar amongst the experimental groups with microcracks running through the matrix as shown from the SEM images in (Figure 18). TC also showed microcracks running through the matrix but also showed voids within the matrix corresponding to possible pull out of the larger pre-polymerised filler (PPF) particles that are present in TC composite, Figure 17. PPF are difficult to silanize due to the lack of active binding sites, therefore they poorly integrate within the resin matrix which may result in easier disintegration when mechanically challenged (Blackham et al., 2009,

Randolph et al., 2016). Analysis of the abrading steatite antagonist was also conducted using the SEM. Scanned samples showed distinct round wear facets corresponding to the opposing wear tracks as shown in Figure 19.

A variety of *in-vitro* wear testing devices has been used to replicate the *in-vivo* masticatory process, however to date no single *in-vitro* wear simulator can simulate the masticatory cycle in the oral environment (Heintze et al., 2012). At best, most wear simulators can provide an indication of the relative ranking of new dental composite formulations and compare them to other commercially available successful formulations (Finlay et al., 2013, Benetti et al., 2016). The wear simulator device used in this study was a variant of the original device used by Harrison and Lewis (Harrison and Lewis, 1975), detailed description is shown in section (3.4.3.1 . It simulates the intermittent sliding action of 'tooth to tooth' contact which remains a major step forward when comparing it to conventional to pin-on disc devices (Lambrechts et al., 2006). Spherical steatite (8 mm in diameter) was used in this study as the abrading antagonist, it has been widely used by several researchers evaluating the wear behaviour of dental composites (Heintze et al., 2005b, Finlay et al., 2013, Altaie et al., 2017). Steatite is a suitable substitute to enamel; it is a synthetic material that is mainly composed of magnesium silicate. It has a comparable surface microhardness and coefficient of friction to enamel (Wassell et al., 1994a, Shortall et al., 2002). Alternative wide range of materials is also available such as human and bovine enamel, stainless steel, porcelain and hydroxyapatite. Although human enamel may be the ideal choice, standardisation of the enamel specimens remains problematic. The loading force used during the test was 4.5 N (Harrison and Lewis, 1975) in a neutral freshly prepared buffer solution (pH 7) to simulate the *in-vivo* oral environment (Antunes and Ramalho, 2009). Samples were also stored for 7 days in distilled water prior to wear testing. Most studies use distilled and deionised water at 37ºC for 24 hours-7 days as storage media prior to mechanical testing to permit post curing polymerisation of the composite specimens and to allow water absorption into the resin matrix which could enhance the mechanical properties through the plasticizing effect. However, over time, the leaching

of the components and the swelling and degradation of the cross-linked matrix in the resin composite and hydrolysis of the filler/matrix interfaces eventually lead to a decrease in the mechanical properties (Ferracane et al., 1998).

Combinations of analytical techniques were employed in this study to evaluate the *in-vitro* wear performance of the materials. Quantitative analysis of the wear tracks was conducted using white light profilometry and the mean volume loss (mm^3) was calculated (Finlay et al., 2013, Arsecularatne et al., 2016, Benetti et al., 2016). To date, confusion still exist on whether the wear depth or volume loss should be reported when evaluating composites wear performance (DeLong, 2006). However, researchers have shown that measuring the volume loss provide a more accurate description of a material's performance and it should be the parameter of choice when reporting *in-vitro* wear (Fleming et al., 2016). Though, regardless of the parameter reported (wear depth or volume loss), the wear *in-vivo* is still dependent on the occlusal factors which continuously change with time and the progression of wear (DeLong, 2006). Therefore, it is suggested that the wear performance of dental composites should be evaluated by using a combination of measurement and analytical techniques to quantify the wear but also to understand the underlying wear mechanism by analysing the wear facets (Altaie et al., 2017). This could provide further insight regarding the material behaviour and the tribology of wear rather than relying on simple ranking. The results showed that prepared experimental composites behaved similarly to the commercial control with minimal wear over 128,000 contacts which is equivalent to 3 months clinical wear using the employed methodology, (Harrison and Lewis, 1975). The null hypothesis was rejected as significant differences were found between group A and D when compared to B, C and TC.

3.6.4 Vickers microhardness

The materials' hardness is a relative measure to its resistance to indentation when a constant load is applied. Therefore by definition, the hardness is a measure of the material's resistance to scratching and abrasion and could indicate the finishing and polishing properties (McCabe, 1990). The surface hardness intuitively seems to be an important property especially in predicting wear resistance of dental composites. However, due to the complexity of the wear process, *in-vitro* studies have been equivocal in showing the correlation between wear and microhardness, (Ferracane, 2011). It has been widely reported that the surface microhardness value is directly proportional to the composite filler content (Ferracane et al., 1998, Kim et al., 2002, Jun et al., 2013b, Randolph et al., 2016). Due to the variation of composite formulations the reported microhardness values of commercial composites ranges between 23-108 (Randolph et al., 2016). Vickers and Knoop microhardness tests are the most widely used methods in evaluating the surface microhardness of dental composites. Vickers microhardness test was conducted in this study when a load of 100 g was applied for 15 s. Data analysis showed that the microhardness values of the experimental composite groups were significantly higher when compared to TC. Experimental composite values ranged between 89-94 (SD=2-4) whereas TC value was 53.5 (SD=3.5). There were no significant differences in the microhardness values between the experimental composites regardless of the resin mixture formulations. Since all experimental groups contained the same amount of filler content (80%wt, 64%vol), the lack of variation in the values is expected. Other researchers also reported a relatively low Vickers hardness value of TC (40.7, SD=1.3) (Randolph et al., 2016). Experimental composites showed high microhardness values which are comparable to the commercially available highly filled dental composites (Randolph et al., 2016). Since FA composites showed significantly higher HV when compared to TC, the null hypothesis was rejected.

3.7 Summary

Model experimental composite formulations were successfully produced with 80%wt (63%vol) filler content. The homogeneity of the composite mixture was comparable to the commercial control. The physical and mechanical properties were acceptable and comparable/higher to the commercial material, Table 12. There were no differences in the DC, and microhardness values between the different experimental composite formulations regardless of the monomer mixture used. However, differences were found when the *in-vitro* wear resistance were evaluated. Composite containing (70BisGMA: 30TEGDMA) and (70BisGMA: 30BisEMA) showed the least wear resistance when compared to other two experimental groups. Therefore, it was concluded that either group B (70BisGMA: 20TEGDMA: 10BisEMA) or C (70BisGMA: 10TEGDMA: 20BisEMA) would be a suitable model dental composite to carry forward for the next part of this. TEGDMA is conventionally associated with higher polymerisation shrinkage (Asmussen, 1984, Braga et al., 2005). Therefore, Group C which contains higher amount of BisEMA was selected as the model composite for the next part of this project.

Table 12: Experimental composites and Tetric Evo ceram (TC) mean degree of conversion (DC) at 40 s curing time, wear resistance (volume loss mm^3) and Vickers microhardness (HV).

Group	DC, (SD)	Wear (mm^3),(SD)	HV,(SD)
TC	51.8 (0.5)	0.023 (0.004)	53.4 (3.5)
30%TEG	59.9 (2.4)	0.060 (0.007)	89.7 (4.0)
20%TEG	59.8 (3.5)	0.019 (0.004)	93.2 (2.8)
10%TEG	61.0 (4.6)	0.021 (0.004)	94.8 (2.0)
0%TEG	61.9 (1.9)	0.031 (0.003)	89.0 (3.3)

Chapter 4: Preparation and characterisation of synthesised Fluorapatite (FA) particles

4.1 Introduction

Dental enamel is the hardest mineralised tissue in the human body; its unique structure provides protection against caries development especially in the presence of fluoride. It consists of hydroxyapatite crystals (HA) arranged into a well organised micro-architectural structure called enamel prisms. Therefore HA is considered a very attractive biomimetic biomaterial for applications in dentistry. Fluorapatite, $Ca_5(PO_4)_3F$, (FA) is the fluorine substituted form of HA, it which the (OH^-) in HA is substituted with (F^-). Various clinical applications of apatites have been suggested; including coating of dental implants to improve the bioactivity and osteointegration (Carradò et al., 2017), direct application to exposed dentine to manage dentine hypersensitivity (EARL, 2007), dental prophylactic agents (Kensche et al., 2017) and the development of experimental bioactive dental restoratives (Arcís et al., 2002, Taheri et al., 2015). Fluorapatite is hexagonally shaped with a highly symmetrical crystallographic structure. It is chemically stable but known to release fluoride in an acidic environment. Fluoride interferes with the caries process by reducing demineralisation and enhancing the remineralisation of enamel and dentine (Cate, 1999). The presence of fluoride in an acidic oral environment results in a physico-chemical interaction between the dissolving hydroxyapatite and the fluoride ions. The calcium and phosphate lost from the hydroxyapatite interacts with the fluoride and returns back to the tooth as fluorapatite (reducing demineralisation). Fluoride also enhances the remineralisation process through enhancing the precipitation of calcium phosphate and consequently reduces caries progression. In addition to that, it has been shown that fluoride has an antibacterial effect towards *Streptococcus mutans* which is the most cariogenic bacteria (Seppa et al., 1993, Loyola-Rodriguez and Garcia-Godoy, 1996, Pandit et al., 2011). To mimic this natural caries resistance of teeth, it was suggested that synthesised fluorapatite crystals could be a suitable and effective chemically stable anti-

caries material (Chen et al., 2006b). In addition to that, the synthesised FA crystals have a unique hexagonal structure in the form of crystals and bundles of crystals which can act as reinforcing filler within the resin matrix of dental composites. Therefore in principle, a dental resin containing FA would be a favourable restorative material for human tooth tissue. Many techniques have been investigated to synthesise apatite including solid state reaction (Rao et al., 1997), ultrasonic pyrolysis (Aizawa et al., 1999), plasma techniques (Yoganand et al., 2010), precipitation (Mobasherpour et al., 2007), solution gelation (Bilton et al., 2010) and the hydrothermal reaction (Chen et al., 2006b). By far, the most widely used methods are either solution precipitation or the hydrothermal reaction (Nayak, 2010).

This chapter will discuss the synthesis of fluorapatite crystals using the hydrothermal synthesis methodology and the characterisation of the produced powder using various analytical techniques to ascertain the crystals morphology and chemical composition, prior to its incorporation as filler in the experimental dental composite.

4.2 Aims

The aim is to develop and characterise fluorapatite particles to be used as secondary filler for preparation of experimental dental composites.

4.3 The null hypothesis

The synthesised fluorapatite in this study will have no morphological and chemical characteristic differences to natural fluorapatite.

4.4 Materials and methods

4.4.1 Fluorapatite (FA) particle synthesis

Fluorapatite crystals were synthesised using a hydrothermal method ($NaH_2PO_4.H_2O$, NaF_2 and EDTA-Ca-Na_2 reaction) which was previously described by (Chen et al., 2006b); this method was also employed by several other researchers to synthesise FA particles for various research applications (Liu et al., Czajka-Jakubowska et al., 2009). 9.36 g of ethylenediamine tetraacetic acid calcium disodium salt (EDTA-Ca-Na_2) and 2.07 g of $NaH_2PO_4 \cdot H_2O$ were mixed with 90 ml of distilled water. This suspension was then stirred continuously until the powder was fully dissolved. The pH was adjusted to 6.0 using NaOH. 0.21 g of NaF was dissolved in 10 ml water (pH 7.0) and stirred continuously and then added to the 90 ml of the first solution. FA crystal growth was achieved by autoclaving the newly prepared EDT-Ca-Na_2/NaH_2PO_4/NaF mixture at 121°C at a pressure of 2.4×10^5 Pa for 10 hours. The resulting solution containing the FA precipitate was then left to cool and the excess liquid was then discarded. The powder was then washed five times by adding 100 ml of distilled water and manually stirring for 2 minutes, followed by drying. After the fifth wash, the suspension was poured onto a flat glass surface and left to dry. Once dried, the powder was collected and manually ground using a mortar and pestle and stored in an airtight vial at room temperature.

4.4.2 Fluorapatite morphological and compositional analyses

4.4.2.1 Scanning Electron Microscope (SEM)

Morphological analysis of the synthesised FA was conducted using SEM. Three FA samples were placed on carbon sample stubs; loose particles were then removed by spraying with compressed air. The samples were then coated with approximately 5 nm of gold using an argon sputter coating unit (Agar Scientific, Stanstead, UK). Samples were then mounted at a 10 mm distance and scanned under low vacuum with an accelerating

voltage of 20Kv. SEM images were then processed using post imaging analysis software to determine particle size distribution (Image J). 20 images were taken at x1000 magnification with 10 mm working distance. 10 measurements were taken from each image (5 for diameter and 5 for the length in μm) and the average was recorded.

4.4.2.2 Energy Dispersive X-Ray Spectroscopy (EDX)

The synthesised FA nanoparticles were further characterised using energy dispersive X-ray spectroscopy (Bruker 129 eV) to obtain their elemental composition. Analysis was carried out using the same samples (n = 3) prepared for SEM imaging. A section of the sample stub was analysed to incorporate as many particles as possible to allow a representative average to be obtained. Images were taken at x1000 and x2000 magnification with 10 mm working distance.

4.4.2.3 X-ray-Diffraction (XRD) analysis

To determine the crystallographic structure of the synthesised FA crystals, XRD analysis was conducted using an X-ray diffractometer (PHILIPS X'PERT, Cambridge, UK). The powder was packed into the sample holder and the diffractometer was run over a 2θ range covering 10-60 °. Generated XRD traces were then compared to a reference pattern (15-0876) for stoichiometric FA obtained from the International Centre for Diffraction Data (ICDD) database.

4.5 Results

4.5.1 Scanning Electron Microscope (SEM)

The synthesised FA exhibited individual hexagonal rod like crystals and bundles, Figure 25 shows the different crystal morphologies identified. Particle size analysis showed that the average crystal diameter ranged between 2-4 (μm) wide and 12-20 (μm) long, Figure 26, to give an aspect ratio of ~1:6.

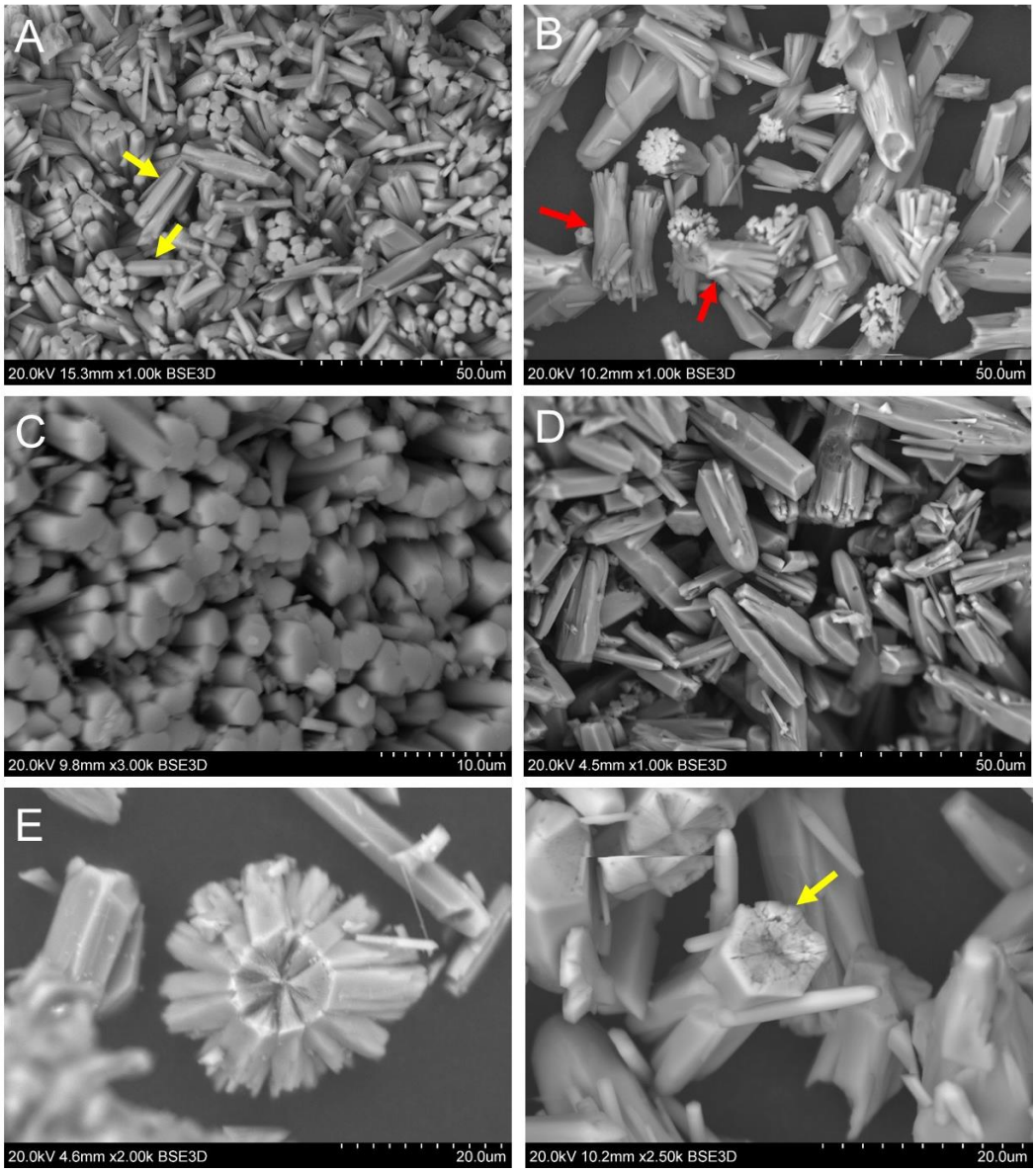

Figure 25: SEM images of the synthesised FA powder. (A) Shows hexagonally shaped rod like crystals. (B) Shows bundles of FA rods (red arrows) and individual FA rods. (C) Shows the top surface of FA rods grown on the surface of the beaker. (D) Shows individual FA crystals precipitated at the bottom of the beaker. (E) Shows as individual bundle with hexagonally shaped centre. (F) Shows an individual hexagonally shaped FA crystal.

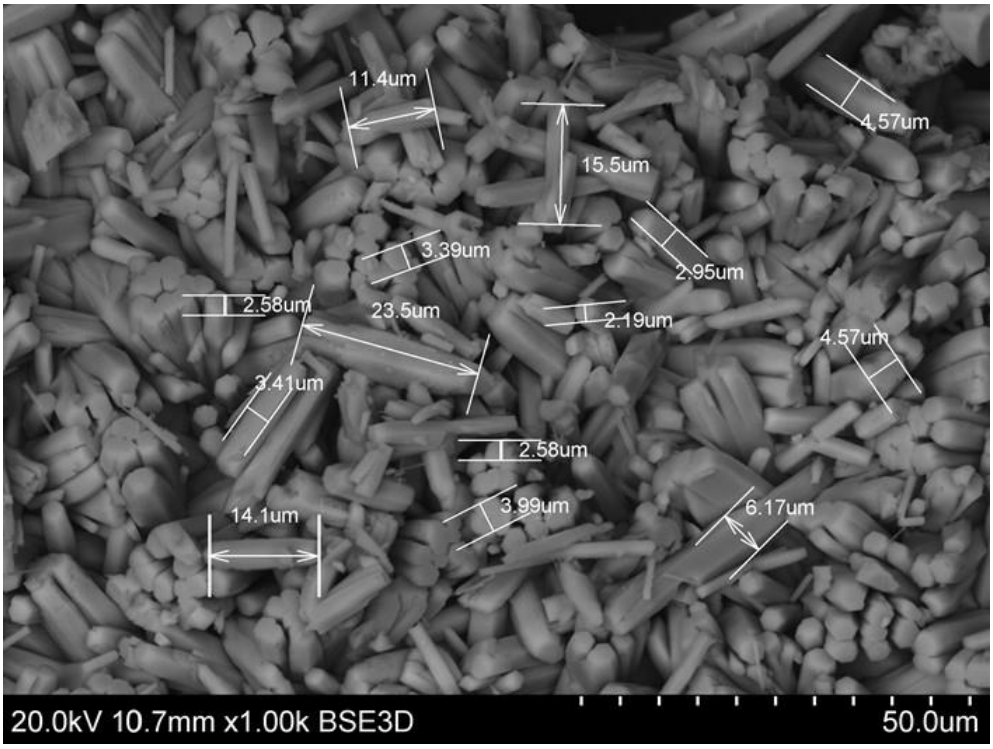

Figure 26: SEM of the FA crystals showing representative range of the average particle size diameter and length (μm).

4.5.2 Energy Dispersive X-Ray Spectroscopy (EDX)

Further characterisation of the synthesised FA particles was conducted using EDX to obtain their elemental composition. EDX spectra showed that the elemental composition of the synthesised FA particles was as expected, Figure 27. Elemental analysis also showed that the Ca:P ratio was in excess of that of stoichiometric FA (calcium rich apatite at 1.77:1 compared to theoretical 1.67:1) and the F content slightly in excess compared to stoichiometric FA, Table 13. Elemental maps were also generated from the SEM images of the FA samples showing P, Ca and F evenly distributed in the crystals, Figure 28.

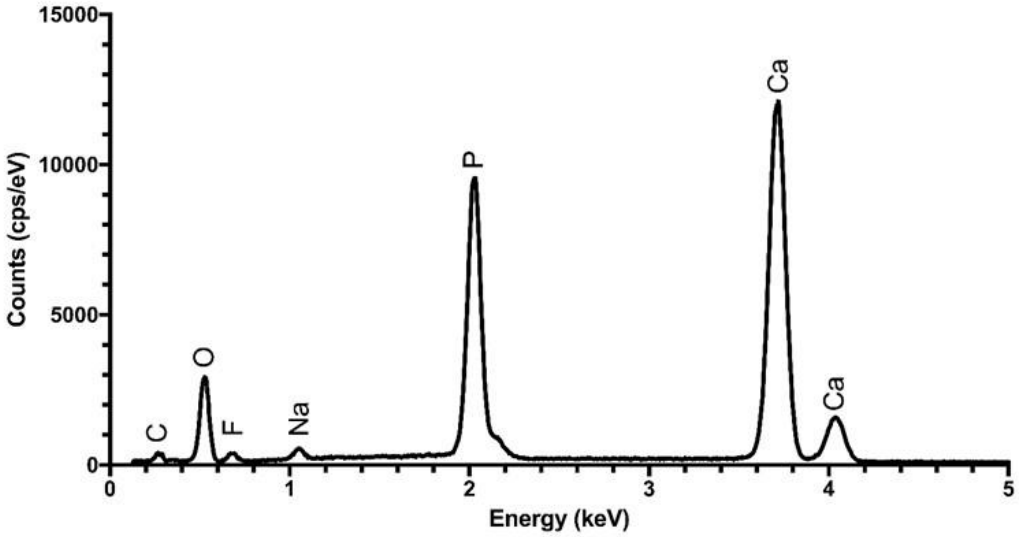

Figure 27: EDX spectrum showing the elemental composition of synthesised FA.

Table 13: Elemental composition of FA in terms of atomic weight% as determined by EDX

Element	Atomic weight%
Ca	22.49±1.3
P	12.64±0.6
F	5.04±0.4
Ca:P	1.77:1
Ca:F	4.46:1

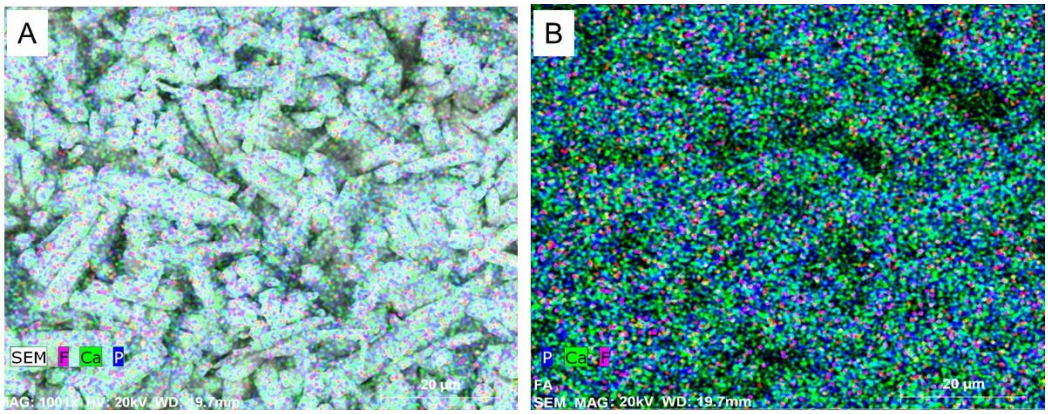

Figure 28: Elemental maps of the FA crystals with P, Ca and F elements shown overlaid on the corresponding SEM image (A) and alone (b).

4.5.3 X-ray-Diffraction (XRD) analysis

XRD traces showed that synthesised FA particles have similar peak positions and relative intensities when compared to the reference trace with the absence of unmatched peaks, Figure 29. The synthesised FA traces showed narrow peaks indicative of a highly crystalline material.

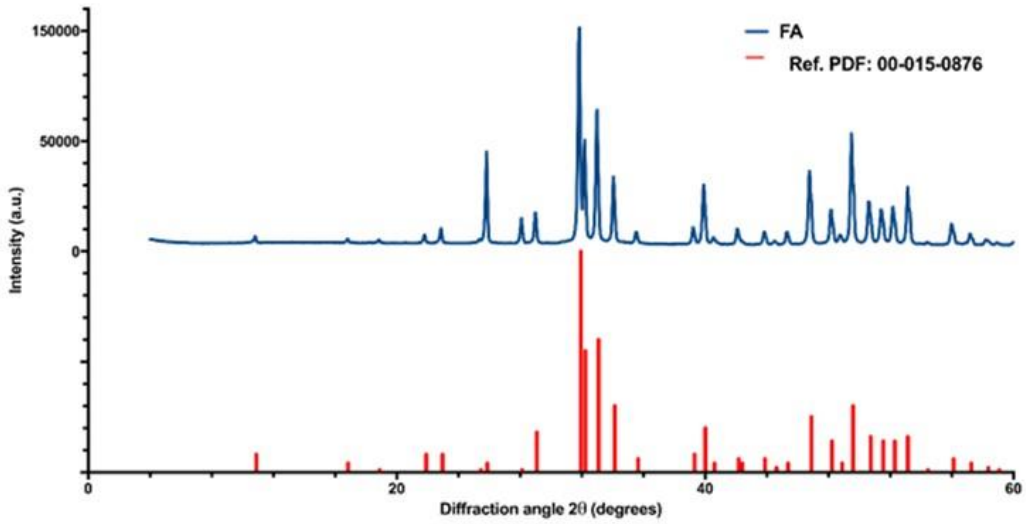

Figure 29: XRD traces of synthesized FA compared to a stoichiometric FA obtained from the International Centre for Diffraction Data (ICDD).

4.6 Discussion

Fluorapatite (FA) crystals were synthesised following the hydrothermal synthesis methodology described by Brian Clarkson's group (Chen et al., 2006b). Various analytical techniques were employed to characterise the morphology and the chemical structure of the synthesised FA including SEM, EDX and XRD. SEM images showed typical hexagonally shaped rod like crystals and bundles of crystals (Figure 25) corresponding to a distinctive FA morphology. Elemental analysis using the EDX showed Ca, P and F peaks which are typical of FA with similar Ca:P and Ca:F ratios to that of stoichiometric FA (Table 13), however the FA was slightly calcium and fluoride rich. The XRD trace (Figure 29) also showed good correlation with that of the ICDD FA reference diffraction pattern. Based on those analytical techniques, strong agreements were found between the synthesised FA to the one produced by Chen *et al* (2006b). Analysis of the particle size distribution showed that FA crystals' average diameter ranged between 2-4 µm and length 12-20 µm as shown in (Figure 26), similar to the dimensions of 1-3 µm in cross section and 10-30 µm in length reported by Chen *et al* (2006b). Filler particle size distribution varies widely in commercial composites materials. Randolph *et al* (2016) conducted a comprehensive analysis of the filler particles size, geometry and content of various commercial dental composites, it was shown that most composite materials have two filler size peaks; with one centred either around 1-2 µm or 10 µm in some materials and the second one around 5-30 µm corresponding to larger filler particles (Randolph et al., 2016). The proposed composition of FA containing composites planned in this study is to incorporate barium glass (D_{50}= 0.7 µm) as a primary filler and FA (2-4 µm diameter and 10-20 µm long) as a secondary filler. Therefore the majority of the experimental FA containing composites will contain submicron filler particles mimicking the majority of the commercially available dental composites. Commercial composites contain fillers with various morphologies from spherical to rough and irregular fillers. Several researchers investigated the effect of various filler morphologies on the mechanical performance of dental composites. To date, there has been no

consensus correlating the size and the shape of filler particles to the mechanical properties of dental composites (Rueggeberg et al., 1993, Turssi et al., 2005, Masouras et al., 2008b, Leprince et al., 2010). Whereas it has been suggested that filler load is the main factor affecting the mechanical properties while the filler size and morphology is considered as a secondary factor that may alter the materials properties (Masouras et al., 2008a, Randolph et al., 2016). The unique morphology of the FA crystals and bundles of crystals could act as reinforcing filler within the resin matrix. Experimental composites containing hydroxyapatite filler showed higher flexural strength in comparison to the control material (Arcís et al., 2002), similar observation were reported by Taheri *et al* (2015). However when the amount of hydroxyapatite incorporated was above a certain level the mechanical properties were negatively affected (Taheri et al., 2015).

The SEM, EDX and XRD data strongly suggested that the FA powder produced exhibited similar chemical composition and morphological features to that produced by Chen *et al* (2006b) whose method was adopted in the study. The FA crystal size was in the range of most conventional fillers used in commercial dental composites; therefore it was felt that the FA powder produced would be a suitable filler to be used in experimental dental composites.

4.7 Summary

Fluorapatite crystals were successfully produced using a reproducible methodology. The morphological and geometrical characteristics of the FA crystals showed favourable properties to be used in resin composites. The FA produced in this chapter will be incorporated as secondary filler in experimental dental composites.

Chapter 5: Development of Fluorapatite containing dental composites

5.1 Introduction

The use of dental composites as a universal restorative has significantly increased over the last few years exceeding amalgam in some countries. This trend is expected to continue due to the Minimata convention and the phase down in the use of mercury containing products (Lynch and Wilson, 2013b). Despite the continuous evolution of dental composites; their long term longevity remains to be problematic. Numerous studies have identified secondary caries and fracture as the two main reasons of failure of dental composites (Burke et al., 1999, Mjor et al., 2000, Bernardo et al., 2007, Demarco et al., 2012b). Therefore, the development of resin composites remains as focal point of research in academia and industry aiming to enhance their properties and clinical service by addressing their perceived shortcomings (Ferracane, 2011, Randolph et al., 2016). A possible approach to prevent secondary caries formation is the addition of agents that inhibit bacterial growth and aid tooth tissue remineralisation. Synthetic fluorapatite resembles the natural dental enamel in colour, chemical composition, surface morphology and structure. It is chemically stable but known to release fluoride in an acidic environment. Therefore, it was suggested that synthesised fluorapatite crystals could be a suitable and effective chemically stable anti-caries material (Chen et al., 2006b). In addition to that, the unique morphology of FA crystals in the form of crystals and bundles of crystals can act as reinforcing filler within the resin matrix of dental composites maintaining the mechanical strength. Therefore the aim of this study is to develop experimental dental composites with FA incorporated as secondary filler to improve the mechanical and the biological properties of resin composites. Characterisation of new materials is essential to predict their performance and clinical success. Therefore experimental materials will be subjected to series of tests to characterise their physical and mechanical properties and fluoride ion release. Wear resistance, fracture toughness and flexural strength have been identified as

the key laboratory mechanical parameters with direct relations to fractures and wear *in-vivo* (Ferracane, 2013a, Heintze et al., 2017). Therefore the mechanical performance of the experimental materials will be evaluated based on these parameters and will be compared to a commercial control (Tetric Evo Ceram).

This chapter will describe the development of FA containing dental composites with various FA concentrations and the characterisation of their properties in relation to commercial dental composites.

5.2 Aims

1- To develop experimental dental composites with fluorapatite incorporated as secondary filler.
2- To characterise the mechanical and physical properties of dental composite formulations FA containing.
3- To measure the fluoride ion release.

5.3 Hypotheses

The null hypotheses are below:

1- There is no significant difference in the degree of conversion of FA containing composites when compared to the commercial control.
2- There are no significant differences in wear resistance, microhardness, fracture toughness, flexural strength and flexural modulus between FA containing composites and to the commercial control.
3- The addition of FA will not significantly affect the experimental materials degree of conversion regardless of the FA concentration used.
4- The addition of FA will not significantly reduce the mechanical properties of the experimental materials regardless of the FA concentration used.
5- FA containing composites will release fluoride under acidic and neutral conditions and no fluoride will be released from the control groups.

5.4 Materials and methods

5.4.1 Preparation of dental composite formulations

Based on the previous physical and mechanical characterisation conducted on the model experimental dental composites, it was decided to select the formulation containing (70: BisGMA, 10: TEGDMA, 20: BisEMA) as the monomer mix of choice to carry forward in this study. Experimental composites were formulated containing BisGMA/TEGMA/BisEMA and barium aluminium silicate glass as the primary filler Table 3. Synthesized fluorapatite (FA) rod-like particles were incorporated at 0 (FA0), 20 (FA20), 30 (FA30) and 40%wt (FA40), replacing the primary glass filler and to maintain an overall filler content of 80wt%.

Five composite formulations were produced following the same protocol previously described (in Chapter 3: section 3.4.1). FA powder was also added sequentially in four increments as detailed earlier. Mixed composites were kept in their containers and sealed with Parafilm (Parafilm®, Bemis company, Inc., UK) and wrapped in aluminium foil and stored at 4°C until use.

5.4.2 Characterisation of FA containing dental composites

5.4.2.1 Scanning Electron Microscopy and Energy Dispersive X-Ray Spectroscopy

EDX attached to the SEM was used to generate elemental maps to evaluate the homogeneity of the composite mixture and the incorporation of FA crystals and bundles within the resin matrix. Composite specimens were prepared as described (in Chapter 3: 3.4.2.1

5.4.3 Degree of Conversion

The degree of conversion (DC) of experimental FA containing dental composites was measured using FTIR-ATR (Spectrum 100, PerkinElmer, UK). Measurements were compared to the DC of 0FA containing composites and Teric Evo Ceram (Ivoclar-Vivadent, Lichtenstein). The

same methodology was followed as previously described (Chapter 3: section 3.4.2.2).

5.4.4 *In-vitro* two body wear

Wear testing (n = 10) and analysis was conducted following the same methodology described (in Chapter 3: section 3.4.3).

5.4.5 Vickers Microhandess (HV)

Vickers microhardness (n = 5) and analysis was conducted following the same methodology described (in Chapter 3: section 3.4.4).

5.4.6 Flexural Modulus and Flexural Strength

5.4.6.1 Specimens preparation

Flexural modulus and flexural strength were determined using a universal testing machine (Instron 3365, MA, USA) equipped with a three-point bending apparatus (n=10) following the ISO 4049 protocol (ISO4049, 2009).Ten composite specimens were prepared for each group with dimensions of 25 × 2 × 2 mm using a custom made split steel mould. Composite was packed incrementally and covered by a cellulose acetate separating strip and a glass microscope slide onto which was placed a 1 kg mass for 20 s in order to compress and level the material. The microscope slide was then removed and each specimen was photo-polymerised for 20 s per side overlapping each section using a light emitting diode (LED) light curing unit with 8 mm diameter tip (Demi Plus, Kerr, Orange Co., CA, USA), irradiance of >1000mW/cm^2, at 23 ± 1ºC. The irradiance was checked prior to use by employing a checkMARK (Bluelight Analytics Inc., Halifax, Canada). Following that, the cellulose acetate strip was removed and each specimen was checked for surface imperfections and polished using silicon carbide (SiC) abrasive papers grid 400 (Struers,Copenhagen, Denmark). The specimens were then stored in distilled water in an incubator maintained at 37 ± 1ºC for seven days before testing.

5.4.6.2 Flexural modulus and flexural strength testing

Specimen thickness and width were measured before testing using digital callipers (±0.01mm) and samples were then loaded on a 20 mm support span with knife edge geometry at 0.75 mm/min cross head speed. The maximum load exerted on the specimen at the point of fracture was recorded and flexural modulus (E) and flexural strength were calculated using Equation (1) and (2) respectively.

Equation 3

$$E(GPa) = \frac{l^3 * \delta}{4 * b * h^3 * 1000}$$

Equation 4

$$\sigma\ (MPa) = \frac{3Fl}{2bh^2}$$

Where

F is the maximum load (N) exerted on the specimen

l is the distance (mm) between the supports

b is the width (mm) at the centre of the specimen

h is the height (mm) at the centre of the specimen

δ is the slope of a force/deformation curve in the elastic region (N/mm)

5.4.7 Fracture Toughness

5.4.7.1 Specimen preparation

The sharp single edge notch beam (SENB) method was used to determine the materials' fracture toughness (K_{1C}) following the ASTM (E399-83) standards . This methodology has also been widely employed in the dental composite literature (Fujishima and Ferracane, 1996, Bonilla et al., 2003, Musanje and Ferracane, 2004, Rodrigues Junior et al., 2008a, Soderholm, 2010). Bar shaped composite specimens were made using custom made split mould (n = 10) with dimensions of 25 x 6 x 3 mm. The mould and specimen configuration are shown in Figure 30 and Figure 31. Composites

were incrementally packed and light cured following the ISO 4049 standards following the same technique detailed in (section 3.4.3.2). Samples were then removed from the mould and a sharp notch (3.0±0.1 mm length x 0.3±0.1 mm width) was cut into each specimen using a diamond disc attached to straight hand piece. The hand piece and the diamond disc were mounted on a custom made jig to precisely cut a 2.8±0.1 mm long notch into the middle of the sample as per the ASTM (E399-83), Figure 32. A razor blade mounted on a custom made Perspex jig was then passed through the notch to create a very sharp notch (0.2±0.01 mm length), Figure 33. A new razor blade was used for each composite group to create the notches. Specimens were then polished using 400 grit silicon carbide (SiC) abrasive papers (Struers,Copenhagen, Denmark) and stored in distilled water in an incubator maintained at 37 ± 1ºC for seven days before testing. SEM images of a representative cracked sample ready for testing is shown in Figure 34.

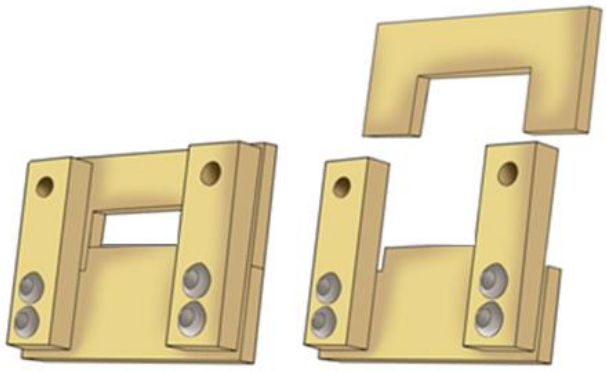

Figure 30: Schematic diagram showing the custom made split mould to produce samples for fracture toughness testing.

(Drawn by Collin Sullivan, LDI)

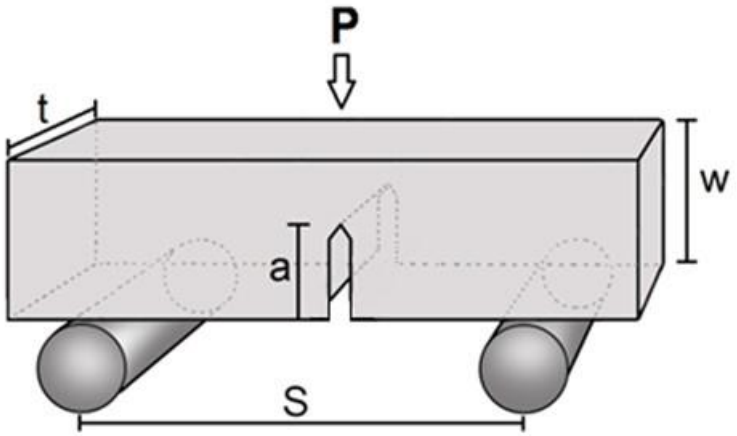

Figure 31: Specimen configuration for fracture toughness determination by the SENB testing method. Specimen geometry (a = 3.0±0.1 mm length x 0.3±0.1 mm width, w = 6 mm and t = 2 mm) ***(Drawn by Collin Sullivan, LDI)***

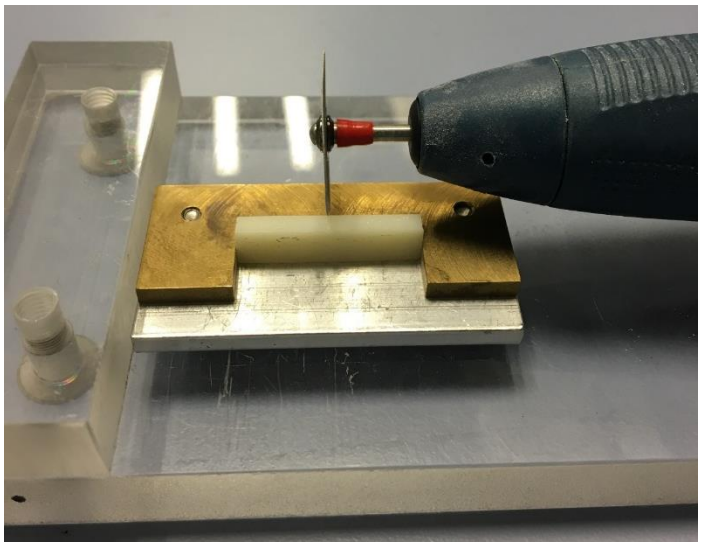

Figure 32: Custom made jig with a diamond disc attached to a securely mounted headpiece to insert the initial crack into the composite specimen.

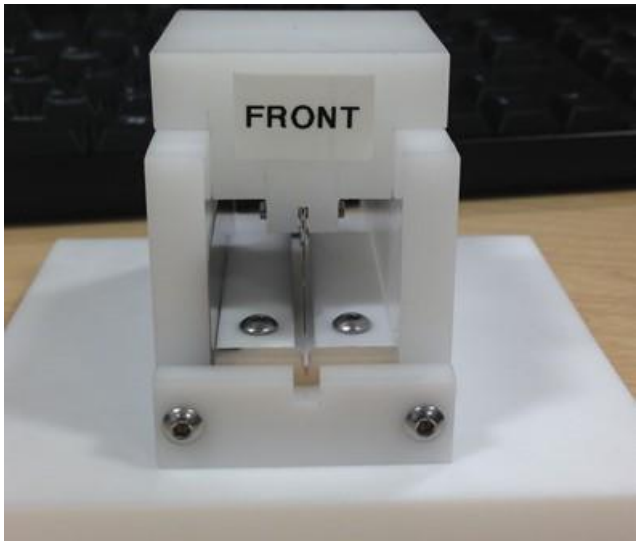

Figure 33: Custom made jig with a changeable razor blade attached to insert the final crack into the composite sample before testing.

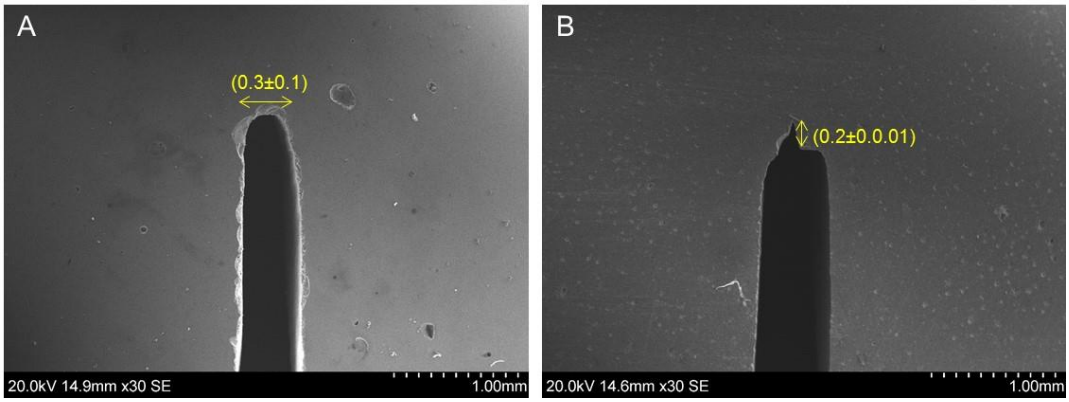

Figure 34: SEM images showing a representative cracked composite sample before testing. (A) The initial crack is created using a diamond disc with dimensions of (2.8±0.01 X 0.3±0.1) and (B) the final crack created after the insertion of the razor blade (0.2±0.01 X 0.02 mm).

5.4.7.2 Fracture toughness testing (SENB)

The notched composite specimens were tested in a three-point bending test with a crosshead speed of 0.5 mm/min in a universal testing machine (Instron 3365, MA, USA), Figure 35. Specimen dimensions were measured prior to testing in three equally spaced positions along the sample and the mean reading was recorded. Calculations of the fracture toughness values were determined using the following equations:

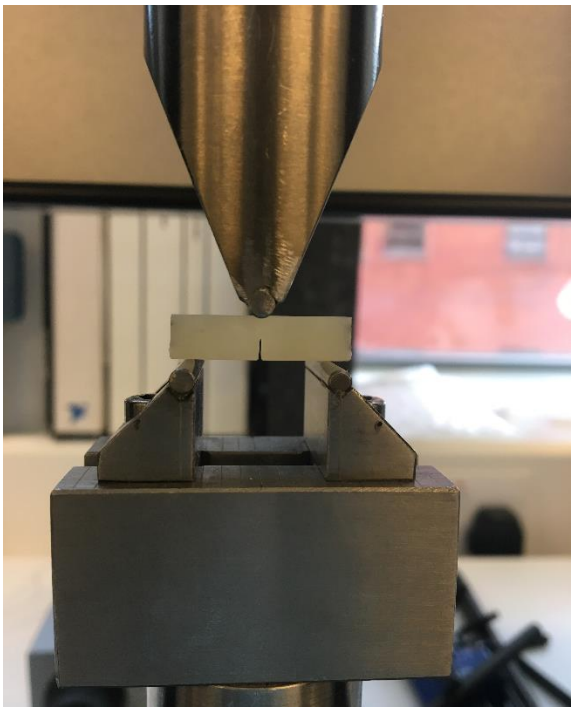

Figure 35: Notched composite specimen mounted on a three-point testing apparatus attached to the Instron machine.

Equation 5

$$K_{1c} = (\frac{3PSa^{1/2}}{2tw^2}) \times f(\frac{a}{w})$$

Where

Equation 6

$$f\left(\frac{a}{w}\right) = 1.93 - 3.07\left(\frac{a}{w}\right) + 14.53\left(\frac{a}{w}\right)^2 - 25.11\left(\frac{a}{w}\right)^3 + 25.80\left(\frac{a}{w}\right)^4$$

P is the maximum load (N) exerted on the specimen

S is the distance (mm) between the supports

w is the width (mm) at the centre of the specimen

t is the thickness (mm) at the centre of the specimen

5.4.8 Fluoride Release

5.4.8.1 Specimen preparation

Disc shaped composite specimens were prepared for each group with dimensions of 6 × 2 mm using a custom made steel mould (n=6). Specimens were prepared following the ISO 4049 standards. Composites were then photo-polymerised in one cycle for 40 s. Following that composites were polished using 400 grit silicon carbide (SiC) abrasive papers (Struers, Copenhagen, Denmark). Fluoride release was conducted in neutral and acidic conditions using distilled water and an acidic buffer solution (pH 4). Fresh buffer solution was made for each test using pH 4 buffer tablets (VDR, Belgium) which was dissolved in distilled water following manufacturer's instructions. The pH values were confirmed using a pH meter (ORION-920A model, Orion Research, UK) which was calibrated before each test. Specimens were then placed in 5 ml of the immersion solution in a sterile polystyrene container with an integral spoon within the cap to aid in sample mounting (30 ml, Elkay Laboratory Products, UK, Ltd). Samples were fixed to the spoon with red dental wax (Metrodent, UK) to allow full immersion of the specimens in the storage medium and to maintain no contacts with walls, Figure 36. The media were changed in each container on daily basis in the first week, then every 7 days up to 1 month and then monthly thereafter.

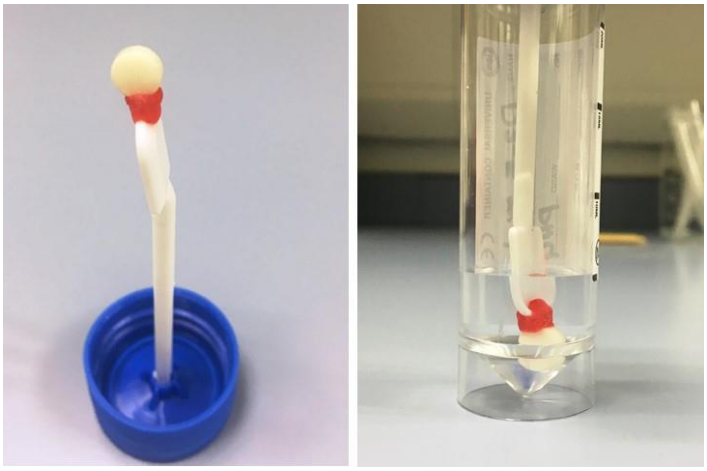

Figure 36: Composite sample fixed on a spoon holder and immersed in the solution in a sample container.

5.4.8.2 Fluoride release testing

The ion-selective method was used to measure the fluoride ion release using an ion-selective electrode (Orion Research, Thermo Scientific, Waltham, MA, USA) connected to an ion analyser. Measurements were taken over 24 hours on daily basis for 7 days, then weekly up to 28 days, then at day 56, 112 and 196. At time of media replacement, each specimen was removed with its integral spoon from the container and the storage solution was stored for analysis. The specimens were then washed with deionised water and dried with a paper towel then they were placed in fresh containers containing 5 ml of the immersing solution for the next measurement. 5 ml of TISAB III (TISAB III concentrate with CDTA, Thermo Fisher science) was added to each storage sample solution and then mixed for 20 s using vortex genie 2 (Scientific industries, USA) prior to measurement. The electrode was then immersed into the solution and concentration reading was recorded.

The instrument was calibrated prior to each testing using five standard sodium fluoride solutions containing 0.01, 0.1, 0.5, 1, 10 and 100 ppm fluoride and a calibration curve was plotted prior to each testing. The concentration reading was recorded in milliVolts (mV) for each sample solution. A logarithmic equation was then used to convert the mV values to ppm following the below equations:

Equation 7

$$\frac{mV1 - mV2}{logC1 - logC2} = \frac{mVs - mV2}{logCs - logC2}$$

Equation 8

$$\frac{logCs - logC2}{logC1 - logC2} = \frac{mVs - mV2}{mV1 - mV2}$$

Equation 9

$$logCs - logC2 = \left(\frac{mVs - mV2}{mV1 - mV2}\right) \times (logC1 - logC2)$$

Equation 10

$$logCs = \left(\frac{mVs - mV2}{mV1 - mV2}\right) logC1 - \left(\frac{mVs - mV2}{mV1 - mV2}\right) logC2 + logC2$$

Equation 11

$$Cs = 10^{logCs}$$

Where

mV1 and *mV2* represent *mV* of standard solutions, *C1* and *C2* represent concentration of standard solutions, *mVs* represents *mV* of testing sample, *Cs* represents concentration of testing sample, *LogCs* represents the concentration of testing sample in ppm, *mV* represents the milliVolts from the analyser reading, *ppm* represents the parts per million.

5.4.8.3 SEM analysis of fluoride releasing composite specimens

Aged and freshly prepared composite specimens were prepared for each fluoridated composite group (n = 3) and evaluated under the SEM. Specimens were prepared using the same protocol used in preparation for fluoride release experiment. Aged specimens were analysed following immersion in acidic medium (pH = 4) for 112 days with daily medium change in the first week and weekly change for the following three weeks. Collected samples were then mounted on an aluminium stub and coated with approximately 5 nm of gold using an argon sputter coating unit (Agar Scientific, Stanstead, UK). Samples were mounted at a 5 mm distance and scanned under low vacuum.

5.5 Results

5.5.1 Scanning Electron Microscopy and Elemental Mapping

SEM images generated showed typical crystalline structure of FA particles homogeneously incorporated within the resin mixture, Figure 37. Further

EDX analysis also showed typical FA elemental compositions corresponding to the incorporated FA crystals, Figure 38.

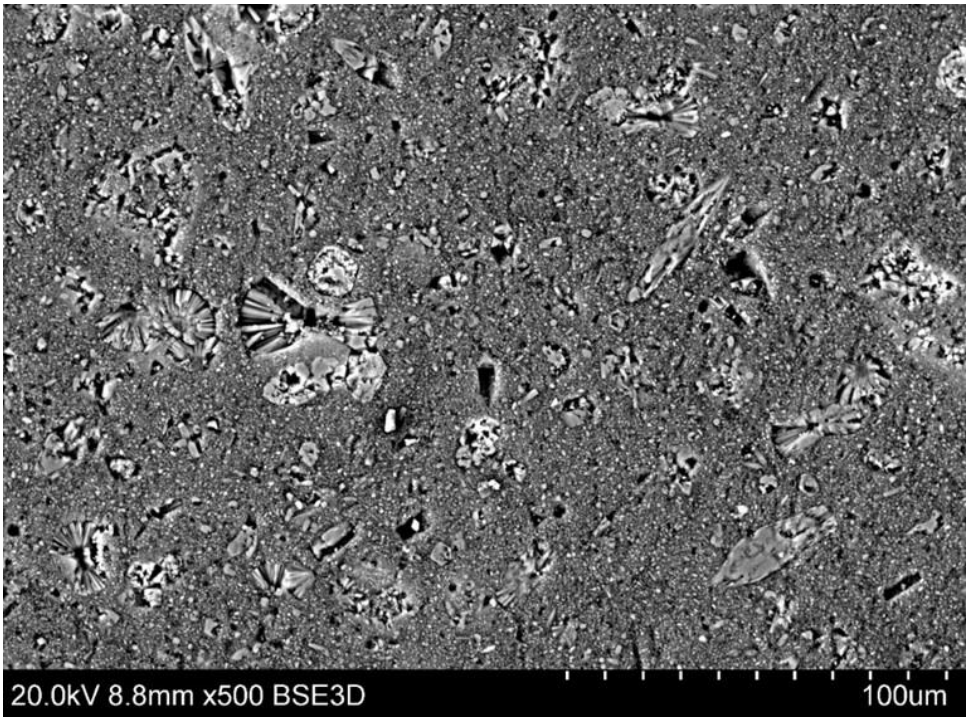

Figure 37: SEM image showing 40FA composite specimen with FA crystals and bundles widely distributed within the resin matrix.

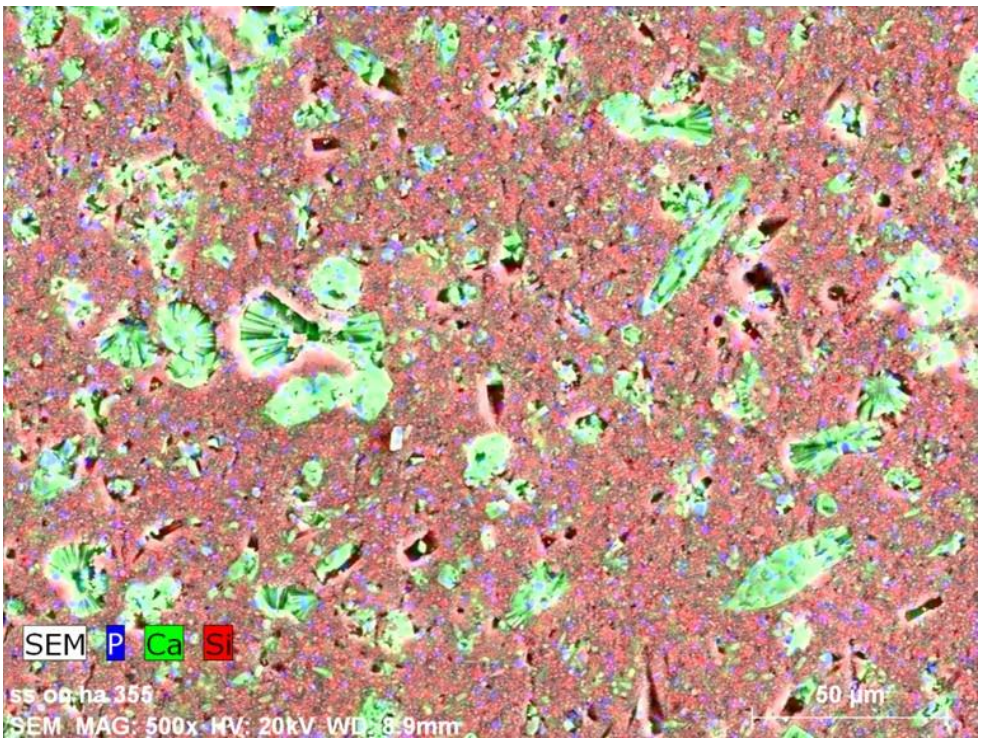

Figure 38: EDX image showing Ca and P corresponding to the FA crystals and Si corresponding to the primary filler.

5.5.2 Degree of Conversion

Figure 39 shows representative FTIR spectra of FA containing composite specimen (30%FA) with typical aromatic and aliphatic key peaks at each time point. The absorption aliphatic (C=C) peak at 1640 cm^{-1} changed with polymerisation whereas the aromatic peak (C=C) at 1607 cm^{-1} remained stable and therefore chosen as the internal standard. The graph also shows that the aliphatic (C=C) peak decreases with the light exposure whereas the aromatic (C=C) peak remains relatively stable during polymerisation.

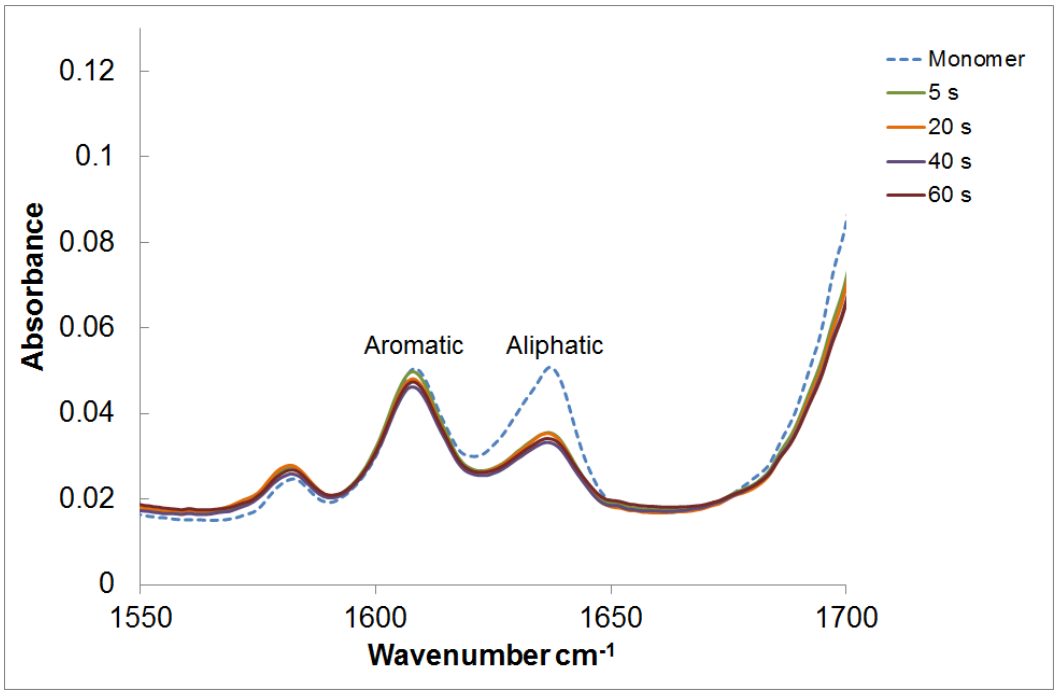

Figure 39: A representative FTIR spectra in region of 1550-1700cm^{-1} from fluorapatite containing composite specimen (30FA).

5.5.2.1 Data distribution

The Shapiro-Wilk test was conducted to evaluate the data distribution. The results showed that all groups were normally distributed as shown in Appendix H, therefore a parametric multi comparison tests One-way ANOVA and the Post Hoc Tukey were carried out.

5.5.2.2 Descriptive and statistical analysis

The mean percentages of the Degree of conversion (DC) are shown in Table 14. FA containing composites showed mean DC of 44-60% at different time intervals. Statistical analysis carried out using the One-way ANOVA showed that there were statistically significant differences between the experimental and the commercial composite groups at different time intervals ($p < 0.05$). Group comparisons were conducted using the post Hoc Tukey test which showed the differences between the groups at different time intervals (Appendix I and Appendix J).

Table 14: Group comparisons showing the mean Degree of Conversion with their standard deviation (SD) for FA containing and commercial composites tested.

Time	TC		0FA		10FA		20FA		30FA		40FA	
	Mean	SD	Mean	SD	Mean	SD	Mean	SD	Mean	SD	Mean	SD
5 s	41.3	7.5	53.9	1.8	53.5	1.5	46.4	2.6	51.6	2.2	45.1	2.9
10 s	41.4	1.3	58.0	4.2	50.6	2.3	53.2	0.5	50.9	4.7	45.3	3.7
20 s	47.3	0.8	56.5	4.1	56.9	1.7	54.8	4.2	56.2	2.0	50.9	2.4
30 s	49.2	1.1	58.1	3.9	53.7	5.5	53.0	6.3	54.6	4.7	50.7	1.9
40 s	51.8	0.5	61.0	4.6	57.8	1.8	54.8	7.2	54.0	5.4	56.6	4.4
50 s	53.0	4.1	62.1	5.1	59.1	3.4	54.8	7.2	61.5	2.8	53.3	4.1
60 s	55.0	3.9	62.9	3.6	56.1	4.8	59.8	4.0	60.4	4.4	55.9	3.9

Commercial and experimental composites comparisons

TC has a significantly lower DC compared to composite groups 0FA, 10FA, 20FA and 30FA at short curing times from 5-20 s ($p < 0.05$). However the DC of TC increases further after curing for extended times (30, 40 and 60 s) with no significant differences compared to all FA containing composite groups ($p > 0.05$), Figure 40. Due to the continuous increase in the DC of 30FA at 50 s, the DC of TC remains significantly lower when compared to 30FA ($p > 0.05$).

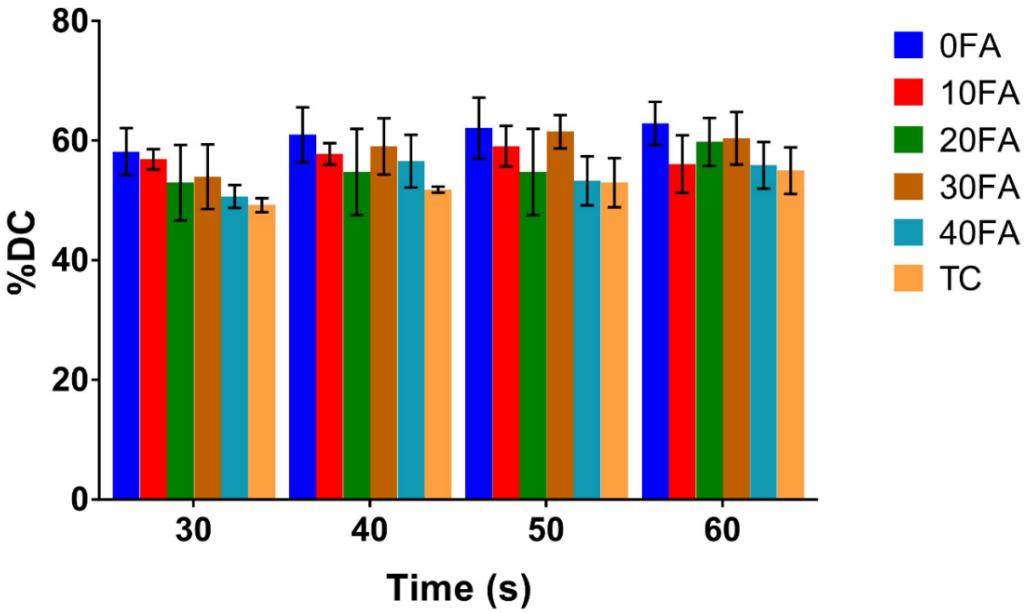

Figure 40: The mean DC with the standard deviation (error bars) for FA containing composites and commercial composite (TC) groups between 30-60 s curing times.

Comparisons between the groups with different FA concentrations

40FA and 20FA composite group showed significantly lower DC when compared to 0FA and 10FA at 5 s curing time ($p < 0.05$). 40FA DC remained significantly lower when compared to 0FA, 10FA, 20FA and 30FA at 10 s curing time ($p < 0.05$). However there were no significant differences between all experimental groups at extended curing times from 20-60 s curing times ($p > 0.05$), Figure 41.

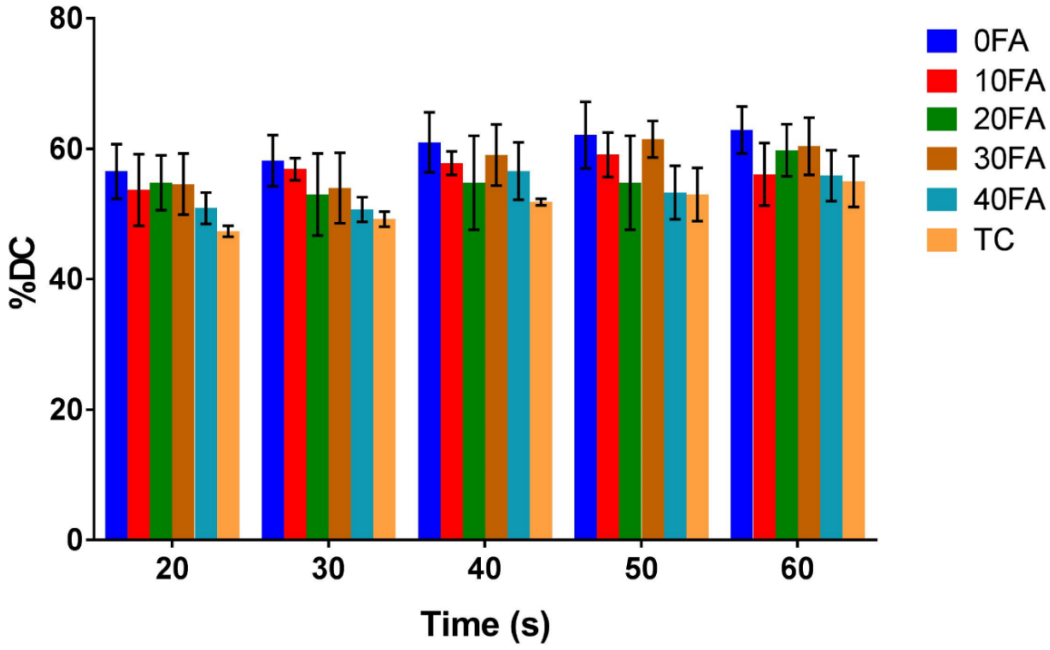

Figure 41: The mean DC with the standard deviation (error bars) for FA containing composites and the control groups (0FA and TC) between 20-60 s curing times.

5.5.3 *In-vitro* wear resistance

5.5.3.1 Data Distribution

The Shapiro-Wilk test was conducted to evaluate the data distribution. The results showed that all groups were not normally distributed as shown in Appendix K, therefore a non-parametric test Kruskal-Wallis was carried out.

5.5.3.2 Descriptive and statistical analysis

The wear results showed that there were no statistically significant differences between the FA composites and TC ($p > 0.05$). There were also no significant differences between the FA containing composites regardless of the percentage of the FA content ($p > 0.05$), Appendix L. The wear values by volume loss (mm^3) are shown in Table 15 and Figure 42.

Table 15: Group comparisons of the volume loss values (mm^3) between FA containing composites and TC

Group	Mean	Median	Std. Deviation
TC	0.023	0.021	0.004
0FA	0.019	0.020	0.004
10FA	0.027	0.023	0.005
20FA	0.026	0.030	0.005
30FA	0.028	0.024	0.008
40FA	0.026	0.020	0.009

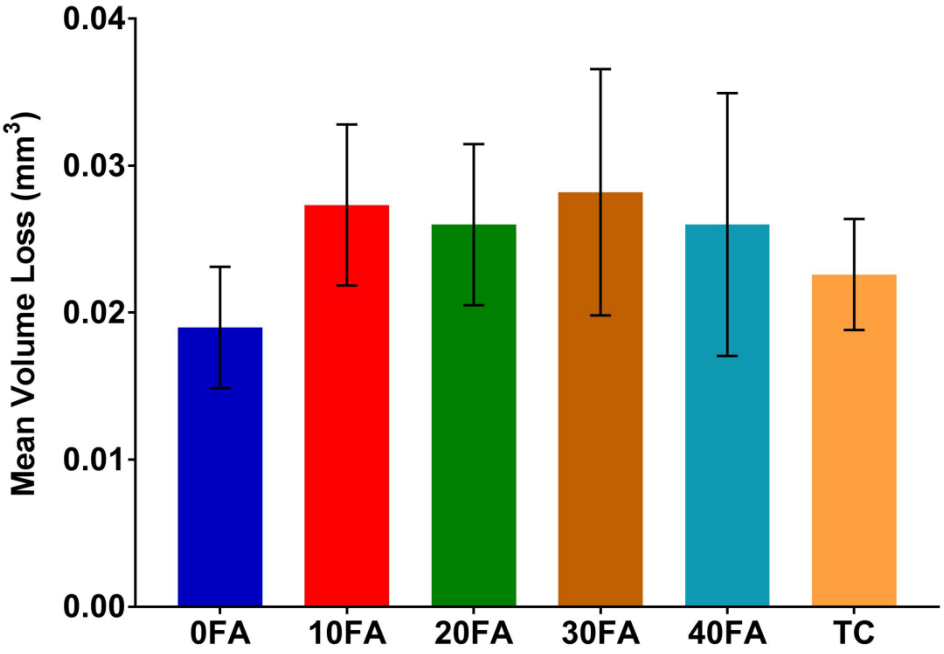

Figure 42: Group comparisons of the mean wear values by volume loss (mm^3) with their standard deviation (error bars) between FA containing composites and TC.

5.5.3.3 Profilometry

The wear tracks of all FA containing groups were shallow as shown in Figure 43. Wear loss measurement were also taken by using the unworn area as a datum for volume loss (mm^3) measurements.

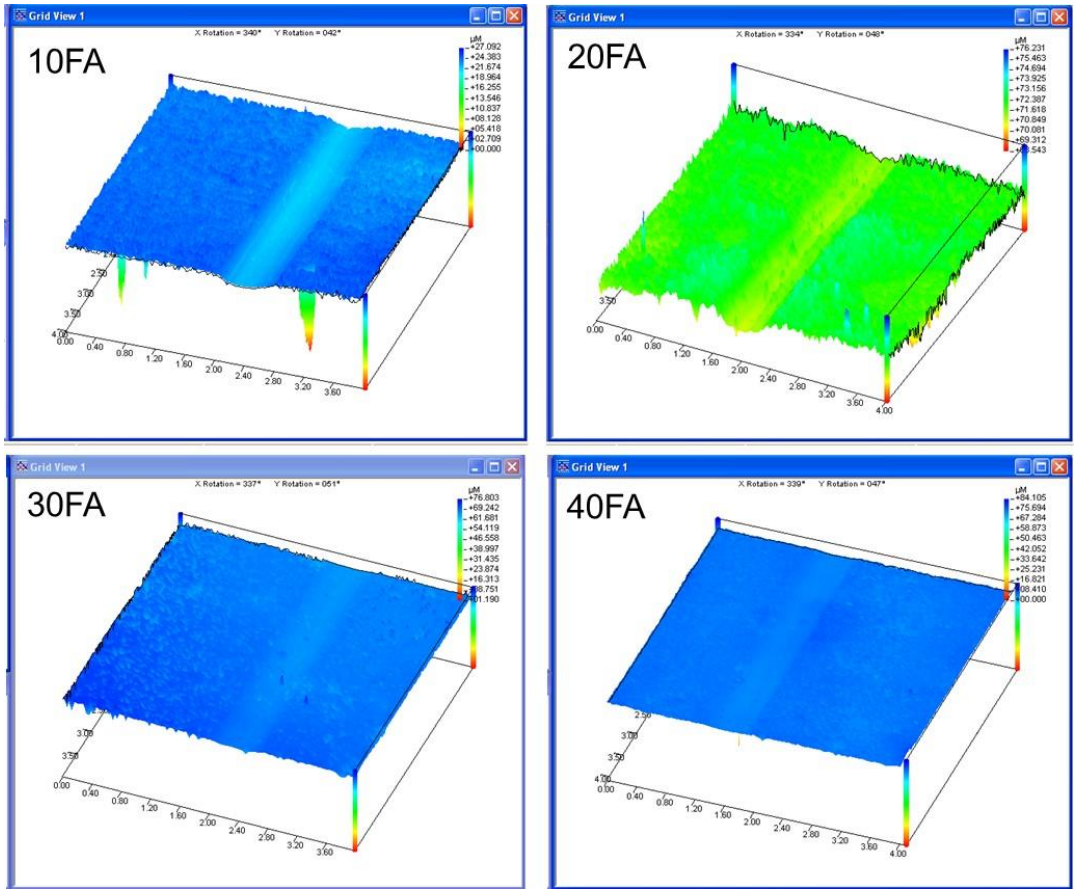

Figure 43: Profilometric scans showing representative wear tracks from the tested FA containing composite groups.

5.5.3.4 SEM and Elemental Mapping

Analysis of the wear tracks of FA containing composites also showed micro grooves within the resin matrix running in the direction of the wear track; damaged and pulled out individual FA crystals were also seen leaving hexagonal voids within the resin matrix. However, larger FA bundles remained imbedded with the resin matrix. Figure 44 shows representative examples of the scanned wear tracks. The steatite abrading antagonists were also analysed, Figure 46 show round shaped wear facets corresponding to the shape of the wear tracks. Magnification of the wear facets showed material deposition on the surface, Figure 48. EDX analysis was conducted to identify the elemental composition of the deposited material, scanned images showed Ca and P elements corresponding to FA and Mg which is one of the main component of steatite, Figure 49.

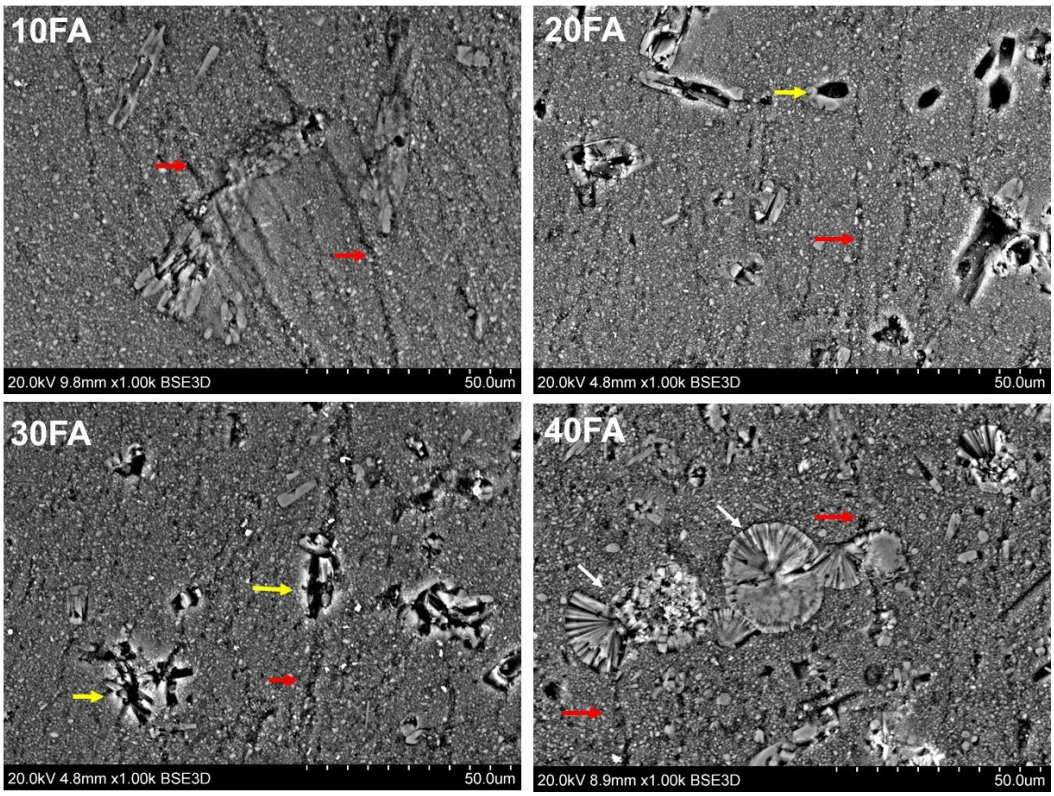

Figure 44: SEM images of the wear tracks of FA containing dental composites. Typical wear track showed vertical micro grooves running through the matrix (red arrows) and pull out and damage to the FA crystals (yellow arrows). Larger FA bundles were still imbedded within the resin matrix (white arrows).

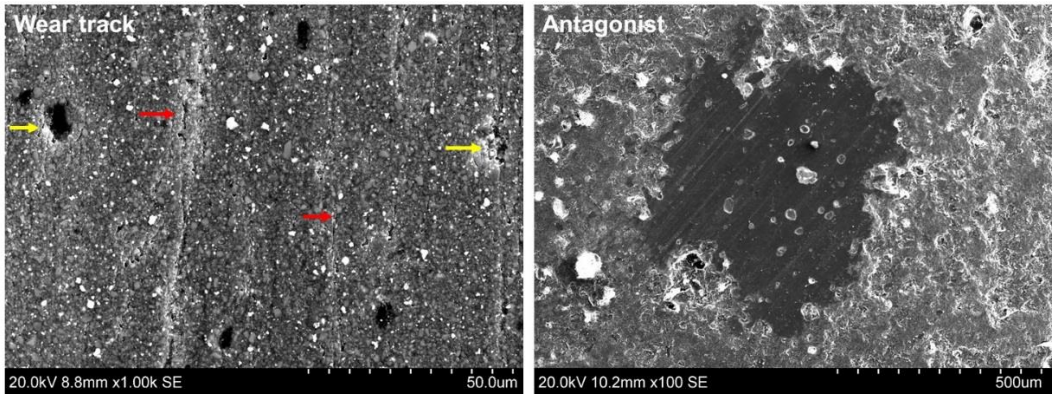

Figure 45: SEM images showing the wear track and the corresponding steatite antagonist of a TC sample. Evident micro-grooves running in the direction of the wear track (red arrows) and voids corresponding to pulled-out filler particles (yellow arrow). Distinctive round wear facet is shown on the abrading antagonist.

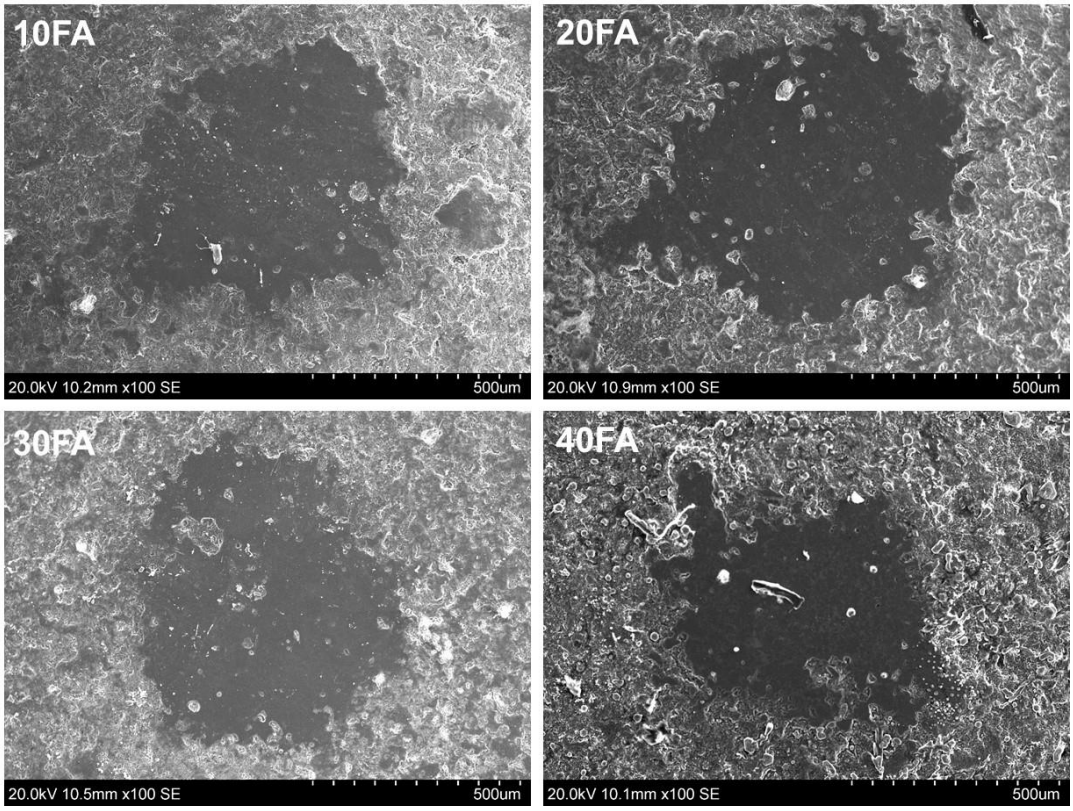

Figure 46: SEM images of the steatite abrading antagonists corresponding to the wear tracks of FA containing composites.

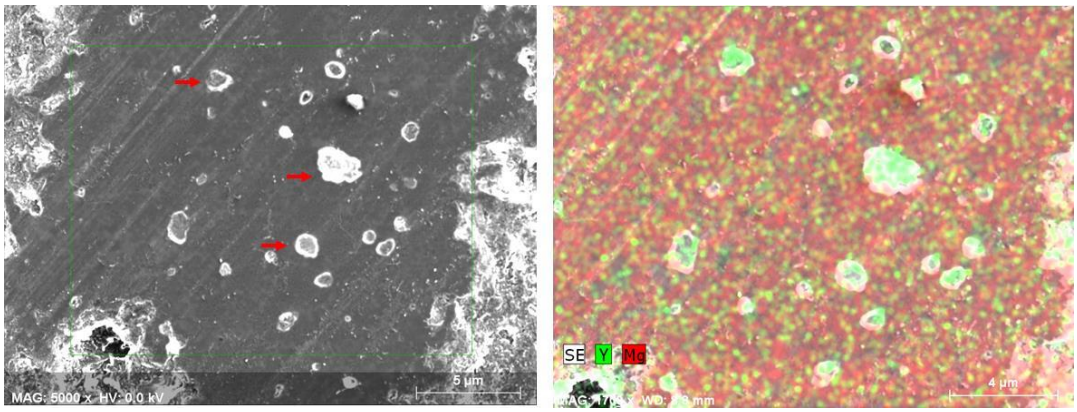

Figure 47: SEM and elemental map of TC antagonist. The SEM shows the wear facet with material deposited on the surface (red arrows). The elemental map shows yttrium element deposition on the surface corresponding to the TC composite filler.

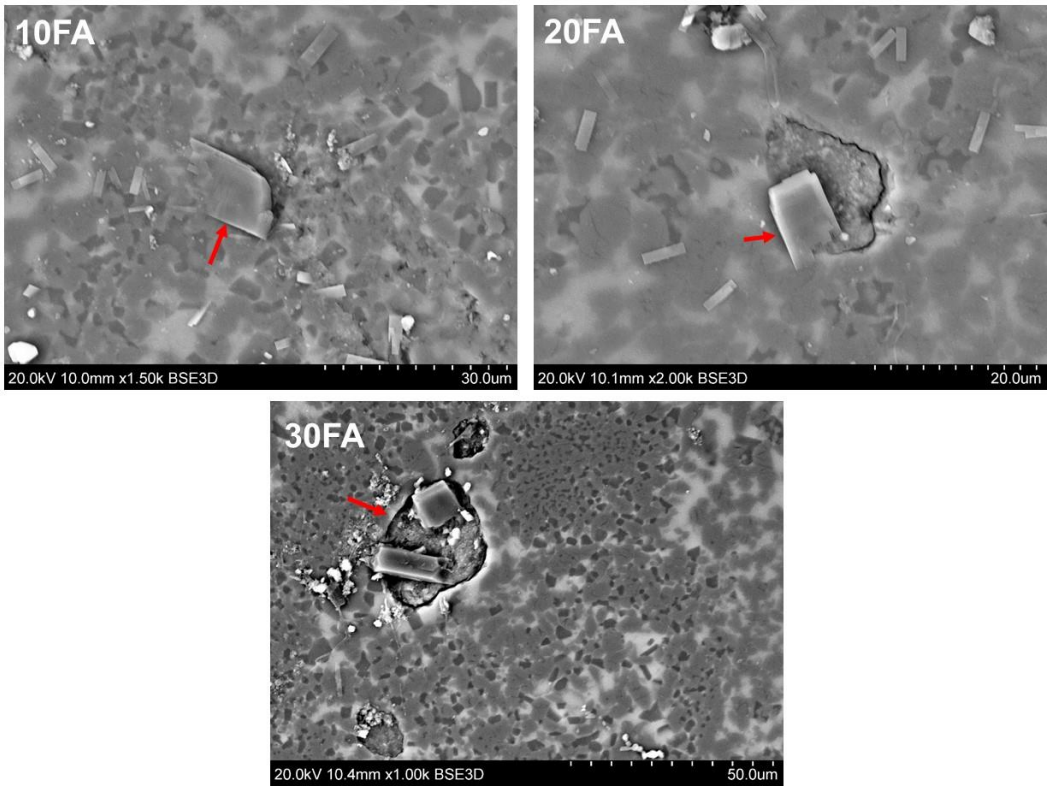

Figure 48: SEM images showing magnifications of the steatite wear facet surfaces corresponding to FA composites. Evident material deposition on the surface is shown (red arrows).

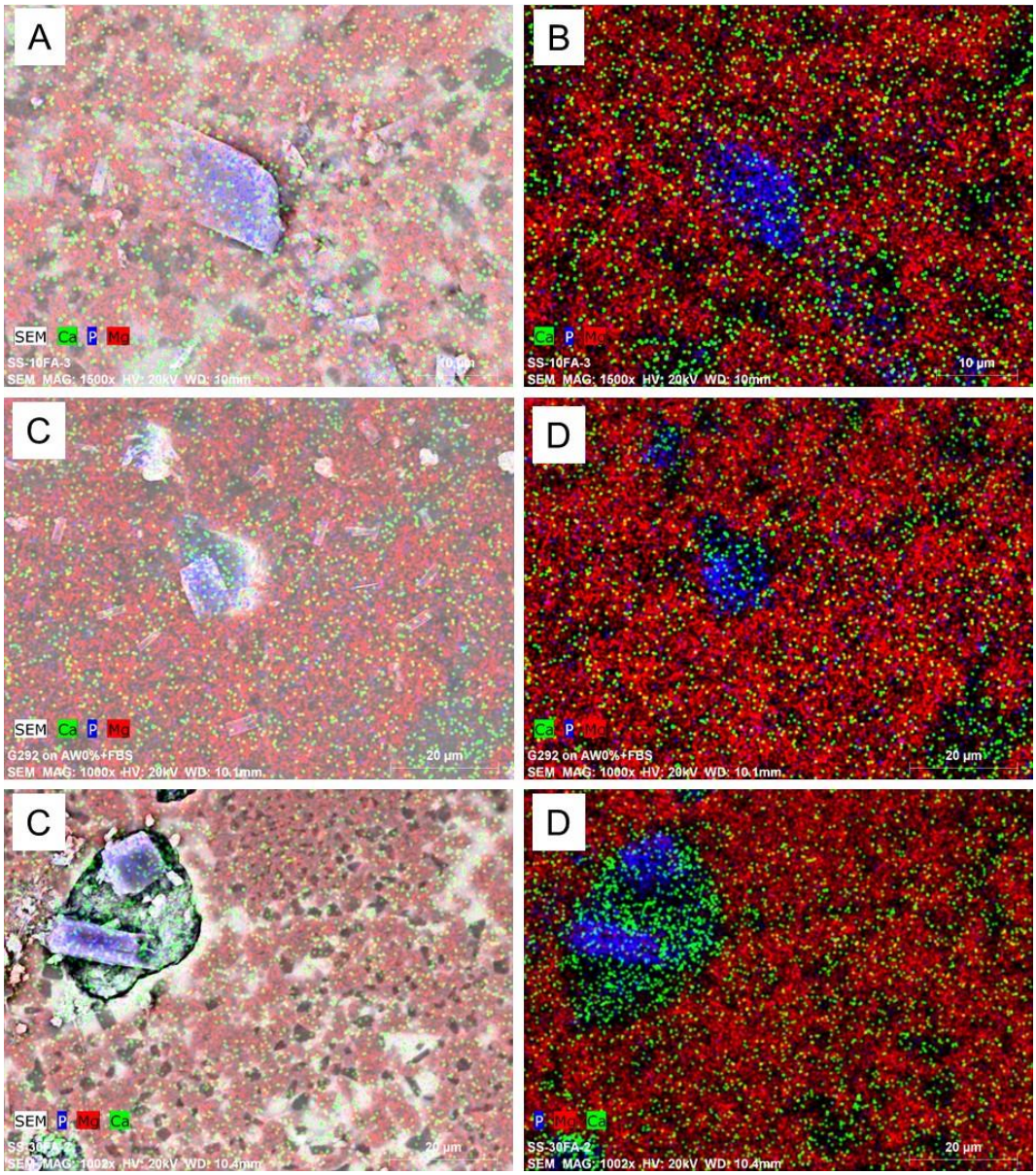

Figure 49: EDX analysis of the steatite wear facet surfaces. Elemental analysis shows Ca and P elements corresponding to the deposited material and Mg which is one of the main components of steatite.

5.5.4 Vickers Microhardness

5.5.4.1 Data Distribution

The Shapiro-Wilk test was conducted to evaluate the data distribution. The results showed that all groups were normally distributed as shown in Appendix M, therefore a parametric multi comparison tests One-way ANOVA and the Post Hoc Tukey were carried out.

5.5.4.2 Descriptive and statistical analysis

Table 16 and Figure 50 show the microhardness results group comparisons. The results showed that TC has a significantly lower HV compared to all the experimental FA composite groups ($p < 0.05$). Whereas there were no statistically significant differences between the FA containing groups regardless of the FA concentration ($p > 0.05$). (Appendix S and Appendix T).

Table 16: Group comparison of HV values between FA containing composites and TC.

Group	Mean	Median	Std. Deviation
TC	53.4	54.3	3.5
0FA	93.2	91.9	2.8
10FA	95.2	94.8	1.6
20FA	94.7	95.1	1.7
30FA	93.9	94.3	2.3
40FA	94.3	94.6	1.9

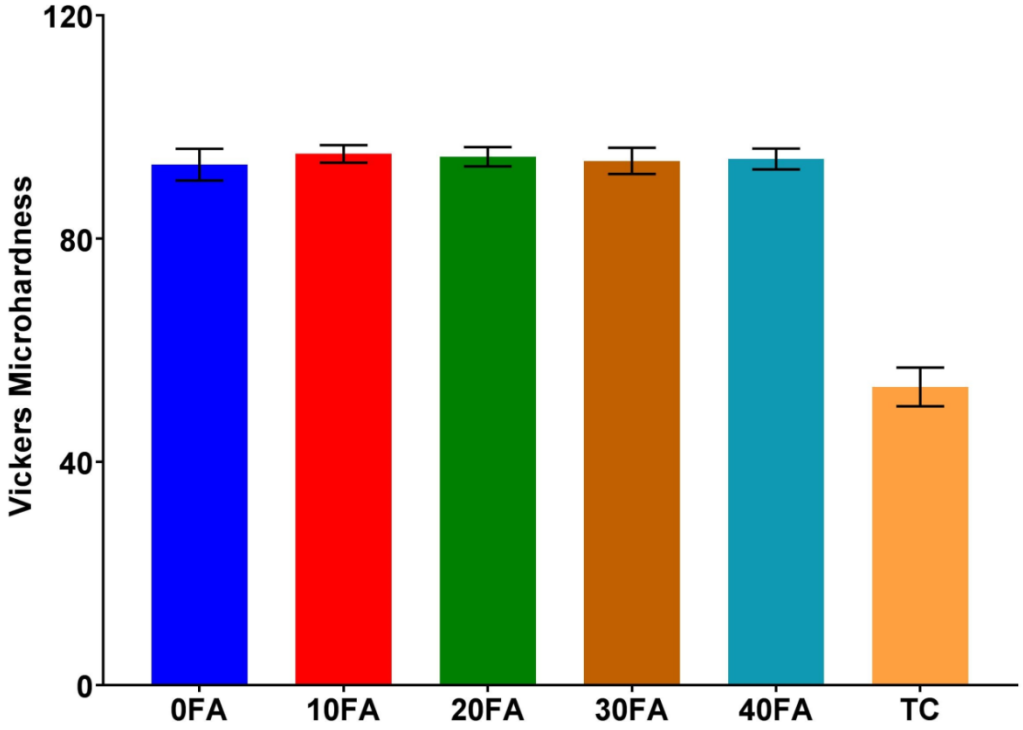

Figure 50: Group comparisons of HV values with their standard deviation (error bars) between FA containing composites and TC.

5.5.5 Flexural strength and flexural modulus

5.5.5.1 Data Distribution

The Shapiro-Wilk test was conducted to evaluate the data distribution. The results showed that the data was not normally distributed as shown in Appendix N, therefore the non-parametric Kruskal-Wallis and the Post Hoc Bonferroni tests were carried out, Appendix O and Appendix P

5.5.5.2 Descriptive and statistical analysis

The flexural strength (MPa) and flexural modulus (GPa) results are shown in Table 17, with group comparisons shown in Figure 51 and Figure 52. 0FA showed the highest flexural strength which was statistically significant when compared to all tested groups ($p < 0.05$). However there were no statistically significant differences in the flexural strength of 10-40FA when compared to TC ($p > 0.05$). The increase in the FA concentration lead to a

decrease in the flexural strength values but this decrease was not statistically significant ($p > 0.05$).

Flexural modulus data also showed that 0FA had the highest flexural modulus value which was statistically significant when compared to all other tested groups ($p < 0.05$). However TC showed the lowest flexural modulus value which was also statistically significant when compared to all FA containing composites ($p < 0.05$). All FA composites showed similar flexural modulus regardless of the amount of FA added ($p > 0.05$).

Table 17: The Flexural strength (MPa) and Flexural modulus (GPa) mean, median and standard deviation (SD) values of the experimental and the commercial dental composites.

DC	Flexural Strength (MPa)			Flexural Modulus (GPa)		
	Mean	Median	SD	Mean	Median	SD
TC	88.64	90.39	17.45	10.22	10.56	0.77
0FA	113.12	99.83	30.10	14.63	13.74	1.27
10FA	80.21	73.91	15.76	12.05	11.65	1.89
20FA	80.56	77.93	10.01	12.19	12.30	0.92
30FA	74.54	71.04	12.49	12.08	11.51	1.73
40FA	68.38	67.05	9.40	12.05	12.05	0.01

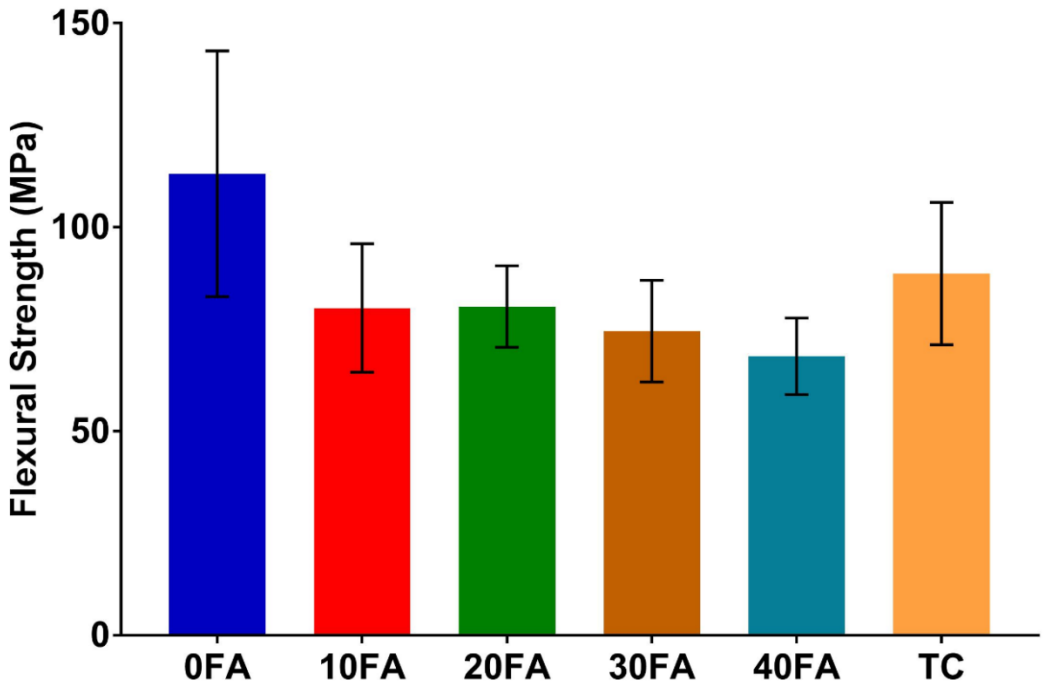

Figure 51: Group comparisons of the flexural strength values (MPa) with their standard deviation (error bars).

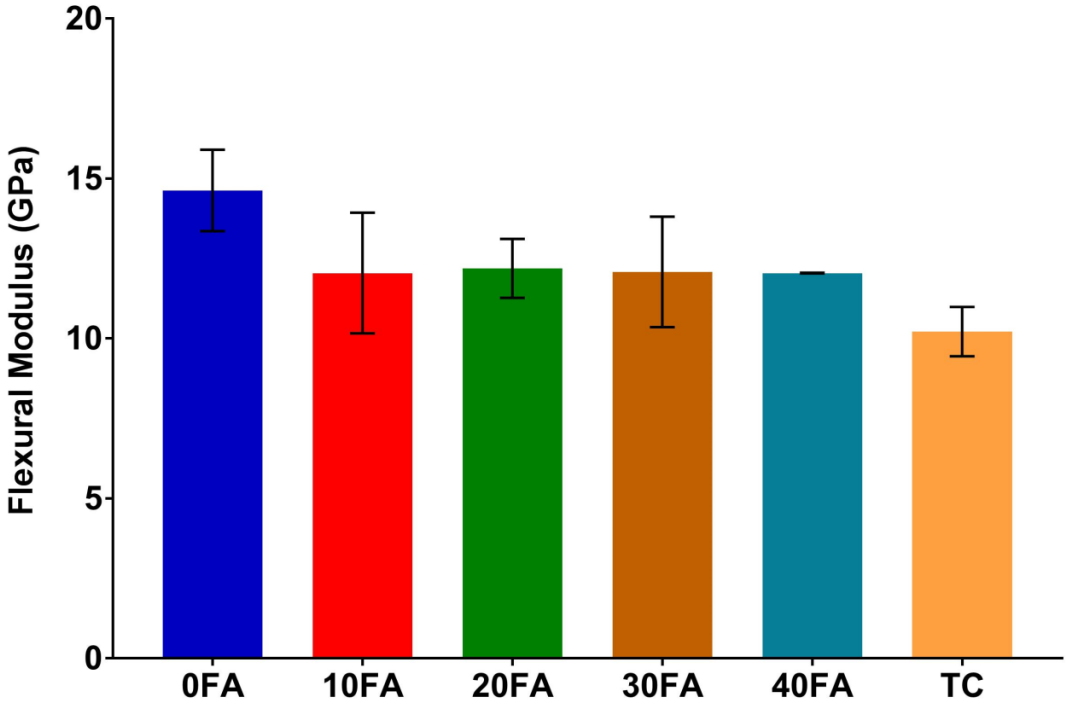

Figure 52: Group comparisons of the flexural modulus values (GPa) with their standard deviation (error bars)

5.5.5.3 SEM observations

Analysis of the fractured surfaces showed micro cracks running through the resin matrix and disintegration of the filler particles leaving a rough fractured surface. Larger pre-polymerised filler particles present in TC were found protruding through the matrix on one fractured surface leaving a corresponding space on the opposing surface, Figure 53 (A and B). 0FA fractured specimen showed a smooth fracture surface with minimal surface irregularity, Figure 53 (C and D). FA containing groups showed very similar fractured surfaces with micro cracks running through the matrix and deflecting around larger FA bundles, scanned surfaces also showed detached smaller FA crystals leaving hexagonal spaces corresponding to their original shape within the matrix, Figure 54.

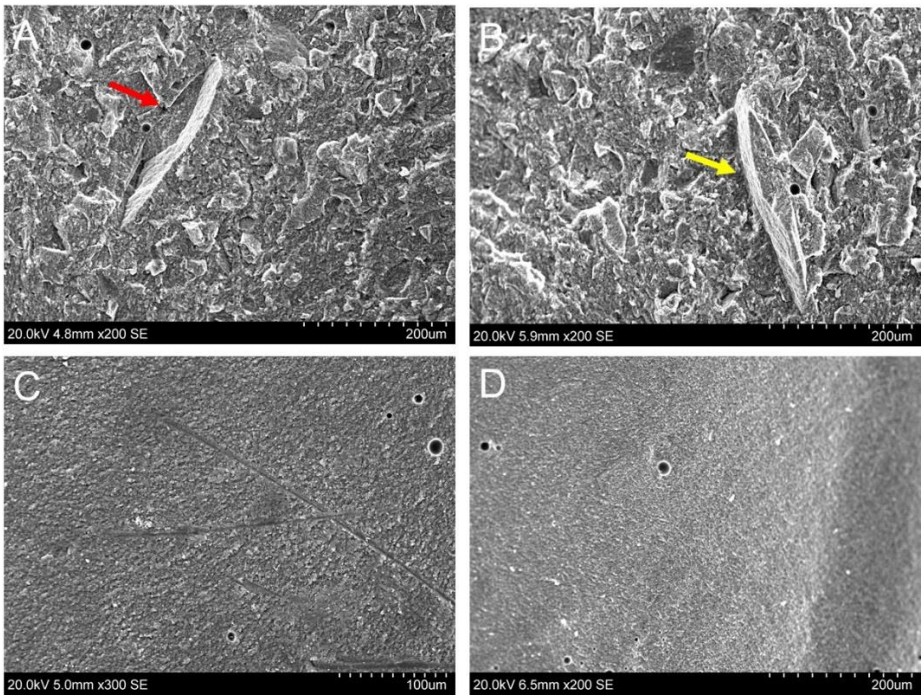

Figure 53: SEM of the fractured surfaces after flexural strength testing. (A,B) Show two opposing fractured surfaces of TC composite specimen with micro cracks running through an irregular matrix, it also shows a large filler particle which has been pull-out leaving a void within the matrix (red arrow); the opposing fractured surface shows the pulled-out filler deposited on the surface (yellow arrow). (C,D) Show the fractured surfaces of 0FA composite specimen with smooth distinct fractured surfaces.

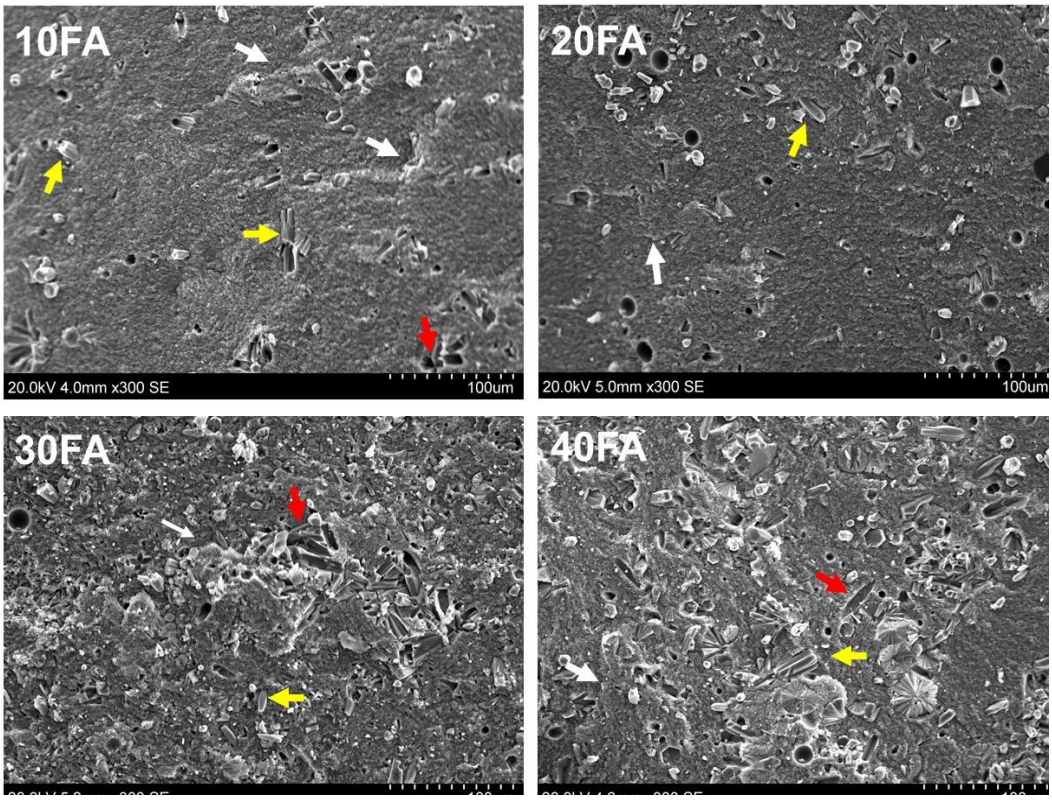

Figure 54: SEM images of the fractured surfaces of FA containing composite specimens post flexural strength testing. Fractured surfaces showed micro cracks (white arrows) and pull-out of FA crystals (yellow arrows) leaving voids corresponding to the lost FA crystals within the matrix (red arrows).

5.5.6 Fracture Toughness (K_{1C})

5.5.6.1 Data Distribution

The Shapiro-Wilk test was conducted to evaluate the data distribution. The results showed that the data was normally distributed as shown in Appendix N, therefore a parametric multi comparison tests One-way ANOVA and the Post Hoc Tukey were carried out, Appendix Q and Appendix R.

5.5.6.2 Descriptive and statistical analysis

Table 18 and Figure 55 show the fracture toughness values ($MPa.m^{(1/2)}$) for the experimental and the commercial composite groups.10FA and 20FA groups showed the lowest fracture toughness values when compared to TC, 30FA and 40FA ($p < 0.05$). The concentration of FA used did not affect the fracture toughness values as the results showed no significant differences between TC, 0FA, 30FA and 40FA ($p > 0.05$).

Table 18: Fracture toughness ($MPa.m^{(1/2)}$) mean, median and standard deviation (SD) of experimental and commercial dental composites.

DC	Mean	Median	SD
TC	1.37	1.38	0.10
0FA	1.29	1.28	0.23
10FA	0.87	0.92	0.14
20FA	0.87	0.87	0.10
30FA	1.46	1.40	0.42
40FA	1.21	1.18	0.06

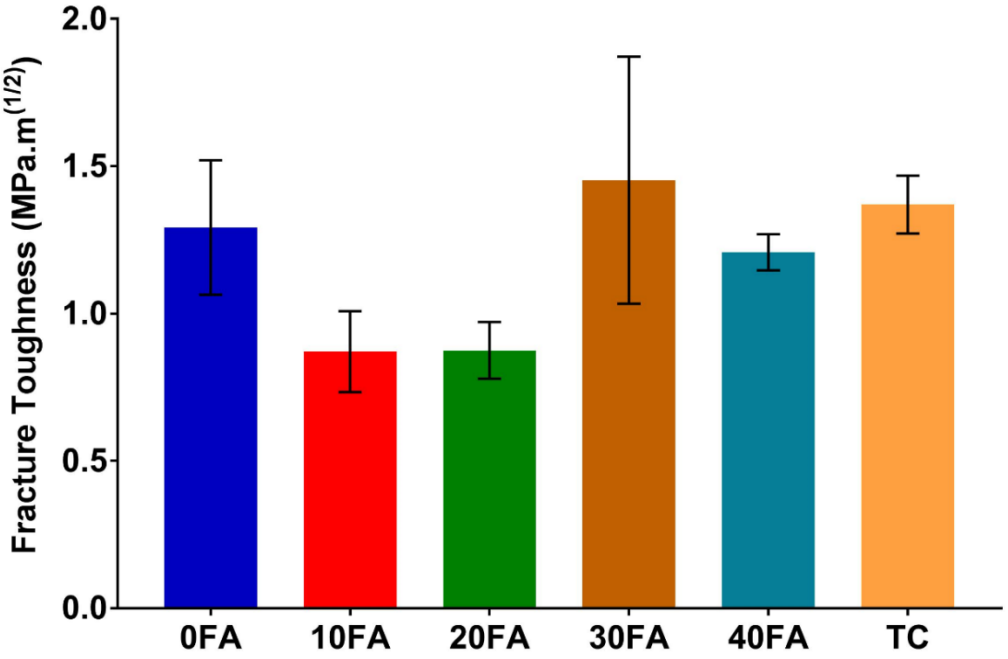

Figure 55: Group comparisons of the fracture toughness values (MPa.m$^{(1/2)}$) with their standard deviation (error bars).

5.5.6.3 SEM observations

Fracture specimens were analysed to evaluate the origin of the fracture line in relation to the pre-cracked area. Figure 56 show representative examples of the fracture lines extending from the pre-inserted notch. Clear cracks were seen extending from the pre-inserted notch with distinctive two fractured surfaces in TC and 0FA composites, however FA containing composites showed clear cracks with FA bundles and rods bridging between the two fractured surfaces as seen in 40FA composite sample shown in Figure 57.

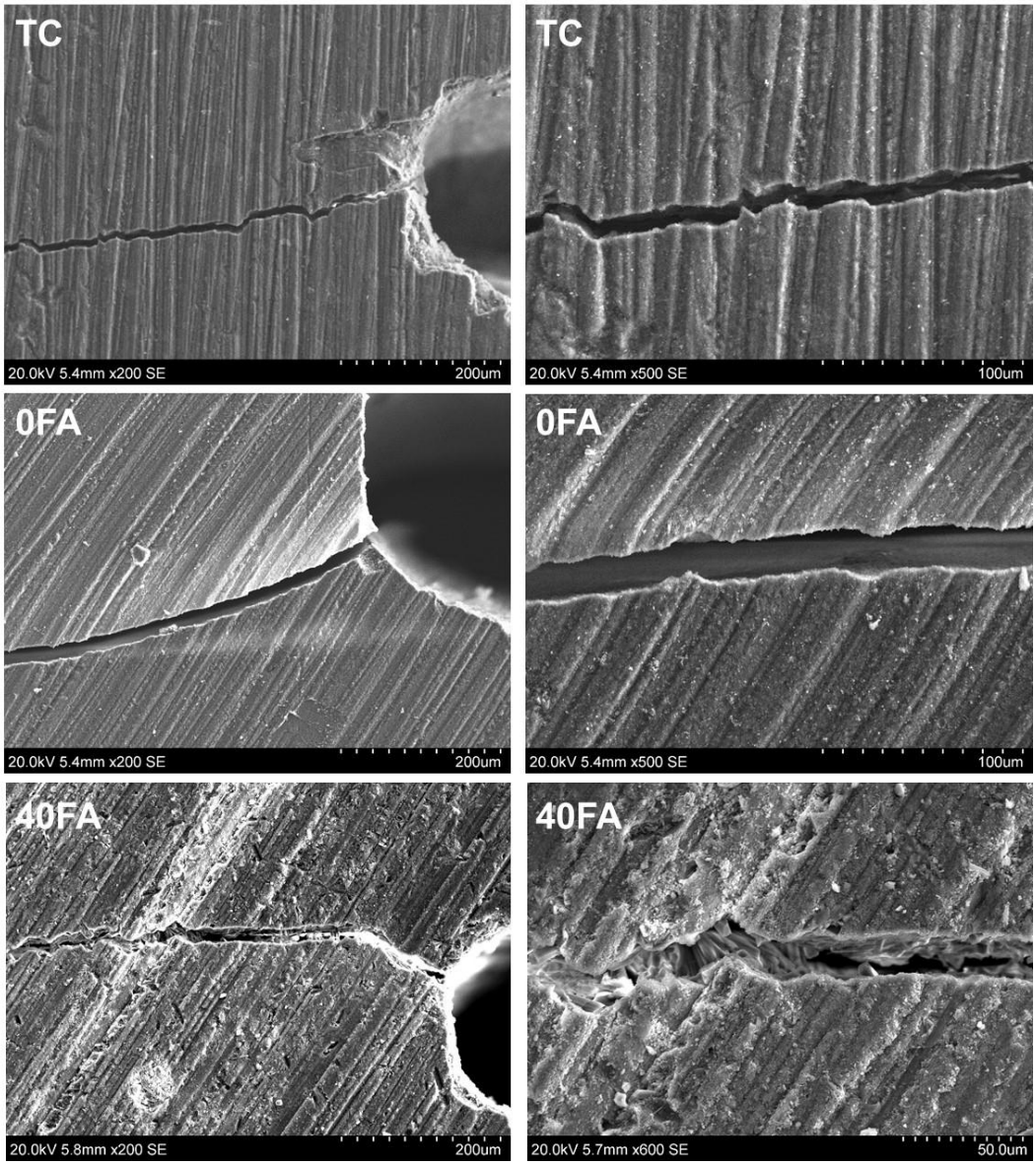

Figure 56: SEM images showing the crack extension from the pre-cracked area and magnifications of the crack line within the samples. TC and 0FA show clear cut crack running through the sample. 40FA shows FA crystals and bundles bridging between the two fractured surfaces.

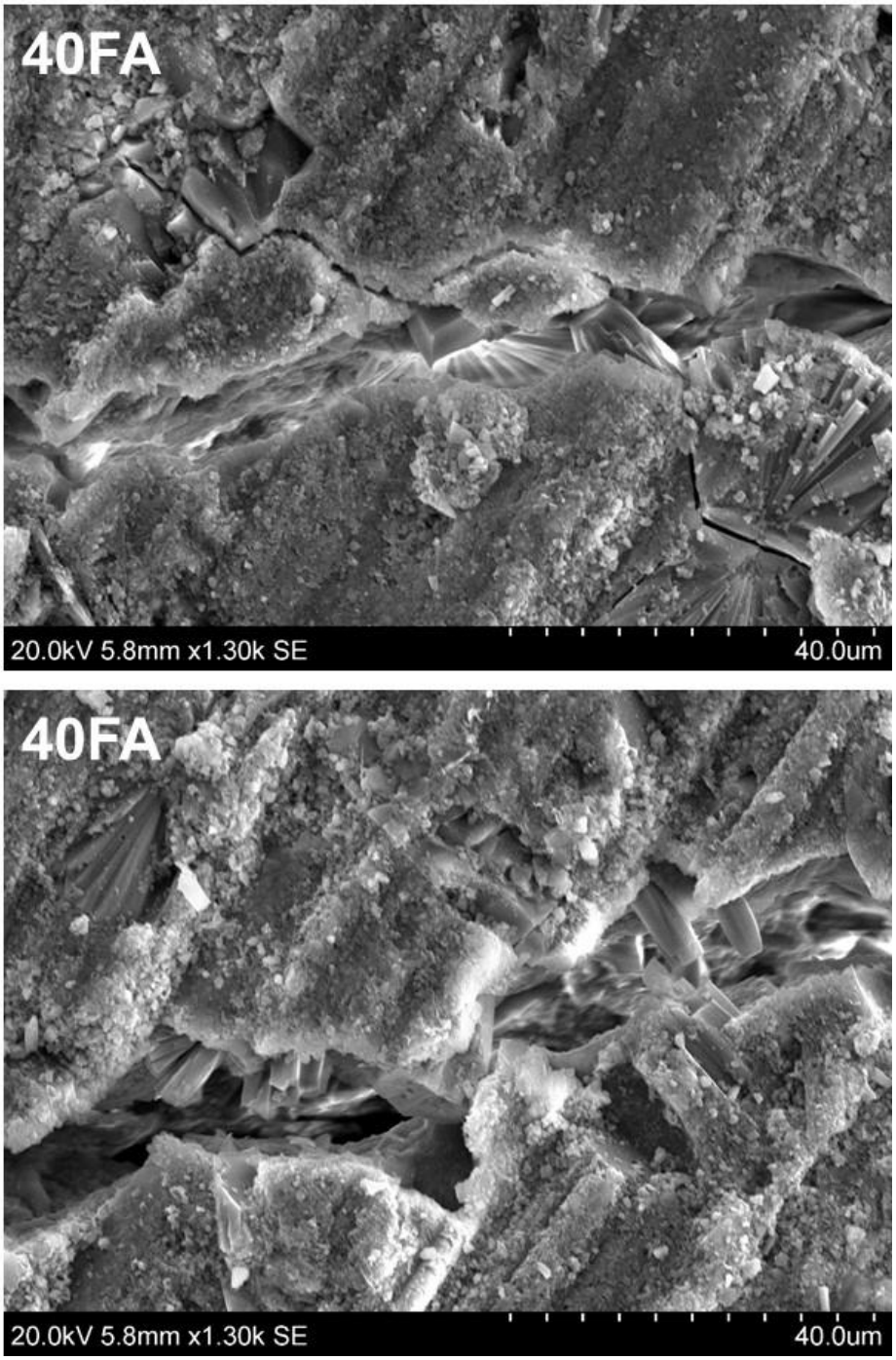

Figure 57: SEM images showing magnifications of the crack line in 40FA composite specimen FA crystals and bundles positioned in the crack line and bridging between the two fractured surfaces.

SEM analysis of the fractured specimens showed three distinct zones: (1) The pre-cracked area shows a flat compact surface with the filler particles tightly embedded within the resin matrix, (2) the transitional zone with an irregular surface and displaced filler/matrix and (3) the fractured surface

with visible crack lines and detached fillers leaving spaces within the resin matrix. Typical example of the fracture zones is shown in Figure 58 (A and B). To identify the fracture mechanisms involved, the two fractured surfaces of each specimen were scanned. SEM observations showed two distinct fracture phenomena: (1) The presecne of major and micro crack lines running through the matrix and (2) The detachment of fillers from the resin matrix leaving spaces corresponding to their shape. The detachment of filler particles was particularly evident in TC which showed detached PPFs deposited on the fractured surfaces leaving spaces within the matrix on the opposing surfaces, representative examples are shown in Figure 58 (C and D) and Figure 59.

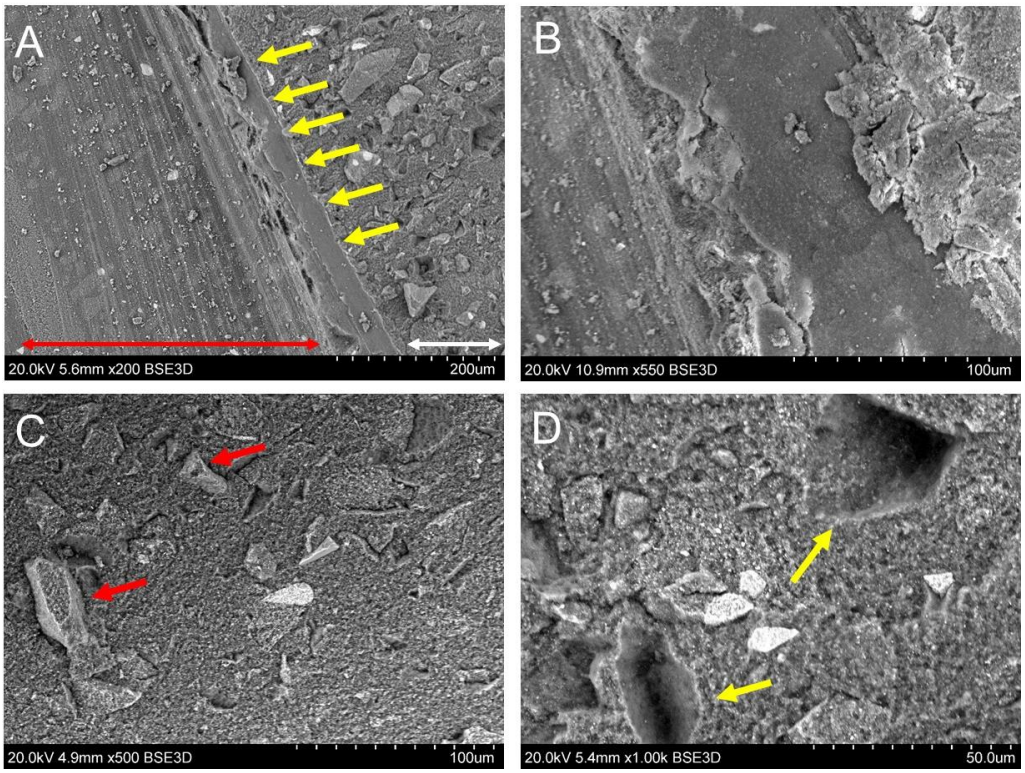

Figure 58: SEM images of a fractured TC specimen. (A) Shows three zones within the specimen: The pre-cracked surface (red arrow), the transitional zone (yellow arrows) and the fractured surface (white arrow). (B) Show magnifications of the transitional zone with pull-out offiller/matrix amongst an irregular surface. (C) Shows the fractured surface with detached filler particles (red arrows) and (D) shows a micro-crack (while arrow) running through the matrix with spaces corresponding to lost fillers (yellow arrows).

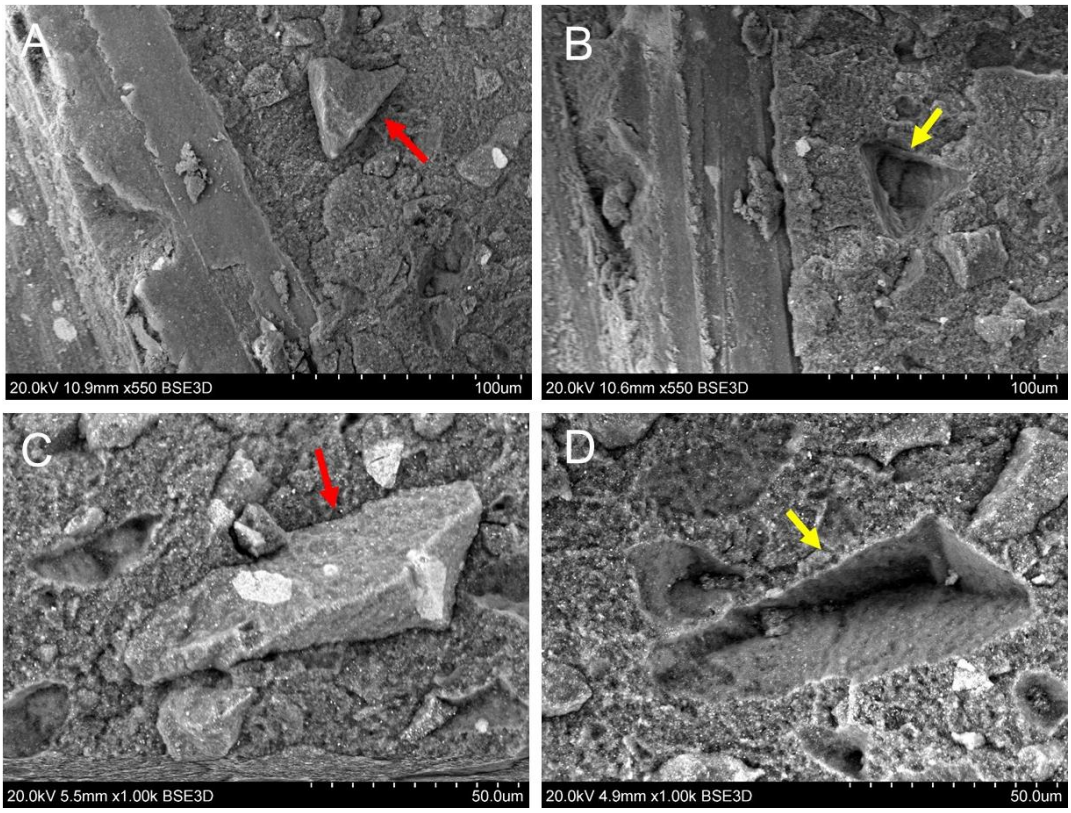

Figure 59: SEM images of two matching fractured surfaces of TC specimen. (A) Shows the fractured zone with evident detached PPF particles deposited on the surface, (B) shows the corresponding fractured surface with evident lost filler particles leaving spaces within the matrix. (C) Shows another detached large PPF on the fractured surface which corresponds to a matching space on the opposing surface shown in (D).

SEM observations of FA containing composites also showed similar transition between the pre-cracked surface and the fractured surface dividing the sample into three distinct zones. Figure 60 (A and B) shows an example of 10FA composite sample with major vertical crack line running through the matrix in the transitional zone, it also shows an intact FA cluster which is imbeded within the matrix at the edge of the fracture zone. Figure 60 (C and D) and Figure 61 show magnifications of the fractured surfaces of 10FA and 20FA composites with similar fracture phenomena to TC, the fractured surfaces showed major and micro crack lines running through the matrix and detached FA crystals from the resin matrix leaving hexagonal spaces corresponding the shape of FA crystals.

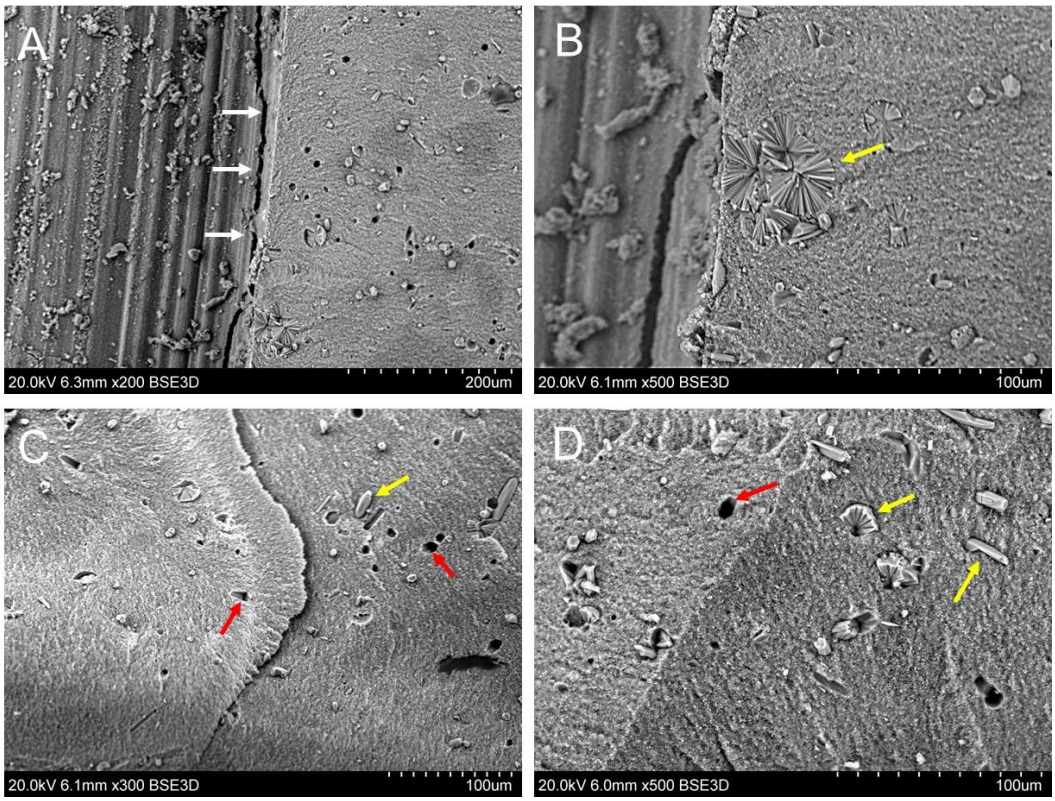

Figure 60: SEM images of 10FA fractured composite specimen. (A) Shows a major crack line running along the transitional zone interface. (B) Shows a cluster of FA (yellow arrow) securely imbedded within the matrix at the edge of the fractured zone. (C,D) show the fractured surface with cracks running through the matrix, detached FA crystals deposited on the surface (yellow arrows) and hexagonal spaces within the matrix corresponding to lost FA crystals (red arrows).

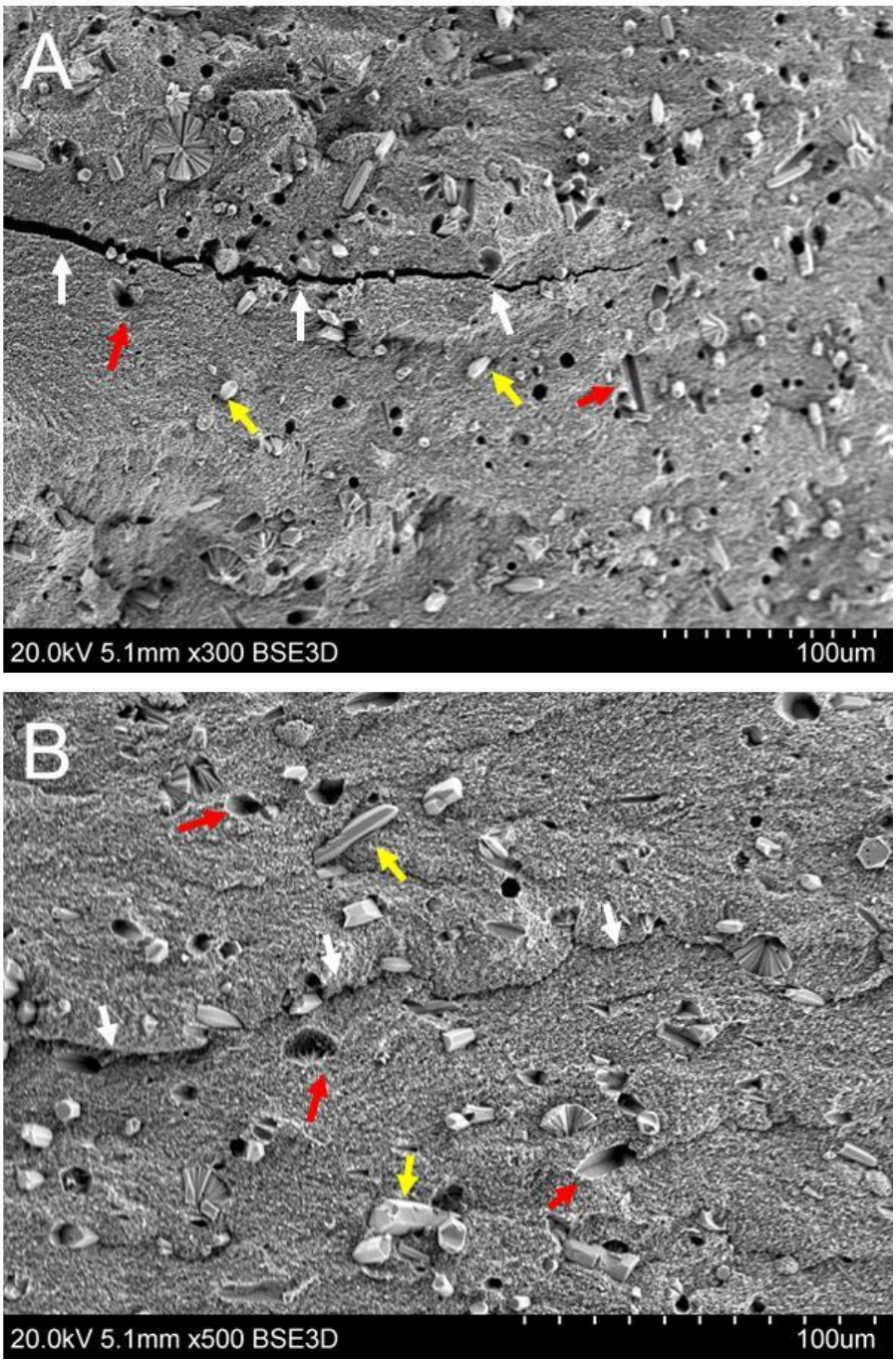

Figure 61: SEM images of 20FA fractured composite specimen. (A) and (B) shows major crack lines running through the matrix (white arrows), detached FA crystals deposited on the surface (yellow arrows) and hexagonal spaces within the resin matrix (red arrows).

Unlike TC and FA composites, 0FA showed compact clear fractured surface with mainly microcracks running through the matrix, representative example is shown in Figure 62.

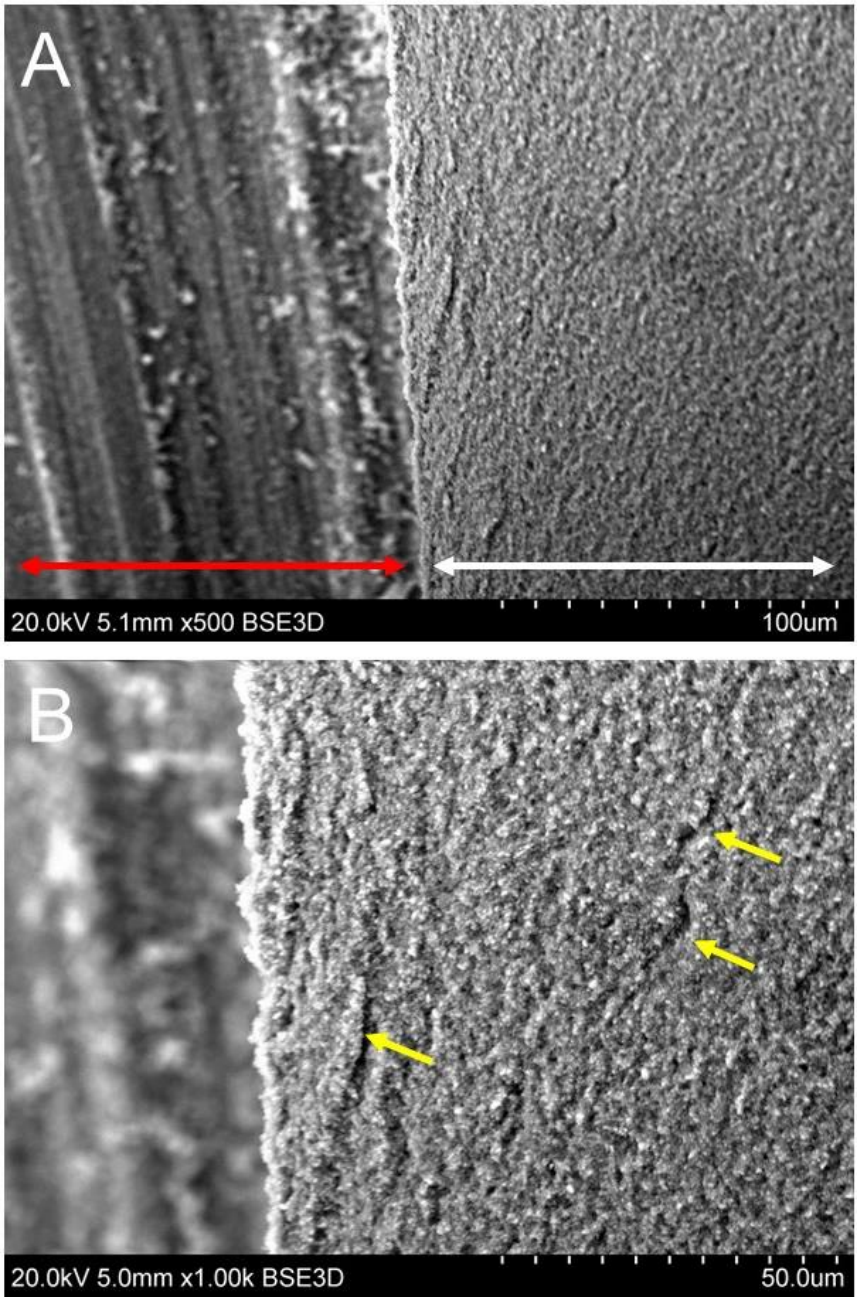

Figure 62: SEM of fractured 0FA composite specimen. (A) Shows the pre-crack zone (red arrow) and the fractured zone (white arrow). (B) shows clear fractured surface with microracks running through the matrix.

30FA and 40FA fractured surfaces also showed similar fracture features to TC, 10FA and 20FA composites. The three fracture zones were evident with fractured surfaces showing interfacial cracking and filler detachment from the resin matrix leaving a rough fractured surface, Figure 63.

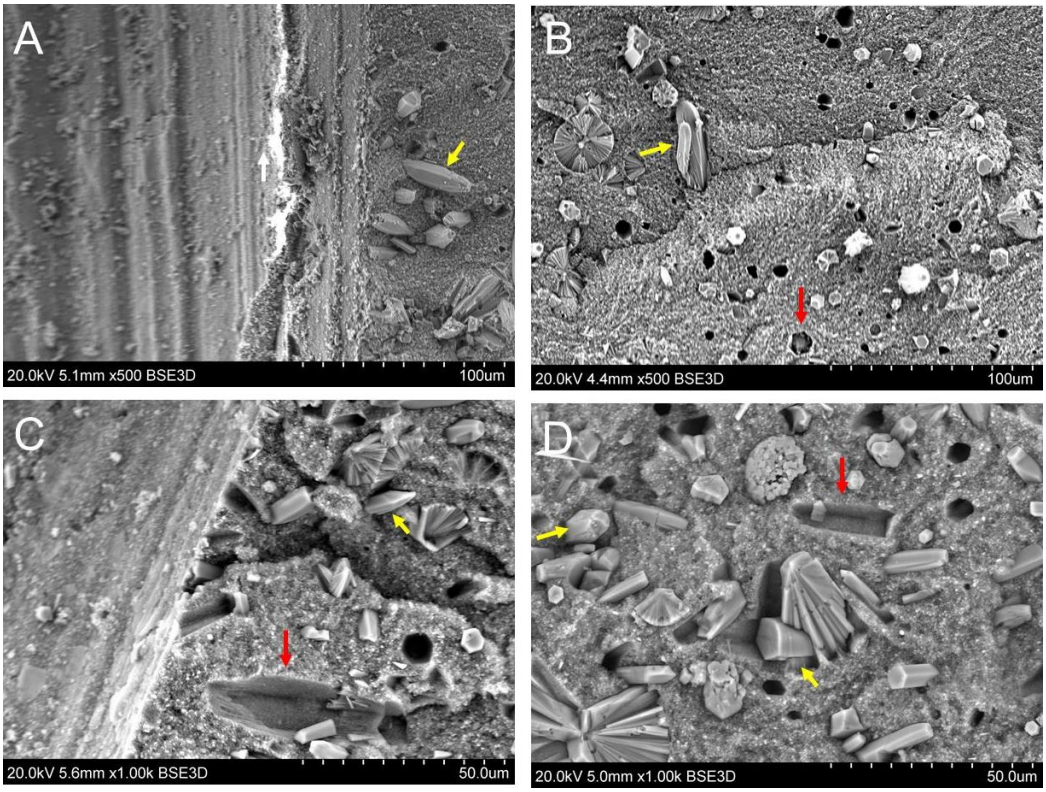

Figure 63: SEM images of fractured 30FA (A,B) and 40FA (C,D) composite specimens. (A,C) Show the three fracture zones with detached FA crystals (yellow arrows) deposited at the edge of the fractured zone and spaces within the matrix corresponding to lost fillers (red arrows). (B,D) Show magnified fractured zone with micro cracks, detached FA fillers (yellow arrow) leaving spaces within the matrix (red arrows).

30FA and 40FA composites specimens also showed distinctive fracture toughening phenomena such as crack deflection and crack bridging near the tip of crack extension. These features were present when the tip of the crack encounters large FA crystals or bundles of crystals, representative examples are shown in Figure 64.

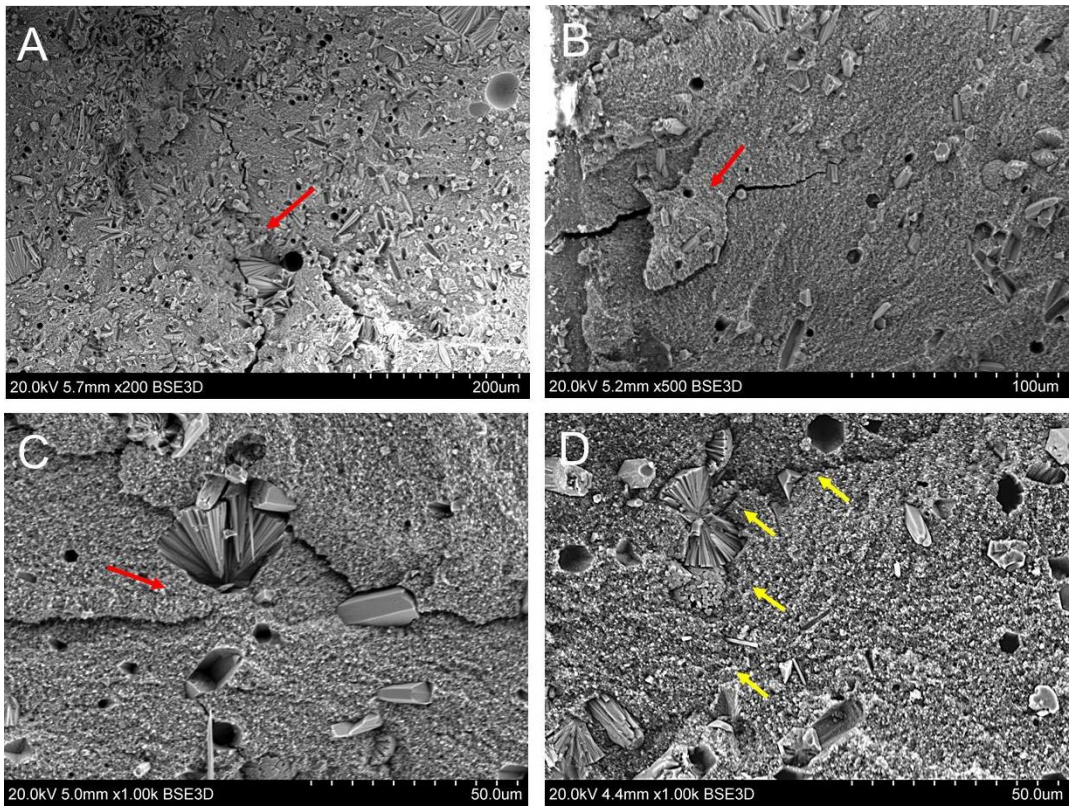

Figure 64: SEM of 30FA and 40FA fractured specimens showing typical fracture toughening mechanisms. (A-C) Show crack deflection and crack bridging (red arrows) when FA bundles are encountered and (D) Shows clear crack deflection when encountering an FA bundle which was broken through the middle (yellow arrows).

5.5.7 Fluoride release

The detection threshold of the ion selected electrode used in this study is > 0.03 µg/cm^2. Therefore, values ≤ 0.03 µg/cm^2 were considered as false negative. Under neutral conditions, the measured fluoride ions from all FA composites and the control groups were below the electrode threshold value (Table 19), therefore it was decided not to continue the measurements under neutral conditions. However under acidic conditions, all FA composites showed detectable fluoride ions (> 0.03 µg/cm^2), therefore a detailed descriptive and statistical analysis were conducted and will be described in the following sections.

Table 19: Measured fluoride ion release (µg/cm^2) in distilled water.

Group	24 hours	48 hours
TC	0.32	0.15
0FA	0.22	0.16
10FA	0.20	0.15
20FA	0.29	0.12
30FA	0.27	0.15
40FA	0.32	0.16

5.5.8 Data distribution

The Shapiro-Wilk test was conducted to evaluate the data distribution. The results showed that all groups were not normally distributed as shown in Appendix U. Therefore non-parametric multi comparison tests Kruskal-Wallis and the Post Hoc Bonferroni were carried out.

5.5.8.1 Descriptive and statistical analysis

The mean cumulative fluoride values (µg/cm^2) for the experimental composites and TC are shown Table 20 and Figure 65. The results showed that there was a significant difference in the fluoride release between the groups at all measured interval times, Appendix V. TC and 0FA groups had negligible amount of fluoride release starting from Day 1 up to Day 196.

5.5.8.2 Fluoride release profile

The pattern of fluoride release was similar amongst all FA containing composites with initial high release on Day 1 followed by a rapid decrease in the amount up to Day 7.

10FA and 20FA composites continued to release small amounts of fluoride at a consistent rate, however there were no significant differences in the cumulative fluoride released at extended time intervals ($p > 0.05$), (Appendix X and Appendix Y).

30FA and 40FA showed consistent increase in the fluoride release over extended period of times, this increase was shown to be significant at Day 196 when compared to Day 112 ($p < 0.05$), (Appendix Z and Appendix AA).

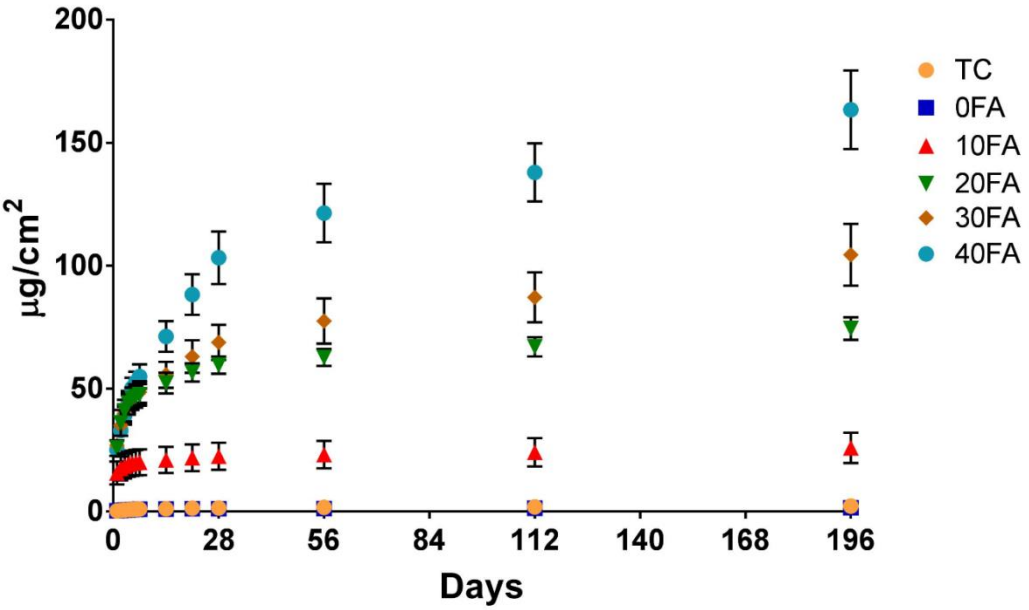

Figure 65: Cumulative fluoride release (µg/cm^2) with their standard deviation (error bars) of experimental and commercial dental composites in pH4 medium.

5.5.8.3 Cumulative fluoride release group comparisons

FA containing composites showed significantly higher cumulative fluoride release over the entire testing period when compared to TC and 0FA ($p < 0.05$). With regard to the cumulative fluoride release in relation to the concentration of FA used, 20FA, 30FA and 40FA showed significantly higher values when compared to 10FA over the entire tested period ($p < 0.05$). However there were no significant differences between 20FA, 30FA and 40 FA in the initial testing period up to Day 7, ($p > 0.05$). Significant differences start to be evident over extended period of times, 40FA showed higher release compared to 20FA and 30 FA at Day 14 and Day 21 ($p < 0.05$). From Day 28 up to Day 196 there were significant differences between all FA containing groups with 40FA showing the highest release (40FA> 30FA > 20FA > 10FA), ($p < 0.05$). Statistical results detailed in Appendix W.

Table 20: The mean fluoride release values (μg/cm^2) with the standard deviation (SD) in pH 4 medium

Day	TC		0FA		10FA		20FA		30FA		40FA	
	Mean	SD	Mean	SD	Mean	SD	Mean	SD	Mean	SD	Mean	SD
1	0.305	0.05	0.37	0.29	15.69	4.73	25.84	3.26	26.98	1.70	25.18	1.93
2	0.49	0.05	0.44	0.29	17.63	4.89	36.16	5.28	35.08	2.89	33.01	2.66
3	0.682	0.08	0.66	0.32	18.56	5.07	41.05	4.46	40.06	3.34	39.04	4.02
4	0.823	0.11	0.76	0.32	19.27	5.13	44.00	4.61	43.83	3.89	44.92	4.90
5	0.93	0.15	0.84	0.31	19.67	5.17	45.94	4.54	46.65	3.86	50.2	4.89
6	0.982	0.16	0.92	0.30	19.90	5.20	46.78	4.45	47.84	4.00	52.67	4.99
7	1.055	0.17	1.03	0.29	20.09	5.24	47.60	4.42	49.02	3.88	54.98	5.61
14	1.202	0.17	1.10	0.29	21.06	5.32	52.3	4.20	56.12	4.78	71.22	7.21
21	1.383	0.18	1.16	0.29	21.91	5.44	56.57	3.77	63.54	6.29	88.25	10.03
28	1.507	0.18	1.2	0.29	22.5	5.56	59.66	3.56	69.3	6.92	103.28	13.13
56	1.733	0.13	1.25	0.28	23.17	5.67	62.76	3.52	77.96	8.88	121.41	14.68
112	1.952	0.13	1.45	0.30	24.11	5.85	67.03	3.89	87.63	9.91	138.01	14.56
196	2.253	0.13	1.62	0.32	25.92	6.23	74.41	4.61	104.91	12.47	163.48	18.31

5.5.8.4 SEM observations

Analysis of the fluoride releasing specimens after immersion in pH 4 buffer solution showed evident dissolution of the FA crystals. Figure 66 and Figure 67 show representative examples of FA crystals before and after immersion in the acidic medium. Surface dissolution of the FA crystals is visible within 24 hours, which then become more evident by Day 28. Most of the FA crystals deposited on the surface would completely dissolve by day 112 leaving voids corresponding to their shapes within the resin matrix.

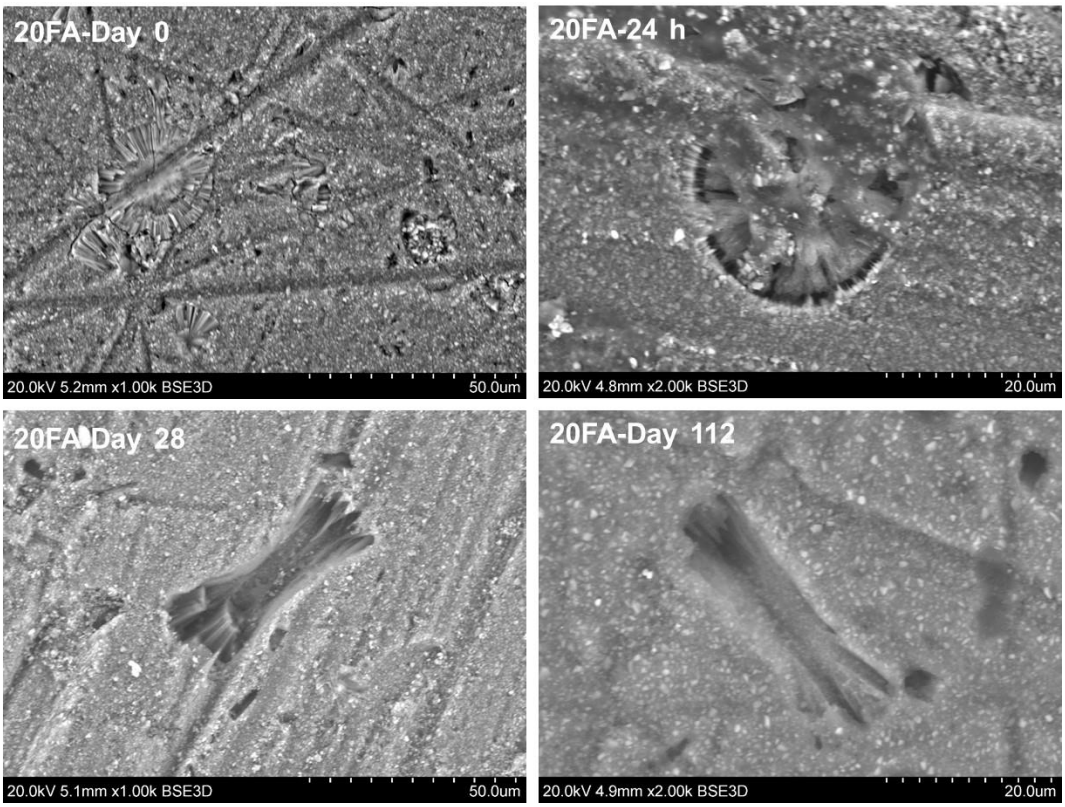

Figure 66: SEM images of 20FA composite specimen before and after immersion in pH 4 solution. AT Day 0: FA crystals are shown to be embedded within the resin matrix, within 24 hours of immersion, FA crystals starts to dissolve at the top surface and continues to dissolve on Day 28 until complete dissolution by Day 112.

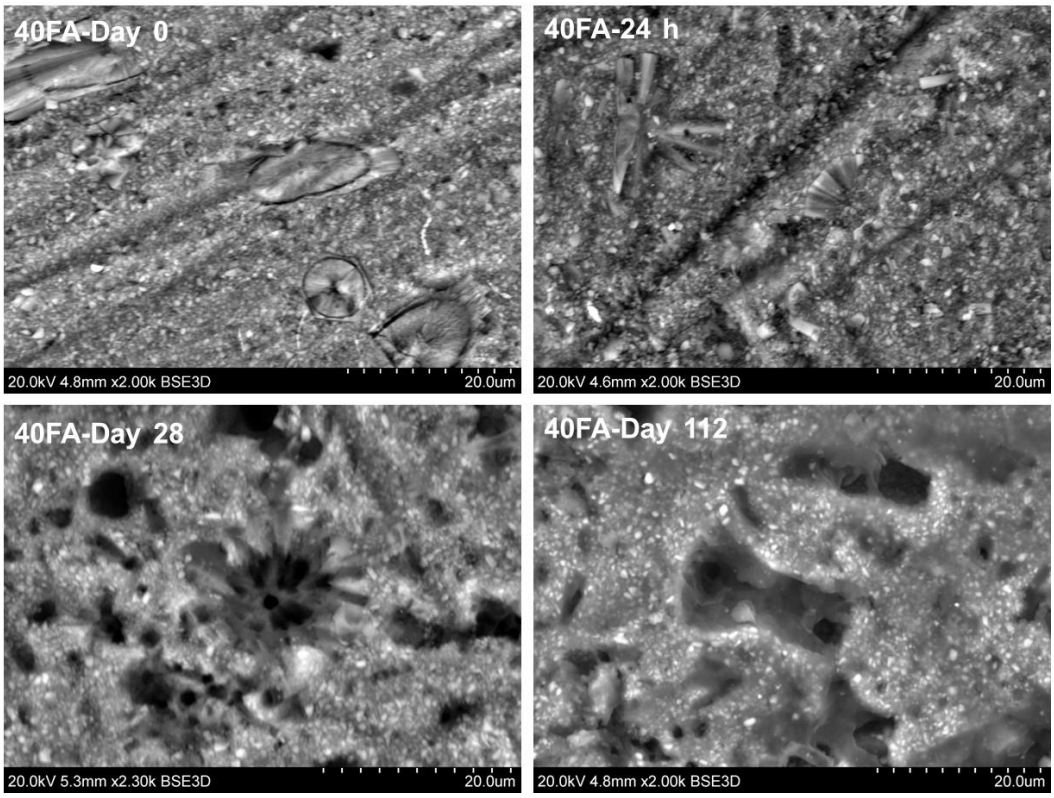

Figure 67: SEM images of 40FA composite specimens before and after immersion in pH 4 buffer solution. Intact FA crystals present at Day 0, partially dissolved FA crystals within 24 hours, more evident dissolution of the FA at Day 28 and complete dissolution at Day 112 leaving voids within the resin matrix.

5.5.8.5 Elemental mapping

Elemental mapping was conducted to analyse the dissolved FA crystals. Figure 68 show representative examples of FA containing composites before immersion in the acidic medium. Ca and P correspond to the FA crystals while Si correspond to the primary filler (barium aluminium silicate glass). After immersion in pH 4 buffer solution, the amount of Ca and P deplete leaving abundant Si particles around the dissolved FA crystals, Figure 69.

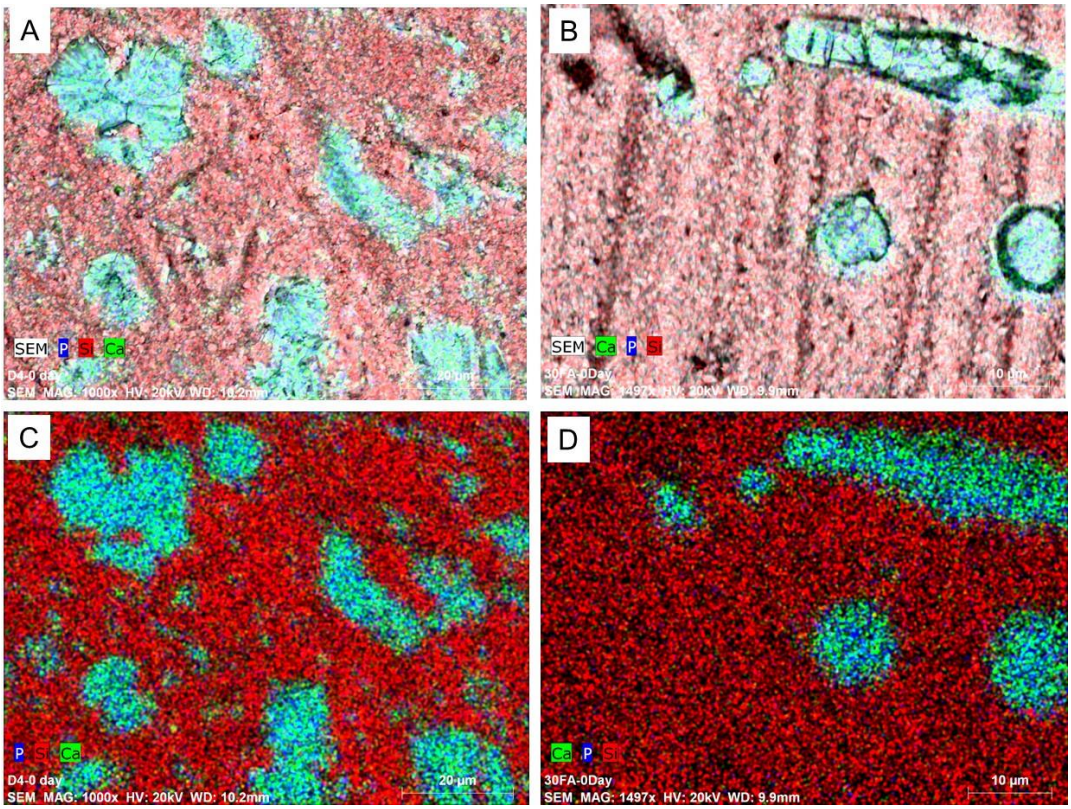

Figure 68: EDX maps of 20FA composite specimens before immersion in the acidic medium. (A,B) SEM with elemental mapping showing Ca and P corresponding to the FA crystals surrounded by Si particles which correspond to the primary filler. (C,D) show the corresponding elemental maps with Ca, P and Si.

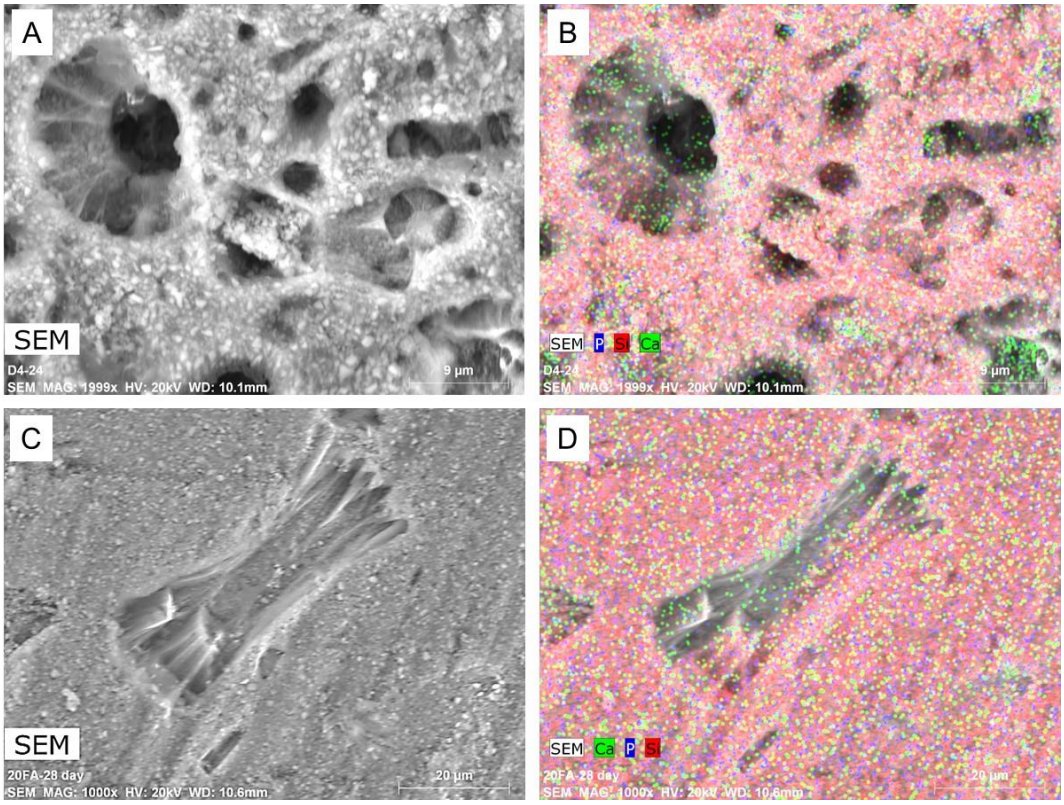

Figure 69: SEM and EDX images of aged composite specimens in pH 4 buffer solution for 28 days. (A,B) show dissolved FA crystals in a 40FA specimen with lack of P and Ca and abundant Si particles. (C,D) dissolved FA bundle in a 20FA composite specimen with no detected Ca or P.

5.6 Discussion

5.6.1 FA composite preparation and characterisation

Experimental FA containing composites were prepared following the same methodology described in (Chapter 3). The model dental monomer mixture (70BisGMA: 10TEGDMA: 20BisEMA) was selected as the experimental resin control and base mix based on the data reported in (Chapter 3). The synthesised FA powder produced in (Chapter 4) was incorporated at 10,20, 30 and 40wt% in addition to barium silicate glass to produce highly filled dental composites with overall filler content of 80%wt (63-67%vol). The homogeneity of the composite mixtures was characterised using SEM and elemental mapping. SEM analysis showed that the FA crystals and the primary glass fillers were widely distributed within the resin mixture which was similar to the commercial control filler/resin distribution pattern. Although the FA produced was not silane coupled, the unique morphology of the FA crystals and bundles of crystals may have aided in their embedding within the resin matrix, (Figure 37). The elemental maps also confirmed the main components of FA (Ca,P and F) corresponding to the embedded FA crystals (Figure 38). Therefore, it was concluded that the methodology employed in this study was suitable to produce homogenous FA containing dental composites. However, to chemically induce the filler/resin interaction, conventional fillers utilised in dental composites are usually coupled with bifunctional agent such as silane (Ferracane, 2011). Consequently incorporating silanated glass fillers provide superior mechanical performance (Ferracane et al., 1998, Drummond, 2008, Marovic et al., 2014). Experimental composites produced in this study contain silanated primary glass filler and un-silanated FA crystals. FA crystals were used without the intention to silane couple them in order to evaluate their behaviour and potential fluoride release which could be prevented if the surface was coupled. However it was recognised that the lack of coupling may result in reduced mechanical properties. Most experimental dental composites with proposed bioactivity were initially produced by incorporating novel fillers such as calcium phosphate particles

and bioactive glass (BAG) without the intention to silane couple them due to the same aforementioned reason (Davis et al., 2014, Aljabo et al., 2015, Alania et al., 2016). Experimental dental containing composites were successfully produced with FA incorporated at 10-40%wt while maintaining overall filler content of 80%wt (63-67%vol). The materials were then subjected to series tests to further characterise their properties and compare them to the commercial control.

5.6.2 Degree of conversion (DC)

The DC of TC recorded was in the range of 41.3-55.0% and 45.1-61.5% for FA containing composites. Group comparisons between at short curing times (5-20 s) showed that the DC of TC is significantly lower when compared to 10FA, 20FA and 30FA composite groups ($p < 0.05$). However the DC of TC increases further after curing for extended times (30, 40 and 60 s) with no significant differences compared to all FA containing composite groups ($p > 0.05$). Though the only exception was around 50 s curing time, as the DC of TC remains significantly lower when compared to 30FA ($p > 0.05$), this is due to the continuous increase in the DC of 30FA group when cured for 50 s, (Figure 40, section 5.4.3). Therefore the null hypothesis rejected when FA composites were compared to TC.

Comparisons were also made to evaluate the effect of FA concentration on the DC of the experimental groups. At short curing times, differences were found between the FA containing groups. The data showed that at short curing times (5 s) 40FA and 20FA groups showed lower DC when compared to 0FA and 10FA groups. The DC of 40FA group continue to remain significantly lower when compared to 0FA,10FA, 20FA and 30FA groups. The variation in the degree of conversion at 5 s could be due to the post-polymerisation curing effect due to the potential delay between the light exposure and the analysis which could have led to some post-curing effect of the specimens (Burtscher, 1993, Par et al., 2014). However 40FA continues to show lower DC at 10 s when compared to the other experimental groups. The polymerisation process is affected by several factors including the material's composition, photoinitiator chemistry, curing

protocol, specimen geometry, surrounding temperature and the presence of oxygen. Light transmission through the material is a key factor in determining the extent of polymerisation. Insufficient light transmission is associated with surface reflection (Burtscher, 1993, Ilie and Hickel, 2007), scattering effect of the filler particles (Par et al., 2014), absorption (Chen et al., 2007) and the interfacial resin/filler refraction (Shortall et al., 2008). The Refractive index of FA is around 1.63 whereas barium glass index is around 1.53, and the reported BisGMA: TEGDMA (70:30%) is around 1.52 (Shortall et al., 2008).

Resin matrix polymerisation results in a change in the materials optical properties and an increase in the refractive index due to the increasing viscosity and the density of the cross-linked polymer. As the refractive index of the resin approaches to that of the filler, the scattering at the interfacial filler/resin reduces which results in higher light transmission. Polymerisation rate increases with time, however a time delay in reaching maximum light transmission could result in lower maximum rates of polymerisation despite a possibly higher ultimate DC (Lovell et al., 1999, Shortall et al., 2008). Therefore due to the higher FA content in 40FA group a possible delay in the light transmission could result in lower polymerisation rate and ultimately lower DC at short curing times. DC at extended curing times (20-60 s) ranged between 50.9-61.5% with no significant differences between all the FA containing groups regardless of the FA concentration, (Figure 41, section 5.4.3). Therefore the null hypothesis was rejected.

Several researchers also investigated the DC of novel experimental dental composites. Aljabo *et al* (2015) developed experimental highly filled dental composites (overall 80%wt) with reactive calcium phosphate (CaP) secondary filler incorporated at up to 40%wt, experimental materials showed DC values around 70% on the top surface of the specimens, however a significant increase in the DC was evident at lower levels within the sample (3-4 mm) which was proportional to the CaP content. The reduction in DC was attributed to the scattering effect of the increased secondary filler content, (Aljabo et al., 2015). Experimental dental composites containing dicalcium phosphate dihydrate (DCPD)

nanoparticles showed no significant difference in the DC when compared to the control regardless of the amount of DCPD content, (Alania et al., 2016). The effect of using alternative photoinitiators on the DC of dental composites was also investigated. Palin *et al* (2014) evaluated the DC of monoacylphosphine oxide (MAPO) containing experimental composites using different curing protocols, MAPO materials showed a significantly higher DC when compared to CQ based materials regardless of the curing protocol used (Palin et al., 2014). Generally experimental FA containing dental composites produced in this study showed acceptable DC when compared to the available commercial materials and the different experimental materials with novel filler technologies. The addition of FA did not negatively affect the DC regardless of the concentration used. However due to the potential scattering effect of the FA filler at deeper sections within the restoration, future work should include an evaluation of the DC at deeper levels within the composite specimen.

5.6.3 *In-vitro* wear resistance

Experimental composites were subjected to two body wear test under pH 7 medium following the same methodology described in (Chapter 3: section 3.4.3). Composite specimens were subjected to 4000 cycles (400000 contacts) which is equivalent to 3 months clinical wear (Harrison and Lewis, 1975). Data showed that the wear resistance of FA containing composites was not significantly different when compared to the experimental and the commercial controls ($p > 0.05$). Very minimal wear was detected which ranged between 0.026-0.028 mm^3 (SD= 0.005-0.009). The amount of FA incorporated did not affect the wear resistance of the experimental groups regardless of the FA concentration ($p > 0.05$). It is widely accepted that the *in-vitro* wear resistance is mainly affected by the filler content, and a filler volume fraction of 60% was identified to be the necessary level required for adequate mechanical performance of resin composites (Ilie and Hickel, 2009a). Therefore the high wear resistance of the FA containing composites is mostly attributed to their high filler content (80%wt, 63-67%vol). Although composite wear behaviour is mainly affected by the filler content, the wear remains to be a complex process and not all monomer

mixtures would be expected to behave in a similar manner. However, since the monomer mixture was the same for all experimental groups, the lack of differences was also expected. Nevertheless, extending the wear test may reveal significant differences between the materials with different FA concentrations. SEM and EDX analytical techniques were used to evaluate the mechanisms of wear and the effect of FA incorporation. SEM images showed similar patterns of wear across the experimental groups with two dominant features; (1) cracks running through the matrix in the direction of wear and (2) pull out of individual FA crystals, Figure 44. This pattern was similar to TC in which larger per-polymerised fillers (PPF) were pulled out leaving voids within the resin matrix, Figure 45. The pull-out of FA crystals could be attributed to the lack of coupling of the FA crystals. However, the bundles of crystals remained embedded within the resin matrix which could be due to their unique morphology allowing resin infiltration between the individual crystals within the bundle. However, extending the wear test may also result in disintegration of these bundles. Similarly, the lack of active binding sites in the PPF required for the surface coupling results in poor integration of the PPF within the resin matrix which may result in easier disintegration when mechanically challenged (Blackham et al., 2009, Randolph et al., 2016). In addition to that, the removal of FA crystals and PPFs might have been due to their relatively large size with less favourable area to volume ratio leading to a smaller interface area between filler and polymer per unit volume (Miyasaka, 1996). SEM analysis was also conducted to evaluate the wear facets. Antagonists showed typical round wear facets corresponding to the wear tracks, Figure 46. However magnified images showed material deposition on the surface typical of adhesive wear pattern as shown in Figure 48. To investigate the material deposition; elemental analysis and mapping was conducted using the EDX which confirmed material deposition corresponding to FA elements on the antagonist surface, Figure 49. TC antagonist also showed material deposition corresponding to yttrium which is one of the elements used in the filler components of TC, Figure 47. Adhesive wear results in the transferral of material from the resin composite onto the abrading antagonist by cold welding through friction (Mair, 1992, Mair et al., 1996).

Similar patterns were previously reported in commercial resin composites (Altaie et al., 2017). Steatite is mainly composed on Mg and Si, however since the composite materials used in this study contain Si as part of the filler, Mg was selected for the elemental mapping to differentiate between the material deposition and the steatite surface. This approach provided further insight into the behaviour of FA composites and TC and distinguished the wear mechanisms especially adhesive wear patterns. It was proposed that using a combination of measurement and analytical techniques to quantify the wear provides further insight on the wear mechanisms and the tribology of wear as opposed to simply ranking by amount of resin composite wear (Altaie et al., 2017). However, regardless of the analytical techniques used, it is key to employ accurate and precise measurement techniques that are relevant to clinical wear (DeLong, 2006). The profilometric analyses used in this study were performed across an area of 8 mm length and a 4 mm width with data points recorded every 20 µm interval in the y-direction and every 4 µm in the x-direction, resulting in 150,951 data points for each wear facet which increases the confidence in the mean total wear volume data (Benetti et al., 2016, Fleming et al., 2016) compared with analogue measurements routinely used in dentistry (Heintze et al., 2005b, Heintze et al., 2011, Heintze et al., 2012). Furthermore, the accuracy and precision volumetric loss measurement data was confirmed by identifying the accuracy and precision of data recorded for a 1.0 mm step size which was 1.51 and 0.54 µm, respectively. Experimental composites containing FA showed favourable wear resistance comparable to the controls and addition of FA did not affect the materials' wear resistance.

5.6.4 Vickers Microhardness (HV)

The surface microhardness of FA composites was evaluated following the same methodology described in (Chapter 3: 3.4.4). FA composites showed significantly higher microhardness values ($p < 0.05$) when compared to TC. FA composites HV ranged between 93.9 and 95.2 (SD=1.6-2.3) while TC HV was 53.4 (SD=3.5). The addition of FA did not affect the surface microhardness regardless of the FA content ($p > 0.05$). A direct correlation

has been established between the amount of filler content and the surface microhardness of dental composites (Ferracane et al., 1998, Kim et al., 2002, Jun et al., 2013b, Randolph et al., 2016). However, due to the variation of composite formulations, commercial composites exhibit wide range of surface microhardness (23-108) (Randolph et al., 2016). The high microhardness values of FA composites could be attributed to their high filler content (80%wt, 63-67%vol). In addition to that, FA is a naturally hard material; therefore regardless of the amount of FA incorporated the surface microhardness of the experimental composites remained relatively high. The addition of novel bioactive fillers to resin composites and their effect on the surface microhardness has been evaluated by several researchers. It was reported that experimental composites containing bioactive glass filler (BAG) exhibited microhardness values ranging between 30-70 HV. However the microhardness decreased when the concentration of BAG increased (Hyun et al., 2015). Zang *et al* (2012) reported increased surface microhardness of resin composites when silanated hydroxyapatite whiskers were incorporated within the resin mixture (Zhang and Darvell, 2012). Generally the experimental composites prepared in this study showed high microhardness values which are comparable to most highly filled commercial composites, the addition of FA did not negatively affect the surface microhardness regardless of the amount of FA added. However, since experimental composites showed higher HV compared to TC, the null hypothesis was rejected.

5.6.5 Flexural strength (FS) and flexural modulus (FM)

Strength assessments seem to be an important property to evaluate since all composite restorations are likely to have internal flaws. Therefore, based on the main reasons of failure of dental composites, flexural strength (FS) and flexural modulus (FM) have been identified as important mechanical properties in predicting the clinical performance of dental composites (Ferracane, 2013a). Flexural testing is the standard means for strength testing of dental composites as per (ISO 4049). Some studies also reported a correction between FS and the wear resistance of dental composites (Peutzfeldt and Asmussen, 1992, Ferracane et al., 1997a, Heintze et al.,

2017). Experimental FA containing composites flexural strength and flexural modulus were evaluated following the ISO4049 as previously described in section (5.4.6). The flexural strength values of FA composites ranged between 68.3-80.2 MPa compared with 0FA (112 MPa) and TC (88 MPa), Table 21.

Table 21: The flexural strength (mean, median, standard deviation (SD)) of the experimental and commercial dental composites

DC	Flexural Strength (MPa)		
	Mean	Median	SD
TC	88.64	90.39	17.45
0FA	113.12	99.83	30.10
10FA	80.21	73.91	15.76
20FA	80.56	77.93	10.01
30FA	74.54	71.04	12.49
40FA	68.38	67.05	9.40

The experimental control (0FA) showed the highest flexural strength which was statistically significant when compared to all tested groups ($p < 0.05$). However there were no statistically significant differences in the flexural strength of 10-40FA when compared to TC ($p > 0.05$). The increase in the FA concentration lead to a decrease in the flexural strength values but this decrease was not statistically significant ($p > 0.05$). Generally the reported flexural strength values for commercial dental composites range between 50-160 MPa (Ilie and Hickel, 2009a, Ilie et al., 2013b, Randolph et al., 2016). Dental composite flexural strength has been previously related to the filler volume, a general trend for enhanced mechanical properties was observed when a filler volume of 60% was reached (Ilie and Hickel, 2009a). However it was shown that increasing the filler content beyond 80% by weight results in a significantly lower tensile strength (Htang et al., 1995). Consequently increasing the filler content does not necessarily increase the flexural strength of dental composites. Kim *et al* (2002) investigated the effect of filler loading and morphology on the flexural properties of resin

composites; it was concluded that round fillers enabled higher filler loading which resulted in high flexural strength, whereas irregular and per-polymerised filler allowed intermediate filler loading which reflected on the flexural properties of the materials (Kim et al., 2002). More recently, Randolph *et al* (2016) evaluated the FS of various commercial dental composites; however no general trend was found between the filler size or content and the materials' flexural strength (Randolph et al., 2016). The lack of general trend was attributed to the differences in filler content at similar size distribution, the different matrix compositions and strength measurement sensitivity in relation to sample surface preparations (Randolph et al., 2016). The ISO4049 classifies two types of light cured direct resin composites according to their flexural strength; Type 1: indicated for occlusal restorations (flexural strength values ≥ 80 MPa) and Type 2: classified as filling for other indications (flexural strength ≥ 50 MPa). Aljabo *et al* (2015) evaluated the FS of experimental dental composites containing CaP fillers with different concentrations, the FS values ranged between 100-144 MPa which was then reduced after aging for 1 month in water. They concluded that increasing the concentration of CaP fillers result in a reduction in the flexural strength of dental composites. This reduction was attributed to the lack of coupling agent between the fillers and the resin matrix (Aljabo et al., 2015). Similar observations were reported when dicalciumphosphate dihydrate (DCPD) nanoparticles were incorporated as fillers into experimental dental composites; materials showed FS values ranging between (76-133MPa) in which the FS was reduced by increasing the DCPD concentration (Alania et al., 2016). The reduction of strength was due to different reasons; firstly the DCPD particles have lower cohesive strength when compared to glass, therefore they are much less effective as toughening agents. Also, the DCPD particles were considered as inclusions increasing the risk of crack initiation at low stress levels due to the lack of surface coupling (Alania et al., 2016). The FS of experimental composites containing hydroxyapatite (HA) rods ranged between 70-100 MPa. The addition of 0.2%wt HA increased the FS values when compared to the control (unfilled resin); however by increasing the HA filler concentration, the FS steeply decreased thereafter (Taheri et al., 2015). BAGs containing

resin composites with 72%wt filler content showed FS values ranging between 116.9 - 123.5 MPa; increasing the BAG concentrations also resulted in a numerical decrease in the FS values but this decrease was not statistically significant (Khvostenko et al., 2013). Based on the data generated in this study, experimental composites containing FA showed acceptable FS values which were comparable to the commercial control (TC); the values were also within the acceptable range of FS value recommended by ISO4049 for Type 1 materials which are suitable for occlusal restorations. Generally, the addition of FA resulted in a significant decrease in composites FS when compared to the experimental control (0FA). Increasing the FA concentration resulted in a numerical decrease in the FS values, however it was not statistically significant. The reduction of FS values could be attributed to the lack of coupling of FA fillers which compromises the integration within the resin matrix; the FA fillers in this case may have behaved as large inclusions increasing the risk of crack initiation.

To encourage even stress distribution at the tooth-restoration interface; the flexural modulus of resin based composites should be closely related to that of natural tooth tissues (20-25 GPa) (Kinney et al., 2003). However, restorations also need to exhibit similar toughness to tooth tissue (1.5-2.7 MPa.$m^{(1/2)}$) otherwise they are at risk of being too brittle (Nalla et al., 2003). A positive correction has been established between composite resin flexural modulus and the amount of filler content (Jun et al., 2013a, Shah and Stansbury, 2014, Randolph et al., 2016). The flexural modulus of commercial dental composites measured *in-vitro* range between 3-16 GPa (Leprince et al., 2010, Ilie et al., 2013b, Jun et al., 2013a, Randolph et al., 2016). Experimental FA containing composites showed FM value around 12 GPa whereas 0FA (14.6 GPa) and TC (10.22 GPa), details shown in Table 22.

Table 22: The flexural modulus (mean, median, standard deviation (SD)) of the experimental and commercial dental composites

DC	Flexural Modulus (GPa)		
	Mean	Median	SD
TC	10.22	10.56	0.77
0FA	14.63	13.74	1.27
10FA	12.05	11.65	1.89
20FA	12.19	12.30	0.92
30FA	12.08	11.51	1.73
40FA	12.05	12.05	0.01

Flexural modulus data showed that the experimental control (0FA) had the highest flexural modulus value when compared to all other tested groups ($p < 0.05$). However TC (commercial control) showed the lowest flexural modulus value which was also statistically significant when compared to all FA containing composites ($p < 0.05$). All FA composites showed similar flexural modulus which was not affected by increasing the FA concentration ($p > 0.05$). Based on the data, the addition of FA resulted in a decrease in the FM values of resin composites; however this did not correlate to the amount of FA added. The lack of correlation could be attributed to the high filler content of all FA composites (63-67%vol) (Ilie and Hickel, 2009a, Randolph et al., 2016). However when compared to 0FA, a general reduction was evident across all FA composites; the most likely explanation is related to lack of surface coupling of FA fillers allowing easier crack extension around the FA fillers. However it would be of an interest to increase the FA concentration further where possible differences might be more evident and a critical level of FA concentration might be established. Generally, all FA composites maintained relatively acceptable FM values which are comparable to most highly filled commercial dental composites, and in this study were significantly higher than TC. The reduced flexural modulus of TC is mostly attributed to the lower modulus of PPF compared to glass; similar findings were also previously reported (Kim et al., 2002, Ilie

et al., 2013b, Randolph et al., 2016). Experimental composites containing CaP fillers showed a relatively low flexural modulus (2.1-4.0 GPa) which was reduced by increasing the CaP filler content (Aljabo et al., 2015). Similarly resin monomer mixtures containing hydroxyapatite filler showed FM values ranging between 1.7-2.5 GPa (Taheri et al., 2015).

Fractographic analysis was also conducted using the SEM where the fracture surfaces were scanned and analysed to establish a better understanding of the fracture mechanisms involved. SEM images of FA composites showed micro cracks and exposed FA crystals suggesting that the fracture occurred at the matrix/filler interface. Images of the opposing fractured surfaces showed several FA crystals protruding from the matrix on one surface leaving spaces within the matrix of the corresponding fractured surface which suggest that FA crystals detached from the matrix upon fracture, representative examples shown in Figure 54. Similar observations were found in TC fractured surfaces where large PPF fillers were protruding through the matrix in one surface leaving a space corresponding to the detached filler on the opposing fractured surface, example shown in Figure 53. Unlike FA composites and TC, 0FA specimens showed smooth fractured surfaces due to the uniform filler type and size distribution, Figure 53.

5.6.6 Fracture toughness (K_{1c})

Fractured toughness has been identified as one of the most important mechanical properties necessary in predicating the material's clinical performance. Since all restorations are likely to contain internal flaws, fracture toughness may be the most critical factor in determining the fracture resistance *in-vivo* which could be presented as chipping or bulk fracture of the restoration (Ferracane, 2013a, Heintze et al., 2017). The single edge notched beam method following the ASTM (E399-12-e2) is the most widely used methodology in determining the fracture toughness of resin composites (Heintze et al., 2017). Therefore, the same methodology was used in this study which is described in details in section (5.4.7). The most reported fracture toughness values of dental composites range between 1-2.5 $MPa.m^{(1/2)}$ (Ilie et al., 2012, Jun et al., 2013a). Studies have been equivocal on whether there is a correlation between resin composites fracture toughness and the amount of filler loading. Several studies were in agreement that there is a correlation between the filler volume fraction and the fracture toughness of resin composites (Kovarik and Fairhurst, 1993, Kim et al., 1994, Ferracane et al., 1998, Ilie et al., 2012). However, a critical filler volume fraction of 57% has been identified after which the fracture toughness of the material starts to plateau until reaching 65% filler volume. Adversely, increasing the filler volume further exceeding 65%vol resulted in a slight reduction in the fracture toughness. This reduction is attributed to increasing the flaws (voids, porosities, filler agglomerates) incorporated due to increased material viscosity (Ilie et al., 2012). However, several other studies suggested that the fracture toughness of resin based materials are highly dependent on the morphology of the composite microstructure rather than filler volume fraction or filler size (Kim et al., 2002, Shah et al., 2009a, Shah et al., 2009b, Elbishari et al., 2012, Ornaghi et al., 2012). Previous studies suggested that the microstructure of resin based composites that maintain good matrix/particle adhesion while endorsing important toughening mechanisms such as crack bridging and crack deflection provide superior fracture and fatigue properties (Manhart et al., 2000, Shah et al., 2009b, Shah et al., 2009a, Elbishari et al., 2012, Ornaghi et al., 2012).

In this study, the fracture toughness values of the tested composites groups were variable with FA composites ranging between 0.8-1.4 MPa.m$^{(1/2)}$, 0FA (1.2 MPa.m$^{(1/2)}$) and TC (1.3 MPa.m$^{(1/2)}$), details shown in Table 23.

Table 23: The fracture toughness (mean, median, standard deviation (SD)) of the experimental and commercial dental composites

Fracture toughness (MPa.m$^{(1/2)}$)			
DC	**Mean**	**Median**	**SD**
TC	1.37	1.38	0.10
0FA	1.29	1.28	0.23
10FA	0.87	0.92	0.14
20FA	0.87	0.87	0.10
30FA	1.46	1.40	0.42
40FA	1.21	1.18	0.06

10FA and 20FA groups showed the lowest fracture toughness values when compared to TC, 30FA and 40FA ($p < 0.05$). However 30FA and 40FA showed higher fracture toughness values which were comparable to the controls ($p > 0.05$). The addition of higher concentration of FA resulted in enhanced fracture toughness of the experimental dental composites. Fractographic analysis was conducted using the SEM to evaluate the fractured surfaces and the mechanism of failure in relation to the experimental materials composition. Crack extension analysis of the matching cracked surfaces showed that cracks extended from the pre-inserted notch which then propagated through the resin/matrix interface. Detached FA crystals were detected between the two fractured surfaces of FA composites, crack extension examples shown in Figure 56. Analysed fractured specimens showed three distinct fracture zones; (1) the pre-cracked area which has a flat compact surface with the filler particles tightly imbedded within the resin matrix, (2) the transitional zone with an irregular surface and displaced filler/matrix and (3) the fractured surface with visible crack lines and detached fillers leaving spaces within the resin matrix. Example of the fracture zones are shown in Figure 58 (A and B). The main mechanism of failure identified for all FA containing composites and TC

were (1) crack propagation between the filler particles either near or at the filler/resin interface and (2) filler particles debonding from the resin matrix leaving spaces corresponding to their shape on one surface and protruding through the matrix on the opposite surface, Figure 59. In contrast 0FA specimens showed smooth fractured surfaces with predominantly microcracks running through the matrix, Figure 62. 10FA and 20FA showed both failure mechanisms; cracks were initiated from the pre-cracked area which then continued to extend through the filler/resin interface and detached individual FA crystals protruding on one surface and leaving hexagonal spaces on the opposing surface, Figure 60 and Figure 61. Due to the lack of surface coupling; FA crystals may have behaved as internal flaws allowing crack propagation as they were easily detached from the resin matrix leading to interfacial debonding. The present observations generally agree with other researchers who identified interfacial debonding as one of the main reasons of reduced fracture properties of dental composites (Chan et al., 2007, Shah et al., 2009b, Khvostenko et al., 2013). Similar observations were found in TC fractured surfaces in which PPFs were cleanly detached from the resin matrix leaving spaces corresponding to their original shape on the opposing surface, typical examples shown in Figure 58 (C and D) and Figure 59. As mentioned earlier, PPFs lack the active binding sites for effective surface coupling which compromises their interaction with the resin matrix and consequently results in easier detachment under loading. 30FA and 40FA fractured specimens also showed the typical failure mechanisms explained earlier (Figure 63), however distinctive fracture toughening mechanisms were also observed including crack deflection and bridging around the larger FA crystals and bundles of crystals, Figure 64. The unique morphology of FA crystals allowed microscopic crack deflection and crack bridging which sustained a portion of the applied load that otherwise would have gone towards crack extension. Similar observations were reported when bioactive glass (BAG) fillers were used increasing the fracture toughness of experimental dental composites (Khvostenko et al., 2013). Crack deflection and bridging are the two toughening mechanisms that often act together in which crack deflection leads to crack bridging (Shah et al., 2009a, Shah et al., 2009b),

similar to natural tooth tissues by which the enamel and dentine are toughened (Imbeni et al., 2005, Bajaj and Arola, 2009, Bechtle et al., 2010). Those toughening mechanisms were more evident when higher concentrations of FA were used, this might have attributed to the increased fracture toughness of 30FA and 40FA when compared to 10FA and 20FA. Generally FA composites showed acceptable fracture toughness values which are comparable to commercial dental composites especially in 30FA and 40FA composites. Although interfacial debonding was evident across all FA composites, the addition of higher amounts of FA aided in material toughening due to crack deflection and bridging around the FA fillers. Therefore the null hypothesis was rejected when comparisons were made between the FA composites as composite fracture toughness increased by increasing the FA concentration.

5.6.7 Fluoride ion release

Fluoride has been identified as an effective agent in slowing caries progression through enhancing the remineralisation and reducing the demineralisation of enamel and dentine (Cate, 1999). Therefore, the idea of fluoride releasing restoratives is very attractive to maintain constant fluoride release in the mouth and in close proximity to demineralising tooth tissue. Fluoride-releasing dental materials present the necessary properties to be effective against caries progression, however their effectiveness have been critically reviewed (Wiegand et al., 2007, Cury et al., 2016). Various fluoride releasing restoratives are currently available such as glass ionomer cements (GIC), resin modified glass ionomers (RMGIC), compomers and fluoride containing composites. The amount of daily and ccumulative fluoride release from these restoratives varies in the literature and is dependent on the type of storage medium (Wiegand et al., 2007). Generally, the highest amount of fluoride release is shown to be in acidic environments and lowest in artificial saliva (Karantakis et al., 2000, Imazato et al., 2001, Moszner and Salz, 2001). However, the kinetics and pattern of fluoride release is similar amongst all restoratives. Most materials initially release high amounts of fluoride (within 24-48 hours), however this initial burst rapidly diminishes with time and long term release continues at much

lower rates (Karantakis et al., 2000, Yap et al., 2002a, Attar and Turgut, 2003). Composites have been shown to release the lowest amounts of fluoride in the long term when compared to GIC, RMGIC and compomers (Karantakis et al., 2000, Vermeersch et al., 2001, Wiegand et al., 2007). The ion selective electrode method (ISE) has been widely used by researchers to measure the total fluoride ions (free and complex fluoride ions) released from dental restoratives. Following this methodology acetic buffer solution (TISAB) is usually added to release free fluoride ions from the complex fluoride ions (Itota et al., 2004a, Itota et al., 2004b, Durner et al., 2012). The ion selective method was used in this study to measure the fluoride ion release under neutral and acidic conditions. The protocol used in this study was daily fluoride measurements for the first week, followed by weekly measurements for the first month and monthly measurements up to 196 days. Fluoride was measured for extended periods to have a better insight into the long term fluoride releasing ability of the experimental materials. This protocol was used to avoid fluoride saturation by continued fluoride release; therefore the media was changed on daily bases, then weekly then monthly for each specimen. Fresh distilled water (pH = 7.0±0.2) was used as the neutral medium and freshly prepared acidic medium using pH 4 buffer tablets (VDR, Belgium) in distilled water. The pH value was confirmed for each prepared solution after calibrating the pH meter (ORION-920A model, Orion Research, Sussex, UK). Similar protocol was followed by several researchers evaluating the fluoride release of various restorative materials (Bell et al., 1999, Preston et al., 1999, Karantakis et al., 2000, Attar and Onen, 2002). The ion selective method is the most widely used technique for fluoride ion release. This is due to its high reliability, great selectivity and specificity for fluoride ions and generally easy to use. The instrument was calibrated every 2 hours during fluoride measurements using standard solutions to account for any temperature change which might have an effect on the fluoride measurements (Itota et al., 2004b). TISAB was added to the standard and the sample solutions to de-complex the fluoride ions and to prevent the interference of hydroxide ions (OH^-) which have similar ionic charge and ion radius to fluoride ions (F^-), TISAB also aid in pH regulation for solutions with pH ranging between

5-7 (McNeill et al., 2001, McCabe et al., 2002, Itota et al., 2004b). Under neutral conditions, no fluoride release was detected from the FA composites and the control groups; therefore it was decided not to continue the experiment under neutral condition as none of the groups released fluoride over the first 48 hours (Table 19). However, under acidic conditions, all FA composites released significant amounts of fluoride when compared to the control groups ($p < 0.05$). All FA composites showed similar pattern and amount of fluoride release which was at its highest in the first day. TC and 0FA did not release fluoride over the entire tested period. The detection threshold of the ion selective electrode used in this study is > 0.03 µg/cm^2. Therefore some fluoride maybe detected from the control materials which could be a false positive measurement due to the level of sensitivity of the electrode or due to the accumulation of fluoride ions around the electrode membrane. However, to minimise the chances of this accumulation; the electrode was cleaned with fluoride free-tooth paste and thoroughly washed with deionised water in-between measurements taken from each composite group. Following the initial release, the fluoride release started to decrease from day two up to day 7. 10FA and 20FA composites continued to release small amounts of fluoride at a consistent rate, however there were no significant differences in the cumulative fluoride released at extended time intervals ($p > 0.05$). 30FA and 40FA showed consistent increase in the fluoride release over extended period of times, this increase was shown to be significant at Day 196 when compared to Day 112 ($p < 0.05$). FA containing composites showed significantly higher cumulative fluoride release over the entire testing period when compared to TC and 0FA ($p < 0.05$). Generally the amount of fluoride released was proportional to the concentration of FA used (cumulative release profile shown in Figure 65). The cumulative release of FA composites ranged between (20.0-54.9 µg/cm^2) in the first week which increased to (25.9-163.4 µg/cm^2) by day 196, Table 20. Data showed that 20FA, 30FA and 40FA showed significantly higher values when compared to 10FA over the entire tested period ($p < 0.05$). However there were no significant differences between 20FA, 30FA and 40 FA in the initial testing period up to Day 7, ($p > 0.05$). Significant differences started to become evident over extended period of

times, 40FA showed higher release when compared to 20FA and 30 FA at Day 14 and Day 21 ($p < 0.05$). From Day 28 up to Day 196 significant differences were present between all FA containing groups with 40FA showing the highest release (40FA> 30FA > 20FA > 10FA), ($p < 0.05$).

SEM and elemental mapping were also conducted to evaluate the mechanism of fluoride release. Scans of fluoride releasing specimens showed evident dissolution of the FA crystals after immersion in pH 4 medium. Figure 66 and Figure 67 show representative examples of FA crystals before and after immersion in the acidic medium. Surface dissolution of the FA crystals is visible within 24 hours, which then become more evident by Day 28. Most of the FA crystals on the surface completely dissolved by day 112 leaving voids corresponding to their shapes within the resin matrix. Elemental maps also confirmed that FA crystals were dissolving as the amount of detected calcium and phosphate start to deplete after immersion in the acidic medium leaving abundant silica particles around the dissolved FA crystals (Figure 68 and Figure 69). Fluorapatite is a chemically stable material but known to release fluoride under acidic conditions (Chen et al., 2006a). The results of this study showed that FA maintained the same behaviour when added to resin composites, as all FA composites released fluoride when they were subjected to pH 4 medium due to the dissolution of FA crystals. However, the FA crystals remained stable under neutral conditions. Since enamel demineralisation starts when the pH drops below 5.5, FA composites could be a suitable restorative material to minimise demineralisation and progression of recurrent caries around resin composites. FA composites could potentially be a “smart” restorative that releases fluoride only when it is required as the pH drops in the oral cavity. To date, there has been no consensus on the amount of fluoride required for a restorative material to be effective against recurrent caries; however it is generally suggested that the effect of fluoride releasing restoratives is mostly due to the localised fluoridation adjacent to the demineralisation zones rather than elevation of fluoride levels in saliva. It has been reported that localised small amounts of fluoride approximately in the ranges of 0.03-0.08 ppm and 0.63-1.3 µg F^-

/cm^2/day is sufficient to shift the equilibrium from demineralisation to re-mineralisation (Rawls, 1995, Wiegand et al., 2007). Therefore all FA composites showed fluoride release within the range considered to be effective in preventing demineralisation. In addition to that, the amount of fluoride is considerably higher when compared to the commercially available fluoride releasing dental composites (Karantakis et al., 2000, Vermeersch et al., 2001).

5.7 Summary

Fluoride was released from all FA composites only under acidic conditions which was proportional to the amount of added FA. Fluoride was released due to the dissolution of FA crystals when the pH dropped. The null hypothesis was rejected as fluoride release was only detected under acidic conditions.

Chapter 6: General Discussion and summary

Over the last decades the state of art of resin composites has changed dramatically. Researchers have focused on enhancing the materials' longevity to increase their clinical service by reducing their perceived shortcomings such as polymerisation stress (Gonçalves et al., 2010), handling (Lee et al., 2006), depth of cure (Sevkusic et al., 2014), aesthetics (Mikhail et al., 2013) and most importantly strength (Kim et al., 2002). Substantial progress has been achieved which placed resin composites in a prominent place amongst restorative materials as a "universal restorative" suitable for anterior and posterior use (Burke, 2004, Mitchell et al., 2007, Vidnes-Kopperud et al., 2009, Burke et al., 2017). Most important changes have evolved around the reinforcing filler which was purposely reduced in size from macro to a nano level which produced materials that are more easily and effectively polished and demonstrate greater wear resistance (Ferracane, 2011). The use of nano particles significantly improved the aesthetic properties and strength (Curtis et al., 2009) in addition to increasing the depth of cure since refraction and scattering are reduced (Fujita et al., 2011). Developments also focused on the polymer matrix to reduce polymerisation shrinkage and more importantly polymerisation stress within the material, such as thiol-ene monomers (Carioscia et al., 2005, Cramer et al., 2010) and epoxy resin chemistry (Ernst et al., 2004, Weinmann et al., 2005). In addition to that, pre-polymerised filler particles were also developed to reduce polymerisation stress and provide superior polishing properties (Senawongse and Pongprueksa, 2007, Ferracane et al., 2014).

Despite the significant developments of resin based composites, most recent systematic reviews showed that recurrent caries and clinical fractures of composite restorations remain to be the most common reasons of failure (Bernardo et al., 2007, Soncini et al., 2007, Sunnegardh-Gronberg et al., 2009, Demarco et al., 2012a, Beck et al., 2015a). The latter is especially important when composite resin is used in posterior teeth (van de Sande et al., 2013). The development of an effective antimicrobial resin composite has been progressing at a slower rate. Several strategies have

been adopted by researchers to introduce antimicrobial dental composites by modifications to the resin matrix, the filler components and the use of novel antibacterial polymers (Beyth et al., 2014). Fluoride has been the most widely used anti-caries agent, however the effectiveness of fluoride containing restoratives has been critically reviewed (Wiegand et al., 2007, Cury et al., 2016). More recently bioactive glass fillers (BAG) have been used as alternative/secondary filler for experimental resin based composites (Hyun et al., 2015, Alania et al., 2016). BAGs are represented by amorphous calcium, sodium phosphosilicate materials which are able to precipitate a biologically active hydroxycarbonate layer on their surfaces when they are exposed to bodily fluids. Therefore, they exhibit promising bioactive properties that can interact with the surrounding environment. However, their use and effectiveness in resin composites is still under investigation. Therefore, researchers continue to focus their efforts to develop new composite formulations with superior physical, mechanical properties and additional antimicrobial properties to produce materials with enhanced performance and extended clinical service.

The aim of this study was to develop novel fluorapatite containing resin composites with potential antimicrobial properties while maintaining good mechanical and physical properties. Successful composite formulations were produced incorporating FA as secondary filler at up to 40%wt filler content while maintaining overall filler content of 80%wt.

The addition of FA did not affect the degree of conversion of the experimental materials regardless of the amount of FA incorporated. The degree of conversion ranged between 50.9-61.5% which lies within the range of most commercial resin composites and the recommended degree of conversion suitable for occlusal restorations (Ferracane et al., 1997c, Silikas et al., 2000). However there was a difference in the refractive index of FA when compared to the resin mixture used. Therefore, optimizing filler/resin refractive index mismatch could also provide increased curing depth and assist in shade-matching (Shortall et al., 2008). Therefore it is worth considering using different resin formulations with refractive index similar to FA to further enhance their depth of cure and shade matching.

The mechanical performance of FA composites was similar/better than the commercial control. The wear resistance was similar to TC and 0FA and the addition of FA did not reduce the wear resistance. The high wear resistance of all FA composites is mostly attributed to the high filler content (80%wt, 63-67%vol) exceeding the filler volume fraction (60%vol) claimed to be necessary for resin composites to maintain adequate mechanical strength and wear resistance (Ilie and Hickel, 2009a). However, the wear process remains complex and the mechanism of wear was different between FA composites, TC and 0FA. SEM images showed similar patterns of wear across the experimental groups with two dominant features; (1) cracks running through the matrix in the direction of wear and (2) pull out of individual FA crystals. A similar pattern was observed in TC where larger pre-polymerised fillers (PPF) were pulled out leaving voids within the resin matrix. The absence of surface coupling of FA crystals and the lack of active binding sites in the PPF required for the surface coupling results in poor integration of these fillers within the resin matrix which may result in easier disintegration when mechanically challenged (Blackham et al., 2009, Aljabo et al., 2015, Randolph et al., 2016). Therefore it is worth investigating the effect of surface coupling of the FA crystals on the wear behaviour of FA composites. In addition to that, the removal of FA crystals and PPFs could also be attributed to their relatively large size with less favourable area to volume ratio leading to a smaller interface area between filler and polymer per unit volume (Miyasaka, 1996). Generally combinations of wear mechanisms were present across all composite groups, however FA composites showed a secondary adhesive wear mechanism where the FA crystals were transferred onto the abrading antagonist by cold welding through friction (Mair, 1992, Mair et al., 1996). TC also showed similar behaviour where material deposition corresponding to yttrium was evident on the abrading steatite antagonist. The use of the combination of analytical techniques such as SEM and EDX allowed further insight into the material behaviour and the unique wear processes involved. Similar findings were previously reported including commercial resin composites such as Filtek supreme XTE (3M ESPE, USA) and Kalore (GC America, USA) (Altaie et al., 2017). Whilst short-term wear testing

(equivalent of 6 month *in-vivo*) was shown to not discern as well between resin composite formulations compared to extended wear testing (equivalent of 18 and 36 months *in-vivo*) (Finlay et al., 2013), it did provide significant insights into the *in-vitro* wear behaviour of the different composite formulations (Finlay et al., 2013, Altaie et al., 2017). Therefore it is proposed that further insights into the wear behaviour of FA composites with different FA concentration could be obtained following an extended wear test. Nevertheless, FA composites showed favourable wear resistance comparable to the controls regardless of the concentration of FA used.

Generally, FA composites showed high microhardness values which were comparable to most highly filled commercial composites; the addition of FA also did not negatively affect the surface microhardness regardless of the amount incorporated. FA composite HV ranged between 93.9 to 95.2 (SD=1.6-2.3) while TC HV was 53.4 (SD=3.5). A direct correlation has been established between the amount of filler content and the surface microhardness of dental composites (Ferracane et al., 1998, Kim et al., 2002, Jun et al., 2013b, Randolph et al., 2016). Therefore, the high microhardness values of FA composites are mostly attributed to their high filler content. Experimental FA composites also showed superior microhardness properties when compared to other experimental composites such as BAG containing composites. It was reported that experimental composites containing BAG exhibited microhardness values ranging between 30-70 HV. However the microhardness decreased when the concentration of BAG increased (Hyun et al., 2015). The surface microhardness was also shown to increase when silanated hydroxyapatite whiskers were incorporated within experimental resin composites mixtures (Zhang and Darvell, 2012).

Evaluation of the experimental materials' strength was also a crucial part of this study to characterise their mechanical performance and the effect of FA incorporation. Strength assessments were based on the important mechanical properties identified to be most effective in predicting the clinical performance of dental composites (Ferracane, 2013a, Heintze et al., 2017), this included fracture toughness (K_{1C}), flexural strength (FS) and

flexural modulus (FM) testing. The most recent systematic review showed that there were significant moderate/strong correlations between fracture toughness and clinical fractures and flexural strength with clinical wear (Heintze et al., 2017).

The flexural strength values of FA composites ranged between 68.3-80.2 MPa compared to higher values for 0FA (112 MPa) and TC (88 MPa),Table 24. The experimental control (0FA) showed the highest flexural strength which was statistically significant when compared to all tested groups ($p < 0.05$). However there were no statistically significant differences in the flexural strength of 10-40FA when compared to TC ($p > 0.05$). The increase in the FA concentration lead to an apparent decrease in the flexural strength but this decrease was not statistically significant ($p > 0.05$). The reduction of FS values could also be attributed to the lack of coupling of FA fillers which compromises the integration within the resin matrix; the FA fillers in this case may have behaved as large inclusions increasing the risk of crack initiation. Similar observations were reported by Aljabo *et al* (2015) for CaP fillers with different concentrations; the FS values ranged between 100-144 MPa which was then reduced after aging for 1 month in water. They concluded that increasing the concentration of CaP fillers resulted in a reduction in the flexural strength of dental composites. This reduction was attributed to the lack of coupling agent between the fillers and the resin matrix (Aljabo et al., 2015). Similar observations were reported when unsilanated filler particles were incorporated into resin composites such as dicalciumphosphate dihydrate (DCPD) nanoparticles; materials showed FS values ranging between (76-133MPa) in which the FS was reduced by increasing the DCPD concentration (Alania et al., 2016). As with the FA particles in this study, DCPD particles were considered as inclusions increasing the risk of crack initiation at low stress levels due to the lack of surface coupling (Alania et al., 2016). Hydroxyapatite (HA) containing experimental composites showed FS values ranging between 70-100 MPa, the addition of 0.2%wt HA increased the FS values when compared to the control (unfilled resin), however the FS values steeply decreased when the HA filler concentration

was increased (Taheri et al., 2015). BAGs containing resin composites with 72%wt filler content showed FS values ranging between 116.9 - 123.5 MPa, increasing the BAG concentrations also resulted in a numerical decrease in the FS values but this decrease was not statistically significant (Khvostenko et al., 2013). It was also reported that the use of silanated BAG fillers increased the flexural strength of experimental resin composites from 70.3 MPa (un-silanized) to 106.6 MPa (silanized) (Oral et al., 2014). Nevertheless, experimental composites containing FA showed acceptable FS values which were comparable to the commercial control (TC); the values were also within the acceptable range of FS value recommended by ISO4049 for Type 1 materials which are suitable for occlusal restorations (Flexural strength values ≥ 80 MPa).

Generally, all FA composites maintained relatively acceptable FM values which are comparable to most highly filled commercial dental composites, and in this study were significantly higher than TC. Experimental FA containing composites showed FM value around 12 GPa compared with 0FA (14.6 GPa) and TC (10.22 GPa), Table 24. Generally the addition of FA resulted in a decrease in the FM values when compared to 0FA. This reduction is mostly attributed to the lack of surface coupling of FA crystals which compromises the resin/filler interaction and the particles are less effectively contributing to the overall stiffness of the material. However, all FA composites showed similar flexural modulus values which were not affected by increasing the FA concentration (10-40%FA), ($p > 0.05$). The lack of correlation could be attributed to the high filler content of all FA composites (63-67%vol) (Ilie and Hickel, 2009a, Randolph et al., 2016). However it would be of an interest to investigate the effect of increasing the FA concentration further to establish the critical level of FA after which the FM values may significantly be reduced. FA composites showed superior FM properties when compared to other experimental composites. It was reported that composites containing CaP fillers showed a relatively low flexural modulus (2.1-4.0 GPa) which was reduced by increasing the CaP filler content (Aljabo et al., 2015). Similarly resin monomer mixtures

containing hydroxyapatite filler showed FM values ranging between 1.7-2.5 GPa (Taheri et al., 2015).

The fracture toughness values of the tested composites groups were variable with FA composites ranging between 0.8-1.4 MPa.m$^{(1/2)}$, 0FA (1.2 MPa.m$^{(1/2)}$) and TC (1.3 MPa.m$^{(1/2)}$), Table 24.10FA and 20FA groups showed the lowest fracture toughness values when compared to TC, 30FA and 40FA ($p < 0.05$). However 30FA and 40FA showed higher fracture toughness values which were comparable to the controls ($p > 0.05$). Interestingly, the addition of higher concentration of FA resulted in enhanced fracture toughness of the experimental dental composites. The most reported fracture toughness values of dental composites range between 1-2.5 MPa.m$^{(1/2)}$ (Ilie et al., 2012, Jun et al., 2013a). The literature has been equivocal on whether there is a correlation between resin composites fracture toughness and the amount of filler loading. Several studies reported correlations between the filler volume fraction and the fracture toughness of resin composites (Kovarik and Fairhurst, 1993, Kim et al., 1994, Ferracane et al., 1998, Ilie et al., 2012). However, several other studies suggested that the fracture toughness of resin based materials are highly dependent on the morphology of the composite microstructure rather than filler volume fraction or filler size (Kim et al., 2002, Shah et al., 2009a, Shah et al., 2009b, Elbishari et al., 2012, Ornaghi et al., 2012). It was suggested that the microstructure of resin based composites that maintain good matrix/particle adhesion while endorsing important toughening mechanisms such as crack bridging and crack deflection provide superior fracture and fatigue properties (Manhart et al., 2000, Shah et al., 2009b, Shah et al., 2009a, Elbishari et al., 2012, Ornaghi et al., 2012). Applying these mechanisms could explain the increased fracture toughness values of resin composites when higher amounts of FA are incorporated. The lack of silane coupling of the FA fillers results in poorer integration of the fillers within the resin matrix, therefore they are considered as internal flaws allowing crack propagation as they are easily detached from the resin matrix leading to interfacial debonding. Generally these observations were evident from the SEM images of the fractured surfaces which agree with

other researchers who identified interfacial debonding as one of the main reasons of reduced fracture properties of dental composites (Chan et al., 2007, Shah et al., 2009b, Khvostenko et al., 2013). However, the unique morphology of FA crystals especially the bundles of crystals also allowed microscopic crack deflection and crack bridging which sustained a portion of the applied load that otherwise would have gone towards crack extension. Crack deflection and bridging are the two toughening mechanisms that often act together in which crack defection lead to crack bridging (Shah et al., 2009a, Shah et al., 2009b), similar to natural tooth tissues by which the enamel and dentine are toughened (Imbeni et al., 2005, Bajaj and Arola, 2009, Bechtle et al., 2010). Those toughening mechanisms were more evident when higher concentrations of FA were used, Figure 64. Therefore, the increased fracture toughness of 30FA and 40FA when compared to 10FA and 20FA could be explained by to those toughening mechanisms due to wider availability of the FA bundles overcoming the lack of surface coupling issue. This study therefore highlights the importance of filler morphology as well as amount of filler in affecting key mechanical properties. Kostenko *et al* (2013) reported similar observations of fracture toughening mechanisms when bioactive glass (BAG) fillers were used which resulted in acceptable fracture toughness of experimental dental composites. Generally all FA composites exhibited adequate mechanical performance when compared to the commercial control;

All FA composites showed similar wear resistance to 0FA and TC regardless of the FA concentration

1- All FA composites showed superior microhardness (HV) when compared to TC, performing at a similar level of most highly filled commercial composites.
2- All FA composites showed similar flexural strength to TC; however the addition of FA resulted in a decrease in the FS values when compared to 0FA.

3- All FA composites showed similar flexural modulus to TC; however the addition of FA resulted in reduced FS values when compared to 0FA.
4- 30FA and 40FA showed similar fracture toughness values when compared to TC and 0FA.

Although all FA composites behaved similarity to the commercial control, the lack of surface coupling of the FA crystals was the primary reason for the reduced flexural strength, flexural modulus and fracture toughness of FA composites when compared to 0FA. However, interesting observations were found when higher concentrations of FA were incorporated which lead to endorsed toughening mechanisms increasing the fracture toughness of the most highly filled FA composites. The importance of filler surface coupling was recognised to enhance the filler/resin interaction and consequently a lack of coupling may result in compromised mechanical properties (Kim et al., 2002, Ilie et al., 2013b, Randolph et al., 2016). However, experimental composites produced in this study contained silanated primary glass filler and un-silanated FA crystals. FA crystals were used without the intention to silane couple them in order to evaluate their behaviour and potential fluoride release which could be prevented if the surface was coupled. A similar approach is usually adopted by most researchers developing experimental dental composites with proposed bioactivity, most materials were initially produced by incorporating novel fillers such as calcium phosphate particles and bioactive glass (BAG) without the intention to silane couple them due to the same aforementioned reason (Davis et al., 2014, Aljabo et al., 2015, Alania et al., 2016).

Table 24: Flexural strength (FS), Flexural modulus (FM) and Fracture toughness (K_{1c}) data of FA composites and the control groups

DC	FS (MPa)(SD)	FM (GPa)(SD)	K_{1c} (MPa.m$^{(1/2)}$)(SD)
TC	88.6 (17.4)	10.2 (0.7)	1.3 (0.1)
0FA	113.1 (30.1)	14.6 (1.2)	1.2 (0.2)
10FA	80.2 (15.7)	12.0 (1.8)	0.8 (0.1)
20FA	80.5 (10.0)	12.1 (0.9)	0.8 (0.1)
30FA	74.5 (12.4)	12.0 (1.7)	1.4 (0.4)
40FA	68.3 (9.4)	12.0 (0.01)	1.2 (0.06)

Selected correlation analysis was also conducted to investigate the relationship between the different composite formulations and their mechanical behaviour. Pearson's correlation tests were conducted between Vickers hardness (HV) wear, flexural strength (FS), flexural modulus (FM) and fracture toughness. The correlation coefficient "*r* value" closer ±1 is considered as a perfect correlation while *r* values ranging between;

- 00-0.19 "very weak"
- 0.20-0.39 "weak"
- 0.40-0.59 "moderate"
- 0.60-0.79 "strong"
- 0.80-1.0 "very strong"

Results showed direct positive moderate linear correlations between FM and FS ($r = 0.549$, $p = 0.000$), as shown in the corresponding scatter plot Figure 70. However, no other correlations were found amongst other tests, Table 25 and Figure 71. The relationship between FM and FS has been widely reported in the literature where a high linear correlation was found amongst most resin composites studied. The correlation between wear and microhardness of resin composites has been investigated by several researchers, however the complexity of the wear process caused conflicting reports in the literature (Manhart et al., 2000, Mandikos et al.,

2001, Ferracane, 2013a). This study showed no correlation between HV and the wear resistance of the materials tested. Fracture toughness also did not correlate to any of the other mechanical properties tested in this study, although a moderately strong correlation was previously reported between FS and fracture toughness (Manhart et al., 2000, Kim et al., 2002, Takahashi et al., 2011, Jun et al., 2013a). However, the relationship between FS and fracture toughness requires further investigation as the pre-cracking approach and testing variables were shown to significantly affect the fracture toughness value of resin composites (Ferracane et al., 1987, Zhao et al., 1997, Tantbirojn et al., 2003).

Table 25: Pearson's correlations between the mechanical tests conducted.

Tests correlations		*r*	*p*-value
Wear	Vickers hardness	-0.160	0.446
	Flexural strength	-0.099	0.603
	Flexural modulus	-0.034	0.859
	Fracture Toughness	0.074	0.698
Flexural strength	wear	-0.099	0.603
	Flexural modulus	**0.549****	0.000
	Fracture Toughness	0.108	0.412
Flexural modulus	wear	-0.034	0.859
	Flexural strength	**0.549****	0.000
	Fracture Toughness	0.039	0.765
Fracture Toughness	wear	0.074	0.698
	Flexural strength	0.108	0.412
	Flexural modulus	0.039	0.765

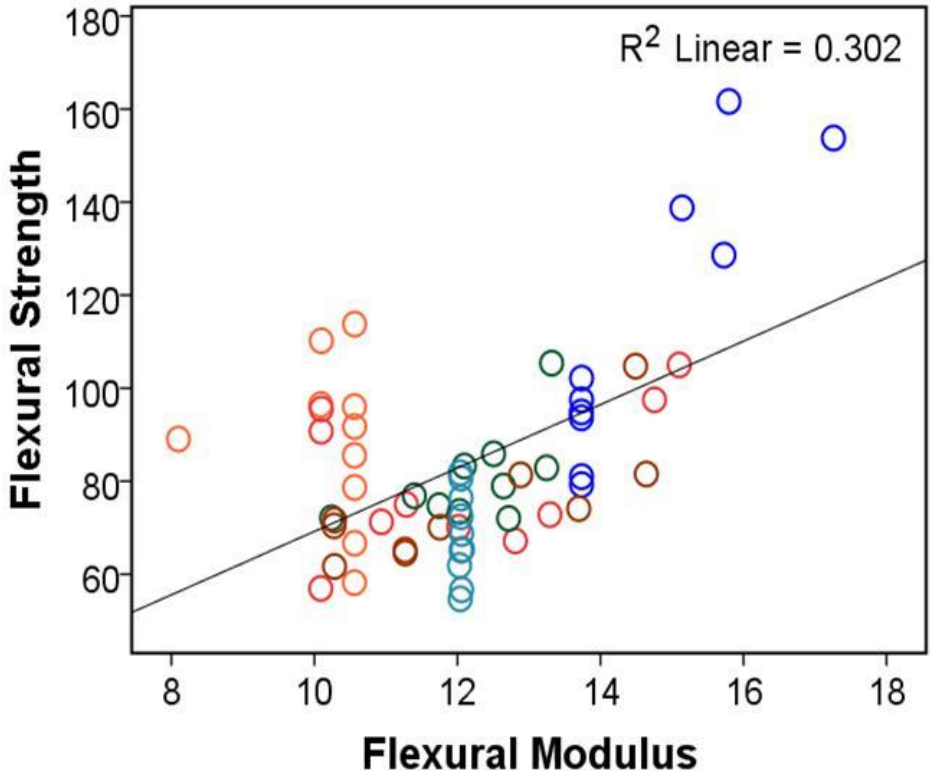

Figure 70: Scatter plot showing the correlation between flexural strength (MPa) and flexural modulus (GPa).

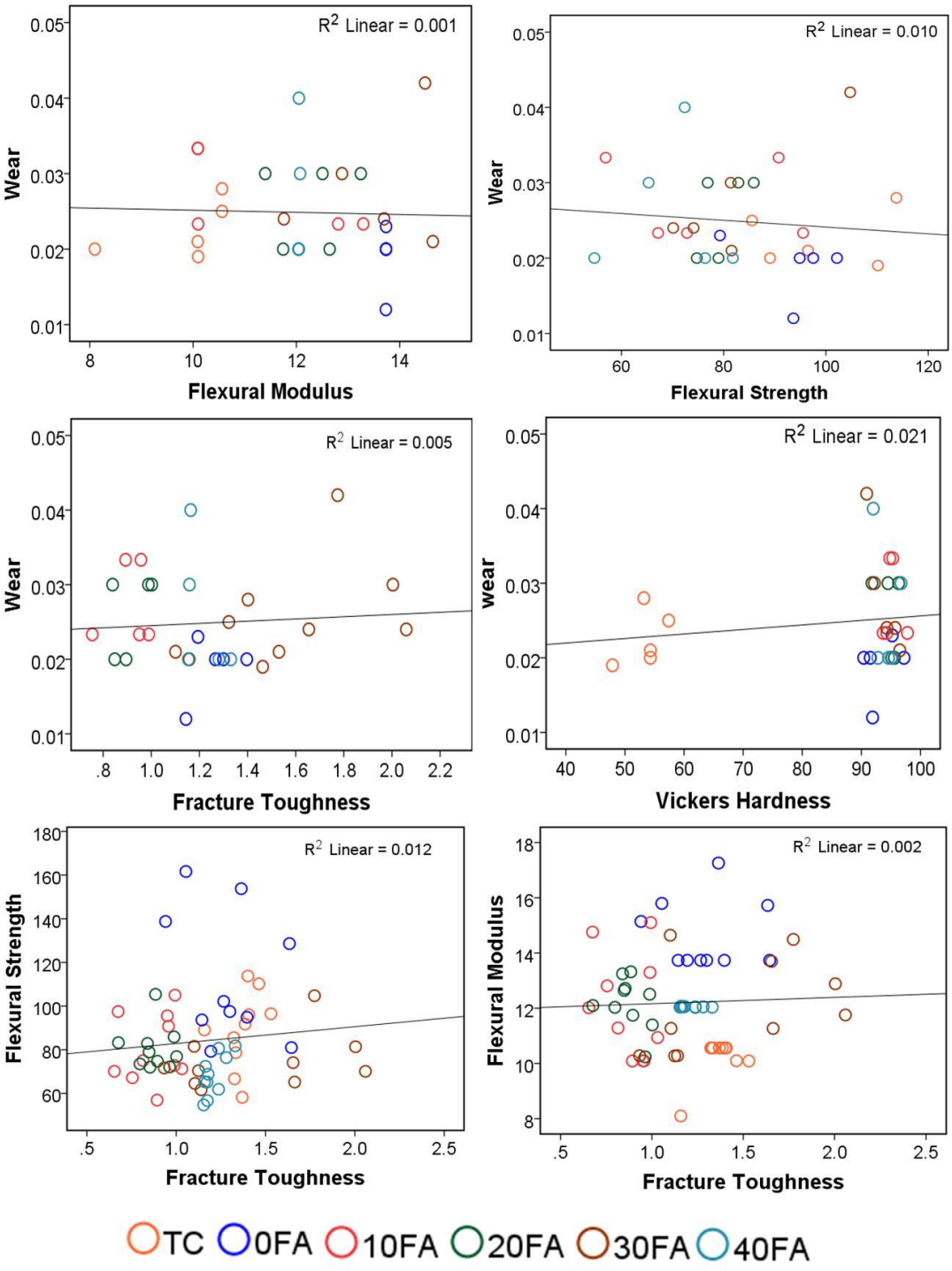

Figure 71: Scatter plots showing correlations between the mechanical properties tested including wear (mean volume loss mm^3), vickers hardness (HV), flexural strength (MPa), flexural modulus (GPa) and fracture toughness ($MPa.m^{(1/2)}$).

Calcium and fluoride ions are widely known to be effective in strengthening the tooth tissue through enhancement of the remineralisation process (Cury and Tenuta, 2009, Fejerskov O et al., 2015) . Therefore a restorative material that is capable of releasing these ions adjacent to the demineralised tooth tissue would be expected to enhance the formation of caries resistant fluoroapatite on the tooth and consequently results in reduced caries progression. Studies have shown that the fluoride concentrations in plaque adjacent to fluoride releasing restorations is significantly higher than fluoride levels in plaque following the use of fluoride containing mouthwashes, 7–21 μgF^- and 1–5 μgF^- per gram of plaque respectively (Duckworth et al., 1987, Benelli et al., 1993, Forss et al., 1995). Given the large number of composites restorations placed nowadays, composites that contain available sources of these ions may have substantial advantages compared to those that do not release these ions. Various fluoride releasing restoratives are currently available such as glass ionomer cements (GIC), resin modified glass ionomers (RMGIC), compomers and fluoride containing composites. Composites have been shown to release the lowest amounts of fluoride in the long term when compared to GIC, RMGIC and compomers (Karantakis et al., 2000, Vermeersch et al., 2001, Wiegand et al., 2007). Most commercial composites formulations contain soluble source of fluoride incorporated into the filler system such as strontium fluoride (SrF_2) and ytterbium trifluoride (YbF_3). More recently experimental materials with alternative novel filler systems such as bioactive glass fillers (BAGs) were developed and are still under investigation; when used in resin composites they may possess potential bioactive properties that could inhibit caries progression (Hyun et al., 2015, Alania et al., 2016). An alternative approach was employed in this study by using an alternative filler system through the incorporation of synthesised fluorapatite crystals as secondary filler. To mimic the natural caries resistance of teeth, it was suggested that synthesised fluorapatite crystals could be a suitable and effective chemically stable anti-caries material (Chen et al., 2006b).

Furthermore, synthesised FA crystals have a unique hexagonal structure in the form of crystals and bundles of crystals which can act as reinforcing filler within the resin matrix of dental composites. Experimental composites prepared in this study contained 10-40% FA. Composites specimens were immersed in neutral and acidic media for evaluation of fluoride ion release using the ion selective electrode methodology. The protocol used in this study was daily fluoride measurements for the first week, followed by weekly measurements for the first month and monthly measurements up to 196 days. Under neutral conditions, no fluoride release was detected from the FA composites and the control groups suggesting a lack of loosely bound or surface bound fluoride; therefore it was decided not to continue the experiment under neutral condition as none of the groups released fluoride over the first 48 hours, (Table 19). However, under acidic conditions, all FA composites released statistically significant amounts of fluoride when compared to the control groups ($p < 0.05$). The lack of fluoride ion release under neutral medium present a favourable property of these materials as fluoride would only be required when the pH drops causing tooth tissue demineralisation. All FA composites showed similar pattern and amount of fluoride release which was at its highest in the first day. Following the initial release, the amount of fluoride release started to slow down from day two up to day 7. 10FA and 20FA composites continued to release small amounts of fluoride at a consistent rate, however there were no significant differences in the cumulative fluoride released at extended time intervals ($p > 0.05$). 30FA and 40FA showed consistent increase in the fluoride release over extended period of times; this increase was shown to be significant at Day 196 when compared to Day 112 ($p < 0.05$). FA containing composites showed significantly higher cumulative fluoride release over the entire testing period when compared to TC and 0FA ($p < 0.05$). Generally the amount of fluoride released was proportional to the concentration of FA used (cumulative release profile shown in Figure 65). The cumulative release of FA composites ranged between (20.0-54.9 µg/cm^2) in the first week which increased to (25.9-163.4 µg/cm^2)

by day 196, Table 20. These values are shown to be higher than the cumulative fluoride release from commercial resin composites which was reported to be less than 0.5 µg/mm^2 during a period of 90-120 days (Karantakis et al., 2000, Vermeersch et al., 2001). To date, there has been no consensus on the amount of fluoride required for a restorative material to be effective against recurrent caries; however it is generally suggested that the effect of fluoride releasing restoratives is mostly due to the localised fluoridation adjacent to the demineralisation zones rather than elevation of fluoride levels in saliva. It has been reported that localised small amounts of fluoride approximately in the ranges of 0.03-0.08 ppm and 0.63-1.3 µg F^-/cm^2/day is sufficient to shift the equilibrium from demineralisation to re-mineralisation (Rawls, 1995, Wiegand et al., 2007). Therefore all FA composites showed fluoride release within the range considered to be effective in preventing demineralisation. In addition to that, the amount of fluoride is considerably higher when compared to the commercially available fluoride releasing dental composites (Karantakis et al., 2000, Vermeersch et al., 2001). The mechanism by which fluoride was released from the FA composites was due to the dissolution of the FA crystals when subjected to acidic environmental which was evident from the SEM images. The initial high daily release followed by a reduced but sustained release may simply be due to the fact that at extended time points, there was little FA remaining. SEM showed that the FA rods could be completely dissolved at these time points, leaving holes where crystals had once been. It is important to reflect that this was an accelerated degradation study and that a patient's exposure to acid in the oral cavity is infrequent and episodic in nature and that saliva effectively buffers the acid challenges a patient experiences due to eating/drinking (Walters et al., 2016, Fonseca et al., 2017). Nevertheless, it would be worth measuring mechanical properties of these degraded materials to see if there was a reduction in mechanical properties as a consequence of the presence of voids. The dissolution of the FA crystals also suggests calcium and phosphate ions release. Therefore it is certainly worth investigating the calcium and phosphate ion release from the FA composites using the

same protocol used for fluoride ion release. In addition to that, it is worth investigating the materials' behaviour using pH cycling models to mimic the demineralisation and remineralisation processes and to use in-situ/biofilm models. This may provide further insight into the behaviour of FA composites which might be a suitable "smart" composite that react with the surrounding environment and may prevent recurrent caries progression.

Limitations of this study are also acknowledged such as the lack of surface coupling of fluorapatite fillers. Surface coupling may further enhance the mechanical properties of FA composites; conversely the fluoride releasing properties may be affected. Therefore, further research is suggested to investigate the possibility of surface coupling of FA followed by re-evaluation of the materials properties. In addition to that, clinical translation of these composite formulations would require further extensive research evaluating the effectiveness of ion release on caries formation and progression around FA composites. Further work is therefore suggested and detailed in the next chapter.

In summary, this project suggests an alternative approach to introduce bioactive properties to resin composites by incorporating synthesised fluorapatite as secondary filler. Successful novel fluorapatite containing resin composites were produced which exhibited adequate key physical and mechanical properties comparable to most contemporary commercial resin composites. Additionally these novel formulations have the advantage of short and long term fluoride release under acidic conditions showing promising step toward "smart" fluoride releasing dental composite. Fluorapatite was shown to be a suitable filler to be used in resin composites while maintaining adequate key physical and mechanical properties.

6.1 Limitations of the study

- The lack of surface coupling of the FA fillers is acknowledged which may have attributed to the reduced mechanical properties when compared to the commercial control.
- Tetric Evo ceram was the only commercial composite control used in this study. Therefore it is worth investigating the performance of FA composites when compared to a wider range of commercial dental composites
- *In-vitro* wear testing was conducted for an equivalent of ~3 month clinical wear, however long term wear testing may provide further insight into the materials' behaviour
- Degree of conversion was conducted in real time however further insight could be gained by investigating the depth of cure of FA composites.

6.2 Conclusions

- Highly filled experimental composites were successfully produced incorporating FA as secondary filler.
- The addition of FA did not affect the key physical and mechanical properties of FA composites when compared to the commercial control.
- A direct positive moderate linear correlation was found between flexural modulus and flexural strength of the tested composites in this study.
- The unique morphology of FA crystals endorsed fracture toughening mechanisms of FA composites leading to increased fracture toughness when higher concentration of FA was used.
- FA composites showed short and long term fluoride release under acidic conditions showing a promising step towards a potential “smart” fluoride releasing dental composite.

Chapter 7: Future work

Experimental FA composites would require further development and characterisation to include the below:

- To measure the calcium and phosphate ion release from the FA resin composites.
- Evaluate the effect of surface coupling of the FA crystals on the mechanical properties of FA resin composites.
- Evaluate the effect of surface coupling on the fluoride, calcium and phosphate ion release.
- To evaluate the effect of aging on the mechanical properties of FA composites.
- Incorporation of FA filler with different resin formulations with similar refractive index to enhance the depth of cure properties
- To evaluate the optical properties including translucency and opacity for optimum shade matching.
- To evaluate the polishability and the surface roughness of FA resin composites.
- To evaluate the effect of fluoride ion release using pH cycling models mimicking the demineralisation and remineralisation processes.
- To evaluate the effect of fluoride ion release using in-situ/biofilm models.
- To translate the experimental materials for clinical use and conduct a clinical trial evaluating the clinical performance of the experimental FA resin composites compared to conventional composites *in-vivo*.

Chapter 8: References

ASTM E399-12-e2. Standard Test Method for Linear-Elastic Plane-Strain Fracture Toughness KIc of Metallic Materials.

ISO 4049 (2009). Polymer-based restorative materials.

ABBAS, G., FLEMING, G. J. P., HARRINGTON, E., SHORTALL, A. C. C. & BURKE, F. J. T. 2003. Cuspal movement and microleakage in premolar teeth restored with a packable composite cured in bulk or in increments. *Journal of Dentistry,* 31**,** 437-444.

AIZAWA, M., HANAZAWA, T., ITATANI, K., HOWELL, F. S. & KISHIOKA, A. 1999. Characterization of hydroxyapatite powders prepared by ultrasonic spray-pyrolysis technique. *Journal of Materials Science,* 34**,** 2865-2873.

ALANIA, Y., CHIARI, M. D. S., RODRIGUES, M. C., ARANA-CHAVEZ, V. E., BRESSIANI, A. H. A., VICHI, F. M. & BRAGA, R. R. 2016. Bioactive composites containing TEGDMA-functionalized calcium phosphate particles: Degree of conversion, fracture strength and ion release evaluation. *Dental Materials,* 32**,** e374-e381.

ALJABO, A., XIA, W., LIAQAT, S., KHAN, M. A., KNOWLES, J. C., ASHLEY, P. & YOUNG, A. M. 2015. Conversion, shrinkage, water sorption, flexural strength and modulus of re-mineralizing dental composites. *Dental Materials,* 31**,** 1279-1289.

ALSHAAFI, M., HAENEL, T., SULLIVAN, B., LABRIE, D., ALQAHTANI, M. Q. & PRICE, R. B. 2016. Effect of a broad-spectrum LED curing light on the Knoop microhardness of four posterior resin based composites at 2, 4 and 6-mm depths. *J Dent,* 45**,** 14-8.

ALTAIE, A. 2012. *Wear Resistance of Contemporary Dental Composites.* MSc thesis, University of Leeds, UK.

ALTAIE, A., BUBB, N. L., FRANKLIN, P., DOWLING, A. H., FLEMING, G. J. P. & WOOD, D. J. 2017. An approach to understanding tribological behaviour of dental composites through volumetric wear loss and wear mechanism determination; beyond material ranking. *Journal of Dentistry,* 59**,** 41-47.

ALVAREZ-GAYOSSO, C., BARCELO-SANTANA, F., GUERRERO-IBARRA, J., SAEZ-ESPINOLA, G. & CANSECO-MARTINEZ, M. A. 2004. Calculation of contraction rates due to shrinkage in light-cured composites. *Dental Materials,* 20**,** 228-235.

AMIROUCHE-KORICHI, A., MOUZALI, M. & WATTS, D. C. 2009. Effects of monomer ratios and highly radiopaque fillers on degree of conversion and shrinkage-strain of dental resin composites. *Dental Materials,* 25**,** 1411-1418.

ANTONUCCI, J. M., DICKENS, S. H., FOWLER, B. O., XU, H. H. K. & MCDONOUGH, W. G. 2005. Chemistry of silanes: Interfaces in dental polymers and composites. *Journal of Research of the National Institute of Standards and Technology,* 110**,** 541-558.

ANTUNES, P. V. & RAMALHO, A. 2009. Influence of pH values and aging time on the tribological behaviour of posterior restorative materials. *Wear,* 267**,** 718-725.

ARCíS, R. W., LÓPEZ-MACIPE, A., TOLEDANO, M., OSORIO, E., RODRíGUEZ-CLEMENTE, R., MURTRA, J., FANOVICH, M. A. & PASCUAL, C. D. 2002. Mechanical properties of visible light-cured resins reinforced with hydroxyapatite for dental restoration. *Dental Materials,* 18**,** 49-57.

ARENDS, J., DIJKMAN, G. E. H. M. & DIJKMAN, A. G. 1995. Review of Fluoride Release and Secondary Caries Reduction by Fluoridating Composites. *Advances in dental research,* 9**,** 367-376.

ARIKAWA, H., KANIE, T., FUJII, K., TAKAHASHI, H. & BAN, S. 2008. Effect of Inhomogeneity of Light from Light Curing Units on the Surface Hardness of Composite Resin. *Dental Materials Journal,* 27**,** 21-28.

ARSECULARATNE, J. A., CHUNG, N. R. & HOFFMAN, M. 2016. An in vitro study of the wear behaviour of dental composites. *Biosurface and Biotribology,* 2**,** 102-113.

ASMUSSEN, E. 1982. Factors affecting the quantity of remaining double bonds in restorative resin polymers. *Scand J Dent Res,* 90**,** 490-6.

ASMUSSEN, E. 1984. Softening of BISGMA-based polymers by ethanol and by organic acids of plaque. *Scandinavian Journal of Dental Research,* 92**,** 257-261.

ÁSTVALDSDÓTTIR, Á., DAGERHAMN, J., VAN DIJKEN, J. W., NAIMI-AKBAR, A., SANDBORGH-ENGLUND, G., TRANÆUS, S. & NILSSON, M. 2015. Longevity of posterior resin composite restorations in adults–a systematic review. *Journal of Dentistry,* 43**,** 934-954.

ATAI, M. & WATTS, D. C. 2006. A new kinetic model for the photopolymerization shrinkage-strain of dental composites and resin-monomers. *Dental Materials,* 22**,** 785-791.

ATTAR, N. & ONEN, A. 2002. Fluoride release and uptake characteristics of aesthetic restorative materials. *J Oral Rehabil,* 29**,** 791-8.

ATTAR, N. & TURGUT, M. D. 2003. Fluoride release and uptake capacities of fluoride-releasing restorative materials. *Oper Dent,* 28**,** 395-402.

AYDIN SEVINC, B. & HANLEY, L. 2010. Antibacterial activity of dental composites containing zinc oxide nanoparticles. *J Biomed Mater Res B Appl Biomater,* 94**,** 22-31.

BAJAJ, D. & AROLA, D. D. 2009. On the R-curve behavior of human tooth enamel. *Biomaterials,* 30**,** 4037-4046.

BALKENHOL, M., KOEHLER, H., ORBACH, K. & WOESTMANN, B. 2009. Fracture toughness of cross-linked and non-cross-linked temporary crown and fixed partial denture materials. *Dental Materials,* 25**,** 917-928.

BAROUDI, K., SALEH, A. M., SILIKAS, N. & WATTS, D. C. 2007. Shrinkage behaviour of flowable resin-composites related to conversion and filler-fraction. *Journal of Dentistry,* 35**,** 651-655.

BEAZOGLOU, T., EKLUND, S., HEFFLEY, D., MEIERS, J., BROWN, L. J. & BAILIT, H. 2007. Economic impact of regulating the use of amalgam restorations. *Public Health Rep,* 122**,** 657-63.

BECHTLE, S., HABELITZ, S., KLOCKE, A., FETT, T. & SCHNEIDER, G. A. 2010. The fracture behaviour of dental enamel. *Biomaterials,* 31**,** 375-384.

BECK, F., LETTNER, S., GRAF, A., BITRIOL, B., DUMITRESCU, N., BAUER, P., MORITZ, A. & SCHEDLE, A. 2015a. Survival of direct resin restorations in posterior teeth within a 19-year period (1996-2015): A meta-analysis of prospective studies. *Dent Mater,* 31**,** 958-85.

BECK, F., LETTNER, S., GRAF, A., BITRIOL, B., DUMITRESCU, N., BAUER, P., MORITZ, A. & SCHEDLE, A. 2015b. Survival of direct resin restorations in posterior teeth within a 19-year period (1996–2015): A meta-analysis of prospective studies. *Dental Materials,* 31**,** 958-985.

BEER F, J. R., DEWOLF J, MAZUREK D. 2008. *Mechanics of Materials. 5th ed.*, McGraw-Hill Companies.

BELL, A., CREANOR, S. L., FOYE, R. H. & SAUNDERS, W. P. 1999. The effect of saliva on fluoride release by a glass-ionomer filling material. *J Oral Rehabil,* 26**,** 407-12.

BENELLI, E., SERRA, M. C., RODRIGUES JR, A. & CURY, J. A. 1993. In situ Anticariogenic Potential of Glass Ionomer Cement. *Caries Research,* 27**,** 280-284.

BENETTI, A. R., LARSEN, L., DOWLING, A. H. & FLEMING, G. J. P. 2016. Assessment of wear facets produced by the ACTA wear machine. *Journal of Dentistry,* 45**,** 19-25.

BERNARDO, M., LUIS, H., MARTIN, M. D., LEROUX, B. G., RUE, T., LEITAO, J. & DEROUEN, T. A. 2007. Survival and reasons for failure of amalgam versus composite posterior restorations placed in a randomized clinical trial. *Journal of the American Dental Association,* 138**,** 775-783.

BEYTH, N., FARAH, S., DOMB, A. J. & WEISS, E. I. 2014. Antibacterial dental resin composites. *Reactive and Functional Polymers,* 75**,** 81-88.

BEYTH, N., YUDOVIN-FARBER, I., BAHIR, R., DOMB, A. J. & WEISS, E. I. 2006. Antibacterial activity of dental composites containing quaternary ammonium polyethylenimine nanoparticles against Streptococcus mutans. *Biomaterials,* 27**,** 3995-4002.

BEYTH, N., YUDOVIN-FARBER, I., PEREZ-DAVIDI, M., DOMB, A. J. & WEISS, E. I. 2010a. Polyethyleneimine nanoparticles incorporated

into resin composite cause cell death and trigger biofilm stress in vivo. *Proc Natl Acad Sci U S A,* 107**,** 22038-43.

BEYTH, N., YUDOVIN-FEARBER, I., DOMB, A. J. & WEISS, E. I. 2010b. Long-term antibacterial surface properties of composite resin incorporating polyethyleneimine nanoparticles. *Quintessence International,* 41**,** 827-835.

BILTON, M., BROWN, A. & MILNE, S. Sol-gel synthesis and characterisation of nano-scale hydroxyapatite. Journal of Physics: Conference Series, 2010. IOP Publishing, 012052.

BLACKHAM, J. T., VANDEWALLE, K. S. & LIEN, W. 2009. Properties of Hybrid Resin Composite Systems Containing Prepolymerized Filler Particles. *Operative Dentistry,* 34**,** 697-702.

BONILLA, E. D., YASHAR, M. & CAPUTO, A. A. 2003. Fracture toughness of nine flowable resin composites. *The Journal of Prosthetic Dentistry,* 89**,** 261-267.

BOUILLAGUET, S., GAMBA, J., FORCHELET, J., KREJCI, I. & WATAHA, J. C. 2006. Dynamics of composite polymerization mediates the development of cuspal strain. *Dental Materials,* 22**,** 896-902.

BOWEN RL. 1962. *Dental Filling Materials Comprising of Vinyl-Silane Treated Fused Silica and Binder Consisting of the Reaction Product of Bisphenol And Glycidyl Methacrylate. US Patent 3, 066,112*.

BRAEM, M., FINGER, W., VAN DOREN, V. E., LAMBRECHTS, P. & VANHERLE, G. 1989. Mechanical properties and filler fraction of dental composites. *Dental Materials,* 5**,** 346-349.

BRAGA, R. R., BALLESTER, R. Y. & FERRACANE, J. L. 2005. Factors involved in the development of polymerization shrinkage stress in resin-composites: a systematic review. *Dental Materials,* 21**,** 962-970.

BRAGA, R. R. & FERRACANE, J. L. 2002. Contraction stress related to degree of conversion and reaction kinetics. *J Dent Res,* 81**,** 114-8.

BRAUN, A. R., FRANKENBERGER, R. & KRAMER, N. 2001. Clinical performance and margin analysis of ariston pHc versus Solitaire I as posterior restorations after 1 year. *Clin Oral Investig,* 5**,** 139-47.

BURKE, F., WILSON, N., CREANOR, S. & BRUNTON, P. 2017. Materials used by UK dentists: Results of a Questionare. *IADR.* San Francisco, USA.

BURKE, F. J., CHEUNG, S. W., MJOR, I. A. & WILSON, N. H. 1999. Reasons for the placement and replacement of restorations in vocational training practices. *Primary dental care : journal of the Faculty of General Dental Practitioners (UK),* 6**,** 17-20.

BURKE, F. J. T. 2004. Amalgam to tooth-coloured materials - implications for clinical practice and dental education: governmental restrictions and amalgam-usage survey results. *Journal of Dentistry,* 32**,** 343-350.

BURTSCHER, P. 1993. Stability of radicals in cured composite materials. *Dental Materials,* 9**,** 218-221.

CARIOSCIA, J. A., LU, H., STANBURY, J. W. & BOWMAN, C. N. 2005. Thiol-ene oligomers as dental restorative materials. *Dental Materials,* 21**,** 1137-1143.

CARRADÒ, A., PERRIN-SCHMITT, F., LE, Q. V., GIRAUDEL, M., FISCHER, C., KOENIG, G., JACOMINE, L., BEHR, L., CHALOM, A., FIETTE, L., MORLET, A. & POURROY, G. 2017. Nanoporous hydroxyapatite/sodium titanate bilayer on titanium implants for improved osteointegration. *Dental Materials,* 33**,** 321-332.

CATE, J. M. 1999. Current concepts on the theories of the mechanism of action of fluoride. *Acta Odontol Scand,* 57**,** 325-9.

CHAN, K., LEE, Y.-D., NICOLELLA, D., FURMAN, B., WELLINGHOFF, S. & RAWLS, R. 2007. Improving fracture toughness of dental nanocomposites by interface engineering and micromechanics. *Engineering fracture mechanics,* 74**,** 1857-1871.

CHEN, H., SUN, K., TANG, Z., LAW, R. V., MANSFIELD, J. F. & CLARKSON, B. H. 2006a. Synthesis of Fluorapatite Nanorods and Nanowires by Direct Precipitation from Solution. *Crystal growth & design,* 6**,** 1504-1508.

CHEN, H., TANG, Z., LIU, J., SUN, K., CHANG, S. R., PETERS, M. C., MANSFIELD, J. F., CZAJKA-JAKUBOWSKA, A. & CLARKSON, B. H. 2006b. Acellular Synthesis of a Human Enamel-like Microstructure. *Advanced Materials,* 18**,** 1846-1851.

CHEN, Y. C., FERRACANE, J. L. & PRAHL, S. A. 2007. Quantum yield of conversion of the photoinitiator camphorquinone. *Dent Mater,* 23**,** 655-64.

CONDON, J. R. & FERRACANE, J. L. 1997. In vitro wear of composite with varied cure, filler level, and filler treatment. *Journal of Dental Research,* 76**,** 1405-1411.

CONDON, J. R. & FERRACANE, J. L. 2002. Reduced polymerization stress through non-bonded nanofiller particles. *Biomaterials,* 23**,** 3807-3815.

COOK, W. D. 1992. Thermal aspects of the kinetics of dimethacrylate photopolymerization. *Polymer,* 33**,** 2152-2161.

COOLEY, R. L., SANDOVAL, V. A. & BARNWELL, S. E. 1988. Fluoride release and color stability of a fluoride-containing composite resin. *Quintessence Int,* 19**,** 899-904.

CORNELL, J. A., JORDAN, J. S., ELLIS, S. & ROSE, E. E. 1957. A method of comparing the wear resistance of various materials used for artificial teeth. *Journal of the American Dental Association (1939),* 54**,** 608-14.

CORRER, G. M., ALONSO, R. C. B., SOBRINHO, L. C., PUPPIN-RONTANI, R. M. & FERRACANE, J. L. 2006. In vitro wear of resin-

based materials - Simultaneous corrosive and abrasive wear. *Journal of Biomedical Materials Research Part B-Applied Biomaterials,* 78B**,** 105-114.

CRAMER, N. B., COUCH, C. L., SCHRECK, K. M., CARIOSCIA, J. A., BOULDEN, J. E., STANSBURY, J. W. & BOWMAN, C. N. 2010. Investigation of thiol-ene and thiol-ene–methacrylate based resins as dental restorative materials. *Dental Materials,* 26**,** 21-28.

CURTIS, A. R., PALIN, W. M., FLEMING, G. J. P., SHORTALL, A. C. C. & MARQUIS, P. M. 2009. The mechanical properties of nanofilled resin-based composites: The impact of dry and wet cyclic pre-loading on bi-axial flexure strength. *Dental Materials,* 25**,** 188-197.

CURY, J. A., DE OLIVEIRA, B. H., DOS SANTOS, A. P. & TENUTA, L. M. 2016. Are fluoride releasing dental materials clinically effective on caries control? *Dent Mater,* 32**,** 323-33.

CURY, J. A. & TENUTA, L. M. A. 2009. Enamel remineralization: Controlling the caries disease or treating early caries lesions? *Brazilian oral research,* 23**,** 23-30.

CZAJKA-JAKUBOWSKA, A. E., LIU, J., CHANG, S. R. & CLARKSON, B. H. 2009. The effect of the surface characteristics of various substrates on fluorapatite crystal growth, alignment, and spatial orientation. *Med Sci Monit,* 15**,** MT84-8.

DA ROSA RODOLPHO, P. A., DONASSOLLO, T. A., CENCI, M. S., LOGUERCIO, A. D., MORAES, R. R., BRONKHORST, E. M., OPDAM, N. J. & DEMARCO, F. F. 2011. 22-Year clinical evaluation of the performance of two posterior composites with different filler characteristics. *Dent Mater,* 27**,** 955-63.

DA VEIGA, A. M. A., CUNHA, A. C., FERREIRA, D. M. T. P., DA SILVA FIDALGO, T. K., CHIANCA, T. K., REIS, K. R. & MAIA, L. C. 2016. Longevity of direct and indirect resin composite restorations in permanent posterior teeth: A systematic review and meta-analysis. *Journal of Dentistry,* 54**,** 1-12.

DAVIS, H. B., GWINNER, F., MITCHELL, J. C. & FERRACANE, J. L. 2014. Ion release from, and fluoride recharge of a composite with a fluoride-containing bioactive glass. *Dental Materials,* 30**,** 1187-1194.

DELONG, R. 2006. Intra-oral restorative materials wear: Rethinking the current approaches: How to measure wear. *Dental Materials,* 22**,** 702-711.

DEMARCO, F. F., CORREA, M. B., CENCI, M. S., MORAES, R. R. & OPDAM, N. J. 2012a. Longevity of posterior composite restorations: not only a matter of materials. *Dent Mater,* 28**,** 87-101.

DEMARCO, F. F., CORREA, M. B., CENCI, M. S., MORAES, R. R. & OPDAM, N. J. M. 2012b. Longevity of posterior composite restorations: Not only a matter of materials. *Dental Materials,* 28**,** 87-101.

DEMARCO, F. F., CORRÊA, M. B., CENCI, M. S., MORAES, R. R. & OPDAM, N. J. M. 2012c. Longevity of posterior composite restorations: Not only a matter of materials. *Dental Materials,* 28**,** 87-101.

DEWAELE, M., TRUFFIER-BOUTRY, D., DEVAUX, J. & LELOUP, G. 2006. Volume contraction in photocured dental resins: the shrinkage-conversion relationship revisited. *Dent Mater,* 22**,** 359-65.

DHONDT, C., DE MAEYER, E. & VERBEECK, R. 2001. Fluoride Release from Glass Ionomer Activated with Fluoride Solutions. *Journal of Dental Research,* 80**,** 1402-1406.

DIJKMAN, G. E., DE VRIES, J., LODDING, A. & ARENDS, J. 1993. Long-term fluoride release of visible light-activated composites in vitro: a correlation with in situ demineralisation data. *Caries Res,* 27**,** 117-23.

DOS SANTOS, G., ALTO, R. M., SAMPAIO FILHO, H., DA SILVA, E. & FELLOWS, C. 2008. Light transmission on dental resin composites. *Dental Materials,* 24**,** 571-576.

DRUMMOND, J. L. 2008. Degradation, Fatigue, and Failure of Resin Dental Composite Materials. *Journal of Dental Research,* 87**,** 710-719.

DUCKWORTH, R., MORGAN, S. & MURRAY, A. 1987. Fluoride in saliva and plaque following use of fluoride-containing mouthwashes. *Journal of Dental Research,* 66**,** 1730-1734.

DURNER, J., OBERMAIER, J., DRAENERT, M. & ILIE, N. 2012. Correlation of the degree of conversion with the amount of elutable substances in nano-hybrid dental composites. *Dental Materials,* 28**,** 1146-1153.

EARL, J. S. 2007. *Hydroxyapatite nanoparticles and dentine tubule infiltration. PhD thesis, University of Leeds.*

EICK, J. D., KOTHA, S. P., CHAPPELOW, C. C., KILWAY, K. V., GIESE, G. J., GLAROS, A. G. & PINZINO, C. S. 2007. Properties of silorane-based dental resins and composites containing a stress-reducing monomer. *Dental Materials,* 23**,** 1011-1017.

EL-SAFTY, S., SILIKAS, N. & WATTS, D. C. 2012. Creep deformation of restorative resin-composites intended for bulk-fill placement. *Dental Materials,* 28**,** 928-935.

ELBISHARI, H., SILIKAS, N. & SATTERTHWAITE, J. 2012. Filler size of resin-composites, percentage of voids and fracture toughness: is there a correlation? *Dental Materials Journal,* 31**,** 523-527.

ERNST, C.-P., MEYER, G. R., KLÖCKER, K. & WILLERSHAUSEN, B. 2004. Determination of polymerization shrinkage stress by means of a photoelastic investigation. *Dental Materials,* 20**,** 313-321.

FEJERSKOV O, CURY JA, TENUTA LMA & V., M. 2015. *Fluorides incaries control. In: Fejerskov O, Kidd E, editors. Dental caries:the disease*

and its clinical management. , third ed. Oxford:Wiley Blackwell; p. 245–76.

FEJERSKOV O, C. B. 1996. *Dynamics of caries lesion formation.,* Copenhagen: Munksgaard. p 187–213., Fejerskov O, Ekstrand J, Burt BA.

FERRACANE, J., ANTONIO, R. & MATSUMOTO, H. 1987. Variables Affecting the Fracture Toughness of Dental Composites, and'. *Journal of Dental Research,* 66**,** 1140-1145.

FERRACANE, J., CONDON, J. & MITCHEM, J. 1997a. Correlating abrasive wear to mechanical properties of experimental dental composites. Transactions of the Academy of Dental Materials A-21.

FERRACANE, J. L. 1985. Correlation between hardness and degree of conversion during the setting reaction of unfilled dental restorative resins. *Dental Materials,* 1**,** 11-14.

FERRACANE, J. L. 1994. Elution of leachable components from composites. *J Oral Rehabil,* 21**,** 441-52.

FERRACANE, J. L. 2011. Resin composite—State of the art. *Dental Materials,* 27**,** 29-38.

FERRACANE, J. L. 2013a. Resin-based composite performance: Are there some things we can't predict? *Dental Materials,* 29**,** 51-58.

FERRACANE, J. L. 2013b. Resin-based composite performance: Are there some things we can’t predict? *Dental Materials,* 29**,** 51-58.

FERRACANE, J. L., BERGE, H. X. & CONDON, J. R. 1998. In vitro aging of dental composites in water - Effect of degree of conversion, filler volume, and filler/matrix coupling. *Journal of Biomedical Materials Research,* 42**,** 465-472.

FERRACANE, J. L. & GREENER, E. H. 1984. Fourier transform infrared analysis of degree of polymerization in unfilled resins--methods comparison. *J Dent Res,* 63**,** 1093-5.

FERRACANE, J. L. & GREENER, E. H. 1986a. The effect of resin formulation on the degree of conversion and mechanical properties of dental restorative resins. *Journal of Biomedical Materials Research,* 20**,** 121-131.

FERRACANE, J. L. & GREENER, E. H. 1986b. The effect of resin formulation on the degree of conversion and mechanical properties of dental restorative resins. *J Biomed Mater Res,* 20**,** 121-31.

FERRACANE, J. L., MITCHEM, J. C., CONDON, J. R. & TODD, R. 1997b. Wear and marginal breakdown of composites with various degrees of cure. *Journal of Dental Research,* 76**,** 1508-1516.

FERRACANE, J. L., MITCHEM, J. C., CONDON, J. R. & TODD, R. 1997c. Wear and marginal breakdown of composites with various degrees of cure. *J Dent Res,* 76**,** 1508-16.

FERRACANE, J. L., PFEIFER, C. S. & HILTON, T. J. 2014. Microstructural features of current resin composite materials. *Current Oral Health Reports,* 1**,** 205-212.

FINLAY, N., HAHNEL, S., DOWLING, A. H. & FLEMING, G. J. P. 2013. The in vitro wear behavior of experimental resin-based composites derived from a commercial formulation. *Dental Materials,* 29**,** 365-374.

FINLAY, N., HAHNEL S FAU - DOWLING, A. H., DOWLING AH FAU - FLEMING, G. J. P. & FLEMING, G. J. The in vitro wear behavior of experimental resin-based composites derived from a commercial formulation.

FLEMING, G. J. P., REILLY, E., DOWLING, A. H. & ADDISON, O. 2016. Data acquisition variability using profilometry to produce accurate mean total volumetric wear and mean maximum wear depth measurements for the OHSU oral wear simulator. *Dental Materials,* 32**,** e176-e184.

FLOYD, C. J. E. & DICKENS, S. H. 2006. Network structure of Bis-GMA- and UDMA-based resin systems. *Dental Materials,* 22**,** 1143-1149.

FONSECA, A. S. Q. S., LABRUNA MOREIRA, A. D., DE ALBUQUERQUE, P. P. A. C., DE MENEZES, L. R., PFEIFER, C. S. & SCHNEIDER, L. F. J. 2017. Effect of monomer type on the CC degree of conversion, water sorption and solubility, and color stability of model dental composites. *Dental Materials,* 33**,** 394-401.

FORSS, H., NÄSE, L. & SEPPÄ, L. 1995. Fluoride Concentration, Mutans Streptococci and Lactobacilli in Plaque from Old Glass Ionomer Fillings. *Caries Research,* 29**,** 50-53.

FUJISHIMA, A. & FERRACANE, J. L. 1996. Comparison of four modes of fracture toughness testing for dental composites. *Dental Materials,* 12**,** 38-43.

FUJITA, K., IKEMI, T. & NISHIYAMA, N. 2011. Effects of particle size of silica filler on polymerization conversion in a light-curing resin composite. *Dental Materials,* 27**,** 1079-1085.

FURTOS, G., COSMA, V., PREJMEREAN, C., MOLDOVAN, M., BRIE, M., COLCERIU, A., VEZSENYI, L., SILAGHI-DUMITRESCU, L. & SIRBU, C. 2005. Fluoride release from dental resin composites. *Materials Science and Engineering: C,* 25**,** 231-236.

FURUSE, A. Y., MONDELLI, J. & WATTS, D. C. 2011. Network structures of Bis-GMA/TEGDMA resins differ in DC, shrinkage-strain, hardness and optical properties as a function of reducing agent. *Dent Mater,* 27**,** 497-506.

GAROUSHI, S., SÄILYNOJA, E., VALLITTU, P. K. & LASSILA, L. 2013. Physical properties and depth of cure of a new short fiber reinforced composite. *Dental Materials,* 29**,** 835-841.

GAUTHIER, M., STANGEL, I., ELLIS, T. & ZHU, X. 2005. Oxygen inhibition in dental resins. *Journal of Dental Research,* 84**,** 725-729.

GHAZAL, M., YANG, B., LUDWIG, K. & KERN, M. 2008. Two-body wear of resin and ceramic denture teeth in comparison to human enamel. *Dental Materials,* 24**,** 502-507.

GONÇALVES, F., PFEIFER, C. C. S., STANSBURY, J. W., NEWMAN, S. M. & BRAGA, R. R. 2010. Influence of matrix composition on polymerization stress development of experimental composites. *Dental Materials,* 26**,** 697-703.

GREGOR, L., BORTOLOTTO, T., FEILZER, A. J. & KREJCI, I. 2013. Shrinkage Kinetics of a Methacrylate- and a Silorane-based Resin Composite: Effect on Marginal Integrity. *Journal of Adhesive Dentistry,* 15**,** 245-250.

HADIS, M., LEPRINCE, J. G., SHORTALL, A. C., DEVAUX, J., LELOUP, G. & PALIN, W. M. 2011. High irradiance curing and anomalies of exposure reciprocity law in resin-based materials. *Journal of Dentistry,* 39**,** 549-557.

HAHNEL, S., DOWLING, A. H., EL-SAFTY, S. & FLEMING, G. J. P. 2012. The influence of monomeric resin and filler characteristics on the performance of experimental resin-based composites (RBCs) derived from a commercial formulation. *Dental Materials,* 28**,** 416-423.

HAHNEL, S., SCHULTZ, S., TREMPLER, C., ACH, B., HANDEL, G. & ROSENTRITT, M. 2011. Two-body wear of dental restorative materials. *Journal of the Mechanical Behavior of Biomedical Materials,* 4**,** 237-244.

HARRISON, A. & DRAUGHN, R. A. 1976. Abrasive wear, tensile strength, and hardness of dental composite resins--is there a relationship. *Journal of Prosthetic Dentistry,* 36**,** 395-398.

HARRISON, A. & LEWIS, T. T. 1975. The development of an brasion testing machine for dental materials *Journal of Biomedical Materials Research,* 9**,** 341-353.

HEINTZE, S. D. 2006. How to qualify and validate wear simulation devices and methods. *Dental Materials,* 22**,** 712-734.

HEINTZE, S. D., BARKMEIER, W. W., LATTA, M. A. & ROUSSON, V. 2011. Round robin test: wear of nine dental restorative materials in six different wear simulators - supplement to the round robin test of 2005. *Dent Mater,* 27**,** e1-9.

HEINTZE, S. D., FAOUZI, M., ROUSSON, V. & ÖZCAN, M. 2012. Correlation of wear in vivo and six laboratory wear methods. *Dental Materials,* 28**,** 961-973.

HEINTZE, S. D., ILIE, N., HICKEL, R., REIS, A., LOGUERCIO, A. & ROUSSON, V. 2017. Laboratory mechanical parameters of composite resins and their relation to fractures and wear in clinical trials—A systematic review. *Dental Materials,* 33**,** e101-e114.

HEINTZE, S. D. & ROUSSON, V. 2012. Clinical effectiveness of direct class II restorations - a meta-analysis. *The journal of adhesive dentistry,* 14**,** 407-31.

HEINTZE, S. D., ROUSSON, V. & HICKEL, R. 2015. Clinical effectiveness of direct anterior restorations—a meta-analysis. *Dental Materials,* 31**,** 481-495.

HEINTZE, S. D., ZAPPINI, G. & ROUSSON, V. 2005a. Wear of ten dental restorative materials in five wear simulators—Results of a round robin test. *Dental Materials,* 21**,** 304-317.

HEINTZE, S. D., ZAPPINI, G. & ROUSSON, V. 2005b. Wear of ten dental restorative materials in five wear simulators - Results of a round robin test. *Dental Materials,* 21**,** 304-317.

HENCH, L. L. 2006. The story of Bioglass®. *Journal of Materials Science: Materials in Medicine,* 17**,** 967-978.

HICKS, J., GARCIA-GODOY, F., DONLY, K. & FLAITZ, C. 2003. Fluoride-releasing restorative materials and secondary caries. *Journal of the California Dental Association,* 31**,** 229-245.

HILTON, T. J. 2002. Can modern restorative procedures and materials reliably seal cavities? In vitro investigations. Part 1. *American Journal of Dentistry,* 15**,** 198-210.

HOFMANN, N., RENNER, J., HUGO, B. & KLAIBER, B. 2002. Elution of leachable components from resin composites after plasma arc vs. standard or soft-start halogen light irradiation. *Journal of Dentistry,* 30**,** 223-232.

HTANG, A., OHSAWA, M. & MATSUMOTO, H. 1995. Fatigue resistance of composite restorations: Effect of filler content. *Dental Materials,* 11**,** 7-13.

HU, X., MARQUIS, P. M. & SHORTALL, A. C. 2003. Influence of filler loading on the two-body wear of a dental composite. *Journal of Oral Rehabilitation,* 30**,** 729-737.

HU, X., SHORTALL, A. C. & MARQUIS, P. M. 2002. Wear of three dental composites under different testing conditions. *Journal of Oral Rehabilitation,* 29**,** 756-764.

HYUN, H.-K., SALEHI, S. & FERRACANE, J. L. 2015. Biofilm formation affects surface properties of novel bioactive glass-containing composites. *Dental Materials,* 31**,** 1599-1608.

ILIE, N., BUCUTA, S. & DRAENERT, M. 2013a. Bulk-fill resin-based composites: an in vitro assessment of their mechanical performance. *Operative Dentistry,* 38**,** 618-625.

ILIE, N. & HICKEL, R. 2007. Quality of curing in relation to hardness, degree of cure and polymerization depth measured on a nano-hybrid composite. *Am J Dent,* 20**,** 263-8.

ILIE, N. & HICKEL, R. 2009a. Investigations on mechanical behaviour of dental composites. *Clinical Oral Investigations,* 13**,** 427.

ILIE, N. & HICKEL, R. 2009b. Macro-, micro-and nano-mechanical investigations on silorane and methacrylate-based composites. *Dental Materials,* 25**,** 810-819.

ILIE, N., HICKEL, R., VALCEANU, A. S. & HUTH, K. C. 2012. Fracture toughness of dental restorative materials. *Clinical Oral Investigations,* 16**,** 489-498.

ILIE, N., HILTON, T. J., HEINTZE, S. D., HICKEL, R., WATTS, D. C., SILIKAS, N., STANSBURY, J. W., CADENARO, M. & FERRACANE, J. L. 2017. Academy of Dental Materials guidance—Resin composites: Part I—Mechanical properties. *Dental Materials*.

ILIE, N., JELEN, E., CLEMENTINO-LUEDEMANN, T. & HICKEL, R. 2007. Low-shrinkage composite for dental application. *Dental Materials Journal,* 26**,** 149-155.

ILIE, N., RENCZ, A. & HICKEL, R. 2013b. Investigations towards nano-hybrid resin-based composites. *Clinical Oral Investigations,* 17**,** 185-193.

IMAZATO, S., MCCABE, J. F., TARUMI, H., EHARA, A. & EBISU, S. 2001. Degree of conversion of composites measured by DTA and FTIR. *Dental Materials,* 17**,** 178-183.

IMAZATO, S., RUSSELL, R. R. & MCCABE, J. F. 1995. Antibacterial activity of MDPB polymer incorporated in dental resin. *J Dent,* 23**,** 177-81.

IMBENI, V., KRUZIC, J. J., MARSHALL, G. W., MARSHALL, S. J. & RITCHIE, R. O. 2005. The dentin-enamel junction and the fracture of human teeth. *Nat Mater,* 4**,** 229-232.

ISMAIL, H. M. 2016. *Further Development of a Novel Fluoride Releasing Acrylic Orthodontic Adhesive.* PhD, University of Newcastle.

ITOTA, T., CARRICK, T. E., RUSBY, S., AL-NAIMI, O. T., YOSHIYAMA, M. & MCCABE, J. F. 2004a. Determination of fluoride ions released from resin-based dental materials using ion-selective electrode and ion chromatograph. *Journal of Dentistry,* 32**,** 117-122.

ITOTA, T., CARRICK, T. E., YOSHIYAMA, M. & MCCABE, J. F. 2004b. Fluoride release and recharge in giomer, compomer and resin composite. *Dental Materials,* 20**,** 789-795.

JÄGGI F 2015. Filling materials—quantity reports. Corporate MarketInsight, Ivoclar Vivadent.

JUN, S. K., KIM, D. A., GOO, H. J. & LEE, H. H. 2013a. Investigation of the correlation between the different mechanical properties of resin composites. *Dental Materials Journal,* 32**,** 48-57.

JUN, S. K., KIM, D. A., GOO, H. J. & LEE, H. H. 2013b. Investigation of the correlation between the different mechanical properties of resin composites. *Dent Mater J,* 32**,** 48-57.

KANCA, J. & SUH, B. I. 1999. Pulse activation: Reducing resin-based composite contraction stresses at the enamel cavosurface margins. *American Journal of Dentistry,* 12**,** 107-112.

KARANTAKIS, P., HELVATJOGLOU-ANTONIADES, M., THEODORIDOU-PAHINI, S. & PAPADOGIANNIS, Y. 2000. Fluoride release from three glass ionomers, a compomer, and a composite resin in water, artificial saliva, and lactic acid. *Oper Dent,* 25**,** 20-5.

KAWASHITA, M., TSUNEYAMA, S., MIYAJI, F., KOKUBO, T., KOZUKA, H. & YAMAMOTO, K. 2000. Antibacterial silver-containing silica glass prepared by sol–gel method. *Biomaterials,* 21**,** 393-398.

KENSCHE, A., HOLDER, C., BASCHE, S., TAHAN, N., HANNIG, C. & HANNIG, M. 2017. Efficacy of a mouthrinse based on hydroxyapatite to reduce initial bacterial colonisation in situ. *Archives of Oral Biology,* 80**,** 18-26.

KHVOSTENKO, D., MITCHELL, J. C., HILTON, T. J., FERRACANE, J. L. & KRUZIC, J. J. 2013. Mechanical performance of novel bioactive glass containing dental restorative composites. *Dental Materials,* 29**,** 1139-1148.

KIM, K., PARK, J., IMAI, Y. & KISHI, T. 1994. Microf racture Mechanisms of Dental Resin Composites Containing Spherically-shaped Filler Particles. *Journal of Dental Research,* 73**,** 499-504.

KIM, K. H., ONG, J. L. & OKUNO, O. 2002. The effect of filler loading and morphology on the mechanical properties of contemporary composites. *Journal of Prosthetic Dentistry,* 87**,** 642-649.

KINNEY, J. H., MARSHALL, S. J. & MARSHALL, G. W. 2003. The Mechanical Properties of Human Dentin: a Critical Review and Re-evaluation of the Dental Literature. *Critical Reviews in Oral Biology & Medicine,* 14**,** 13-29.

KOPPERUD, H. M., JOHNSEN, G. F., LAMOLLE, S., KLEVEN, I. S., WELLENDORF, H. & HAUGEN, H. J. 2013. Effect of short LED lamp exposure on wear resistance, residual monomer and degree of conversion for Filtek Z250 and Tetric EvoCeram composites. *Dental Materials,* 29**,** 824-834.

KOVARIK, R. E. & FAIRHURST, C. W. 1993. Effect of Griffith precracks on measurement of composite fracture toughness. *Dent Mater,* 9**,** 222-8.

LAMBRECHTS, P., DEBELS, E., VAN LANDUYT, K., PEUMANS, M. & VAN MEERBEEK, B. 2006. How to simulate wear? Overview of existing methods. *Dental Materials,* 22**,** 693-701.

LEE, J.-H., UM, C.-M. & LEE, I.-B. 2006. Rheological properties of resin composites according to variations in monomer and filler composition. *Dental Materials,* 22**,** 515-526.

LEMON, M. T., JONES, M. S. & STANSBURY, J. W. 2007. Hydrogen bonding interactions in methacrylate monomers and polymers. *J Biomed Mater Res A,* 83**,** 734-46.

LEPRINCE, J., PALIN, W. M., MULLIER, T., DEVAUX, J., VREVEN, J. & LELOUP, G. 2010. Investigating filler morphology and mechanical properties of new low-shrinkage resin composite types. *J Oral Rehabil,* 37**,** 364-76.

LEPRINCE, J. G., HADIS, M., SHORTALL, A. C., FERRACANE, J. L., DEVAUX, J., LELOUP, G. & PALIN, W. M. 2011. Photoinitiator type and applicability of exposure reciprocity law in filled and unfilled photoactive resins. *Dent Mater,* 27**,** 157-64.

LEPRINCE, J. G., LEVEQUE, P., NYSTEN, B., GALLEZ, B., DEVAUX, J. & LELOUP, G. 2012. New insight into the “depth of cure” of dimethacrylate-based dental composites. *Dental Materials,* 28**,** 512-520.

LEPRINCE, J. G., PALIN, W. M., HADIS, M. A., DEVAUX, J. & LELOUP, G. 2013. Progress in dimethacrylate-based dental composite technology and curing efficiency. *Dent Mater,* 29**,** 139-56.

LEPRINCE, J. G., PALIN, W. M., VANACKER, J., SABBAGH, J., DEVAUX, J. & LELOUP, G. 2014. Physico-mechanical characteristics of commercially available bulk-fill composites. *Journal of Dentistry,* 42**,** 993-1000.

LEUNG, D., SPRATT, D. A., PRATTEN, J., GULABIVALA, K., MORDAN, N. J. & YOUNG, A. M. 2005. Chlorhexidine-releasing methacrylate dental composite materials. *Biomaterials,* 26**,** 7145-7153.

LIEN, W. & VANDEWALLE, K. S. 2010. Physical properties of a new silorane-based restorative system. *Dental Materials,* 26**,** 337-344.

LIM, B. S., FERRACANE, J. L., CONDON, J. R. & ADEY, J. D. 2002. Effect of filler fraction and filler surface treatment on wear of microfilled composites. *Dental Materials,* 18**,** 1-11.

LINDBERG, A., PEUTZFELDT, A. & VAN DIJKEN, J. W. 2005. Effect of power density of curing unit, exposure duration, and light guide distance on composite depth of cure. *Clin Oral Investig,* 9**,** 71-6.

LIU, J., JIN T FAU - CHANG, S., CHANG S FAU - CZAJKA-JAKUBOWSKA, A., CZAJKA-JAKUBOWSKA A FAU - ZHANG, Z., ZHANG Z FAU - NOR, J. E., NOR JE FAU - CLARKSON, B. H. & CLARKSON, B. H. The effect of novel fluorapatite surfaces on osteoblast-like cell adhesion, growth, and mineralization.

LOHBAUER, U., FRANKENBERGER, R., KRAMER, N. & PETSCHELT, A. 2006. Strength and fatigue performance versus filler fraction of different types of direct dental restoratives. *J Biomed Mater Res B Appl Biomater,* 76**,** 114-20.

LOVELL, L. G., STANSBURY, J. W., SYRPES, D. C. & BOWMAN, C. N. 1999. Effects of Composition and Reactivity on the Reaction Kinetics

of Dimethacrylate/Dimethacrylate Copolymerizations. *Macromolecules,* 32**,** 3913-3921.

LOYOLA-RODRIGUEZ, J. P. & GARCIA-GODOY, F. 1996. Antibacterial activity of fluoride release sealants on mutans streptococci. *J Clin Pediatr Dent,* 20**,** 109-11.

LUTZ, E., KREJCI, I. & OLDENBURG, T. R. 1986. Elimination of polymerization stresses at the margins of posterior composite resin restorations: a new restorative technique. *Quintessence international (Berlin, Germany : 1985),* 17**,** 777-84.

LUTZ, F., KREJCI, I. & BARBAKOW, F. 1992. Chewing pressure vs wear of composites and opposing enamel cusps. *Journal of Dental Research,* 71**,** 1525-1529.

LYNCH, C. D., FRAZIER, K. B., MCCONNELL, R. J., BLUM, I. R. & WILSON, N. H. 2011. Minimally invasive management of dental caries: contemporary teaching of posterior resin-based composite placement in U.S. and Canadian dental schools. *J Am Dent Assoc,* 142**,** 612-20.

LYNCH, C. D., SHORTALL, A. C., STEWARDSON, D., TOMSON, P. L. & BURKE, F. J. 2007. Teaching posterior composite resin restorations in the United Kingdom and Ireland: consensus views of teachers. *Br Dent J,* 203**,** 183-7.

LYNCH, C. D. & WILSON, N. H. F. 2013a. Managing the phase-down of amalgam: part I. Educational and training issues. *Br Dent J,* 215**,** 109-113.

LYNCH, C. D. & WILSON, N. H. F. 2013b. Managing the phase-down of amalgam: part II. Implications for practising arrangements and lessons from Norway. *Br Dent J,* 215**,** 159-162.

MADHYASTHA, P., KOTIAN, R., PAI, V. & KHADER, A. 2013. Fluoride Release from Glass Ionomer Cements: Effect of Temperature, Time Interval and Storage Condition. *Journal of Contemporary Dentistry,* 3**,** 68-73.

MAIR, L. H. 1992. Wear in dentistry – current terminology. *Journal of Dentistry,* 20**,** 140-144.

MAIR, L. H., STOLARSKI, T. A., VOWLES, R. W. & LLOYD, C. H. 1996. Wear: Mechanisms, manifestations and measurement. Report of a workshop. *Journal of Dentistry,* 24**,** 141-148.

MANDIKOS, M. N., MCGIVNEY, G. P., DAVIS, E., BUSH, P. J. & CARTER, J. M. 2001. A comparison of the wear resistance and hardness of indirect composite resins. *The Journal of Prosthetic Dentistry,* 85**,** 386-395.

MANHART, J., CHEN, H. Y. & HICKEL, R. 2009. Three-year results of a randomized controlled clinical trial of the posterior composite QuiXfil in class I and II cavities. *Clin Oral Investig,* 13**,** 301-7.

MANHART, J., KUNZELMANN, K. H., CHEN, H. Y. & HICKEL, R. 2000. Mechanical properties of new composite restorative materials. *Journal of Biomedical Materials Research,* 53**,** 353-361.

MANOJLOVIC, D., DRAMIĆANIN, M. D., MILETIC, V., MITIĆ-ĆULAFIĆ, D., JOVANOVIĆ, B. & NIKOLIĆ, B. 2017. Cytotoxicity and genotoxicity of a low-shrinkage monomer and monoacylphosphine oxide photoinitiator: Comparative analyses of individual toxicity and combination effects in mixtures. *Dental Materials,* 33**,** 454-466.

MANOJLOVIC, D., DRAMIĆANIN, M. D., MILOSEVIC, M., ZEKOVIĆ, I., CVIJOVIĆ-ALAGIĆ, I., MITROVIC, N. & MILETIC, V. 2016. Effects of a low-shrinkage methacrylate monomer and monoacylphosphine oxide photoinitiator on curing efficiency and mechanical properties of experimental resin-based composites. *Materials Science and Engineering: C,* 58**,** 487-494.

MARINHO, V. C., HIGGINS, J. P., SHEIHAM, A. & LOGAN, S. 2004. Combinations of topical fluoride (toothpastes, mouthrinses, gels, varnishes) versus single topical fluoride for preventing dental caries in children and adolescents. *Cochrane Database Syst Rev***,** CD002781.

MAROVIC, D., TARLE, Z., HILLER, K. A., MÜLLER, R., RISTIC, M., ROSENTRITT, M., SKRTIC, D. & SCHMALZ, G. 2014. Effect of silanized nanosilica addition on remineralizing and mechanical properties of experimental composite materials with amorphous calcium phosphate. *Clinical Oral Investigations,* 18**,** 783-792.

MASOURAS, K., AKHTAR, R., WATTS, D. C. & SILIKAS, N. 2008a. Effect of filler size and shape on local nanoindentation modulus of resin-composites. *J Mater Sci Mater Med,* 19**,** 3561-6.

MASOURAS, K., SILIKAS, N. & WATTS, D. C. 2008b. Correlation of filler content and elastic properties of resin-composites. *Dental Materials,* 24**,** 932-939.

MCCABE, J. 1990. *Applied dental materials*, Oxford, England: Blackwell Scientific Publications.

MCCABE, J., YAN, Z., AL NAIMI, O., MAHMOUD, G. & ROLLAND, S. 2011. Smart materials in dentistry. *Australian Dental Journal,* 56**,** 3-10.

MCCABE, J. F., CARRICK, T. E. & SIDHU, S. K. 2002. Determining low levels of fluoride released from resin based dental materials. *Eur J Oral Sci,* 110**,** 380-4.

MCNEILL, C. J., WILTSHIRE, W. A., DAWES, C. & LAVELLE, C. L. 2001. Fluoride release from new light-cured orthodontic bonding agents. *Am J Orthod Dentofacial Orthop,* 120**,** 392-7.

MIAN, R. I. 2011. *Tribochemical Behaviour of Contemporary Dental Resin Composites.* MSc MSc thesis, University of Leeds.

MIKHAIL, S. S., SCHRICKER, S. R., AZER, S. S., BRANTLEY, W. A. & JOHNSTON, W. M. 2013. Optical characteristics of contemporary dental composite resin materials. *Journal of Dentistry,* 41**,** 771-778.

MITCHELL, R. J., KOIKE, M. & OKABE, T. 2007. Posterior amalgam restorations—usage, regulation, and longevity. *Dental Clinics of North America,* 51**,** 573-589.

MIYASAKA, T. 1996. Effect of Shape and Size of Silanated Fillers on Mechanical Properties of Experimental Photo Cure Composite Resins. *Dental Materials Journal,* 15**,** 98-110,249.

MJOR, I. A., MOORHEAD, J. E. & DAHL, J. E. 2000. Reasons for replacement of restorations in permanent teeth in general dental practice. *International Dental Journal,* 50**,** 361-366.

MOAD, G. & SOLOMON, D. 1995. *The chemistry of free radical polymerization* London, Pergamon.

MOBASHERPOUR, I., HESHAJIN, M. S., KAZEMZADEH, A. & ZAKERI, M. 2007. Synthesis of nanocrystalline hydroxyapatite by using precipitation method. *Journal of Alloys and Compounds,* 430**,** 330-333.

MOHSEN, N. M. & CRAIG, R. G. 1995. EFFECT OF SILANATION OF FILLERS ON THEIR DISPERSABILITY BY MONOMER SYSTEMS. *Journal of Oral Rehabilitation,* 22**,** 183-189.

MOORE, B. K., PLATT, J. A., BORGES, G., CHU, T. M. & KATSILIERI, I. 2008. Depth of cure of dental resin composites: ISO 4049 depth and microhardness of types of materials and shades. *Oper Dent,* 33**,** 408-12.

MORAES, R. R., SINHORETI, M. A., CORRER-SOBRINHO, L., OGLIARI, F. A., PIVA, E. & PETZHOLD, C. L. 2010. Preparation and evaluation of dental resin luting agents with increasing content of bisphenol-A ethoxylated dimethacrylate. *J Biomater Appl,* 24**,** 453-73.

MOSZNER, N. & SALZ, U. 2001. New developments of polymeric dental composites. *Progress in Polymer Science (Oxford),* 26**,** 535-576.

MUSANJE, L. & FERRACANE, J. L. 2004. Effects of resin formulation and nanofiller surface treatment on the properties of experimental hybrid resin composite. *Biomaterials,* 25**,** 4065-4071.

MUSANJE, L., FERRACANE, J. L. & SAKAGUCHI, R. L. 2009. Determination of the optimal photoinitiator concentration in dental composites based on essential material properties. *Dent Mater,* 25**,** 994-1000.

MUSANJE, L., SHU, M. & DARVELL, B. W. 2001. Water sorption and mechanical behaviour of cosmetic direct restorative materials in artificial saliva. *Dental Materials,* 17**,** 394-401.

NALLA, R. K., KINNEY, J. H. & RITCHIE, R. O. 2003. Effect of orientation on the in vitro fracture toughness of dentin: the role of toughening mechanisms. *Biomaterials,* 24**,** 3955-3968.

NAYAK, A. K. 2010. Hydroxyapatite synthesis methodologies: an overview. *International Journal of ChemTech Research,* 2**,** 903-907.

NEUMANN, M. G., MIRANDA, W. G., SCHMITT, C. C., RUEGGEBERG, F. A. & CORREA, I. C. 2005. Molar extinction coefficients and the photon absorption efficiency of dental photoinitiators and light curing units. *Journal of Dentistry,* 33**,** 525-532.

NEUMANN, M. G., SCHMITT, C. C., FERREIRA, G. C. & CORRÊA, I. C. 2006. The initiating radical yields and the efficiency of polymerization for various dental photoinitiators excited by different light curing units. *Dental Materials,* 22**,** 576-584.

NICHOLSON, J. & CZARNECKA, B. 2004. The release of ions by compomers under neutral and acidic conditions. *Journal of Oral Rehabilitation,* 31**,** 665-670.

NIHEI, T., DABANOGLU, A., TERANAKA, T., KURATA, S., OHASHI, K., KONDO, Y., YOSHINO, N., HICKEL, R. & KUNZELMANN, K.-H. 2008. Three-body-wear resistance of the experimental composites containing filler treated with hydrophobic silane coupling agents. *Dental Materials,* 24**,** 760-764.

OGUNYINKA, A., PALIN, W. M., SHORTALL, A. C. & MARQUIS, P. M. 2007. Photoinitiation chemistry affects light transmission and degree of conversion of curing experimental dental resin composites. *Dental Materials,* 23**,** 807-813.

OPDAM, N. J. M., VAN DE SANDE, F. H., BRONKHORST, E., CENCI, M. S., BOTTENBERG, P., PALLESEN, U., GAENGLER, P., LINDBERG, A., HUYSMANS, M. C. D. N. J. M. & VAN DIJKEN, J. W. 2014. Longevity of posterior composite restorations: A systematic review and meta-analysis. *Journal of Dental Research,* 93**,** 943-949.

ORAL, O., LASSILA, L. V., KUMBULOGLU, O. & VALLITTU, P. K. 2014. Bioactive glass particulate filler composite: Effect of coupling of fillers and filler loading on some physical properties. *Dental Materials,* 30**,** 570-577.

ORNAGHI, B. P., MEIER, M. M., ROSA, V., CESAR, P. F., LOHBAUER, U. & BRAGA, R. R. 2012. Subcritical crack growth and in vitro lifetime prediction of resin composites with different filler distributions. *Dental Materials,* 28**,** 985-995.

PAGORIA, D., LEE, A. & GEURTSEN, W. 2005. The effect of camphorquinone (CQ) and CQ-related photosensitizers on the generation of reactive oxygen species and the production of oxidative DNA damage. *Biomaterials,* 26**,** 4091-4099.

PALANIAPPAN, S., ELSEN, L., LIJNEN, I., PEUMANS, M., MEERBEEK, B. V. & LAMBRECHTS, P. 2010. Three-year randomised clinical trial to evaluate the clinical performance, quantitative and qualitative

wear patterns of hybrid composite restorations. *Clinical Oral Investigations,* 14**,** 441-458.

PALANIAPPAN, S., ELSEN, L., LIJNEN, I., PEUMANS, M., VAN MEERBEEK, B. & LAMBRECHTS, P. 2012. Nanohybrid and microfilled hybrid versus conventional hybrid composite restorations: 5-year clinical wear performance. *Clinical Oral Investigations,* 16**,** 181-190.

PALIN, W. M., HADIS, M. A., LEPRINCE, J. G., LELOUP, G., BOLAND, L., FLEMING, G. J. P., KRASTL, G. & WATTS, D. C. 2014. Reduced polymerization stress of MAPO-containing resin composites with increased curing speed, degree of conversion and mechanical properties. *Dental Materials,* 30**,** 507-516.

PALIN, W. M., SENYILMAZ, D. P., MARQUIS, P. M. & SHORTALL, A. C. 2008. Cure width potential for MOD resin composite molar restorations. *Dental Materials,* 24**,** 1083-1094.

PANDIT, S., KIM, G. R., LEE, M. H. & JEON, J. G. 2011. Evaluation of Streptococcus mutans biofilms formed on fluoride releasing and non fluoride releasing resin composites. *J Dent,* 39**,** 780-7.

PAR, M., GAMULIN, O., MAROVIC, D., KLARIC, E. & TARLE, Z. 2014. Effect of temperature on post-cure polymerization of bulk-fill composites. *Journal of Dentistry,* 42**,** 1255-1260.

PEUTZFELDT, A. & ASMUSSEN, E. 1992. Modulus of resilience as predictor for clinical wear of restorative resins. *Dental Materials,* 8**,** 146-148.

PFEIFER, C. S., FERRACANE, J. L., SAKAGUCHI, R. L. & BRAGA, R. R. 2009a. Photoinitiator content in restorative composites: influence on degree of conversion, reaction kinetics, volumetric shrinkage and polymerization stress. *Am J Dent,* 22**,** 206-10.

PFEIFER, C. S., SILVA, L. R., KAWANO, Y. & BRAGA, R. R. 2009b. Bis-GMA co-polymerizations: influence on conversion, flexural properties, fracture toughness and susceptibility to ethanol degradation of experimental composites. *Dent Mater,* 25**,** 1136-41.

PIANELLI, C., DEVAUX, J., BEBELMAN, S. & LELOUP, G. 1999. The micro-Raman spectroscopy, a useful tool to determine the degree of conversion of light-activated composite resins. *J Biomed Mater Res,* 48**,** 675-81.

PICK, B., PELKA, M., BELLI, R., BRAGA, R. R. & LOHBAUER, U. 2011. Tailoring of physical properties in highly filled experimental nanohybrid resin composites. *Dental Materials,* 27**,** 664-669.

PILLIAR, R. M., SMITH, D. C. & MARIC, B. 1986. Fracture Toughness of Dental Composites Determined Using the Short-rod Fracture Toughness Test. *Journal of Dental Research,* 65**,** 1308-1314.

PRESTON, A. J., MAIR, L. H., AGALAMANYI, E. A. & HIGHAM, S. M. 1999. Fluoride release from aesthetic dental materials. *Journal of Oral Rehabilitation,* 26**,** 123-129.

RANDOLPH, L. D., PALIN, W. M., LELOUP, G. & LEPRINCE, J. G. 2016. Filler characteristics of modern dental resin composites and their influence on physico-mechanical properties. *Dental Materials,* 32**,** 1586-1599.

RAO, R. R., ROOPA, H. N. & KANNAN, T. S. 1997. Solid state synthesis and thermal stability of HAP and HAP - beta-TCP composite ceramic powders. *J Mater Sci Mater Med,* 8**,** 511-8.

RAWLS, H. R. 1995. Evaluation of fluoride-releasing dental materials by means of in vitro and in vivo demineralization models: reaction paper. *Advances in dental research,* 9**,** 324-331.

RENCZ, A., HICKEL, R. & ILIE, N. 2012. Curing efficiency of modern LED units. *Clinical Oral Investigations,* 16**,** 173-179.

RODRIGUES JUNIOR, S. A., SCHERRER, S. S., FERRACANE, J. L. & BONA, Á. D. 2008a. Microstructural characterization and fracture behavior of a microhybrid and a nanofill composite. *Dental Materials,* 24**,** 1281-1288.

RODRIGUES JUNIOR, S. A., SCHERRER, S. S., FERRACANE, J. L. & DELLA BONA, A. 2008b. Microstructural characterization and fracture behavior of a microhybrid and a nanofill composite. *Dental Materials,* 24**,** 1281-1288.

RØLLA G, E. J. 1996. *Fluoride in oral fluids and dental plaque.,* Fejerskov O, Ekstrand J, Burt BA. Copenhagen: Munksgaard; p 215–29.

RUEGGEBERG, F. A., CAUGHMAN, W. F., CURTIS, J. W., JR. & DAVIS, H. C. 1993. Factors affecting cure at depths within light-activated resin composites. *American Journal of Dentistry,* 6**,** 91-5.

RUEGGEBERG, F. A., HASHINGER, D. T. & FAIRHURST, C. W. 1990a. Calibration of FTIR conversion analysis of contemporary dental resin composites. *Dental Materials,* 6**,** 241-249.

RUEGGEBERG, F. A., HASHINGER, D. T. & FAIRHURST, C. W. 1990b. Calibration of FTIR conversion analysis of contemporary dental resin composites. *Dent Mater,* 6**,** 241-9.

RUYTER, I. E. & SVENDSEN, S. A. 1978. Remaining methacrylate groups in composite restorative materials. *Acta Odontol Scand,* 36**,** 75-82.

SANKARAPANDIAN, M., SHOBHA, H., KALACHANDRA, S., TAYLOR, D., SHULTZ, A. & MCGRATH, J. 1997. Synthesis of new dental composite matrix dimethacrylates. *Polym Prepr***,** 92-3.

SCHERRER, S. S., BOTSIS, J., STUDER, M., PINI, M., WISKOTT, H. W. A. & BELSER, U. C. 2000. Fracture toughness of aged dental composites in combined mode I and mode II loading. *Journal of Biomedical Materials Research,* 53**,** 362-370.

SCHMALZ, G. 2009. *Resin-based composites. Biocompatibility of Dental Materials. Berlin/Heidelberg/Germany: Springer-Verlag. p. 99–137.*

SCHNEIDER, L. F., CONSANI, S., SAKAGUCHI, R. L. & FERRACANE, J. L. 2009a. Alternative photoinitiator system reduces the rate of stress

development without compromising the final properties of the dental composite. *Dent Mater,* 25**,** 566-72.

SCHNEIDER, L. F. J., CONSANI, S., SAKAGUCHI, R. L. & FERRACANE, J. L. 2009b. Alternative photoinitiator system reduces the rate of stress development without compromising the final properties of the dental composite. *Dental Materials,* 25**,** 566-572.

SCHNEIDER, S. J. 1991. *Engineered materials handbook*, ASM International, USA.

SCOUGALL-VILCHIS, R. J., EACUTE, HOTTA, Y., HOTTA, M., IDONO, T. & YAMAMOTO, K. 2009. Examination of composite resins with electron microscopy, microhardness tester and energy dispersive X-ray microanalyzer. *Dental Materials Journal,* 28**,** 102-112.

SEHGAL, V., SHETTY, V. S., MOGRA, S., BHAT, G., EIPE, M., JACOB, S. & PRABU, L. 2007. Evaluation of antimicrobial and physical properties of orthodontic composite resin modified by addition of antimicrobial agents—an in-vitro study. *American Journal of Orthodontics and Dentofacial Orthopedics,* 131**,** 525-529.

SENAWONGSE, P. & PONGPRUEKSA, P. 2007. Surface roughness of nanofill and nanohybrid resin composites after polishing and brushing. *Journal of Esthetic and Restorative Dentistry,* 19**,** 265-273.

SEPPA, L., FORSS, H. & OGAARD, B. 1993. The effect of fluoride application on fluoride release and the antibacterial action of glass ionomers. *J Dent Res,* 72**,** 1310-4.

SEVKUSIC, M., SCHUSTER, L., ROTHMUND, L., DETTINGER, K., MAIER, M., HICKEL, R., VAN LANDHUYT, K. L., DURNER, J., HOGG, C. & REICHL, F. X. 2014. The elution and breakdown behavior of constituents from various light-cured composites. *Dent Mater,* 30**,** 619-31.

SHAH, M. B., FERRACANE, J. L. & KRUZIC, J. J. 2009a. R-curve behavior and micromechanisms of fracture in resin based dental restorative composites. *Journal of the Mechanical Behavior of Biomedical Materials,* 2**,** 502-511.

SHAH, M. B., FERRACANE, J. L. & KRUZIC, J. J. 2009b. R-curve behavior and toughening mechanisms of resin-based dental composites: Effects of hydration and post-cure heat treatment. *Dental Materials,* 25**,** 760-770.

SHAH, P. K. & STANSBURY, J. W. 2014. Role of filler and functional group conversion in the evolution of properties in polymeric dental restoratives. *Dental Materials,* 30**,** 586-593.

SHORTALL, A. C., FELIX, C. J. & WATTS, D. C. 2015. Robust spectrometer-based methods for characterizing radiant exitance of dental LED light curing units. *Dental Materials,* 31**,** 339-350.

SHORTALL, A. C., HU, X. Q. & MARQUIS, P. M. 2002. Potential countersample materials for in vitro simulation wear testing. *Dental Materials,* 18**,** 246-254.

SHORTALL, A. C., PALIN, W. M. & BURTSCHER, P. 2008. Refractive Index Mismatch and Monomer Reactivity Influence Composite Curing Depth. *Journal of Dental Research,* 87**,** 84-88.

SIDERIDOU, I., TSERKI, V. & PAPANASTASIOU, G. 2002. Effect of chemical structure on degree of conversion in light-cured dimethacrylate-based dental resins. *Biomaterials,* 23**,** 1819-1829.

SIDERIDOU, I. D. & ACHILIAS, D. S. 2005. Elution study of unreacted Bis-GMA, TEGDMA, UDMA, and Bis-EMA from light-cured dental resins and resin composites using HPLC. *J Biomed Mater Res B Appl Biomater,* 74**,** 617-26.

SILIKAS, N., ELIADES, G. & WATTS, D. C. 2000. Light intensity effects on resin-composite degree of conversion and shrinkage strain. *Dental Materials,* 16**,** 292-296.

SILIKAS, N. & WATTS, D. C. 1999. Rheology of urethane dimethacrylate and diluent formulations. *Dental Materials,* 15**,** 257-261.

SKJORLAND, K. K. 1973. Plaque accumulation on different dental filling materials. *Scandinavian Journal of Dental Research,* 81**,** 538-42.

SODERHOLM, K.-J. 2010. Review of the fracture toughness approach. *Dental Materials,* 26**,** e63-e77.

SODERHOLM, K. J. M., LAMBRECHTS, P., SARRETT, D., ABE, Y., YANG, M. C. K., LABELLA, R., YILDIZ, E. & WILLEMS, G. 2001. Clinical wear performance of eight experimental dental composites over three years determined by two measuring methods. *European Journal of Oral Sciences,* 109**,** 273-281.

SONCINI, J. A., MASEREJIAN, N. N., TRACHTENBERG, F., TAVARES, M. & HAYES, C. 2007. The longevity of amalgam versus compomer/composite restorations in posterior primary and permanent teeth: findings From the New England Children's Amalgam Trial. *J Am Dent Assoc,* 138**,** 763-72.

STANSBURY, J. W. 2012. Dimethacrylate network formation and polymer property evolution as determined by the selection of monomers and curing conditions. *Dental Materials,* 28**,** 13-22.

STANSBURY, J. W. & DICKENS, S. H. 2001. Determination of double bond conversion in dental resins by near infrared spectroscopy. *Dent Mater,* 17**,** 71-9.

STGERMAIN, H., SWARTZ, M. L., PHILLIPS, R. W., MOORE, B. K. & ROBERTS, T. A. 1985. Properties of Microfilled Composite Resins as Influenced by Filler Content. *Journal of Dental Research,* 64**,** 155-160.

SUNNEGARDH-GRONBERG, K., VAN DIJKEN, J. W., FUNEGARD, U., LINDBERG, A. & NILSSON, M. 2009. Selection of dental materials and longevity of replaced restorations in Public Dental Health clinics in northern Sweden. *J Dent,* 37**,** 673-8.

SUZUKI, S., LEINFELDER, K. F., KAWAI, K. & TSUCHITANI, Y. 1995. Effect of particle variation on wear rates of posterior composites. *American Journal of Dentistry,* 8**,** 173-178.

TAHERI, M. M., ABDUL KADIR, M. R., SHOKUHFAR, T., HAMLEKHAN, A., SHIRDAR, M. R. & NAGHIZADEH, F. 2015. Fluoridated hydroxyapatite nanorods as novel fillers for improving mechanical properties of dental composite: Synthesis and application. *Materials & Design,* 82**,** 119-125.

TAKAHASHI, H., FINGER, W. J., ENDO, T., KANEHIRA, M., KOOTTATHAPE, N., KOMATSU, M. & BALKENHOL, M. 2011. Comparative evaluation of mechanical characteristics of nanofiller containing resin composites. *Am J Dent,* 24**,** 264-70.

TANAGAWA, M., YOSHIDA, K., MATSUMOTO, S., YAMADA, T. & ATSUTA, M. 1999. Inhibitory effect of antibacterial resin composite against Streptococcus mutans. *Caries Res,* 33**,** 366-71.

TANOUE, N., ATSUTA, M. & MATSUMURA, H. 2003. Properties of a new photo-activated composite polymerized with three different laboratory photo-curing units. *Journal of Oral Rehabilitation,* 30**,** 832-836.

TANTBIROJN, D., RETIEF, D. H. & RUSSELL, C. M. 1992. Enamel, cementum and dentin fluoride uptake from a fluoride releasing resin composite. *Am J Dent,* 5**,** 226-32.

TANTBIROJN, D., VERSLUIS, A., CHENG, Y.-S. & DOUGLAS, W. 2003. Fracture toughness and microhardness of a composite: do they correlate? *Journal of Dentistry,* 31**,** 89-95.

TEN CATE JM, F. J. 1996. *Physicochemical aspects of fluoride–enamel interactions.* , n: Fejerskov O, Ekstrand J,Burt BA. Copenhagen: Munksgaard; 252–72.

THEOCHAROPOULOS, A., ZHOU, L., HILL, R. & CATTELL, M. 2010. Wear quantification of human enamel and dental glass-ceramics using white light profilometry. *Wear,* 269**,** 930-936.

THOMAIDIS, S., KAKABOURA, A., MUELLER, W. D. & ZINELIS, S. 2013. Mechanical properties of contemporary composite resins and their interrelations. *Dental Materials,* 29**,** E132-E141.

TILLER, J. C., LEE, S. B., LEWIS, K. & KLIBANOV, A. M. 2002. Polymer surfaces derivatized with poly(vinyl-N-hexylpyridinium) kill airborne and waterborne bacteria. *Biotechnol Bioeng,* 79**,** 465-71.

TOPARLI, M. & AKSOY, T. 1998. Fracture toughness determination of composite resin and dentin composite resin adhesive interfaces by laboratory testing and finite element models. *Dental Materials,* 14**,** 287-293.

TURSSI, C. P., FERRACANE, J. L. & VOGEL, K. 2005. Filler features and their effects on wear and degree of conversion of particulate dental resin composites. *Biomaterials,* 26**,** 4932-4937.

VAN DE SANDE, F. H., OPDAM, N. J., RODOLPHO, P. A., CORREA, M. B., DEMARCO, F. F. & CENCI, M. S. 2013. Patient risk factors' influence on survival of posterior composites. *J Dent Res,* 92**,** 78S-83S.

VAN DIJKEN, J. W. V. 2000. Direct resin composite inlays/onlays: an 11 year follow-up. *Journal of Dentistry,* 28**,** 299-306.

VANDEWALLE, K. S., ROBERTS, H. W. & RUEGGEBERG, F. A. 2008. Power distribution across the face of different light guides and its effect on composite surface microhardness. *J Esthet Restor Dent,* 20**,** 108-17; discussion 118.

VENHOVEN, B. A. M., DE GEE, A. J., WERNER, A. & DAVIDSON, C. L. 1996. Influence of filler parameters on the mechanical coherence of dental restorative resin composites. *Biomaterials,* 17**,** 735-740.

VERMEERSCH, G., LELOUP, G. & VREVEN, J. 2001. Fluoride release from glass-ionomer cements, compomers and resin composites. *J Oral Rehabil,* 28**,** 26-32.

VIDNES-KOPPERUD, S., TVEIT, A. B., GAARDEN, T., SANDVIK, L. & ESPELID, I. 2009. Factors influencing dentists' choice of amalgam and tooth-colored restorative materials for Class II preparations in younger patients. *Acta Odontol Scand,* 67**,** 74-79.

WACHTMAN JB, C. W., MATTHEWSON MJ. 2009. *Mechanical properties of ceramics. 2nd ed.* , Hoboken, NJ:Wiley Inc.

WALTERS, N. J., XIA, W., SALIH, V., ASHLEY, P. F. & YOUNG, A. M. 2016. Poly(propylene glycol) and urethane dimethacrylates improve conversion of dental composites and reveal complexity of cytocompatibility testing. *Dental Materials,* 32**,** 264-277.

WASSELL, R. W., MCCABE, J. F. & WALLS, A. W. G. 1994a. A 2-body frictional wear test. *Journal of Dental Research,* 73**,** 1546-1553.

WASSELL, R. W., MCCABE, J. F. & WALLS, A. W. G. 1994b. Wear characteristics in a 2-body wear test. *Dental Materials,* 10**,** 269-274.

WATANABE, H., KHERA, S. C., VARGAS, M. A. & QIAN, F. 2008. Fracture toughness comparison of six resin composites. *Dental Materials,* 24**,** 418-425.

WEINMANN, W., THALACKER, C. & GUGGENBERGER, R. 2005. Siloranes in dental composites. *Dental Materials,* 21**,** 68-74.

WICHT, M. J., HAAK, R., KNEIST, S. & NOACK, M. J. 2005. A triclosan-containing compomer reduces Lactobacillus spp. predominant in advanced carious lesions. *Dental Materials,* 21**,** 831-836.

WIEGAND, A., BUCHALLA, W. & ATTIN, T. 2007. Review on fluoride-releasing restorative materials--fluoride release and uptake characteristics, antibacterial activity and influence on caries formation. *Dent Mater,* 23**,** 343-62.

WILLIAMS, J., BILLINGTON, R. & PEARSON, G. 1999. The influence of sample dimensions on fluoride ion release from a glass ionomer restorative cement. *Biomaterials,* 20**,** 1327-1337.

WILLIAMS, J. A., BILLINGTON, R. W. & PEARSON, G. J. 2001. A long term study of fluoride release from metal-containing conventional and resin-modified glass-ionomer cements. *J Oral Rehabil,* 28**,** 41-7.

XU, H. H. K., MOREAU, J. L., SUN, L. & CHOW, L. C. 2010a. Novel CaF(2) Nanocomposite with High Strength and Fluoride Ion Release. *Journal of Dental Research,* 89**,** 739-745.

XU, H. H. K., WEIR, M. D., SUN, L., MOREAU, J. L., TAKAGI, S., CHOW, L. C. & ANTONUCCI, J. M. 2010b. Strong Nanocomposites with Ca, PO(4), and F Release for Caries Inhibition. *Journal of Dental Research,* 89**,** 19-28.

XU, X. & BURGESS, J. O. 2003a. Compressive strength, fluoride release and recharge of fluoride-releasing materials. *Biomaterials,* 24**,** 2451-61.

XU, X. & BURGESS, J. O. 2003b. Compressive strength, fluoride release and recharge of fluoride-releasing materials. *Biomaterials,* 24**,** 2451-2461.

YAMAMOTO, K., OHASHI, S., AONO, M., KOKUBO, T., YAMADA, I. & YAMAUCHI, J. 1996. Antibacterial activity of silver ions implanted in SiO2 filler on oral streptococci. *Dental Materials,* 12**,** 227-229.

YAN, Z., SIDHU, S., MAHMOUD, G., CARRICK, T. & MCCABE, J. 2007. Effects of temperature on the fluoride release and recharging ability of glass ionomers. *Operative Dentistry,* 32**,** 138-143.

YAP, A. U., KHOR, E. & FOO, S. H. 1999. Fluoride release and antibacterial properties of new-generation tooth-colored restoratives. *Operative Dentistry,* 24**,** 297-305.

YAP, A. U., THAM, S. Y., ZHU, L. Y. & LEE, H. K. 2002a. Short-term fluoride release from various aesthetic restorative materials. *Oper Dent,* 27**,** 259-65.

YAP, A. U. J., CHEW, C. L., ONG, L. & TEOH, S. H. 2002b. Environmental damage and occlusal contact area wear of composite restoratives. *Journal of Oral Rehabilitation,* 29**,** 87-97.

YOGANAND, C., SELVARAJAN, V., ROUABHIA, M., CANNILLO, V. & SOLA, A. Bioactivity of thermal plasma synthesized bovine hydroxyapatite/glass ceramic composites. Journal of Physics: Conference Series, 2010. IOP Publishing, 012099.

YOSHIDA, K., TANAGAWA, M. & ATSUTA, M. 1999. Characterization and inhibitory effect of antibacterial dental resin composites incorporating silver-supported materials. *J Biomed Mater Res,* 47**,** 516-22.

ZAKIR, M., AL KHERAIF, A. A. A., ASIF, M., WONG, F. S. L. & REHMAN, I. U. 2013. A comparison of the mechanical properties of a modified

silorane based dental composite with those of commercially available composite material. *Dental Materials,* 29**,** E53-E59.

ZHANG, H. & DARVELL, B. W. 2012. Mechanical properties of hydroxyapatite whisker-reinforced bis-GMA-based resin composites. *Dental Materials,* 28**,** 824-830.

ZHAO, D., BOTSIS, J. & DRUMMOND, J. L. 1997. Fracture studies of selected dental restorative composites. *Dental Materials,* 13**,** 198-207.

Chapter 9: Appendices

Appendix A: One- Way ANOVA volume loss (TC,A,B,C,D)

ANOVA					
Volume_loss (TC,A,B,C,D)					
	Sum of Squares	df	Mean Square	F	Sig.
Between Groups	.01	4.00	.00	68.42	.00
Within Groups	.00	20.00	.00		
Total	.01	24.00			

Appendix B: Post Hoc Tukey volume loss (TC,A,B,C,D)

Multiple Comparisons						
Dependent Variable: Volume_loss (TC,A,B,C,D)						
Tukey HSD						
(I) DC	(J) DC	Mean Difference (I-J)	Std. Error	Sig.	95% Confidence Interval	
					Lower Bound	Upper Bound
TC	A	-.04*	.00	.00	-.05	-.03
	B	-.01	.00	.08	-.02	.00
	C	.00	.00	.73	-.01	.01
	D	.00	.00	.96	-.01	.01
A	TC	.04*	.00	.00	.03	.05
	B	.03*	.00	.00	.02	.04
	C	.04*	.00	.00	.03	.05
	D	.04*	.00	.00	.03	.05
B	TC	.00	.00	.73	-.01	.01
	A	-.04*	.00	.00	-.05	-.03
	C	-.01*	.00	.01	-.02	.00
	D	.00	.00	.98	-.01	.01
C	TC	.00	.00	.96	-.01	.01

	A	-.04*	.00	.00	-.05	-.03
	B	-.01*	.00	.02	-.02	.00
	D	.00	.00	.98	-.01	.01
D	TC	.01	.00	.08	.00	.02
	A	-.03*	.00	.00	-.04	-.02
	B	.01*	.00	.01	.00	.02
	C	.01*	.00	.02	.00	.02
*. The mean difference is significant at the 0.05 level. If less than 0.05 data is not normally distributed.						

Appendix C: One- Way ANOVA HV (TC,A,B,C,D)

ANOVA					
HV					
	Sum of Squares	df	Mean Square	F	Sig.
Between Groups	5974.33	4.00	1493.58	148.24	.00
Within Groups	201.51	20.00	10.08		
Total	6175.84	24.00			

Appendix D: Post Hoc Tukey HV (TC,A,B,C,D)

Multiple Comparisons

Dependent Variable: HV

Tukey HSD

(I) DC	(J) DC	Mean Difference (I-J)	Std. Error	Sig.	95% Confidence Interval	
					Lower Bound	Upper Bound
TC	A	-36.30*	2.01	.00	-42.31	-30.29
	B	-35.58*	2.01	.00	-41.59	-29.57
	C	-39.82*	2.01	.00	-45.83	-33.81
	D	-41.38*	2.01	.00	-47.39	-35.37
A	TC	36.30*	2.01	.00	30.29	42.31
	B	.72	2.01	1.00	-5.29	6.73
	C	-3.52	2.01	.43	-9.53	2.49
	D	-5.08	2.01	.12	-11.09	.93
B	TC	39.82*	2.01	.00	33.81	45.83
	A	3.52	2.01	.43	-2.49	9.53
	C	4.24	2.01	.25	-1.77	10.25
	D	-1.56	2.01	.93	-7.57	4.45
C	A	41.38*	2.01	.00	35.37	47.39
	B	5.08	2.01	.12	-.93	11.09
	C	5.80	2.01	.06	-.21	11.81
	D	1.56	2.01	.93	-4.45	7.57
D	TC	35.58*	2.01	.00	29.57	41.59
	B	-.72	2.01	1.00	-6.73	5.29
	C	-4.24	2.01	.25	-10.25	1.77
	D	-5.80	2.01	.06	-11.81	.21

*. The mean difference is significant at the 0.05 level.

Appendix E: Normality test results DC (TC,A,B,C,D)

	Tests of Normality-DC (TC,A,B,C,D)			
Group	Time	Shapiro-Wilk		
		Statistic	df	Sig.
TC	DC_5s	.887	5	.344
	DC_10s	.840	5	.166
	DC_20s	.907	5	.448
	DC_30s	.970	5	.873
	DC_40s	.882	5	.317
	DC_50s	.865	5	.247
	DC_60s	.949	5	.728
A	DC_5s	.970	5	.876
	DC_10s	.989	5	.975
	DC_20s	.958	5	.791
	DC_30s	.810	5	.098
	DC_40s	.855	5	.211
	DC_50s	.948	5	.720
	DC_60s	.968	5	.860
B	DC_5s	.974	5	.899
	DC_10s	.844	5	.177
	DC_20s	.939	5	.659
	DC_30s	.858	5	.222
	DC_40s	.805	5	.089
	DC_50s	.868	5	.258
	DC_60s	.942	5	.678
C	DC_5s	.875	5	.287
	DC_10s	.846	5	.182
	DC_20s	.876	5	.292
	DC_30s	.869	5	.263
	DC_40s	.865	5	.246
	DC_50s	.821	5	.119
	DC_60s	.800	5	.081
D	DC_5s	.950	5	.736
	DC_10s	.948	5	.719
	DC_20s	.899	5	.402
	DC_30s	.898	5	.398
	DC_40s	.931	5	.602
	DC_50s	.855	5	.210
	DC_60s	.777	5	.052
	*. This is a lower bound of the true significance.			

Appendix F: One- Way ANOVA DC (TC,A,B,C,D)

ANOVA-Degree of Conversion TC,A,B,C,D						
		Sum of Squares	df	Mean Square	F	Sig.
DC_5s	Between Groups	754.29	4.00	188.57	12.59	.00
	Within Groups	299.58	20.00	14.98		
	Total	1053.87	24.00			
DC_10s	Between Groups	954.97	4.00	238.74	31.97	.00
	Within Groups	149.35	20.00	7.47		
	Total	1104.31	24.00			
DC_20s	Between Groups	429.07	4.00	107.27	15.49	.00
	Within Groups	138.53	20.00	6.93		
	Total	567.60	24.00			
DC_30s	Between Groups	483.34	4.00	120.83	13.43	.00
	Within Groups	179.92	20.00	9.00		
	Total	663.26	24.00			
DC_40s	Between Groups	328.65	4.00	82.16	9.40	.00
	Within Groups	174.86	20.00	8.74		
	Total	503.51	24.00			
DC_50s	Between Groups	414.63	4.00	103.66	7.75	.00
	Within Groups	267.57	20.00	13.38		
	Total	682.20	24.00			
DC_60s	Between Groups	322.64	4.00	80.66	18.87	.00
	Within Groups	85.50	20.00	4.27		
	Total	408.14	24.00			

Appendix G: Post Hoc Tukey DC (TC,A,B,C,D)

Multiple Comparisons- Degree of Conversion TC,A,B,C,D							
Tukey HSD							
Dependent Variable	(I) DC	(J) DC	Mean Difference (I-J)	Std. Error	Sig.	95% Confidence Interval	
						Lower Bound	Upper Bound
DC_5s	TC	A	-10.904*	2.448	.002	-18.229	-3.579
		B	-11.759*	2.448	.001	-19.084	-4.435
		C	-16.385*	2.448	.000	-23.709	-9.060
		D	-12.592*	2.448	.000	-19.917	-5.268
	A	TC	10.904*	2.448	.002	3.579	18.229
		B	-.856	2.448	.997	-8.180	6.469
		C	-5.481	2.448	.206	-12.805	1.844
		D	-1.689	2.448	.956	-9.013	5.636
	B	TC	11.759*	2.448	.001	4.435	19.084
		A	.856	2.448	.997	-6.469	8.180
		C	-4.625	2.448	.354	-11.950	2.700
		D	-.833	2.448	.997	-8.158	6.492
	C	TC	16.385*	2.448	.000	9.060	23.709
		A	5.481	2.448	.206	-1.844	12.805
		B	4.625	2.448	.354	-2.700	11.950
		D	3.792	2.448	.545	-3.533	11.117
	D	TC	12.592*	2.448	.000	5.268	19.917
		A	1.689	2.448	.956	-5.636	9.013
		B	.833	2.448	.997	-6.492	8.158
		C	-3.792	2.448	.545	-11.117	3.533
DC_10s	TC	A	-12.595*	1.728	.000	-17.767	-7.424
		B	-12.968*	1.728	.000	-18.139	-7.796
		C	-17.016*	1.728	.000	-22.187	-11.844
		D	-16.550*	1.728	.000	-21.721	-11.378
	A	TC	12.595*	1.728	.000	7.424	17.767
		B	-.372	1.728	.999	-5.544	4.800
		C	-4.420	1.728	.117	-9.592	.752
		D	-3.954	1.728	.190	-9.126	1.217
	B	TC	12.968*	1.728	.000	7.796	18.139
		A	.372	1.728	.999	-4.800	5.544
		C	-4.048	1.728	.173	-9.220	1.124
		D	-3.582	1.728	.270	-8.754	1.589
	C	TC	17.016*	1.728	.000	11.844	22.187
		A	4.420	1.728	.117	-.752	9.592
		B	4.048	1.728	.173	-1.124	9.220
		D	.466	1.728	.999	-4.706	5.637

	D	TC	16.550*	1.728	.000	11.378	21.721
		A	3.954	1.728	.190	-1.217	9.126
		B	3.582	1.728	.270	-1.589	8.754
		C	-.466	1.728	.999	-5.637	4.706
DC_20s	TC	A	-8.158*	1.665	.001	-13.139	-3.177
		B	-10.654*	1.665	.000	-15.635	-5.673
		C	-11.663*	1.665	.000	-16.644	-6.682
		D	-9.163*	1.665	.000	-14.144	-4.182
	A	TC	8.158*	1.665	.001	3.177	13.139
		B	-2.496	1.665	.575	-7.477	2.485
		C	-3.505	1.665	.256	-8.486	1.476
		D	-1.005	1.665	.973	-5.986	3.976
	B	TC	10.654*	1.665	.000	5.673	15.635
		A	2.496	1.665	.575	-2.485	7.477
		C	-1.010	1.665	.972	-5.990	3.971
		D	1.491	1.665	.895	-3.490	6.472
	C	TC	11.663*	1.665	.000	6.682	16.644
		A	3.505	1.665	.256	-1.476	8.486
		B	1.010	1.665	.972	-3.971	5.990
		D	2.500	1.665	.573	-2.481	7.481
	D	TC	9.163*	1.665	.000	4.182	14.144
		A	1.005	1.665	.973	-3.976	5.986
		B	-1.491	1.665	.895	-6.472	3.490
		C	-2.500	1.665	.573	-7.481	2.481
DC_30s	TC	A	-11.326*	1.897	.000	-17.002	-5.649
		B	-10.891*	1.897	.000	-16.568	-5.215
		C	-11.747*	1.897	.000	-17.424	-6.071
		D	-8.953*	1.897	.001	-14.630	-3.277
	A	TC	11.326*	1.897	.000	5.649	17.002
		B	.434	1.897	.999	-5.242	6.111
		C	-.422	1.897	.999	-6.098	5.255
		D	2.373	1.897	.723	-3.304	8.049
	B	TC	10.891*	1.897	.000	5.215	16.568
		A	-.434	1.897	.999	-6.111	5.242
		C	-.856	1.897	.991	-6.532	4.820
		D	1.938	1.897	.842	-3.738	7.615
	C	TC	11.747*	1.897	.000	6.071	17.424
		A	.422	1.897	.999	-5.255	6.098
		B	.856	1.897	.991	-4.820	6.532
		D	2.794	1.897	.591	-2.882	8.471
	D	TC	8.953*	1.897	.001	3.277	14.630
		A	-2.373	1.897	.723	-8.049	3.304

		B	-1.938	1.897	.842	-7.615	3.738
		C	-2.794	1.897	.591	-8.471	2.882
DC_40s	TC	A	-8.070*	1.870	.003	-13.666	-2.474
		B	-10.156*	1.870	.000	-15.752	-4.560
		C	-7.970*	1.870	.003	-13.566	-2.374
		D	-9.171*	1.870	.001	-14.767	-3.575
	A	TC	8.070*	1.870	.003	2.474	13.666
		B	-2.085	1.870	.797	-7.681	3.511
		C	.101	1.870	1.000	-5.495	5.697
		D	-1.101	1.870	.975	-6.697	4.495
	B	TC	10.156*	1.870	.000	4.560	15.752
		A	2.085	1.870	.797	-3.511	7.681
		C	2.186	1.870	.768	-3.410	7.782
		D	.984	1.870	.984	-4.612	6.580
	C	TC	7.970*	1.870	.003	2.374	13.566
		A	-.101	1.870	1.000	-5.697	5.495
		B	-2.186	1.870	.768	-7.782	3.410
		D	-1.201	1.870	.966	-6.797	4.395
	D	TC	9.171*	1.870	.001	3.575	14.767
		A	1.101	1.870	.975	-4.495	6.697
		B	-.984	1.870	.984	-6.580	4.612
		C	1.201	1.870	.966	-4.395	6.797
DC_50s	TC	A	-9.469*	2.313	.005	-16.392	-2.547
		B	-10.709*	2.313	.001	-17.632	-3.787
		C	-7.593*	2.313	.027	-14.515	-.670
		D	-11.086*	2.313	.001	-18.008	-4.163
	A	TC	9.469*	2.313	.005	2.547	16.392
		B	-1.240	2.313	.982	-8.162	5.682
		C	1.877	2.313	.924	-5.046	8.799
		D	-1.616	2.313	.954	-8.539	5.306
	B	TC	10.709*	2.313	.001	3.787	17.632
		A	1.240	2.313	.982	-5.682	8.162
		C	3.117	2.313	.666	-3.806	10.039
		D	-.376	2.313	1.000	-7.298	6.546
	C	TC	7.593*	2.313	.027	.670	14.515
		A	-1.877	2.313	.924	-8.799	5.046
		B	-3.117	2.313	.666	-10.039	3.806
		D	-3.493	2.313	.568	-10.415	3.429
	D	TC	11.086*	2.313	.001	4.163	18.008
		A	1.616	2.313	.954	-5.306	8.539
		B	.376	2.313	1.000	-6.546	7.298
		C	3.493	2.313	.568	-3.429	10.415

DC_60s	TC	A	-9.245*	1.308	.000	-13.158	-5.332
		B	-8.407*	1.308	.000	-12.320	-4.495
		C	-8.600*	1.308	.000	-12.513	-4.687
		D	-9.460*	1.308	.000	-13.373	-5.547
	A	TC	9.245*	1.308	.000	5.332	13.158
		B	.837	1.308	.966	-3.076	4.750
		C	.645	1.308	.987	-3.268	4.558
		D	-.215	1.308	1.000	-4.128	3.698
	B	TC	8.407*	1.308	.000	4.495	12.320
		A	-.837	1.308	.966	-4.750	3.076
		C	-.192	1.308	1.000	-4.105	3.721
		D	-1.052	1.308	.926	-4.965	2.861
	C	TC	8.600*	1.308	.000	4.687	12.513
		A	-.645	1.308	.987	-4.558	3.268
		B	.192	1.308	1.000	-3.721	4.105
		D	-.860	1.308	.963	-4.773	3.053
	D	TC	9.460*	1.308	.000	5.547	13.373
		A	.215	1.308	1.000	-3.698	4.128
		B	1.052	1.308	.926	-2.861	4.965
		C	.860	1.308	.963	-3.053	4.773

*. The mean difference is significant at the 0.05 level.

Appendix H: Normality test results DC (FA composites)

	Tests of Normality-DC (FA composites)			
Group	Time	Shapiro-Wilk		
		Statistic	df	Sig.
TC	DC_5s	.887	5	.344
	DC_10s	.840	5	.166
	DC_20s	.907	5	.448
	DC_30s	.970	5	.873
	DC_40s	.882	5	.317
	DC_50s	.865	5	.247
	DC_60s	.949	5	.728
0FA	DC_5s	.861	5	.233
	DC_10s	.928	5	.580
	DC_20s	.898	5	.400
	DC_30s	.888	5	.349
	DC_40s	.922	5	.546
	DC_50s	.915	5	.500
	DC_60s	.943	5	.689
10FA	DC_5s	.932	5	.610
	DC_10s	.891	5	.364
	DC_20s	.910	5	.470
	DC_30s	.798	5	.079
	DC_40s	.959	5	.798
	DC_50s	.885	5	.332
	DC_60s	.862	5	.235
20FA	DC_5s	.901	5	.417
	DC_10s	.931	5	.603
	DC_20s	.812	5	.101
	DC_30s	.806	5	.091
	DC_40s	.821	5	.119
	DC_50s	.821	5	.119
	DC_60s	.785	5	.061

30FA	DC_5s	.873	5	.277
	DC_10s	.931	5	.603
	DC_20s	.968	5	.861
	DC_30s	.939	5	.657
	DC_40s	.871	5	.271
	DC_50s	.906	5	.446
	DC_60s	.908	5	.457
40FA	DC_5s	.882	5	.320
	DC_10s	.928	5	.580
	DC_20s	.898	5	.400
	DC_30s	.888	5	.349
	DC_40s	.922	5	.546
	DC_50s	.915	5	.500
	DC_60s	.943	5	.689
*. This is a lower bound of the true significance.				

Appendix I: One- Way ANOVA DC (FA composites)

ANOVA

		Sum of Squares	df	Mean Square	F	Sig.
DoC_5s	Between Groups	551.822	5	110.364	7.604	.000
	Within Groups	348.328	24	14.514		
	Total	900.151	29			
DoC_10s	Between Groups	1054.557	5	210.911	31.562	.000
	Within Groups	160.378	24	6.682		
	Total	1214.936	29			
DoC_20s	Between Groups	344.611	5	68.922	6.088	.001
	Within Groups	271.718	24	11.322		
	Total	616.329	29			
DoC_30s	Between Groups	240.189	5	48.038	2.391	.068
	Within Groups	482.120	24	20.088		
	Total	722.309	29			
DoC_40s	Between Groups	261.912	5	52.382	2.637	.049
	Within Groups	476.673	24	19.861		
	Total	738.585	29			
DoC_50s	Between Groups	526.534	5	105.307	4.706	.004
	Within Groups	537.010	24	22.375		
	Total	1063.545	29			
DoC_60s	Between Groups	309.885	5	61.977	3.393	.019
	Within Groups	438.410	24	18.267		
	Total	748.295	29			

Appendix J: Post Hoc Tukey DC (FA composites)

Multiple Comparisons							
Tukey HSD							
Dependent Variable	(I) DC	(J) DC	Mean Difference (I-J)	Std. Error	Sig.	95% Confidence Interval	
						Lower Bound	Upper Bound
DoC_5s	TC	0FA	-12.59*	2.36	.00	-19.90	-5.29
		10FA	-12.18*	2.36	.00	-19.49	-4.88
		20FA	-5.17	2.36	.28	-12.47	2.14
		30FA	-10.28*	2.36	.00	-17.59	-2.98
		40FA	-3.74	2.36	.62	-11.04	3.57
	0FA	TC	12.59*	2.36	.00	5.29	19.90
		10FA	.41	2.36	1.00	-6.90	7.71
		20FA	7.43*	2.36	.04	.12	14.73
		30FA	2.31	2.36	.92	-5.00	9.61
		40FA	8.86*	2.36	.01	1.55	16.16
	10FA	TC	12.18*	2.36	.00	4.88	19.49
		0FA	-.41	2.36	1.00	-7.71	6.90
		20FA	7.02	2.36	.06	-.29	14.32
		30FA	1.90	2.36	.96	-5.40	9.21
		40FA	8.45*	2.36	.02	1.14	15.75
	20FA	TC	5.17	2.36	.28	-2.14	12.47
		0FA	-7.43*	2.36	.04	-14.73	-.12
		10FA	-7.02	2.36	.06	-14.32	.29
		30FA	-5.12	2.36	.29	-12.42	2.19
		40FA	1.43	2.36	.99	-5.88	8.73
	30FA	TC	10.28*	2.36	.00	2.98	17.59
		0FA	-2.31	2.36	.92	-9.61	5.00
		10FA	-1.90	2.36	.96	-9.21	5.40
		20FA	5.12	2.36	.29	-2.19	12.42
		40FA	6.55	2.36	.10	-.76	13.85
	40FA	TC	3.74	2.36	.62	-3.57	11.04
		0FA	-8.86*	2.36	.01	-16.16	-1.55
		10FA	-8.45*	2.36	.02	-15.75	-1.14
		20FA	-1.43	2.36	.99	-8.73	5.88
		30FA	-6.55	2.36	.10	-13.85	.76
DoC_10s	TC	0FA	-16.55	1.63	.00	-21.60	-11.49
		10FA	-12.03	1.63	.00	-17.08	-6.97
		20FA	-11.80	1.63	.00	-16.86	-6.75
		30FA	-14.75	1.63	.00	-19.81	-9.70

		40FA	-3.82	1.63	.22	-8.87	1.24
	0FA	TC	16.55	1.63	.00	11.49	21.60
		10FA	4.52	1.63	.10	-.54	9.58
		20FA	4.74	1.63	.07	-.31	9.80
		30FA	1.80	1.63	.88	-3.26	6.85
		40FA	12.73	1.63	.00	7.68	17.79
	10FA	TC	12.03	1.63	.00	6.97	17.08
		0FA	-4.52	1.63	.10	-9.58	.54
		20FA	.22	1.63	1.00	-4.83	5.28
		30FA	-2.72	1.63	.57	-7.78	2.33
		40FA	8.21	1.63	.00	3.16	13.27
	20FA	TC	11.80	1.63	.00	6.75	16.86
		0FA	-4.74	1.63	.07	-9.80	.31
		10FA	-.22	1.63	1.00	-5.28	4.83
		30FA	-2.95	1.63	.48	-8.00	2.11
		40FA	7.99	1.63	.00	2.93	13.04
	30FA	TC	14.75	1.63	.00	9.70	19.81
		0FA	-1.80	1.63	.88	-6.85	3.26
		10FA	2.72	1.63	.57	-2.33	7.78
		20FA	2.95	1.63	.48	-2.11	8.00
		40FA	10.94	1.63	.00	5.88	15.99
	40FA	TC	3.82	1.63	.22	-1.24	8.87
		0FA	-12.73	1.63	.00	-17.79	-7.68
		10FA	-8.21	1.63	.00	-13.27	-3.16
		20FA	-7.99	1.63	.00	-13.04	-2.93
		30FA	-10.94	1.63	.00	-15.99	-5.88
DoC_20s	TC	0FA	-9.16*	2.13	.00	-15.74	-2.58
		10FA	-9.61*	2.13	.00	-16.19	-3.03
		20FA	-7.49*	2.13	.02	-14.07	-.92
		30FA	-7.26*	2.13	.02	-13.84	-.68
		40FA	-3.50	2.13	.58	-10.08	3.08
	0FA	TC	9.16*	2.13	.00	2.58	15.74
		10FA	-.44	2.13	1.00	-7.02	6.14

		20FA	1.67	2.13	.97	-4.91	8.25
		30FA	1.90	2.13	.94	-4.68	8.48
		40FA	5.67	2.13	.12	-.91	12.24
	10FA	TC	9.61*	2.13	.00	3.03	16.19
		0FA	.44	2.13	1.00	-6.14	7.02
		20FA	2.11	2.13	.92	-4.47	8.69
		30FA	2.35	2.13	.88	-4.23	8.93
		40FA	6.11	2.13	.08	-.47	12.69
	20FA	TC	7.49*	2.13	.02	.92	14.07
		0FA	-1.67	2.13	.97	-8.25	4.91
		10FA	-2.11	2.13	.92	-8.69	4.47
		30FA	.23	2.13	1.00	-6.35	6.81
		40FA	4.00	2.13	.44	-2.58	10.58
	30FA	TC	7.26*	2.13	.02	.68	13.84
		0FA	-1.90	2.13	.94	-8.48	4.68
		10FA	-2.35	2.13	.88	-8.93	4.23
		20FA	-.23	2.13	1.00	-6.81	6.35
		40FA	3.76	2.13	.50	-2.82	10.34
	40FA	TC	3.50	2.13	.58	-3.08	10.08
		0FA	-5.67	2.13	.12	-12.24	.91
		10FA	-6.11	2.13	.08	-12.69	.47
		20FA	-4.00	2.13	.44	-10.58	2.58
		30FA	-3.76	2.13	.50	-10.34	2.82
DoC_30s	TC	0FA	-8.95*	2.83	.04	-17.72	-.19
		10FA	-4.56	2.83	.60	-13.32	4.21
		20FA	-3.84	2.83	.75	-12.60	4.93
		30FA	-4.82	2.83	.54	-13.59	3.94
		40FA	-1.45	2.83	1.00	-10.21	7.32
	0FA	TC	8.95*	2.83	.04	.19	17.72
		10FA	4.40	2.83	.64	-4.37	13.16
		20FA	5.11	2.83	.48	-3.65	13.88
		30FA	4.13	2.83	.69	-4.64	12.89
		40FA	7.51	2.83	.12	-1.26	16.27
	10FA	TC	4.56	2.83	.60	-4.21	13.32
		0FA	-4.40	2.83	.64	-13.16	4.37
		20FA	.72	2.83	1.00	-8.05	9.48
		30FA	-.27	2.83	1.00	-9.03	8.50
		40FA	3.11	2.83	.88	-5.66	11.87
	20FA	TC	3.84	2.83	.75	-4.93	12.60
		0FA	-5.11	2.83	.48	-13.88	3.65
		10FA	-.72	2.83	1.00	-9.48	8.05
		30FA	-.99	2.83	1.00	-9.75	7.78

		40FA	2.39	2.83	.96	-6.37	11.16
	30FA	TC	4.82	2.83	.54	-3.94	13.59
		0FA	-4.13	2.83	.69	-12.89	4.64
		10FA	.27	2.83	1.00	-8.50	9.03
		20FA	.99	2.83	1.00	-7.78	9.75
		40FA	3.38	2.83	.84	-5.39	12.14
	40FA	TC	1.45	2.83	1.00	-7.32	10.21
		0FA	-7.51	2.83	.12	-16.27	1.26
		10FA	-3.11	2.83	.88	-11.87	5.66
		20FA	-2.39	2.83	.96	-11.16	6.37
		30FA	-3.38	2.83	.84	-12.14	5.39
DoC_40s	TC	0FA	-9.17*	2.82	.04	-17.89	-.46
		10FA	-6.05	2.82	.30	-14.77	2.66
		20FA	-3.02	2.82	.89	-11.74	5.69
		30FA	-7.22	2.82	.15	-15.94	1.49
		40FA	-4.81	2.82	.54	-13.52	3.91
	0FA	TC	9.17*	2.82	.04	.46	17.89
		10FA	3.12	2.82	.87	-5.60	11.83
		20FA	6.15	2.82	.28	-2.57	14.86
		30FA	1.95	2.82	.98	-6.77	10.66
		40FA	4.36	2.82	.64	-4.35	13.08
	10FA	TC	6.05	2.82	.30	-2.66	14.77
		0FA	-3.12	2.82	.87	-11.83	5.60
		20FA	3.03	2.82	.89	-5.68	11.75
		30FA	-1.17	2.82	1.00	-9.89	7.54
		40FA	1.24	2.82	1.00	-7.47	9.96
	20FA	TC	3.02	2.82	.89	-5.69	11.74
		0FA	-6.15	2.82	.28	-14.86	2.57
		10FA	-3.03	2.82	.89	-11.75	5.68
		30FA	-4.20	2.82	.67	-12.92	4.51
		40FA	-1.79	2.82	.99	-10.50	6.93
	30FA	TC	7.22	2.82	.15	-1.49	15.94
		0FA	-1.95	2.82	.98	-10.66	6.77
		10FA	1.17	2.82	1.00	-7.54	9.89
		20FA	4.20	2.82	.67	-4.51	12.92
		40FA	2.41	2.82	.95	-6.30	11.13
	40FA	TC	4.81	2.82	.54	-3.91	13.52
		0FA	-4.36	2.82	.64	-13.08	4.35
		10FA	-1.24	2.82	1.00	-9.96	7.47
		20FA	1.79	2.82	.99	-6.93	10.50
		30FA	-2.41	2.82	.95	-11.13	6.30
DoC_50s	TC	0FA	-11.09*	2.99	.01	-20.34	-1.84

		10FA	-8.12	2.99	.11	-17.37	1.13
		20FA	-3.84	2.99	.79	-13.09	5.41
		30FA	-10.49*	2.99	.02	-19.74	-1.24
		40FA	-2.24	2.99	.97	-11.49	7.01
	0FA	TC	11.09*	2.99	.01	1.84	20.34
		10FA	2.97	2.99	.92	-6.28	12.22
		20FA	7.25	2.99	.19	-2.00	16.50
		30FA	.59	2.99	1.00	-8.66	9.84
		40FA	8.84	2.99	.07	-.41	18.09
	10FA	TC	8.12	2.99	.11	-1.13	17.37
		0FA	-2.97	2.99	.92	-12.22	6.28
		20FA	4.28	2.99	.71	-4.97	13.53
		30FA	-2.38	2.99	.97	-11.63	6.87
		40FA	5.87	2.99	.39	-3.38	15.12
	20FA	TC	3.84	2.99	.79	-5.41	13.09
		0FA	-7.25	2.99	.19	-16.50	2.00
		10FA	-4.28	2.99	.71	-13.53	4.97
		30FA	-6.65	2.99	.26	-15.90	2.60
		40FA	1.60	2.99	.99	-7.65	10.85
	30FA	TC	10.49*	2.99	.02	1.24	19.74
		0FA	-.59	2.99	1.00	-9.84	8.66
		10FA	2.38	2.99	.97	-6.87	11.63
		20FA	6.65	2.99	.26	-2.60	15.90
		40FA	8.25	2.99	.10	-1.00	17.50
	40FA	TC	2.24	2.99	.97	-7.01	11.49
		0FA	-8.84	2.99	.07	-18.09	.41
		10FA	-5.87	2.99	.39	-15.12	3.38
		20FA	-1.60	2.99	.99	-10.85	7.65
		30FA	-8.25	2.99	.10	-17.50	1.00
DoC_60s	TC	0FA	-9.46*	2.70	.02	-17.82	-1.10
		10FA	-2.65	2.70	.92	-11.01	5.70
		20FA	-6.41	2.70	.21	-14.76	1.95
		30FA	-6.94	2.70	.14	-15.30	1.42
		40FA	-2.44	2.70	.94	-10.79	5.92
	0FA	TC	9.46*	2.70	.02	1.10	17.82
		10FA	6.81	2.70	.16	-1.55	15.16
		20FA	3.05	2.70	.86	-5.31	11.41
		30FA	2.52	2.70	.93	-5.84	10.88
		40FA	7.02	2.70	.14	-1.33	15.38
	10FA	TC	2.65	2.70	.92	-5.70	11.01
		0FA	-6.81	2.70	.16	-15.16	1.55
		20FA	-3.75	2.70	.73	-12.11	4.60

		30FA	-4.29	2.70	.62	-12.64	4.07
		40FA	.22	2.70	1.00	-8.14	8.58
	20FA	TC	6.41	2.70	.21	-1.95	14.76
		0FA	-3.05	2.70	.86	-11.41	5.31
		10FA	3.75	2.70	.73	-4.60	12.11
		30FA	-.53	2.70	1.00	-8.89	7.83
		40FA	3.97	2.70	.69	-4.39	12.33
	30FA	TC	6.94	2.70	.14	-1.42	15.30
		0FA	-2.52	2.70	.93	-10.88	5.84
		10FA	4.29	2.70	.62	-4.07	12.64
		20FA	.53	2.70	1.00	-7.83	8.89
		40FA	4.50	2.70	.57	-3.85	12.86
	40FA	TC	2.44	2.70	.94	-5.92	10.79
		0FA	-7.02	2.70	.14	-15.38	1.33
		10FA	-.22	2.70	1.00	-8.58	8.14
		20FA	-3.97	2.70	.69	-12.33	4.39
		30FA	-4.50	2.70	.57	-12.86	3.85

*. The mean difference is significant at the 0.05 level.

Appendix K: Normality test results wear (TC,0FA-40FA)

Tests of Normality-Volume loss (TC,0FA-40FA)			
DC-Volume loss	Shapiro-Wilk		
	Statistic	df	Sig.
TC	.903	5	.429
0FA	.786	5	.062
10FA	.684	5	.006
20FA	.684	5	.006
30FA	.845	5	.180
40FA	.771	5	.046
*. This is a lower bound of the true significance.			

Appendix L: Kruskal-Wallis test wear (TC,0FA-40FA)

Test Statisticsa,b	
	Volume_loss
Chi-Square	8.96
df	5.00
Asymp. Sig.	0.11
a. Kruskal Wallis Test	
b. Grouping Variable: DC	

Appendix M: Normality test results HV (TC,0FA-40FA)

Tests of Normality-TC,0FA-40FA			
HV	Shapiro-Wilk		
	Statistic	df	Sig.
TC	.904	5	.430
0FA	.904	5	.432
10FA	.881	5	.314
20FA	.886	5	.336
30FA	.946	5	.708
40FA	.966	5	.851

Appendix N: Normality test results FS,FM and K1C (TC,0FA-40FA)

Tests of Normality- Shapiro-Wilk									
	Flexural Modulus			Flexural Strength			Fracture Toughness		
	Statistic	df	Sig.	Statistic	df	Sig.	Statistic	df	Sig.
TC	.520	10	.000	.965	10	.838	.937	10	.517
0FA	.749	10	.003	.890	10	.168	.959	10	.774
10FA	.894	10	.187	.926	10	.407	.895	10	.193
20FA	.904	10	.241	.800	10	.014	.942	10	.580
30FA	.875	10	.113	.837	10	.041	.872	10	.104
40FA	.953	10	.706	.954	10	.712	.842	10	.047

Appendix O: Kruskal Wallis test FS and FM

Test Statistics[a,b]		
	Flexural_Modulus	Flexural_Strength
Chi-Square	30.224	22.541
df	5	5
Asymp. Sig.	.000	.000
a. Kruskal Wallis Test		
b. Grouping Variable: DC		

Appendix P: Post Hoc Bonferroni FS and FM

Multiple Comparisons							
Bonferroni							
Dependent Variable	(I) DC	(J) DC	Mean Difference (I-J)	Std. Error	Sig.	95% Confidence Interval	
						Lower Bound	Upper Bound
Flexural_Modulus	TC	0FA	-4.41*	.57	.00	-6.15	-2.68
		10FA	-1.83*	.57	.03	-3.56	-.09
		20FA	-1.97*	.57	.01	-3.71	-.24
		30FA	-1.86*	.57	.03	-3.60	-.13
		40FA	-1.83*	.57	.03	-3.57	-.09
	0FA	TC	4.41*	.57	.00	2.68	6.15
		10FA	2.59*	.57	.00	.85	4.32
		20FA	2.44*	.57	.00	.70	4.18
		30FA	2.55*	.57	.00	.81	4.29
		40FA	2.58*	.57	.00	.85	4.32
	10FA	TC	1.83*	.57	.03	.09	3.56
		0FA	-2.59*	.57	.00	-4.32	-.85
		20FA	-.15	.57	1.00	-1.88	1.59
		30FA	-.04	.57	1.00	-1.77	1.70
		40FA	.00	.57	1.00	-1.74	1.74
	20FA	TC	1.97*	.57	.01	.24	3.71
		0FA	-2.44*	.57	.00	-4.18	-.70
		10FA	.15	.57	1.00	-1.59	1.88
		30FA	.11	.57	1.00	-1.63	1.85
		40FA	.14	.57	1.00	-1.59	1.88
	30FA	TC	1.86*	.57	.03	.13	3.60
		0FA	-2.55*	.57	.00	-4.29	-.81
		10FA	.04	.57	1.00	-1.70	1.77
		20FA	-.11	.57	1.00	-1.85	1.63
		40FA	.03	.57	1.00	-1.70	1.77
	40FA	TC	1.83*	.57	.03	.09	3.57
		0FA	-2.58*	.57	.00	-4.32	-.85
		10FA	.00	.57	1.00	-1.74	1.74
		20FA	-.14	.57	1.00	-1.88	1.59
		30FA	-.03	.57	1.00	-1.77	1.70
Flexural_Strength	TC	0FA	-24.48*	7.75	.04	-48.30	-.67
		10FA	8.43	7.75	1.00	-15.38	32.24
		20FA	8.08	7.75	1.00	-15.73	31.89
		30FA	14.09	7.75	1.00	-9.72	37.90
		40FA	20.26	7.75	.17	-3.55	44.07
	0FA	TC	24.48*	7.75	.04	.67	48.30

		10FA	32.91*	7.75	.00	9.10	56.73
		20FA	32.56*	7.75	.00	8.75	56.37
		30FA	38.58*	7.75	.00	14.76	62.39
		40FA	44.74*	7.75	.00	20.93	68.55
	10FA	TC	-8.43	7.75	1.00	-32.24	15.38
		0FA	-32.91*	7.75	.00	-56.73	-9.10
		20FA	-.35	7.75	1.00	-24.16	23.46
		30FA	5.66	7.75	1.00	-18.15	29.47
		40FA	11.83	7.75	1.00	-11.98	35.64
	20FA	TC	-8.08	7.75	1.00	-31.89	15.73
		0FA	-32.56*	7.75	.00	-56.37	-8.75
		10FA	.35	7.75	1.00	-23.46	24.16
		30FA	6.02	7.75	1.00	-17.80	29.83
		40FA	12.18	7.75	1.00	-11.63	35.99
	30FA	TC	-14.09	7.75	1.00	-37.90	9.72
		0FA	-38.58*	7.75	.00	-62.39	-14.76
		10FA	-5.66	7.75	1.00	-29.47	18.15
		20FA	-6.02	7.75	1.00	-29.83	17.80
		40FA	6.17	7.75	1.00	-17.65	29.98
	40FA	TC	-20.26	7.75	.17	-44.07	3.55
		0FA	-44.74*	7.75	.00	-68.55	-20.93
		10FA	-11.83	7.75	1.00	-35.64	11.98
		20FA	-12.18	7.75	1.00	-35.99	11.63
		30FA	-6.17	7.75	1.00	-29.98	17.65

*. The mean difference is significant at the 0.05 level.

Appendix Q: One way ANOVA Fracture Toughness (TC,0FA-40FA)

ANOVA					
Fracture_Toughness					
	Sum of Squares	df	Mean Square	F	Sig.
Between Groups	3.142	5	.628	13.986	.000
Within Groups	2.426	54	.045		
Total	5.569	59			

Appendix R: Post Hoc Tukey test Fracture Toughness (TC,0FA-40FA)

Multiple Comparisons						
Dependent Variable: Fracture_Toughness						
Tukey HSD						
(I) DC	(J) DC	Mean Difference (I-J)	Std. Error	Sig.	95% Confidence Interval	
					Lower Bound	Upper Bound
TC	0FA	.08	.09	.97	-.20	.36
	10FA	.50*	.09	.00	.22	.78
	20FA	.49*	.09	.00	.21	.78
	30FA	-.09	.09	.94	-.37	.19
	40FA	.16	.09	.54	-.12	.44
0FA	TC	-.08	.09	.97	-.36	.20
	10FA	.42*	.09	.00	.14	.70
	20FA	.42*	.09	.00	.14	.70
	30FA	-.16	.09	.53	-.44	.12
	40FA	.08	.09	.95	-.20	.37
10FA	TC	-.50*	.09	.00	-.78	-.22
	0FA	-.42*	.09	.00	-.70	-.14
	20FA	.00	.09	1.00	-.28	.28
	30FA	-.58*	.09	.00	-.86	-.30
	40FA	-.34*	.09	.01	-.62	-.06
20FA	TC	-.49*	.09	.00	-.78	-.21
	0FA	-.42*	.09	.00	-.70	-.14
	10FA	.00	.09	1.00	-.28	.28
	30FA	-.58*	.09	.00	-.86	-.30
	40FA	-.33*	.09	.01	-.61	-.05
30FA	TC	.09	.09	.94	-.19	.37
	0FA	.16	.09	.53	-.12	.44
	10FA	.58*	.09	.00	.30	.86
	20FA	.58*	.09	.00	.30	.86
	40FA	.25	.09	.11	-.03	.53

40FA	TC	-.16	.09	.54	-.44	.12
	0FA	-.08	.09	.95	-.37	.20
	10FA	.34*	.09	.01	.06	.62
	20FA	.33*	.09	.01	.05	.61
	30FA	-.25	.09	.11	-.53	.03
*. The mean difference is significant at the 0.05 level.						

Appendix S: One- Way ANOVA DC (FA composites)

ANOVA-HV (TC,0FA-40FA)					
HV					
	Sum of Squares	df	Mean Square	F	Sig.
Between Groups	6957.69	5.00	1391.54	241.10	.00
Within Groups	138.52	24.00	5.77		
Total	7096.21	29.00			

Appendix T: Post Hoc Tukey DC (FA composites)

Multiple Comparisons						
Dependent Variable: HV						
Tukey HSD						
(I) DC	(J) DC	Mean Difference (I-J)	Std. Error	Sig.	95% Confidence Interval	
					Lower Bound	Upper Bound
TC	0FA	-39.82*	1.52	.00	-44.52	-35.12
	10FA	-41.76*	1.52	.00	-46.46	-37.06
	20FA	-41.24*	1.52	.00	-45.94	-36.54
	30FA	-40.50*	1.52	.00	-45.20	-35.80
	40FA	-40.84*	1.52	.00	-45.54	-36.14
0FA	TC	39.82*	1.52	.00	35.12	44.52
	10FA	-1.94	1.52	.79	-6.64	2.76
	20FA	-1.42	1.52	.93	-6.12	3.28
	30FA	-.68	1.52	1.00	-5.38	4.02
	40FA	-1.02	1.52	.98	-5.72	3.68

10FA	TC	41.76*	1.52	.00	37.06	46.46
	0FA	1.94	1.52	.79	-2.76	6.64
	20FA	.52	1.52	1.00	-4.18	5.22
	30FA	1.26	1.52	.96	-3.44	5.96
	40FA	.92	1.52	.99	-3.78	5.62
20FA	TC	41.24*	1.52	.00	36.54	45.94
	0FA	1.42	1.52	.93	-3.28	6.12
	10FA	-.52	1.52	1.00	-5.22	4.18
	30FA	.74	1.52	1.00	-3.96	5.44
	40FA	.40	1.52	1.00	-4.30	5.10
30FA	TC	40.50*	1.52	.00	35.80	45.20
	0FA	.68	1.52	1.00	-4.02	5.38
	10FA	-1.26	1.52	.96	-5.96	3.44
	20FA	-.74	1.52	1.00	-5.44	3.96
	40FA	-.34	1.52	1.00	-5.04	4.36
40FA	TC	40.84*	1.52	.00	36.14	45.54
	0FA	1.02	1.52	.98	-3.68	5.72
	10FA	-.92	1.52	.99	-5.62	3.78
	20FA	-.40	1.52	1.00	-5.10	4.30
	30FA	.34	1.52	1.00	-4.36	5.04

*. The mean difference is significant at the 0.05 level.

Appendix U: Normality test results (F release ppm)

Test of Normality (F release microgram)				
Group	Day	Shapiro-Wilk		
		Statistic	df	Sig.
TC	Day 1-ppm	.991	6	.990
	Day 2-ppm	.969	6	.889
	Day 3-ppm	.953	6	.761
	Day 4-ppm	.919	6	.498
	Day 5-ppm	.900	6	.374
	Day6-ppm	.896	6	.352
	Day7-ppm	.907	6	.418
	Day14-ppm	.895	6	.343
	Day21-ppm	.889	6	.312
	Day28-ppm	.846	6	.145
	Day56-ppm	.873	6	.240
	Day112-ppm	.792	6	.049
	Day196-ppm	.862	6	.197
0FA	Day 1-ppm	.786	6	.044
	Day 2-ppm	.802	6	.061
	Day 3-ppm	.921	6	.511
	Day 4-ppm	.945	6	.698
	Day 5-ppm	.958	6	.803
	Day6-ppm	.965	6	.854
	Day7-ppm	.960	6	.822
	Day14-ppm	.968	6	.879
	Day21-ppm	.973	6	.913
	Day28-ppm	.972	6	.905
	Day56-ppm	.965	6	.854
	Day112-ppm	.975	6	.923
	Day196-ppm	.986	6	.978
10FA	Day 1-ppm	.860	6	.189
	Day 2-ppm	.892	6	.330

	Day 3-ppm	.891	6	.322
	Day 4-ppm	.895	6	.343
	Day 5-ppm	.902	6	.386
	Day6-ppm	.907	6	.415
	Day7-ppm	.905	6	.405
	Day14-ppm	.933	6	.604
	Day21-ppm	.942	6	.677
	Day28-ppm	.944	6	.694
	Day56-ppm	.944	6	.689
	Day112-ppm	.950	6	.739
	Day196-ppm	.920	6	.502
20FA	Day 1-ppm	.873	6	.238
	Day 2-ppm	.836	6	.121
	Day 3-ppm	.860	6	.188
	Day 4-ppm	.849	6	.155
	Day 5-ppm	.854	6	.171
	Day6-ppm	.856	6	.175
	Day7-ppm	.857	6	.179
	Day14-ppm	.873	6	.238
	Day21-ppm	.884	6	.286
	Day28-ppm	.918	6	.489
	Day56-ppm	.968	6	.876
	Day112-ppm	.917	6	.482
	Day196-ppm	.877	6	.257
30FA	Day 1-ppm	.849	6	.154
	Day 2-ppm	.941	6	.664
	Day 3-ppm	.954	6	.773
	Day 4-ppm	.916	6	.478
	Day 5-ppm	.926	6	.549
	Day6-ppm	.902	6	.388
	Day7-ppm	.884	6	.287

	Day14-ppm	.839	6	.128
	Day21-ppm	.732	6	.013
	Day28-ppm	.781	6	.039
	Day56-ppm	.718	6	.010
	Day112-ppm	.893	6	.332
	Day196-ppm	.948	6	.726
40FA	Day 1-ppm	.879	6	.264
	Day 2-ppm	.987	6	.981
	Day 3-ppm	.939	6	.649
	Day 4-ppm	.875	6	.245
	Day 5-ppm	.846	6	.145
	Day6-ppm	.870	6	.227
	Day7-ppm	.859	6	.187
	Day14-ppm	.855	6	.174
	Day21-ppm	.867	6	.214
	Day28-ppm	.927	6	.557
	Day56-ppm	.947	6	.712
	Day112-ppm	.972	6	.906
	Day196-ppm	.920	6	.508

Appendix V: Kruskal-Wallis test F release microgram

Test Statistics[a,b]			
	Chi-Square	df	Asymp. Sig.
Day 1-ppm	29.920	5	.000
Day 2-ppm	29.742	5	.000
Day 3-ppm	29.538	5	.000
Day 4-ppm	29.335	5	.000
Day 5-ppm	30.142	5	.000
Day6-ppm	30.379	5	.000
Day7-ppm	30.668	5	.000
Day14-ppm	32.209	5	.000
Day21-ppm	32.835	5	.000
Day28-ppm	33.483	5	.000
Day56-ppm	33.757	5	.000
Day112-ppm	33.907	5	.000
Day196-ppm	34.054	5	.000
a. Kruskal Wallis Test			
b. Grouping Variable: DC			

Appendix W: Post Hoc Bonferroni group comparisons F release (microgram)

Multiple Comparisons							
Bonferroni							
Dependent Variable	(I) DC	(J) DC	Mean Difference (I-J)	Std. Error	Sig.	95% Confidence Interval	
						Lower Bound	Upper Bound
Day 1-ppm	TC	0FA	-.07	1.48	1.00	-4.80	4.66
		10FA	-15.38*	1.48	.00	-20.11	-10.65
		20FA	-25.54*	1.48	.00	-30.27	-20.80
		30FA	-26.67*	1.48	.00	-31.40	-21.94
		40FA	-24.87*	1.48	.00	-29.60	-20.14
	0FA	TC	.07	1.48	1.00	-4.66	4.80
		10FA	-15.31*	1.48	.00	-20.04	-10.58
		20FA	-25.47*	1.48	.00	-30.20	-20.74
		30FA	-26.60*	1.48	.00	-31.34	-21.87
		40FA	-24.80*	1.48	.00	-29.54	-20.07
	10FA	TC	15.38*	1.48	.00	10.65	20.11
		0FA	15.31*	1.48	.00	10.58	20.04
		20FA	-10.16*	1.48	.00	-14.89	-5.42
		30FA	-11.29*	1.48	.00	-16.02	-6.56
		40FA	-9.49*	1.48	.00	-14.22	-4.76
	20FA	TC	25.54*	1.48	.00	20.80	30.27
		0FA	25.47*	1.48	.00	20.74	30.20
		10FA	10.16*	1.48	.00	5.42	14.89
		30FA	-1.14	1.48	1.00	-5.87	3.60
		40FA	.67	1.48	1.00	-4.07	5.40
	30FA	TC	26.67*	1.48	.00	21.94	31.40
		0FA	26.60*	1.48	.00	21.87	31.34
		10FA	11.29*	1.48	.00	6.56	16.02
		20FA	1.14	1.48	1.00	-3.60	5.87
		40FA	1.80	1.48	1.00	-2.93	6.53
	40FA	TC	24.87*	1.48	.00	20.14	29.60
		0FA	24.80*	1.48	.00	20.07	29.54
		10FA	9.49*	1.48	.00	4.76	14.22
		20FA	-.67	1.48	1.00	-5.40	4.07
		30FA	-1.80	1.48	1.00	-6.53	2.93
Day 2-ppm	TC	0FA	.05	1.93	1.00	-6.11	6.21
		10FA	-17.14*	1.93	.00	-23.30	-10.97
		20FA	-35.67*	1.93	.00	-41.83	-29.51
		30FA	-34.59*	1.93	.00	-40.75	-28.42

		40FA	-32.52*	1.93	.00	-38.68	-26.35
	0FA	TC	-.05	1.93	1.00	-6.21	6.11
		10FA	-17.19*	1.93	.00	-23.35	-11.02
		20FA	-35.72*	1.93	.00	-41.88	-29.56
		30FA	-34.64*	1.93	.00	-40.80	-28.47
		40FA	-32.57*	1.93	.00	-38.73	-26.40
	10FA	TC	17.14*	1.93	.00	10.97	23.30
		0FA	17.19*	1.93	.00	11.02	23.35
		20FA	-18.53*	1.93	.00	-24.69	-12.37
		30FA	-17.45*	1.93	.00	-23.61	-11.29
		40FA	-15.38*	1.93	.00	-21.54	-9.22
	20FA	TC	35.67*	1.93	.00	29.51	41.83
		0FA	35.72*	1.93	.00	29.56	41.88
		10FA	18.53*	1.93	.00	12.37	24.69
		30FA	1.08	1.93	1.00	-5.08	7.24
		40FA	3.15	1.93	1.00	-3.01	9.31
	30FA	TC	34.59*	1.93	.00	28.42	40.75
		0FA	34.64*	1.93	.00	28.47	40.80
		10FA	17.45*	1.93	.00	11.29	23.61
		20FA	-1.08	1.93	1.00	-7.24	5.08
		40FA	2.07	1.93	1.00	-4.09	8.23
	40FA	TC	32.52*	1.93	.00	26.35	38.68
		0FA	32.57*	1.93	.00	26.40	38.73
		10FA	15.38*	1.93	.00	9.22	21.54
		20FA	-3.15	1.93	1.00	-9.31	3.01
		30FA	-2.07	1.93	1.00	-8.23	4.09
Day 3-ppm	TC	0FA	.02	2.01	1.00	-6.40	6.44
		10FA	-17.88*	2.01	.00	-24.30	-11.46
		20FA	-40.36*	2.01	.00	-46.78	-33.95
		30FA	-39.38*	2.01	.00	-45.80	-32.96
		40FA	-38.35*	2.01	.00	-44.77	-31.94
	0FA	TC	-.02	2.01	1.00	-6.44	6.40
		10FA	-17.90*	2.01	.00	-24.32	-11.48
		20FA	-40.38*	2.01	.00	-46.80	-33.97
		30FA	-39.40*	2.01	.00	-45.82	-32.98
		40FA	-38.37*	2.01	.00	-44.79	-31.96
	10FA	TC	17.88*	2.01	.00	11.46	24.30
		0FA	17.90*	2.01	.00	11.48	24.32
		20FA	-22.49*	2.01	.00	-28.90	-16.07
		30FA	-21.50*	2.01	.00	-27.92	-15.08
		40FA	-20.48*	2.01	.00	-26.89	-14.06
	20FA	TC	40.36*	2.01	.00	33.95	46.78

		0FA	40.38*	2.01	.00	33.97	46.80
		10FA	22.49*	2.01	.00	16.07	28.90
		30FA	.99	2.01	1.00	-5.43	7.40
		40FA	2.01	2.01	1.00	-4.41	8.43
	30FA	TC	39.38*	2.01	.00	32.96	45.80
		0FA	39.40*	2.01	.00	32.98	45.82
		10FA	21.50*	2.01	.00	15.08	27.92
		20FA	-.99	2.01	1.00	-7.40	5.43
		40FA	1.03	2.01	1.00	-5.39	7.44
	40FA	TC	38.35*	2.01	.00	31.94	44.77
		0FA	38.37*	2.01	.00	31.96	44.79
		10FA	20.48*	2.01	.00	14.06	26.89
		20FA	-2.01	2.01	1.00	-8.43	4.41
		30FA	-1.03	2.01	1.00	-7.44	5.39
Day 4-ppm	TC	0FA	.07	2.20	1.00	-6.94	7.07
		10FA	-18.45*	2.20	.00	-25.46	-11.44
		20FA	-43.18*	2.20	.00	-50.18	-36.17
		30FA	-43.01*	2.20	.00	-50.01	-36.00
		40FA	-44.10*	2.20	.00	-51.11	-37.09
	0FA	TC	-.07	2.20	1.00	-7.07	6.94
		10FA	-18.52*	2.20	.00	-25.52	-11.51
		20FA	-43.24*	2.20	.00	-50.25	-36.23
		30FA	-43.07*	2.20	.00	-50.08	-36.07
		40FA	-44.17*	2.20	.00	-51.17	-37.16
	10FA	TC	18.45*	2.20	.00	11.44	25.46
		0FA	18.52*	2.20	.00	11.51	25.52
		20FA	-24.73*	2.20	.00	-31.73	-17.72
		30FA	-24.56*	2.20	.00	-31.56	-17.55
		40FA	-25.65*	2.20	.00	-32.66	-18.64
	20FA	TC	43.18*	2.20	.00	36.17	50.18
		0FA	43.24*	2.20	.00	36.23	50.25
		10FA	24.73*	2.20	.00	17.72	31.73
		30FA	.17	2.20	1.00	-6.84	7.17
		40FA	-.93	2.20	1.00	-7.93	6.08
	30FA	TC	43.01*	2.20	.00	36.00	50.01
		0FA	43.07*	2.20	.00	36.07	50.08
		10FA	24.56*	2.20	.00	17.55	31.56
		20FA	-.17	2.20	1.00	-7.17	6.84
		40FA	-1.09	2.20	1.00	-8.10	5.91
	40FA	TC	44.10*	2.20	.00	37.09	51.11
		0FA	44.17*	2.20	.00	37.16	51.17
		10FA	25.65*	2.20	.00	18.64	32.66

		20FA	.93	2.20	1.00	-6.08	7.93
		30FA	1.09	2.20	1.00	-5.91	8.10
Day 5-ppm	TC	0FA	.09	2.19	1.00	-6.89	7.07
		10FA	-18.74*	2.19	.00	-25.72	-11.76
		20FA	-45.01*	2.19	.00	-51.98	-38.03
		30FA	-45.72*	2.19	.00	-52.70	-38.74
		40FA	-49.27*	2.19	.00	-56.25	-42.29
	0FA	TC	-.09	2.19	1.00	-7.07	6.89
		10FA	-18.83*	2.19	.00	-25.81	-11.85
		20FA	-45.10*	2.19	.00	-52.08	-38.12
		30FA	-45.81*	2.19	.00	-52.79	-38.83
		40FA	-49.36*	2.19	.00	-56.34	-42.38
	10FA	TC	18.74*	2.19	.00	11.76	25.72
		0FA	18.83*	2.19	.00	11.85	25.81
		20FA	-26.26*	2.19	.00	-33.24	-19.28
		30FA	-26.98*	2.19	.00	-33.96	-20.00
		40FA	-30.53*	2.19	.00	-37.50	-23.55
	20FA	TC	45.01*	2.19	.00	38.03	51.98
		0FA	45.10*	2.19	.00	38.12	52.08
		10FA	26.26*	2.19	.00	19.28	33.24
		30FA	-.72	2.19	1.00	-7.70	6.26
		40FA	-4.26	2.19	.91	-11.24	2.72
	30FA	TC	45.72*	2.19	.00	38.74	52.70
		0FA	45.81*	2.19	.00	38.83	52.79
		10FA	26.98*	2.19	.00	20.00	33.96
		20FA	.72	2.19	1.00	-6.26	7.70
		40FA	-3.55	2.19	1.00	-10.52	3.43
	40FA	TC	49.27*	2.19	.00	42.29	56.25
		0FA	49.36*	2.19	.00	42.38	56.34
		10FA	30.53*	2.19	.00	23.55	37.50
		20FA	4.26	2.19	.91	-2.72	11.24
		30FA	3.55	2.19	1.00	-3.43	10.52
Day6-ppm	TC	0FA	.07	2.21	1.00	-6.98	7.11
		10FA	-18.92*	2.21	.00	-25.96	-11.87
		20FA	-45.80*	2.21	.00	-52.85	-38.75
		30FA	-46.86*	2.21	.00	-53.91	-39.82
		40FA	-51.69*	2.21	.00	-58.73	-44.64
	0FA	TC	-.07	2.21	1.00	-7.11	6.98
		10FA	-18.98*	2.21	.00	-26.03	-11.93
		20FA	-45.87*	2.21	.00	-52.91	-38.82
		30FA	-46.93*	2.21	.00	-53.97	-39.88
		40FA	-51.75*	2.21	.00	-58.80	-44.70

	10FA	TC	18.92*	2.21	.00	11.87	25.96
		0FA	18.98*	2.21	.00	11.93	26.03
		20FA	-26.89*	2.21	.00	-33.93	-19.84
		30FA	-27.95*	2.21	.00	-34.99	-20.90
		40FA	-32.77*	2.21	.00	-39.82	-25.72
	20FA	TC	45.80*	2.21	.00	38.75	52.85
		0FA	45.87*	2.21	.00	38.82	52.91
		10FA	26.89*	2.21	.00	19.84	33.93
		30FA	-1.06	2.21	1.00	-8.11	5.98
		40FA	-5.89	2.21	.18	-12.93	1.16
	30FA	TC	46.86*	2.21	.00	39.82	53.91
		0FA	46.93*	2.21	.00	39.88	53.97
		10FA	27.95*	2.21	.00	20.90	34.99
		20FA	1.06	2.21	1.00	-5.98	8.11
		40FA	-4.82	2.21	.56	-11.87	2.22
	40FA	TC	51.69*	2.21	.00	44.64	58.73
		0FA	51.75*	2.21	.00	44.70	58.80
		10FA	32.77*	2.21	.00	25.72	39.82
		20FA	5.89	2.21	.18	-1.16	12.93
		30FA	4.82	2.21	.56	-2.22	11.87
Day7-ppm	TC	0FA	.03	2.28	1.00	-7.25	7.30
		10FA	-19.04*	2.28	.00	-26.31	-11.76
		20FA	-46.55*	2.28	.00	-53.82	-39.27
		30FA	-47.97*	2.28	.00	-55.24	-40.69
		40FA	-53.93*	2.28	.00	-61.20	-46.65
	0FA	TC	-.03	2.28	1.00	-7.30	7.25
		10FA	-19.07*	2.28	.00	-26.34	-11.79
		20FA	-46.57*	2.28	.00	-53.85	-39.30
		30FA	-48.00*	2.28	.00	-55.27	-40.72
		40FA	-53.96*	2.28	.00	-61.23	-46.68
	10FA	TC	19.04*	2.28	.00	11.76	26.31
		0FA	19.07*	2.28	.00	11.79	26.34
		20FA	-27.51*	2.28	.00	-34.78	-20.23
		30FA	-28.93*	2.28	.00	-36.21	-21.66
		40FA	-34.89*	2.28	.00	-42.17	-27.61
	20FA	TC	46.55*	2.28	.00	39.27	53.82
		0FA	46.57*	2.28	.00	39.30	53.85
		10FA	27.51*	2.28	.00	20.23	34.78
		30FA	-1.42	2.28	1.00	-8.70	5.85
		40FA	-7.38*	2.28	.04	-14.66	-.11
	30FA	TC	47.97*	2.28	.00	40.69	55.24
		0FA	48.00*	2.28	.00	40.72	55.27

		10FA	28.93*	2.28	.00	21.66	36.21
		20FA	1.42	2.28	1.00	-5.85	8.70
		40FA	-5.96	2.28	.21	-13.23	1.32
	40FA	TC	53.93*	2.28	.00	46.65	61.20
		0FA	53.96*	2.28	.00	46.68	61.23
		10FA	34.89*	2.28	.00	27.61	42.17
		20FA	7.38*	2.28	.04	.11	14.66
		30FA	5.96	2.28	.21	-1.32	13.23
Day14-ppm	TC	0FA	.10	2.59	1.00	-8.16	8.36
		10FA	-19.86*	2.59	.00	-28.12	-11.60
		20FA	-51.10*	2.59	.00	-59.37	-42.84
		30FA	-54.92*	2.59	.00	-63.19	-46.66
		40FA	-70.01*	2.59	.00	-78.28	-61.75
	0FA	TC	-.10	2.59	1.00	-8.36	8.16
		10FA	-19.96*	2.59	.00	-28.22	-11.70
		20FA	-51.20*	2.59	.00	-59.47	-42.94
		30FA	-55.02*	2.59	.00	-63.29	-46.76
		40FA	-70.11*	2.59	.00	-78.38	-61.85
	10FA	TC	19.86*	2.59	.00	11.60	28.12
		0FA	19.96*	2.59	.00	11.70	28.22
		20FA	-31.24*	2.59	.00	-39.51	-22.98
		30FA	-35.06*	2.59	.00	-43.33	-26.80
		40FA	-50.15*	2.59	.00	-58.42	-41.89
	20FA	TC	51.10*	2.59	.00	42.84	59.37
		0FA	51.20*	2.59	.00	42.94	59.47
		10FA	31.24*	2.59	.00	22.98	39.51
		30FA	-3.82	2.59	1.00	-12.08	4.44
		40FA	-18.91*	2.59	.00	-27.18	-10.65
	30FA	TC	54.92*	2.59	.00	46.66	63.19
		0FA	55.02*	2.59	.00	46.76	63.29
		10FA	35.06*	2.59	.00	26.80	43.33
		20FA	3.82	2.59	1.00	-4.44	12.08
		40FA	-15.09*	2.59	.00	-23.36	-6.83
	40FA	TC	70.01*	2.59	.00	61.75	78.28
		0FA	70.11*	2.59	.00	61.85	78.38
		10FA	50.15*	2.59	.00	41.89	58.42
		20FA	18.91*	2.59	.00	10.65	27.18
		30FA	15.09*	2.59	.00	6.83	23.36
Day21-ppm	TC	0FA	.22	3.20	1.00	-9.98	10.42
		10FA	-20.53*	3.20	.00	-30.73	-10.33
		20FA	-55.19*	3.20	.00	-65.39	-44.99
		30FA	-62.15*	3.20	.00	-72.35	-51.96

		40FA	-86.87*	3.20	.00	-97.06	-76.67
	0FA	TC	-.22	3.20	1.00	-10.42	9.98
		10FA	-20.75*	3.20	.00	-30.95	-10.55
		20FA	-55.41*	3.20	.00	-65.61	-45.21
		30FA	-62.38*	3.20	.00	-72.57	-52.18
		40FA	-87.09*	3.20	.00	-97.29	-76.89
	10FA	TC	20.53*	3.20	.00	10.33	30.73
		0FA	20.75*	3.20	.00	10.55	30.95
		20FA	-34.66*	3.20	.00	-44.86	-24.46
		30FA	-41.62*	3.20	.00	-51.82	-31.43
		40FA	-66.34*	3.20	.00	-76.53	-56.14
	20FA	TC	55.19*	3.20	.00	44.99	65.39
		0FA	55.41*	3.20	.00	45.21	65.61
		10FA	34.66*	3.20	.00	24.46	44.86
		30FA	-6.96	3.20	.56	-17.16	3.23
		40FA	-31.68*	3.20	.00	-41.87	-21.48
	30FA	TC	62.15*	3.20	.00	51.96	72.35
		0FA	62.38*	3.20	.00	52.18	72.57
		10FA	41.62*	3.20	.00	31.43	51.82
		20FA	6.96	3.20	.56	-3.23	17.16
		40FA	-24.71*	3.20	.00	-34.91	-14.52
	40FA	TC	86.87*	3.20	.00	76.67	97.06
		0FA	87.09*	3.20	.00	76.89	97.29
		10FA	66.34*	3.20	.00	56.14	76.53
		20FA	31.68*	3.20	.00	21.48	41.87
		30FA	24.71*	3.20	.00	14.52	34.91
Day28-ppm	TC	0FA	.31	3.83	1.00	-11.90	12.52
		10FA	-20.99*	3.83	.00	-33.20	-8.78
		20FA	-58.16*	3.83	.00	-70.37	-45.94
		30FA	-67.80*	3.83	.00	-80.01	-55.59
		40FA	-101.77*	3.83	.00	-113.98	-89.56
	0FA	TC	-.31	3.83	1.00	-12.52	11.90
		10FA	-21.30*	3.83	.00	-33.51	-9.09
		20FA	-58.46*	3.83	.00	-70.67	-46.25
		30FA	-68.11*	3.83	.00	-80.32	-55.89
		40FA	-102.08*	3.83	.00	-114.29	-89.87
	10FA	TC	20.99*	3.83	.00	8.78	33.20
		0FA	21.30*	3.83	.00	9.09	33.51
		20FA	-37.17*	3.83	.00	-49.38	-24.96
		30FA	-46.81*	3.83	.00	-59.02	-34.60
		40FA	-80.78*	3.83	.00	-92.99	-68.57
	20FA	TC	58.16*	3.83	.00	45.94	70.37

		0FA	58.46*	3.83	.00	46.25	70.67
		10FA	37.17*	3.83	.00	24.96	49.38
		30FA	-9.64	3.83	.26	-21.85	2.57
		40FA	-43.62*	3.83	.00	-55.83	-31.41
	30FA	TC	67.80*	3.83	.00	55.59	80.01
		0FA	68.11*	3.83	.00	55.89	80.32
		10FA	46.81*	3.83	.00	34.60	59.02
		20FA	9.64	3.83	.26	-2.57	21.85
		40FA	-33.98*	3.83	.00	-46.19	-21.76
	40FA	TC	101.77*	3.83	.00	89.56	113.98
		0FA	102.08*	3.83	.00	89.87	114.29
		10FA	80.78*	3.83	.00	68.57	92.99
		20FA	43.62*	3.83	.00	31.41	55.83
		30FA	33.98*	3.83	.00	21.76	46.19
Day56-ppm	TC	0FA	.48	4.34	1.00	-13.36	14.32
		10FA	-21.44*	4.34	.00	-35.27	-7.60
		20FA	-61.03*	4.34	.00	-74.87	-47.19
		30FA	-76.23*	4.34	.00	-90.07	-62.39
		40FA	-119.67*	4.34	.00	-133.51	-105.83
	0FA	TC	-.48	4.34	1.00	-14.32	13.36
		10FA	-21.92*	4.34	.00	-35.76	-8.08
		20FA	-61.51*	4.34	.00	-75.35	-47.67
		30FA	-76.71*	4.34	.00	-90.55	-62.87
		40FA	-120.15*	4.34	.00	-133.99	-106.31
	10FA	TC	21.44*	4.34	.00	7.60	35.27
		0FA	21.92*	4.34	.00	8.08	35.76
		20FA	-39.59*	4.34	.00	-53.43	-25.75
		30FA	-54.80*	4.34	.00	-68.63	-40.96
		40FA	-98.24*	4.34	.00	-112.08	-84.40
	20FA	TC	61.03*	4.34	.00	47.19	74.87
		0FA	61.51*	4.34	.00	47.67	75.35
		10FA	39.59*	4.34	.00	25.75	53.43
		30FA	-15.20*	4.34	.02	-29.04	-1.36
		40FA	-58.64*	4.34	.00	-72.48	-44.80
	30FA	TC	76.23*	4.34	.00	62.39	90.07
		0FA	76.71*	4.34	.00	62.87	90.55
		10FA	54.80*	4.34	.00	40.96	68.63
		20FA	15.20*	4.34	.02	1.36	29.04
		40FA	-43.44*	4.34	.00	-57.28	-29.60
	40FA	TC	119.67*	4.34	.00	105.83	133.51
		0FA	120.15*	4.34	.00	106.31	133.99
		10FA	98.24*	4.34	.00	84.40	112.08

		20FA	58.64*	4.34	.00	44.80	72.48
		30FA	43.44*	4.34	.00	29.60	57.28
Day112-ppm	TC	0FA	.50	4.47	1.00	-13.75	14.76
		10FA	-22.15*	4.47	.00	-36.41	-7.90
		20FA	-65.07*	4.47	.00	-79.33	-50.82
		30FA	-85.68*	4.47	.00	-99.93	-71.42
		40FA	-136.06*	4.47	.00	-150.32	-121.80
	0FA	TC	-.50	4.47	1.00	-14.76	13.75
		10FA	-22.66*	4.47	.00	-36.91	-8.40
		20FA	-65.58*	4.47	.00	-79.83	-51.32
		30FA	-86.18*	4.47	.00	-100.44	-71.92
		40FA	-136.56*	4.47	.00	-150.82	-122.31
	10FA	TC	22.15*	4.47	.00	7.90	36.41
		0FA	22.66*	4.47	.00	8.40	36.91
		20FA	-42.92*	4.47	.00	-57.18	-28.66
		30FA	-63.52*	4.47	.00	-77.78	-49.26
		40FA	-113.91*	4.47	.00	-128.16	-99.65
	20FA	TC	65.07*	4.47	.00	50.82	79.33
		0FA	65.58*	4.47	.00	51.32	79.83
		10FA	42.92*	4.47	.00	28.66	57.18
		30FA	-20.60*	4.47	.00	-34.86	-6.34
		40FA	-70.99*	4.47	.00	-85.24	-56.73
	30FA	TC	85.68*	4.47	.00	71.42	99.93
		0FA	86.18*	4.47	.00	71.92	100.44
		10FA	63.52*	4.47	.00	49.26	77.78
		20FA	20.60*	4.47	.00	6.34	34.86
		40FA	-50.39*	4.47	.00	-64.64	-36.13
	40FA	TC	136.06*	4.47	.00	121.80	150.32
		0FA	136.56*	4.47	.00	122.31	150.82
		10FA	113.91*	4.47	.00	99.65	128.16
		20FA	70.99*	4.47	.00	56.73	85.24
		30FA	50.39*	4.47	.00	36.13	64.64
Day196-ppm	TC	0FA	.63	5.53	1.00	-17.01	18.27
		10FA	-23.66*	5.53	.00	-41.30	-6.02
		20FA	-72.15*	5.53	.00	-89.79	-54.51
		30FA	-102.65*	5.53	.00	-120.29	-85.01
		40FA	-161.23*	5.53	.00	-178.87	-143.59
	0FA	TC	-.63	5.53	1.00	-18.27	17.01
		10FA	-24.30*	5.53	.00	-41.93	-6.66
		20FA	-72.79*	5.53	.00	-90.42	-55.15
		30FA	-103.29*	5.53	.00	-120.92	-85.65
		40FA	-161.86*	5.53	.00	-179.50	-144.22

	10FA	TC	23.66*	5.53	.00	6.02	41.30
		0FA	24.30*	5.53	.00	6.66	41.93
		20FA	-48.49*	5.53	.00	-66.13	-30.85
		30FA	-78.99*	5.53	.00	-96.63	-61.35
		40FA	-137.57*	5.53	.00	-155.21	-119.93
	20FA	TC	72.15*	5.53	.00	54.51	89.79
		0FA	72.79*	5.53	.00	55.15	90.42
		10FA	48.49*	5.53	.00	30.85	66.13
		30FA	-30.50*	5.53	.00	-48.14	-12.86
		40FA	-89.08*	5.53	.00	-106.72	-71.44
	30FA	TC	102.65*	5.53	.00	85.01	120.29
		0FA	103.29*	5.53	.00	85.65	120.92
		10FA	78.99*	5.53	.00	61.35	96.63
		20FA	30.50*	5.53	.00	12.86	48.14
		40FA	-58.58*	5.53	.00	-76.22	-40.94
	40FA	TC	161.23*	5.53	.00	143.59	178.87
		0FA	161.86*	5.53	.00	144.22	179.50
		10FA	137.57*	5.53	.00	119.93	155.21
		20FA	89.08*	5.53	.00	71.44	106.72
		30FA	58.58*	5.53	.00	40.94	76.22

*. The mean difference is significant at the 0.05 level.

Appendix X: Post Hoc Bonferroni 10FA cumulative release (micrograms)

Multiple Comparisons-cumulative (micrograms)						
Dependent Variable: 10%FA-Acidic						
Bonferroni						
(I) Day	(J) Day	Mean Difference (I-J)	Std. Error	Sig.	95% Confidence Interval	
					Lower Bound	Upper Bound
Day 1	Day 2	-1.94	3.09	1.00	-13.04	9.16
	Day 3	-2.88	3.09	1.00	-13.98	8.23
	Day 4	-3.59	3.09	1.00	-14.69	7.51
	Day 5	-3.99	3.09	1.00	-15.09	7.11
	Day 6	-4.21	3.09	1.00	-15.31	6.89
	Day 7	-4.41	3.09	1.00	-15.51	6.69
	Day 14	-5.38	3.09	1.00	-16.48	5.72
	Day 21	-6.23	3.09	1.00	-17.33	4.87
	Day 28	-6.81	3.09	1.00	-17.91	4.29
	Day 56	-7.48	3.09	1.00	-18.58	3.62
	Day 112	-8.42	3.09	.65	-19.52	2.68
	Day 196	-10.23	3.09	.12	-21.33	.87
Day 2	Day 1	1.94	3.09	1.00	-9.16	13.04
	Day 3	-.93	3.09	1.00	-12.03	10.17
	Day 4	-1.65	3.09	1.00	-12.75	9.45
	Day 5	-2.05	3.09	1.00	-13.15	9.06
	Day 6	-2.27	3.09	1.00	-13.37	8.83
	Day 7	-2.47	3.09	1.00	-13.57	8.64
	Day 14	-3.44	3.09	1.00	-14.54	7.67
	Day 21	-4.29	3.09	1.00	-15.39	6.81
	Day 28	-4.87	3.09	1.00	-15.97	6.23
	Day 56	-5.54	3.09	1.00	-16.64	5.56
	Day 112	-6.48	3.09	1.00	-17.58	4.62
	Day 196	-8.29	3.09	.73	-19.39	2.81
Day 3	Day 1	2.88	3.09	1.00	-8.23	13.98
	Day 2	.93	3.09	1.00	-10.17	12.03
	Day 4	-.71	3.09	1.00	-11.81	10.39
	Day 5	-1.11	3.09	1.00	-12.21	9.99
	Day 6	-1.34	3.09	1.00	-12.44	9.76
	Day 7	-1.53	3.09	1.00	-12.63	9.57
	Day 14	-2.50	3.09	1.00	-13.60	8.60
	Day 21	-3.35	3.09	1.00	-14.45	7.75
	Day 28	-3.94	3.09	1.00	-15.04	7.17
	Day 56	-4.61	3.09	1.00	-15.71	6.49

	Day 112	-5.55	3.09	1.00	-16.65	5.56
	Day 196	-7.36	3.09	1.00	-18.46	3.74
Day 4	Day 1	3.59	3.09	1.00	-7.51	14.69
	Day 2	1.65	3.09	1.00	-9.45	12.75
	Day 3	.71	3.09	1.00	-10.39	11.81
	Day 5	-.40	3.09	1.00	-11.50	10.70
	Day 6	-.62	3.09	1.00	-11.72	10.48
	Day 7	-.82	3.09	1.00	-11.92	10.28
	Day 14	-1.79	3.09	1.00	-12.89	9.31
	Day 21	-2.64	3.09	1.00	-13.74	8.46
	Day 28	-3.22	3.09	1.00	-14.32	7.88
	Day 56	-3.90	3.09	1.00	-15.00	7.21
	Day 112	-4.83	3.09	1.00	-15.93	6.27
	Day 196	-6.64	3.09	1.00	-17.74	4.46
Day 5	Day 1	3.99	3.09	1.00	-7.11	15.09
	Day 2	2.05	3.09	1.00	-9.06	13.15
	Day 3	1.11	3.09	1.00	-9.99	12.21
	Day 4	.40	3.09	1.00	-10.70	11.50
	Day 6	-.23	3.09	1.00	-11.33	10.88
	Day 7	-.42	3.09	1.00	-11.52	10.68
	Day 14	-1.39	3.09	1.00	-12.49	9.71
	Day 21	-2.24	3.09	1.00	-13.34	8.86
	Day 28	-2.82	3.09	1.00	-13.92	8.28
	Day 56	-3.50	3.09	1.00	-14.60	7.60
	Day 112	-4.43	3.09	1.00	-15.53	6.67
	Day 196	-6.25	3.09	1.00	-17.35	4.86
Day 6	Day 1	4.21	3.09	1.00	-6.89	15.31
	Day 2	2.27	3.09	1.00	-8.83	13.37
	Day 3	1.34	3.09	1.00	-9.76	12.44
	Day 4	.62	3.09	1.00	-10.48	11.72
	Day 5	.23	3.09	1.00	-10.88	11.33
	Day 7	-.20	3.09	1.00	-11.30	10.91
	Day 14	-1.17	3.09	1.00	-12.27	9.94
	Day 21	-2.02	3.09	1.00	-13.12	9.08
	Day 28	-2.60	3.09	1.00	-13.70	8.50
	Day 56	-3.27	3.09	1.00	-14.37	7.83
	Day 112	-4.21	3.09	1.00	-15.31	6.89
	Day 196	-6.02	3.09	1.00	-17.12	5.08
Day 7	Day 1	4.41	3.09	1.00	-6.69	15.51
	Day 2	2.47	3.09	1.00	-8.64	13.57
	Day 3	1.53	3.09	1.00	-9.57	12.63
	Day 4	.82	3.09	1.00	-10.28	11.92

	Day 5	.42	3.09	1.00	-10.68	11.52
	Day 6	.20	3.09	1.00	-10.91	11.30
	Day 14	-.97	3.09	1.00	-12.07	10.13
	Day 21	-1.82	3.09	1.00	-12.92	9.28
	Day 28	-2.40	3.09	1.00	-13.50	8.70
	Day 56	-3.08	3.09	1.00	-14.18	8.02
	Day 112	-4.01	3.09	1.00	-15.11	7.09
	Day 196	-5.83	3.09	1.00	-16.93	5.28
Day 14	Day 1	5.38	3.09	1.00	-5.72	16.48
	Day 2	3.44	3.09	1.00	-7.67	14.54
	Day 3	2.50	3.09	1.00	-8.60	13.60
	Day 4	1.79	3.09	1.00	-9.31	12.89
	Day 5	1.39	3.09	1.00	-9.71	12.49
	Day 6	1.17	3.09	1.00	-9.94	12.27
	Day 7	.97	3.09	1.00	-10.13	12.07
	Day 21	-.85	3.09	1.00	-11.95	10.25
	Day 28	-1.43	3.09	1.00	-12.53	9.67
	Day 56	-2.11	3.09	1.00	-13.21	8.99
	Day 112	-3.04	3.09	1.00	-14.14	8.06
	Day 196	-4.86	3.09	1.00	-15.96	6.25
Day 21	Day 1	6.23	3.09	1.00	-4.87	17.33
	Day 2	4.29	3.09	1.00	-6.81	15.39
	Day 3	3.35	3.09	1.00	-7.75	14.45
	Day 4	2.64	3.09	1.00	-8.46	13.74
	Day 5	2.24	3.09	1.00	-8.86	13.34
	Day 6	2.02	3.09	1.00	-9.08	13.12
	Day 7	1.82	3.09	1.00	-9.28	12.92
	Day 14	.85	3.09	1.00	-10.25	11.95
	Day 28	-.58	3.09	1.00	-11.68	10.52
	Day 56	-1.26	3.09	1.00	-12.36	9.85
	Day 112	-2.19	3.09	1.00	-13.29	8.91
	Day 196	-4.00	3.09	1.00	-15.10	7.10
Day 28	Day 1	6.81	3.09	1.00	-4.29	17.91
	Day 2	4.87	3.09	1.00	-6.23	15.97
	Day 3	3.94	3.09	1.00	-7.17	15.04
	Day 4	3.22	3.09	1.00	-7.88	14.32
	Day 5	2.82	3.09	1.00	-8.28	13.92
	Day 6	2.60	3.09	1.00	-8.50	13.70
	Day 7	2.40	3.09	1.00	-8.70	13.50
	Day 14	1.43	3.09	1.00	-9.67	12.53
	Day 21	.58	3.09	1.00	-10.52	11.68
	Day 56	-.67	3.09	1.00	-11.77	10.43

	Day 112	-1.61	3.09	1.00	-12.71	9.49
	Day 196	-3.42	3.09	1.00	-14.52	7.68
Day 56	Day 1	7.48	3.09	1.00	-3.62	18.58
	Day 2	5.54	3.09	1.00	-5.56	16.64
	Day 3	4.61	3.09	1.00	-6.49	15.71
	Day 4	3.90	3.09	1.00	-7.21	15.00
	Day 5	3.50	3.09	1.00	-7.60	14.60
	Day 6	3.27	3.09	1.00	-7.83	14.37
	Day 7	3.08	3.09	1.00	-8.02	14.18
	Day 14	2.11	3.09	1.00	-8.99	13.21
	Day 21	1.26	3.09	1.00	-9.85	12.36
	Day 28	.67	3.09	1.00	-10.43	11.77
	Day 112	-.94	3.09	1.00	-12.04	10.16
	Day 196	-2.75	3.09	1.00	-13.85	8.35
Day 112	Day 1	8.42	3.09	.65	-2.68	19.52
	Day 2	6.48	3.09	1.00	-4.62	17.58
	Day 3	5.55	3.09	1.00	-5.56	16.65
	Day 4	4.83	3.09	1.00	-6.27	15.93
	Day 5	4.43	3.09	1.00	-6.67	15.53
	Day 6	4.21	3.09	1.00	-6.89	15.31
	Day 7	4.01	3.09	1.00	-7.09	15.11
	Day 14	3.04	3.09	1.00	-8.06	14.14
	Day 21	2.19	3.09	1.00	-8.91	13.29
	Day 28	1.61	3.09	1.00	-9.49	12.71
	Day 56	.94	3.09	1.00	-10.16	12.04
	Day 196	-1.81	3.09	1.00	-12.91	9.29
Day 196	Day 1	10.23	3.09	.12	-.87	21.33
	Day 2	8.29	3.09	.73	-2.81	19.39
	Day 3	7.36	3.09	1.00	-3.74	18.46
	Day 4	6.64	3.09	1.00	-4.46	17.74
	Day 5	6.25	3.09	1.00	-4.86	17.35
	Day 6	6.02	3.09	1.00	-5.08	17.12
	Day 7	5.83	3.09	1.00	-5.28	16.93
	Day 14	4.86	3.09	1.00	-6.25	15.96
	Day 21	4.00	3.09	1.00	-7.10	15.10
	Day 28	3.42	3.09	1.00	-7.68	14.52
	Day 56	2.75	3.09	1.00	-8.35	13.85
	Day 112	1.81	3.09	1.00	-9.29	12.91

Appendix Y: Post Hoc Bonferroni 20FA cumulative release (micrograms)

Multiple Comparisons-cumulative (micrograms)						
Dependent Variable: 20%FA-Acidic						
Bonferroni						
(I) Day	(J) Day	Mean Difference (I-J)	Std. Error	Sig.	95% Confidence Interval	
					Lower Bound	Upper Bound
Day 1	Day 2	-10.32*	2.44	.01	-19.08	-1.55
	Day 3	-15.20*	2.44	.00	-23.97	-6.44
	Day 4	-18.16*	2.44	.00	-26.92	-9.39
	Day 5	-20.09*	2.44	.00	-28.86	-11.33
	Day 6	-20.94*	2.44	.00	-29.71	-12.17
	Day 7	-21.76*	2.44	.00	-30.53	-12.99
	Day 14	-26.46*	2.44	.00	-35.23	-17.69
	Day 21	-30.73*	2.44	.00	-39.50	-21.96
	Day 28	-33.82*	2.44	.00	-42.59	-25.05
	Day 56	-36.92*	2.44	.00	-45.69	-28.15
	Day 112	-41.18*	2.44	.00	-49.95	-32.42
	Day 196	-48.57*	2.44	.00	-57.33	-39.80
Day 2	Day 1	10.32*	2.44	.01	1.55	19.08
	Day 3	-4.89	2.44	1.00	-13.65	3.88
	Day 4	-7.84	2.44	.16	-16.61	.93
	Day 5	-9.78*	2.44	.01	-18.54	-1.01
	Day 6	-10.62*	2.44	.00	-19.39	-1.86
	Day 7	-11.44*	2.44	.00	-20.21	-2.67
	Day 14	-16.15*	2.44	.00	-24.91	-7.38
	Day 21	-20.42*	2.44	.00	-29.18	-11.65
	Day 28	-23.50*	2.44	.00	-32.27	-14.74
	Day 56	-26.60*	2.44	.00	-35.37	-17.84
	Day 112	-30.87*	2.44	.00	-39.63	-22.10
	Day 196	-38.25*	2.44	.00	-47.02	-29.48
Day 3	Day 1	15.20*	2.44	.00	6.44	23.97
	Day 2	4.89	2.44	1.00	-3.88	13.65
	Day 4	-2.95	2.44	1.00	-11.72	5.81
	Day 5	-4.89	2.44	1.00	-13.66	3.88
	Day 6	-5.74	2.44	1.00	-14.50	3.03
	Day 7	-6.56	2.44	.72	-15.32	2.21
	Day 14	-11.26*	2.44	.00	-20.03	-2.49
	Day 21	-15.53*	2.44	.00	-24.30	-6.76
	Day 28	-18.62*	2.44	.00	-27.38	-9.85
	Day 56	-21.72*	2.44	.00	-30.48	-12.95

	Day 112	-25.98*	2.44	.00	-34.75	-17.21
	Day 196	-33.36*	2.44	.00	-42.13	-24.59
Day 4	Day 1	18.16*	2.44	.00	9.39	26.92
	Day 2	7.84	2.44	.16	-.93	16.61
	Day 3	2.95	2.44	1.00	-5.81	11.72
	Day 5	-1.94	2.44	1.00	-10.70	6.83
	Day 6	-2.78	2.44	1.00	-11.55	5.98
	Day 7	-3.60	2.44	1.00	-12.37	5.17
	Day 14	-8.31	2.44	.09	-17.07	.46
	Day 21	-12.58*	2.44	.00	-21.34	-3.81
	Day 28	-15.66*	2.44	.00	-24.43	-6.90
	Day 56	-18.76*	2.44	.00	-27.53	-10.00
	Day 112	-23.03*	2.44	.00	-31.79	-14.26
	Day 196	-30.41*	2.44	.00	-39.18	-21.64
Day 5	Day 1	20.09*	2.44	.00	11.33	28.86
	Day 2	9.78*	2.44	.01	1.01	18.54
	Day 3	4.89	2.44	1.00	-3.88	13.66
	Day 4	1.94	2.44	1.00	-6.83	10.70
	Day 6	-.85	2.44	1.00	-9.61	7.92
	Day 7	-1.67	2.44	1.00	-10.43	7.10
	Day 14	-6.37	2.44	.89	-15.14	2.40
	Day 21	-10.64*	2.44	.00	-19.41	-1.87
	Day 28	-13.73*	2.44	.00	-22.49	-4.96
	Day 56	-16.83*	2.44	.00	-25.59	-8.06
	Day 112	-21.09*	2.44	.00	-29.86	-12.32
	Day 196	-28.47*	2.44	.00	-37.24	-19.70
Day 6	Day 1	20.94*	2.44	.00	12.17	29.71
	Day 2	10.62*	2.44	.00	1.86	19.39
	Day 3	5.74	2.44	1.00	-3.03	14.50
	Day 4	2.78	2.44	1.00	-5.98	11.55
	Day 5	.85	2.44	1.00	-7.92	9.61
	Day 7	-.82	2.44	1.00	-9.59	7.95
	Day 14	-5.52	2.44	1.00	-14.29	3.25
	Day 21	-9.79*	2.44	.01	-18.56	-1.02
	Day 28	-12.88*	2.44	.00	-21.65	-4.11
	Day 56	-15.98*	2.44	.00	-24.75	-7.21
	Day 112	-20.24*	2.44	.00	-29.01	-11.48
	Day 196	-27.63*	2.44	.00	-36.39	-18.86
Day 7	Day 1	21.76*	2.44	.00	12.99	30.53
	Day 2	11.44*	2.44	.00	2.67	20.21
	Day 3	6.56	2.44	.72	-2.21	15.32
	Day 4	3.60	2.44	1.00	-5.17	12.37

	Day 5	1.67	2.44	1.00	-7.10	10.43
	Day 6	.82	2.44	1.00	-7.95	9.59
	Day 14	-4.70	2.44	1.00	-13.47	4.06
	Day 21	-8.97*	2.44	.04	-17.74	-.21
	Day 28	-12.06*	2.44	.00	-20.83	-3.29
	Day 56	-15.16*	2.44	.00	-23.93	-6.39
	Day 112	-19.43*	2.44	.00	-28.19	-10.66
	Day 196	-26.81*	2.44	.00	-35.57	-18.04
Day 14	Day 1	26.46*	2.44	.00	17.69	35.23
	Day 2	16.15*	2.44	.00	7.38	24.91
	Day 3	11.26*	2.44	.00	2.49	20.03
	Day 4	8.31	2.44	.09	-.46	17.07
	Day 5	6.37	2.44	.89	-2.40	15.14
	Day 6	5.52	2.44	1.00	-3.25	14.29
	Day 7	4.70	2.44	1.00	-4.06	13.47
	Day 21	-4.27	2.44	1.00	-13.04	4.50
	Day 28	-7.36	2.44	.29	-16.13	1.41
	Day 56	-10.46*	2.44	.00	-19.23	-1.69
	Day 112	-14.72*	2.44	.00	-23.49	-5.95
	Day 196	-22.10*	2.44	.00	-30.87	-13.34
Day 21	Day 1	30.73*	2.44	.00	21.96	39.50
	Day 2	20.42*	2.44	.00	11.65	29.18
	Day 3	15.53*	2.44	.00	6.76	24.30
	Day 4	12.58*	2.44	.00	3.81	21.34
	Day 5	10.64*	2.44	.00	1.87	19.41
	Day 6	9.79*	2.44	.01	1.02	18.56
	Day 7	8.97*	2.44	.04	.21	17.74
	Day 14	4.27	2.44	1.00	-4.50	13.04
	Day 28	-3.09	2.44	1.00	-11.86	5.68
	Day 56	-6.19	2.44	1.00	-14.96	2.58
	Day 112	-10.45*	2.44	.00	-19.22	-1.68
	Day 196	-17.83*	2.44	.00	-26.60	-9.07
Day 28	Day 1	33.82*	2.44	.00	25.05	42.59
	Day 2	23.50*	2.44	.00	14.74	32.27
	Day 3	18.62*	2.44	.00	9.85	27.38
	Day 4	15.66*	2.44	.00	6.90	24.43
	Day 5	13.73*	2.44	.00	4.96	22.49
	Day 6	12.88*	2.44	.00	4.11	21.65
	Day 7	12.06*	2.44	.00	3.29	20.83
	Day 14	7.36	2.44	.29	-1.41	16.13
	Day 21	3.09	2.44	1.00	-5.68	11.86
	Day 56	-3.10	2.44	1.00	-11.87	5.67

	Day 112	-7.36	2.44	.29	-16.13	1.40
	Day 196	-14.75*	2.44	.00	-23.51	-5.98
Day 56	Day 1	36.92*	2.44	.00	28.15	45.69
	Day 2	26.60*	2.44	.00	17.84	35.37
	Day 3	21.72*	2.44	.00	12.95	30.48
	Day 4	18.76*	2.44	.00	10.00	27.53
	Day 5	16.83*	2.44	.00	8.06	25.59
	Day 6	15.98*	2.44	.00	7.21	24.75
	Day 7	15.16*	2.44	.00	6.39	23.93
	Day 14	10.46*	2.44	.00	1.69	19.23
	Day 21	6.19	2.44	1.00	-2.58	14.96
	Day 28	3.10	2.44	1.00	-5.67	11.87
	Day 112	-4.26	2.44	1.00	-13.03	4.50
	Day 196	-11.65*	2.44	.00	-20.41	-2.88
Day 112	Day 1	41.18*	2.44	.00	32.42	49.95
	Day 2	30.87*	2.44	.00	22.10	39.63
	Day 3	25.98*	2.44	.00	17.21	34.75
	Day 4	23.03*	2.44	.00	14.26	31.79
	Day 5	21.09*	2.44	.00	12.32	29.86
	Day 6	20.24*	2.44	.00	11.48	29.01
	Day 7	19.43*	2.44	.00	10.66	28.19
	Day 14	14.72*	2.44	.00	5.95	23.49
	Day 21	10.45*	2.44	.00	1.68	19.22
	Day 28	7.36	2.44	.29	-1.40	16.13
	Day 56	4.26	2.44	1.00	-4.50	13.03
	Day 196	-7.38	2.44	.28	-16.15	1.39
Day 196	Day 1	48.57*	2.44	.00	39.80	57.33
	Day 2	38.25*	2.44	.00	29.48	47.02
	Day 3	33.36*	2.44	.00	24.59	42.13
	Day 4	30.41*	2.44	.00	21.64	39.18
	Day 5	28.47*	2.44	.00	19.70	37.24
	Day 6	27.63*	2.44	.00	18.86	36.39
	Day 7	26.81*	2.44	.00	18.04	35.57
	Day 14	22.10*	2.44	.00	13.34	30.87
	Day 21	17.83*	2.44	.00	9.07	26.60
	Day 28	14.75*	2.44	.00	5.98	23.51
	Day 56	11.65*	2.44	.00	2.88	20.41
	Day 112	7.38	2.44	.28	-1.39	16.15

*. The mean difference is significant at the 0.05 level.

Appendix Z: Post Hoc Bonferroni 30FA cumulative release (micrograms)

Multiple Comparisons-cumulative F release micrograms						
Dependent Variable: 30%FA-Acidic						
Bonferroni						
(I) Day	(J) Day	Mean Difference (I-J)	Std. Error	Sig.	95% Confidence Interval	
					Lower Bound	Upper Bound
Day 1	Day 2	-8.10	3.67	1.00	-21.28	5.08
	Day 3	-13.08	3.67	.05	-26.26	.09
	Day 4	-16.85*	3.67	.00	-30.03	-3.68
	Day 5	-19.68*	3.67	.00	-32.85	-6.50
	Day 6	-20.87*	3.67	.00	-34.04	-7.69
	Day 7	-22.05*	3.67	.00	-35.22	-8.87
	Day 14	-29.15*	3.67	.00	-42.32	-15.97
	Day 21	-36.56*	3.67	.00	-49.74	-23.38
	Day 28	-42.33*	3.67	.00	-55.50	-29.15
	Day 56	-50.99*	3.67	.00	-64.16	-37.81
	Day 112	-60.65*	3.67	.00	-73.83	-47.47
	Day 196	-77.93*	3.67	.00	-91.11	-64.75
Day 2	Day 1	8.10	3.67	1.00	-5.08	21.28
	Day 3	-4.98	3.67	1.00	-18.16	8.19
	Day 4	-8.75	3.67	1.00	-21.93	4.42
	Day 5	-11.58	3.67	.19	-24.75	1.60
	Day 6	-12.77	3.67	.07	-25.94	.41
	Day 7	-13.95*	3.67	.03	-27.12	-.77
	Day 14	-21.05*	3.67	.00	-34.22	-7.87
	Day 21	-28.46*	3.67	.00	-41.64	-15.28
	Day 28	-34.23*	3.67	.00	-47.40	-21.05
	Day 56	-42.89*	3.67	.00	-56.06	-29.71
	Day 112	-52.55*	3.67	.00	-65.73	-39.37
	Day 196	-69.83*	3.67	.00	-83.01	-56.65
Day 3	Day 1	13.08	3.67	.05	-.09	26.26
	Day 2	4.98	3.67	1.00	-8.19	18.16
	Day 4	-3.77	3.67	1.00	-16.95	9.41
	Day 5	-6.59	3.67	1.00	-19.77	6.58
	Day 6	-7.78	3.67	1.00	-20.96	5.39
	Day 7	-8.96	3.67	1.00	-22.14	4.21
	Day 14	-16.06*	3.67	.00	-29.24	-2.89
	Day 21	-23.48*	3.67	.00	-36.65	-10.30
	Day 28	-29.24*	3.67	.00	-42.42	-16.07
	Day 56	-37.90*	3.67	.00	-51.08	-24.73

	Day 112	-47.57*	3.67	.00	-60.74	-34.39
	Day 196	-64.85*	3.67	.00	-78.02	-51.67
Day 4	Day 1	16.85*	3.67	.00	3.68	30.03
	Day 2	8.75	3.67	1.00	-4.42	21.93
	Day 3	3.77	3.67	1.00	-9.41	16.95
	Day 5	-2.82	3.67	1.00	-16.00	10.35
	Day 6	-4.01	3.67	1.00	-17.19	9.16
	Day 7	-5.19	3.67	1.00	-18.37	7.98
	Day 14	-12.29	3.67	.11	-25.47	.88
	Day 21	-19.71*	3.67	.00	-32.88	-6.53
	Day 28	-25.47*	3.67	.00	-38.65	-12.30
	Day 56	-34.13*	3.67	.00	-47.31	-20.96
	Day 112	-43.80*	3.67	.00	-56.97	-30.62
	Day 196	-61.08*	3.67	.00	-74.25	-47.90
Day 5	Day 1	19.68*	3.67	.00	6.50	32.85
	Day 2	11.58	3.67	.19	-1.60	24.75
	Day 3	6.59	3.67	1.00	-6.58	19.77
	Day 4	2.82	3.67	1.00	-10.35	16.00
	Day 6	-1.19	3.67	1.00	-14.37	11.98
	Day 7	-2.37	3.67	1.00	-15.55	10.80
	Day 14	-9.47	3.67	.95	-22.65	3.70
	Day 21	-16.89*	3.67	.00	-30.06	-3.71
	Day 28	-22.65*	3.67	.00	-35.83	-9.48
	Day 56	-31.31*	3.67	.00	-44.49	-18.14
	Day 112	-40.98*	3.67	.00	-54.15	-27.80
	Day 196	-58.26*	3.67	.00	-71.43	-45.08
Day 6	Day 1	20.87*	3.67	.00	7.69	34.04
	Day 2	12.77	3.67	.07	-.41	25.94
	Day 3	7.78	3.67	1.00	-5.39	20.96
	Day 4	4.01	3.67	1.00	-9.16	17.19
	Day 5	1.19	3.67	1.00	-11.98	14.37
	Day 7	-1.18	3.67	1.00	-14.36	12.00
	Day 14	-8.28	3.67	1.00	-21.46	4.90
	Day 21	-15.69*	3.67	.01	-28.87	-2.52
	Day 28	-21.46*	3.67	.00	-34.64	-8.28
	Day 56	-30.12*	3.67	.00	-43.30	-16.94
	Day 112	-39.78*	3.67	.00	-52.96	-26.61
	Day 196	-57.06*	3.67	.00	-70.24	-43.89
Day 7	Day 1	22.05*	3.67	.00	8.87	35.22
	Day 2	13.95*	3.67	.03	.77	27.12
	Day 3	8.96	3.67	1.00	-4.21	22.14
	Day 4	5.19	3.67	1.00	-7.98	18.37

	Day 5	2.37	3.67	1.00	-10.80	15.55
	Day 6	1.18	3.67	1.00	-12.00	14.36
	Day 14	-7.10	3.67	1.00	-20.28	6.08
	Day 21	-14.51*	3.67	.02	-27.69	-1.34
	Day 28	-20.28*	3.67	.00	-33.46	-7.10
	Day 56	-28.94*	3.67	.00	-42.12	-15.76
	Day 112	-38.60*	3.67	.00	-51.78	-25.43
	Day 196	-55.88*	3.67	.00	-69.06	-42.71
Day 14	Day 1	29.15*	3.67	.00	15.97	42.32
	Day 2	21.05*	3.67	.00	7.87	34.22
	Day 3	16.06*	3.67	.00	2.89	29.24
	Day 4	12.29	3.67	.11	-.88	25.47
	Day 5	9.47	3.67	.95	-3.70	22.65
	Day 6	8.28	3.67	1.00	-4.90	21.46
	Day 7	7.10	3.67	1.00	-6.08	20.28
	Day 21	-7.41	3.67	1.00	-20.59	5.76
	Day 28	-13.18*	3.67	.05	-26.36	.00
	Day 56	-21.84*	3.67	.00	-35.02	-8.66
	Day 112	-31.50*	3.67	.00	-44.68	-18.33
	Day 196	-48.78*	3.67	.00	-61.96	-35.61
Day 21	Day 1	36.56*	3.67	.00	23.38	49.74
	Day 2	28.46*	3.67	.00	15.28	41.64
	Day 3	23.48*	3.67	.00	10.30	36.65
	Day 4	19.71*	3.67	.00	6.53	32.88
	Day 5	16.89*	3.67	.00	3.71	30.06
	Day 6	15.69*	3.67	.01	2.52	28.87
	Day 7	14.51*	3.67	.02	1.34	27.69
	Day 14	7.41	3.67	1.00	-5.76	20.59
	Day 28	-5.77	3.67	1.00	-18.94	7.41
	Day 56	-14.43*	3.67	.02	-27.60	-1.25
	Day 112	-24.09*	3.67	.00	-37.27	-10.91
	Day 196	-41.37*	3.67	.00	-54.55	-28.19
Day 28	Day 1	42.33*	3.67	.00	29.15	55.50
	Day 2	34.23*	3.67	.00	21.05	47.40
	Day 3	29.24*	3.67	.00	16.07	42.42
	Day 4	25.47*	3.67	.00	12.30	38.65
	Day 5	22.65*	3.67	.00	9.48	35.83
	Day 6	21.46*	3.67	.00	8.28	34.64
	Day 7	20.28*	3.67	.00	7.10	33.46
	Day 14	13.18*	3.67	.05	.00	26.36
	Day 21	5.77	3.67	1.00	-7.41	18.94
	Day 56	-8.66	3.67	1.00	-21.84	4.52

	Day 112	-18.32*	3.67	.00	-31.50	-5.15
	Day 196	-35.60*	3.67	.00	-48.78	-22.43
Day 56	Day 1	50.99*	3.67	.00	37.81	64.16
	Day 2	42.89*	3.67	.00	29.71	56.06
	Day 3	37.90*	3.67	.00	24.73	51.08
	Day 4	34.13*	3.67	.00	20.96	47.31
	Day 5	31.31*	3.67	.00	18.14	44.49
	Day 6	30.12*	3.67	.00	16.94	43.30
	Day 7	28.94*	3.67	.00	15.76	42.12
	Day 14	21.84*	3.67	.00	8.66	35.02
	Day 21	14.43*	3.67	.02	1.25	27.60
	Day 28	8.66	3.67	1.00	-4.52	21.84
	Day 112	-9.66	3.67	.83	-22.84	3.51
	Day 196	-26.94*	3.67	.00	-40.12	-13.77
Day 112	Day 1	60.65*	3.67	.00	47.47	73.83
	Day 2	52.55*	3.67	.00	39.37	65.73
	Day 3	47.57*	3.67	.00	34.39	60.74
	Day 4	43.80*	3.67	.00	30.62	56.97
	Day 5	40.98*	3.67	.00	27.80	54.15
	Day 6	39.78*	3.67	.00	26.61	52.96
	Day 7	38.60*	3.67	.00	25.43	51.78
	Day 14	31.50*	3.67	.00	18.33	44.68
	Day 21	24.09*	3.67	.00	10.91	37.27
	Day 28	18.32*	3.67	.00	5.15	31.50
	Day 56	9.66	3.67	.83	-3.51	22.84
	Day 196	-17.28*	3.67	.00	-30.46	-4.10
Day 196	Day 1	77.93*	3.67	.00	64.75	91.11
	Day 2	69.83*	3.67	.00	56.65	83.01
	Day 3	64.85*	3.67	.00	51.67	78.02
	Day 4	61.08*	3.67	.00	47.90	74.25
	Day 5	58.26*	3.67	.00	45.08	71.43
	Day 6	57.06*	3.67	.00	43.89	70.24
	Day 7	55.88*	3.67	.00	42.71	69.06
	Day 14	48.78*	3.67	.00	35.61	61.96
	Day 21	41.37*	3.67	.00	28.19	54.55
	Day 28	35.60*	3.67	.00	22.43	48.78
	Day 56	26.94*	3.67	.00	13.77	40.12
	Day 112	17.28*	3.67	.00	4.10	30.46

*. The mean difference is significant at the 0.05 level.

Appendix AA: Post Hoc Bonferroni 40FA cumulative release (micrograms)

Multiple Comparisons-cumulative micrograms						
Dependent Variable: 40%FA-Acidic						
Bonferroni						
(I) Day	(J) Day	Mean Difference (I-J)	Std. Error	Sig.	95% Confidence Interval	
					Lower Bound	Upper Bound
Day 1	Day 2	-7.83	5.59	1.00	-27.89	12.23
	Day 3	-13.86	5.59	1.00	-33.91	6.20
	Day 4	-19.75	5.59	.06	-39.80	.31
	Day 5	-25.02*	5.59	.00	-45.08	-4.96
	Day 6	-27.49*	5.59	.00	-47.55	-7.43
	Day 7	-29.81*	5.59	.00	-49.86	-9.75
	Day 14	-46.04*	5.59	.00	-66.09	-25.98
	Day 21	-63.07*	5.59	.00	-83.13	-43.02
	Day 28	-78.10*	5.59	.00	-98.16	-58.05
	Day 56	-96.23*	5.59	.00	-116.28	-76.17
	Day 112	-112.84*	5.59	.00	-132.89	-92.78
	Day 196	-138.31*	5.59	.00	-158.36	-118.25
Day 2	Day 1	7.83	5.59	1.00	-12.23	27.89
	Day 3	-6.03	5.59	1.00	-26.08	14.03
	Day 4	-11.92	5.59	1.00	-31.97	8.14
	Day 5	-17.19	5.59	.24	-37.25	2.87
	Day 6	-19.66	5.59	.06	-39.72	.40
	Day 7	-21.98*	5.59	.02	-42.03	-1.92
	Day 14	-38.21*	5.59	.00	-58.26	-18.15
	Day 21	-55.24*	5.59	.00	-75.30	-35.19
	Day 28	-70.27*	5.59	.00	-90.33	-50.22
	Day 56	-88.40*	5.59	.00	-108.45	-68.34
	Day 112	-105.01*	5.59	.00	-125.06	-84.95
	Day 196	-130.48*	5.59	.00	-150.53	-110.42
Day 3	Day 1	13.86	5.59	1.00	-6.20	33.91
	Day 2	6.03	5.59	1.00	-14.03	26.08
	Day 4	-5.89	5.59	1.00	-25.94	14.17
	Day 5	-11.16	5.59	1.00	-31.22	8.89
	Day 6	-13.63	5.59	1.00	-33.69	6.42
	Day 7	-15.95	5.59	.45	-36.00	4.11
	Day 14	-32.18*	5.59	.00	-52.24	-12.12
	Day 21	-49.22*	5.59	.00	-69.27	-29.16
	Day 28	-64.24*	5.59	.00	-84.30	-44.19
	Day 56	-82.37*	5.59	.00	-102.43	-62.31

	Day 112	-98.98*	5.59	.00	-119.03	-78.92
	Day 196	-124.45*	5.59	.00	-144.50	-104.39
Day 4	Day 1	19.75	5.59	.06	-.31	39.80
	Day 2	11.92	5.59	1.00	-8.14	31.97
	Day 3	5.89	5.59	1.00	-14.17	25.94
	Day 5	-5.27	5.59	1.00	-25.33	14.78
	Day 6	-7.74	5.59	1.00	-27.80	12.31
	Day 7	-10.06	5.59	1.00	-30.11	10.00
	Day 14	-26.29*	5.59	.00	-46.35	-6.24
	Day 21	-43.33*	5.59	.00	-63.38	-23.27
	Day 28	-58.36*	5.59	.00	-78.41	-38.30
	Day 56	-76.48*	5.59	.00	-96.54	-56.43
	Day 112	-93.09*	5.59	.00	-113.14	-73.03
	Day 196	-118.56*	5.59	.00	-138.62	-98.50
Day 5	Day 1	25.02*	5.59	.00	4.96	45.08
	Day 2	17.19	5.59	.24	-2.87	37.25
	Day 3	11.16	5.59	1.00	-8.89	31.22
	Day 4	5.27	5.59	1.00	-14.78	25.33
	Day 6	-2.47	5.59	1.00	-22.53	17.59
	Day 7	-4.79	5.59	1.00	-24.84	15.27
	Day 14	-21.02*	5.59	.03	-41.07	-.96
	Day 21	-38.05*	5.59	.00	-58.11	-18.00
	Day 28	-53.08*	5.59	.00	-73.14	-33.03
	Day 56	-71.21*	5.59	.00	-91.26	-51.15
	Day 112	-87.82*	5.59	.00	-107.87	-67.76
	Day 196	-113.29*	5.59	.00	-133.34	-93.23
Day 6	Day 1	27.49*	5.59	.00	7.43	47.55
	Day 2	19.66	5.59	.06	-.40	39.72
	Day 3	13.63	5.59	1.00	-6.42	33.69
	Day 4	7.74	5.59	1.00	-12.31	27.80
	Day 5	2.47	5.59	1.00	-17.59	22.53
	Day 7	-2.32	5.59	1.00	-22.37	17.74
	Day 14	-18.55	5.59	.12	-38.60	1.51
	Day 21	-35.58*	5.59	.00	-55.64	-15.53
	Day 28	-50.61*	5.59	.00	-70.67	-30.56
	Day 56	-68.74*	5.59	.00	-88.79	-48.68
	Day 112	-85.35*	5.59	.00	-105.40	-65.29
	Day 196	-110.82*	5.59	.00	-130.87	-90.76
Day 7	Day 1	29.81*	5.59	.00	9.75	49.86
	Day 2	21.98*	5.59	.02	1.92	42.03
	Day 3	15.95	5.59	.45	-4.11	36.00
	Day 4	10.06	5.59	1.00	-10.00	30.11

	Day 5	4.79	5.59	1.00	-15.27	24.84
	Day 6	2.32	5.59	1.00	-17.74	22.37
	Day 14	-16.23	5.59	.39	-36.29	3.82
	Day 21	-33.27*	5.59	.00	-53.32	-13.21
	Day 28	-48.30*	5.59	.00	-68.35	-28.24
	Day 56	-66.42*	5.59	.00	-86.48	-46.37
	Day 112	-83.03*	5.59	.00	-103.09	-62.97
	Day 196	-108.50*	5.59	.00	-128.56	-88.45
Day 14	Day 1	46.04*	5.59	.00	25.98	66.09
	Day 2	38.21*	5.59	.00	18.15	58.26
	Day 3	32.18*	5.59	.00	12.12	52.24
	Day 4	26.29*	5.59	.00	6.24	46.35
	Day 5	21.02*	5.59	.03	.96	41.07
	Day 6	18.55	5.59	.12	-1.51	38.60
	Day 7	16.23	5.59	.39	-3.82	36.29
	Day 21	-17.04	5.59	.26	-37.09	3.02
	Day 28	-32.06*	5.59	.00	-52.12	-12.01
	Day 56	-50.19*	5.59	.00	-70.25	-30.13
	Day 112	-66.80*	5.59	.00	-86.85	-46.74
	Day 196	-92.27*	5.59	.00	-112.32	-72.21
Day 21	Day 1	63.07*	5.59	.00	43.02	83.13
	Day 2	55.24*	5.59	.00	35.19	75.30
	Day 3	49.22*	5.59	.00	29.16	69.27
	Day 4	43.33*	5.59	.00	23.27	63.38
	Day 5	38.05*	5.59	.00	18.00	58.11
	Day 6	35.58*	5.59	.00	15.53	55.64
	Day 7	33.27*	5.59	.00	13.21	53.32
	Day 14	17.04	5.59	.26	-3.02	37.09
	Day 28	-15.03	5.59	.71	-35.08	5.03
	Day 56	-33.16*	5.59	.00	-53.21	-13.10
	Day 112	-49.76*	5.59	.00	-69.82	-29.71
	Day 196	-75.23*	5.59	.00	-95.29	-55.18
Day 28	Day 1	78.10*	5.59	.00	58.05	98.16
	Day 2	70.27*	5.59	.00	50.22	90.33
	Day 3	64.24*	5.59	.00	44.19	84.30
	Day 4	58.36*	5.59	.00	38.30	78.41
	Day 5	53.08*	5.59	.00	33.03	73.14
	Day 6	50.61*	5.59	.00	30.56	70.67
	Day 7	48.30*	5.59	.00	28.24	68.35
	Day 14	32.06*	5.59	.00	12.01	52.12
	Day 21	15.03	5.59	.71	-5.03	35.08
	Day 56	-18.13	5.59	.15	-38.18	1.93

	Day 112	-34.73*	5.59	.00	-54.79	-14.68
	Day 196	-60.21*	5.59	.00	-80.26	-40.15
Day 56	Day 1	96.23*	5.59	.00	76.17	116.28
	Day 2	88.40*	5.59	.00	68.34	108.45
	Day 3	82.37*	5.59	.00	62.31	102.43
	Day 4	76.48*	5.59	.00	56.43	96.54
	Day 5	71.21*	5.59	.00	51.15	91.26
	Day 6	68.74*	5.59	.00	48.68	88.79
	Day 7	66.42*	5.59	.00	46.37	86.48
	Day 14	50.19*	5.59	.00	30.13	70.25
	Day 21	33.16*	5.59	.00	13.10	53.21
	Day 28	18.13	5.59	.15	-1.93	38.18
	Day 112	-16.61	5.59	.32	-36.66	3.45
	Day 196	-42.08*	5.59	.00	-62.13	-22.02
Day 112	Day 1	112.84*	5.59	.00	92.78	132.89
	Day 2	105.01*	5.59	.00	84.95	125.06
	Day 3	98.98*	5.59	.00	78.92	119.03
	Day 4	93.09*	5.59	.00	73.03	113.14
	Day 5	87.82*	5.59	.00	67.76	107.87
	Day 6	85.35*	5.59	.00	65.29	105.40
	Day 7	83.03*	5.59	.00	62.97	103.09
	Day 14	66.80*	5.59	.00	46.74	86.85
	Day 21	49.76*	5.59	.00	29.71	69.82
	Day 28	34.73*	5.59	.00	14.68	54.79
	Day 56	16.61	5.59	.32	-3.45	36.66
	Day 196	-25.47*	5.59	.00	-45.53	-5.42
Day 196	Day 1	138.31*	5.59	.00	118.25	158.36
	Day 2	130.48*	5.59	.00	110.42	150.53
	Day 3	124.45*	5.59	.00	104.39	144.50
	Day 4	118.56*	5.59	.00	98.50	138.62
	Day 5	113.29*	5.59	.00	93.23	133.34
	Day 6	110.82*	5.59	.00	90.76	130.87
	Day 7	108.50*	5.59	.00	88.45	128.56
	Day 14	92.27*	5.59	.00	72.21	112.32
	Day 21	75.23*	5.59	.00	55.18	95.29
	Day 28	60.21*	5.59	.00	40.15	80.26
	Day 56	42.08*	5.59	.00	22.02	62.13
	Day 112	25.47*	5.59	.00	5.42	45.53

*. The mean difference is significant at the 0.05 level.